# Developmental Expression of the Proteolipid Protein Gene in the Nervous System

A thesis presented to

the Faculty of Veterinary Medicine

University of Glasgow
for the Degree of Doctor of Philosophy

November 1995

*Peter James Dickinson*



ProQuest LLC.
789 East Eisenhower Parkway
P.O. Box 1346
Ann Arbor, MI 48106 – 1346

# Abstract

Proteolipid protein (PLP) and DM-20 account for more than 50% of total myelin protein in the central nervous system (CNS) and are produced by alternative splicing of the primary *plp* transcript. While PLP is thought to contribute to the stability of the intraperiod line in CNS myelin, little is known about the function of DM-20. It has been suggested that DM-20 may be involved in oligodendrocyte differentiation and survival. The present work confirmed that the marked upregulation of the *plp* gene, and change in transcript ratio from *dm-20* to *plp* predominance, occurs around the time of onset of myelination. In separate areas where myelination commenced at different times, these changes were correlated with the "age" of myelination in that area, rather than the chronological age of the developing CNS as a whole.

Using a combination of semi-quantitative reverse transcription-polymerase chain reaction (RT-PCR) and immunocytochemistry, both transcripts and product were shown to be present in the embryonic mouse spinal cord as early as embryonic day 12 (E12). This expression was linked to the oligodendrocyte progenitor lineage. The presence of DM-20 isoprotein in these oligodendrocyte progenitors challenges previous perceptions that *plp* gene expression occurs only in mature post-mitotic oligodendrocytes. These studies also support the hypothesis that oligodendrocytes originate in a discrete region of the ventral spinal cord.

*Plp* and *dm-20* transcripts were demonstrated in the sciatic nerve, cranial sympathetic trunk and cranial cervical ganglion in the peripheral nervous system (PNS) with *dm-20* being the predominant message present. No developmental change in *plp/dm-20* transcript ratio similar to that seen in the CNS was seen. Nerve transection studies in both sciatic nerves (PNS) and optic nerves (CNS) demonstrated selective downregulation of the *plp* isoform suggesting different regulatory mechanisms for the two isomers, with axonal factors being more important for *plp*.

*Plp* gene expression was present in the olfactory nerve layer (ONL) of the olfactory bulb during both embryogenesis and postnatal life. Transcripts and protein were found to be exclusively *dm-20* and were shown to be present in the olfactory nerve ensheathing cells of the ONL.

The combination of these studies has added further evidence to support the theory of separate functions for the PLP and DM-20 isoproteins. Expression of the *dm-20* isoform appears to be the default pathway in "non-myelin" environments with dramatic upregulation of the *plp* isoform during active myelination.

To my parents and Katey

*Tell a student that the only people who are going to read this great document are the supervisor, two examiners and one or two close friends, and you will be regarded with rank disbelief.*

Steven Rose

# List of Contents

# List of Figures

# List of Tables

# Declaration

I, Peter James Dickinson, do hereby declare that the work carried out in this thesis is original, was carried out by myself or with due acknowledgement, and has not been presented for the award of a degree at any other University.

# Acknowledgements

First and foremost, I would like to thank my supervisor, Professor Ian Griffiths, and Dr. Paul Montague for their support and guidance. Their continued willingness to give advice, despite the amount left unused from the last time, has never ceased to amaze me.

Within the Applied Neurobiology Group, I would like to thank the technical staff for their help, advice and above all their patience. These people include Jenny Barrie, Nan Deary, Douglas Kirkham, Evangelos Kyriakides, Mailis McCulloch and Eilidh MacPhee.

I am grateful to Professor Neil Gorman and Dr. Mike Harvey for enabling me to pursue this study in the Department of Veterinary Surgery and to the Wellcome trust who provided generous funding and fees during this period.

Special thanks are due to Alan May for all the photography.

I am very thankful for all those colleagues who have given their advice and time; Dr. Christine Thomson, Dr. Monica Fanarraga, Dr. Sue Barnett and Dr. Martin Sullivan.

Finally I would like to thank Jim for his support both as a colleague and more importantly as a friend.

# CHAPTER 1. INTRODUCTION

# 1.1.DEVELOPMENT OF THE NERVOUS SYSTEM

Development of the vertebrate nervous system begins with the induction of the neural plate from uncommitted ectoderm. The neural plate then invaginates longitudinally until the lateral extremities of the original plate, the neural folds, meet centrally and fuse over the neural groove to form a neural tube and canal (Schoenwolf and Smith 1990) (Figure 1). The margins of the non-neural ectoderm fuse dorsal to the neural tube and the two layers of ectoderm separate. A longitudinal column of cells arises from the junction of the neural and non-neural ectoderm and lies dorsolaterally on either side of the neural tube throughout its length. These are the neural crest cells which will give rise to the spinal, autonomic and cranial nerve sensory ganglia, melanoblasts of the epidermis and cells of the adrenal medulla. Regional differentiation of the neural epithelium along the cranio-caudal axis is present at the neural plate stage (Roach 1945) and gives rise rostrally to the forebrain and midbrain and caudally to the hindbrain and spinal cord.

The neural tube is divided into three concentric layers (Figure 1). Adjacent to the neural canal is the germinal layer of proliferating neuroepithelial cells. The proliferative function of this layer is ultimately exhausted, and the resulting single layer of cells forms the ependymal lining of the ventricular system. Peripheral to the germinal layer is the mantle layer which will become the grey matter of the definitive spinal cord, nuclei of the brain stem and, after migration to the external surface of the neural tube, the cerebral cortex of the telencephalon. The external layer of the neural tube is the marginal layer which gives rise to the white matter of the brain and spinal cord and contains relatively few cells. The spinal cord is also divided into dorsal and ventral portions at the level of the sulcus limitans, a longitudinal groove present in the lateral wall of the neural canal. The dorsal or alar plate is concerned predominantly with sensory systems, and the ventral or basal plate with motor systems.

Two important structures present during development of the neural tube are the floor plate and the notochord. The floor plate arises from cells at the ventral midline of the neural plate (Schoenwolf and Smith 1990), whilst the notochord is of mesodermal origin and lies ventral to the neural plate (Figure 1). Differentiation of the floor plate appears to be induced by the notochord (Placzek *et al.* 1990), and both structures appear to act as sources of polarising signal in the embryonic tissues. It is likely that these two cell groups are involved in controlling the pattern of cell differentiation along the dorso-ventral axis of the developing nervous system. Moreover, the fate of neuroepithelial precursor cells appears to be dependent on the position that they occupy with respect to the notochord and floor plate (Yamada *et al.* 1991).

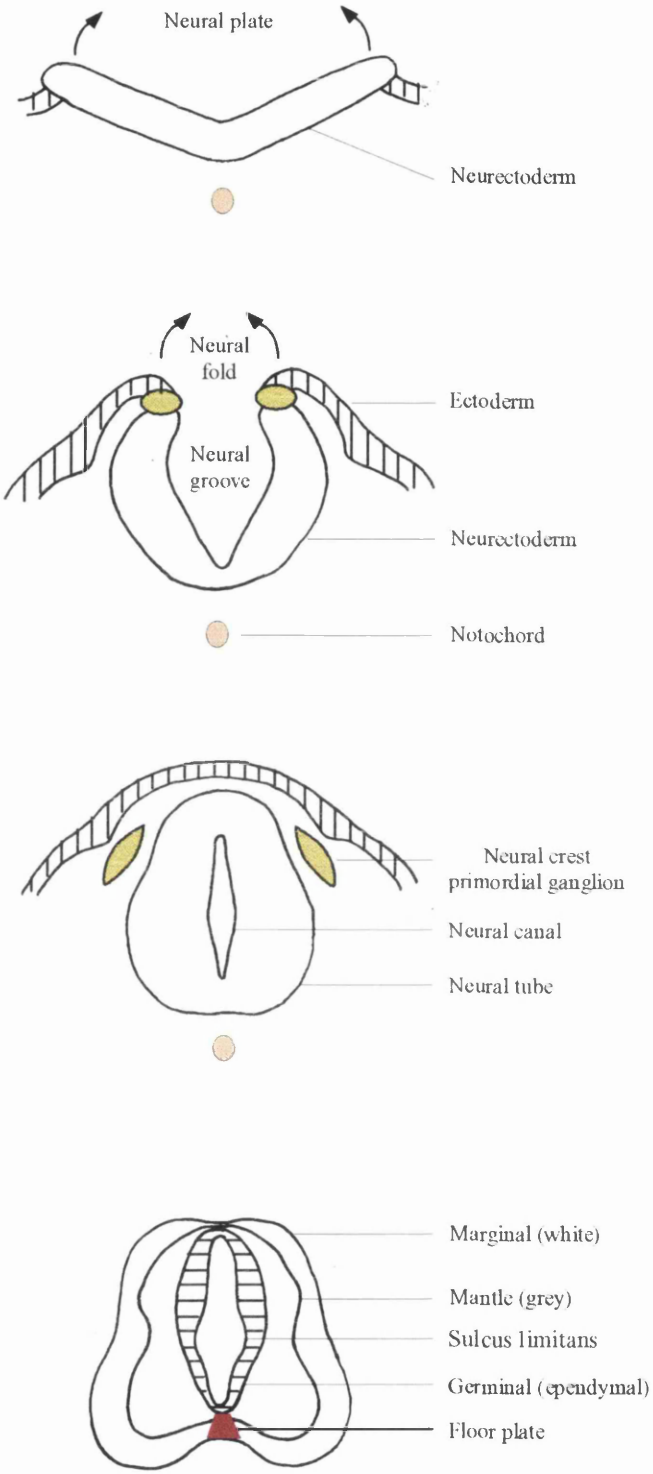


**Figure 1.** Development of the neural tube. Temporal development of the neural tube is demonstrated from the upper to the lower diagram. The embryonic spinal cord can be seen to consist of three concentric layers (lower diagram).

# 1.2.MYELINATION AND THE PROTEOLIPID PROTEIN (*plp*) GENE

## 1.2.1.The myelin sheath

Myelin is a highly specialised extension of the plasma membrane elaborated by specific glial cells in both the central nervous system (CNS) and peripheral nervous system (PNS). In the CNS the myelinating cell is the oligodendrocyte (Bunge *et al.* 1961; Bunge *et al.* 1962), with one oligodendrocyte capable of myelinating many segments of different axons, possibly as many as 60, simultaneously (Bunge 1968; Matthews and Duncan 1971). In the PNS, the Schwann cell fulfils the same function but maintains a 1:1 ratio with the myelin internode (Peters and Muir 1959). The tightly compacted multilamellar sheath surrounds axons and facilitates rapid, saltatory conduction of nerve impulses (Huxley and Staempfli 1949) necessary for integrated function of the vertebrate nervous system. Disruption of the myelin sheath, whether due to developmental abnormalities (dysmyelination) as seen in myelin gene mutations, or due to loss (demyelination) during disease processes, invariably leads to devastating neurological symptoms.

## 1.2.2.CNS/PNS myelin

Although CNS and PNS myelin have general similarities in composition and structure, several differences exist. The manner of formation of the myelin lamellae is identical, however periodicity varies (CNS 10.5-11.5nm/PNS 11.5-12.7nm in specimens for electron microscopy), and CNS sheaths never attain the same thickness as those around axons of similar diameter in the PNS (Fraher 1992). The Schwann cell is surrounded by a basal lamina and the myelin sheath is formed directly from the soma of the Schwann cell whilst the oligodendrocyte lacks a basal lamina and myelination may occur at a distance from the soma by spiral wrapping of numerous extensions of the plasma membrane. Some Schwann cell-like oligodendrocytes have been demonstrated in the developing spinal cord where they are found in close association with the myelin sheath of a single axon (Remahl and Hildebrand 1990). Proteolipid protein (PLP) and myelin basic protein (MBP) are the major proteins present in compact CNS myelin accounting for 50% and 30% total myelin protein respectively (Lees and Brostoff 1984). In the PNS, MBP, although present in compact myelin, comprises only 5-15% total myelin protein and PLP is found in considerably smaller amounts and never in compact myelin. Protein zero ($P_0$) is the major myelin protein in the PNS accounting for over 50% total protein (Greenfield *et al.* 1973). (see 1.3.5.PLP in the peripheral nervous system).

## 1.2.3.Myelin composition (CNS)

### Lipids

Lipid accounts for approximately 70% of the dry weight of myelin (Norton and Cammer 1984). There are no lipids specific to myelin, however the high content of galactosphingolipids, cerebroside (galactosylceramide) and sulphatide is a distinguishing feature of myelin lipid. These three comprise about 65% of total lipid and 45-50% total dry weight of myelin (Norton and Cammer 1984). Myelin lipid is also enriched in cholesterol and ethanolamine phosphoglycerides relative to other membranes. Cerebroside is the most "myelin typical" lipid and within the CNS is a specific marker for oligodendrocytes (Raff *et al.* 1978).

### Proteins

The protein composition of myelin is relatively simple with the major proteins being myelin specific.

a) *Myelin proteolipid protein (PLP)*:

(See 1.3.MYELIN PROTEOLIPID PROTEIN)

b) *Myelin basic protein (MBP)*:

MBP represents ~ 30% total myelin protein and consists of a family of proteins produced by differential gene splicing (de Ferra *et al.* 1985). Four major isoforms exist in rodents with apparent molecular weights up to 20kD. MBP is thought to be important in maintaining the fusion of the major dense line in the compact myelin sheath. Different isoforms have also been reported which predominate during embryogenesis and may have a function unrelated to myelinogenesis (Nakajima *et al.* 1993).

c) *Myelin-associated oligodendrocyte basic protein (MOBP)*:

MOBP is the most recently characterised myelin protein (Yamamoto *et al.* 1994) and is the most abundant after PLP and MBP. Two peptides have been described with apparent molecular weights of 12kD and 25kD. MOBP shares several characteristics with MBP (small, hydrophilic, basic and distributed throughout compact myelin), and may perform a similar function.

e) *2',3'-cyclic nucleotide 3'-phosphodiesterase (CNP)*:

CNP represents ~ 5% total myelin protein (Sprinkle *et al.* 1978) and consists of two peptides with apparent molecular weights of 46kD and 48kD. CNP is part of the Wolfgram fraction of proteins (45-65kD/insoluble in chloroform/methanol). CNP may be

involved in oligodendrocyte differentiation (Scherer *et al.* 1994) or maintenance of the myelin membrane (Trapp 1990).

d) *Myelin associated glycoprotein (MAG)*:

MAG is a minor constituent of CNS myelin protein (~1%) (Quarles *et al.* 1973). It has an apparent molecular weight of 100kD of which 30% is carbohydrate. It localises to periaxonal regions and is thought to be involved in contact between the myelin forming cell and the axon.

f) *Minor proteins*:

Several other CNS myelin proteins have been documented such as: Myelin oligodendrocyte glycoprotein (MOG) (Linington *et al.* 1984); Myelin oligodendrocyte-specific protein (MOSP) (Dyer *et al.* 1991); Oligodendrocyte-myelin glycoprotein (OMgp) (Mikol *et al.* 1993) and $P_2$ (Trapp *et al.* 1983). Although the amounts of these proteins are relatively small this may not reflect their functional significance. Inspection of SDS-PAGE gels from myelin preparations suggests that there are further, as yet uncharacterised proteins.

involved in oligodendrocyte differentiation (Scherer *et al.* 1994) or maintenance of the myelin membrane (Trapp 1990).

d) *Myelin associated glycoprotein (MAG)*:

MAG is a minor constituent of CNS myelin protein (~1%) (Quarles *et al.* 1973). It has an apparent molecular weight of 100kD of which 30% is carbohydrate. It localises to periaxonal regions and is thought to be involved in contact between the myelin forming cell and the axon.

f) *Minor proteins*:

Several other CNS myelin proteins have been documented such as: Myelin oligodendrocyte glycoprotein (MOG) (Linington *et al.* 1984); Myelin oligodendrocyte-specific protein (MOSP) (Dyer *et al.* 1991); Oligodendrocyte-myelin glycoprotein (OMgp) (Mikol *et al.* 1993)and $P_2$ (Trapp *et al.* 1983). Although the amounts of these proteins are relatively small this may not reflect their functional significance. Inspection of SDS-PAGE gels from myelin preparations suggests that there are further, as yet uncharacterised proteins.

# 1.3.MYELIN PROTEOLIPID PROTEIN

Proteolipids are a class of lipoproteins characterised by their solubility in organic solvents, particularly chloroform/methanol mixtures (Folch and Lees 1951) and are found as membrane components in many animal, plant and bacterial cells. Myelin proteolipid protein (PLP/*proteolipid apoprotein/Folch-protein lipophilin/P7*) , which has been shown to have no cross reactivity with other proteolipids (Macklin *et al.* 1982), is the major myelin protein of the CNS and accounts for approximately 50% of total myelin protein (Lees and Brostoff 1984).

PLP is an extremely hydrophobic membrane protein consisting of a 276-residue long polypeptide chain with four strongly hydrophobic sequences linked by highly charged hydrophilic sequences (Stoffel *et al.* 1984). The protein can be isolated by separation from lipids using either acid solvents or detergents. The lipid-free protein (apoprotein) can be converted to a water soluble form by gradual replacement of the organic solvent with water (Lees and Sakura 1978). Protein from mature animals can be resolved on sodium dodecyl sulphate (SDS) polyacrylamide gels into two protein bands, the major PLP component and a minor band corresponding to the isoprotein DM-20, so named due to its apparent molecular mass on SDS gels (DM-20 ~ 20kDa/PLP ~ 24kDa). The actual molecular masses of the two isoproteins are higher than these values (DM-20 ~ 26.5kDa (Nave *et al.* 1987b)/PLP ~ 30kDa (Stoffel *et al.* 1983) ). Lower molecular weight myelin proteolipids have been described in the cow (Chan and Lees 1974; Lepage *et al.* 1986; Vacher-Lepretre *et al.* 1976), mouse (Nussbaum and Mandel 1973) and rat (Campagnoni *et al.* 1976). Two related proteolipid proteins of similar apparent molecular mass to PLP (PIIβ (Helynck *et al.* 1983) in bovine adult CNS) and DM-20 (PIIβ' (Schindler *et al.* 1990) in bovine foetal CNS) have also been reported.

## 1.3.1.The *plp* gene

The *plp* gene (Figure 2) is located on the X-chromosome (Mattei *et al.* 1986; Willard and Riordan 1985) (Xq21.33-22 in man) and is approximately 17kb in size. The gene is composed of seven exons, although an eighth exon has been proposed based on the isolation of a cDNA with a novel 3′ region (Kamholz *et al.* 1992). Two major transcription initiation sites have been described in the rat and mouse around nucleotides −130 and −160 (Macklin *et al.* 1987; Milner *et al.* 1985). However, even at these two sites, there is a degree of heterogeneity with respect to the exact point of initiation. The two major sites appear to be used in a selective manner with the more distal site being utilised in the CNS and the proximal in the PNS (Kamholz *et al.* 1992). *Plp* mRNA is also heterogeneous in terms of the length of the 3′ untranslated region (3′UTR) due to utilisation of alternative polyadenylation sites (Figure 2). Three major transcript sizes are seen; 1.5-1.6kb, 2.4-2.6kb and 3.0-3.4kb, with relative amounts varying between species. By northern analysis the rat has a major band of 3.2kb and a minor band of 1.6kb (Milner *et al.* 1985); the

mouse has major bands of 2.4-2.6kb and 3.0-3.4kb with a minor band of 1.6kb (Gardinier *et al.* 1986; Sorg *et al.* 1987), and the human has a major band of 3.2kb and a minor band of 2.2kb with very little 1.6kb transcript (Kronquist *et al.* 1987). The significance of these multiple transcript sizes is unknown although availability of multiple polyadenylation sequences may confer greater evolutionary tolerance to mutational loss of these important post-transcriptional processing sites. All transcripts are translated to give the same 277 amino acid protein, the amino-terminal methionine being removed post-translationally.
A second isoform, DM-20, is generated by the use of an alternate 5′ splice site in exon 3 (Nave *et al.* 1987b). Exon 3B is deleted from the processed transcript giving a protein identical to PLP apart from the deletion of 35 residues (amino acids 116-150). With the exception of anurans (frogs), in which the *plp* gene is duplicated (Nave *et al.* 1993), these proteins are the products of a single gene.

## Expression

### Tissue expression

Although it was initially thought that *plp* gene expression was restricted to the oligodendrocyte in the CNS it has become apparent that expression occurs in several other cell types. Transcripts can be demonstrated in embryonic and adult peripheral nerve and cranial and spinal ganglia (see 1.3.5.PLP in the peripheral nervous system), the olfactory nerve layer of the olfactory bulb (OB) (see 1.4.THE OLFACTORY BULB) and in unidentified cells in the mouse and rat embryonic brain and spinal cord. Partial transcripts have been found in astrocytes (Macklin 1988) and full length transcripts in some astrocytoma cell lines (Kashima *et al.* 1993). *Plp* and *dm-20* transcripts are found in the C6 glioblastoma cell line (Ikenaka *et al.* 1992; Nave and Lemke 1991) (which has some O-2A-like characteristics) and surprisingly in several "neuronal" cell lines derived from phaeochromocytoma, neuroblastoma or melanoma cells (PC-12, NG108-15, N18-TG, Neuro-2A) (Ikenaka *et al.* 1992). Gene expression in immortalised cell lines is generally under less strict regulatory control than expression in "wild-type" cell cultures resulting in a more complex mRNA profile. The possibility of tumour-derived cell lines expressing "uncharacteristic" genes must therefore not be overlooked. *Dm-20* transcripts have also been identified in heart and localised by *in situ* hybridisation (ISH) to the cardiac myocytes (Campagnoni *et al.* 1992). Protein has been demonstrated in the PNS and OB (Griffiths *et al.* 1995a; Wight *et al.* 1993). Based on the generation of transgenic mice it has been suggested that elements involved in directing tissue specific expression may reside within intron 1 of the gene (Wight *et al.* 1993).
ISH using *plp/dm-20* riboprobes and tissue sections from adult animals demonstrates multiple foci of signal corresponding to the cell bodies of individual oligodendrocytes,

concentrated in the white matter and more sporadically in grey matter. Immunostaining shows a similar pattern with localisation to the compact myelin sheath.

**Postnatal developmental expression**

Interpretation of studies on developmental expression of the *plp* gene can be difficult to correlate due to differences in species studied, whether transcript or product were detected, sensitivity of the assay employed and the area of the CNS involved. However general patterns can be seen. The ratio of PLP/DM-20 protein changes during early myelination. Studies on postnatal rat (LeVine *et al.* 1990), mouse (Gardinier and Macklin 1988), foetal cow (Van Dorsselaer *et al.* 1987) and human (Kronquist *et al.* 1987) have shown that DM-20 predominates during early myelination, whereas PLP is either equivalent or the major isoform in the adult. Production of *plp/dm-20* transcripts and protein (Macklin *et al.* 1983; Naismith *et al.* 1985) appear to parallel myelination and increase dramatically with increasing numbers of myelinating oligodendrocytes in the CNS, with peak levels seen around post-natal day 20 (P20) in the mouse (Campagnoni and Hunkeler 1980; Gardinier *et al.* 1986; Sorg *et al.* 1987) and around P25 in the rat (Milner *et al.* 1985; Naismith *et al.* 1985). Levels of transcript in the adult mouse are approximately 25-30% of those at peak myelination (Gardinier *et al.* 1986; Naismith *et al.* 1985) indicating a high turnover of the protein. The ratio of *plp/dm-20* transcripts in the post-natal rat CNS is always >1 and a ratio of at least 2:1 is present in the adult (LeVine *et al.* 1990; Nave *et al.* 1987b). At the cellular level *plp* transcripts have been demonstrated by ISH as early as P1 in the mouse hind brain (Verity and Campagnoni 1988) and at P0 in the rat lumbosacral cord (Baron *et al.* 1993). Protein is detectable by western blots at P1 in the rat (LeVine *et al.* 1990) and P3 in the mouse (Gardinier and Macklin 1988). DM-20 predominates at this time with predominance of PLP occurring several days later.

**Embryonic expression**

*Plp/dm-20* transcripts have been documented in embryonic brain (Ikenaka *et al.* 1992; Timsit *et al.* 1992a; Timsit *et al.* 1995), spinal cord (Timsit *et al.* 1995; Yu *et al.* 1994) and PNS (Timsit *et al.* 1992a; Timsit *et al.* 1995; Wight *et al.* 1993; Yu *et al.* 1994). Expression of the *plp* gene during embryogenesis is of particular interest for two reasons. Firstly, the expression of a major myelin gene at a time when no myelin sheaths are present (sheaths are seen only after E18 in the mouse) is intriguing and would indicate a non-structural role for the gene. Secondly, the *dm-20* isoform appears to be the sole or predominant transcript present at this time (Ikenaka *et al.* 1992; Timsit *et al.* 1992a) which would potentially implicate it in an alternative function. This is comparable to the peripheral nervous system where PLP/DM-20 is not present in the compact myelin sheath (Griffiths *et al.* 1989; Griffiths *et al.* 1995a; Puckett *et al.* 1987) (see 1.3.5.PLP in the peripheral nervous system); DM-20 is the major isoprotein present (Griffiths *et al.* 1995a;

Ikenaka *et al.* 1992; Pham-Dinh *et al.* 1991) and a non-structural role for DM-20 has also been postulated. Both of these situations contrast with the mature myelinated CNS where PLP is the dominant isoform (see 1.3.1.The *plp* gene), probably acting as a structural protein. DM-20 protein has been isolated from foetal bovine cerebral hemispheres prior to the appearance of white matter (Schindler *et al.* 1990) and *plp/dm-20* transcripts have been localised to the area of the diencephalic basal plate in the mouse as early as E9.5 (Timsit *et al.* 1992a; Timsit *et al.* 1995), the positive cells being thought to represent oligodendrocyte precursors (O-2As). Embryonic expression of other major CNS myelin genes (CNP and MBP), and the major PNS myelin gene $P_{0,}$ in non-myelinating cells has been described (Nakajima *et al.* 1993; Scherer *et al.* 1994; Yu *et al.* 1994; Zhang *et al.* 1995).

There is still some controversy regarding the location and lineage of the cells responsible for embryonic *plp/dm-20* expression in the spinal cord. ISH studies have localised transcripts in the rat to a column of cells either side of the mid-line, just above the floor plate at E12 (Yu *et al.* 1994). This signal was subsequently only detectable at E18 when it was located in the ventral white matter and at later ages throughout the whole of the spinal cord white matter. In contrast, in the mouse, positive cells were found in a slightly more dorsal position at E14.5 (Timsit *et al.* 1995) and such cells progressively colonised the spinal cord between E14.5 and P1, first ventrally and then dorsally, predominantly in the white matter tracts.

*Plp* gene expression in the rat was suggested to be of neuronal origin (Yu *et al.* 1994) based indirectly on the differing temporal and spatial position of the *dm-20+* cells at E12 relative to CNP or platelet derived growth factor α receptor (PDGFαR)+ cells. It has been suggested that CNP and PDGFαR may be early markers of oligodendrocyte precursors in the spinal cord (Pringle *et al.* 1992; Pringle and Richardson 1993; Yu *et al.* 1994). Timsit *et al.* (1995), however were unable to demonstrate co-localisation of neuronal markers TuJ1 (neurone specific tubulin), neurofilament or F4/80 (macrophage/microglial marker) with *dm-20+* cells in either the brain or spinal cord. There is the possibility that *dm-20* may be labelling pluripotent stem cells which may give rise to either neurones or oligodendrocytes (De Vitry *et al.* 1980; Price and Thurlow 1988; Williams *et al.* 1991) and that *dm-20* may be expressed transiently by neuronal precursors (Timsit *et al.* 1995; Yu *et al.* 1994).

Alternatively, *plp* gene expression in the mouse was suggested to be present in oligodendrocyte precursors (Timsit *et al.* 1995). Spatial and temporal position of *plp/dm-20+* cells is in agreement with previous studies using other presumptive oligodendrocyte progenitor markers (PDGFαR and CNP) at E14 (Pringle and Richardson 1993; Yu *et al.* 1994), however a more diffuse labelling of grey and white matter is seen with both of these markers at older ages. In addition, the ventral ventricular zone, adjacent to the central canal has been identified as the probable site of origin of the O-2A lineage. Fok-Seang and Miller (1994), using A2B5 as an O-2A marker, and Warf *et al* (1991) showed that at E14

in the rat, only cells cultured from the ventral cord were capable of giving rise to oligodendrocytes. Noll and Miller (1993) used a combination of BrdU (a thymidine analogue) incorporation and O-2A specific markers (see 1.5.THE O-2A LINEAGE) to locate O-2A cells originating in this area. Ono *et al.* (1995) demonstrated a similar situation in the E6 chick spinal cord with O4+ O-2A progenitors arising close to the dorsal aspect of the floor plate in a similar position to that seen with *plp/dm-20*+ cells in the E12 rat. It is possible that the various presumptive markers may be labelling additional cell types or possibly subsets of the oligodendrocyte lineage. An alternative theory for the origin of oligodendrocytes in the spinal cord is that they originate from radial glial cells in the peripheral white matter (Choi *et al.* 1983; Hirano and Goldman 1988). This is based on the demonstration of radially oriented glial cells exhibiting markers of the O-2A lineage and radial glial cells which appeared to have a combination of oligodendrocyte and astrocytic characteristics. As it is highly likely that at least some of the astrocytes of the spinal cord are derived directly from radial glial cells it was suggested that this could be a common site of origin for both astrocytes and oligodendrocytes. The present body of evidence however, suggests that the ventricular zone is the most likely origin of oligodendrocyte precursors in the spinal cord.

Conflicting evidence is available regarding expression of *plp* in O-2A cultures from neonatal rat brain, with either positive (Lubetzki *et al.* 1991) or negative (Yu *et al.* 1994) northern blots using a *plp/dm-20* probe. This may reflect differences in purity of culture or sensitivity of hybridisation.

## Regulation

The *plp* gene is transcribed by RNA polymerase II. It is a complex transcriptional unit generating several message isoforms. As such, a variety of mechanisms may be involved in determining both total transcript levels and also the relative amounts of the *plp* and *dm-20* isoforms. Gene regulation may occur at three general levels; 1) transcriptional control, usually at the level of rate of transcript initiation; 2) post-transcriptional processing involving factors such as polyadenylation, primary transcript splicing and transcript stability and 3) translational or post-translational control (Darnell Jr. 1982). Regulation of the *plp* gene has been demonstrated at transcriptional, post-transcriptional and translational levels and it has become evident that *plp* gene expression is dependent on a highly complex and integrated system involving numerous regulatory factors, associated intermediate genes and feedback mechanisms working at several levels of regulation. Interpretation of published data regarding *plp* gene transcriptional regulation is difficult due to the diverse experimental approaches employed. Studies involving *in vivo* and *in vitro* systems, or using "wild type" oligodendrocytes or glial cell lines have all been documented. Glial cell lines appear to be partially deregulated and, as a result, exhibit a higher degree of message complexity. Evidence from several studies looking at individual factors influencing *plp*

gene expression and potential regulatory regions of the *plp* gene contains inconsistencies, probably due to the reasons outlined above, and it is presently only possible to give a generalised picture of the regulatory factors influencing *plp* gene expression.

As is the case with most pol II genes, transcriptional regulation appears to be the major controlling step in *plp* gene expression. It is this increased rate of synthesis of pre-mRNA which is primarily responsible for the production of the large amounts of PLP/DM-20 protein required during myelination (Cook *et al.* 1992; Gardinier and Macklin 1990). Several factors have been shown to induce transcription of the *plp* gene including corticosteroids (Zhu *et al.* 1994), cAMP (Nave and Lemke 1991; Ye *et al.* 1992), PDGF (Grinspan *et al.* 1993), high cell density and serum deprivation (Nave and Lemke 1991) and presence of neurones (Giulian *et al.* 1991; Kidd *et al.* 1990; Macklin *et al.* 1986; McPhilemy *et al.* 1990; Scherer *et al.* 1992). Corticosteroids have also, conversely, been demonstrated as down-regulators of *plp* gene expression (Tsuneishi *et al.* 1991). Post-transcriptional control has been inferred based on differences between *plp/dm-20* transcript and protein ratios (LeVine *et al.* 1990). Increased stability of mRNA could account for post-transcriptional rises in message levels, however evidence supporting this is conflicting. Increase in stability of mRNA would be reflected in measured half-life; one group has suggested half-life to be around 25 hours and found no extreme changes (Cook *et al.* 1992). However evidence supporting increased stability both *in vivo* (Gardinier and Macklin 1990), and *in vitro* under the influence of retinoic acid (López-Barahona *et al.* 1993; Zhu *et al.* 1992) has also been presented. Protein kinase C (Asotra and Macklin 1993) may also act at this level as may corticosteroids (Kumar *et al.* 1989). Factors controlling the alternative splicing of pre-mRNA are unknown and involve complex protein/RNA interactions during splice site selection. Thyroid hormone has been shown to effect *plp* gene expression at the transcriptional and translational level (Campagnoni and Macklin 1988), and PLP synthesis is increased at the translational level by hydrocortisone (Verdi *et al.* 1989).

Sequence analysis of 1.5kb of the 5′ flanking region of the human, rat, and mouse *plp* genes revealed that the proximal region from −250 to +100 (+1=the most upstream transcription start site) is highly conserved in the three species (~ 95% identity) (Janz and Stoffel 1993). Regions further upstream are only about 50% identical. This indicates that the evolutionary conserved proximal region may contain *cis*-regulatory sequences essential for the functional expression of the *plp* gene. *Cis*-elements act as recognition targets for *trans*-acting factors, the protein products of regulatory genes. Both physical analysis (using footprinting and gel shifts) and functional analysis (using reporter genes) of *cis*-regulatory elements have been performed in cultured cells and transgenic mice. These studies demonstrated that both positive and negative *cis*-regulatory sites involved in regulation of the *plp* gene are located in the 5′ non-coding region (Berndt *et al.* 1992; Cambi and Kamholz 1994; Nave and Lemke 1991) and possibly in intron 1 (Wight *et al.*

1993) (Figure 2.) Although there is interspecies variation, some of these sites are highly conserved and are also present in other myelin specific genes such as MBP, MAG and $P_0$ suggesting common *trans* acting factors giving co-ordinated regulation of myelin gene expression (Berndt *et al.* 1992; Nave and Lemke 1991). It is not clear which *cis*-regulatory area(s) confer glial specific expression, however glial specific expression of a *plp/lac* Z transgenic fusion-gene containing 2.4kb upstream sequence extending to the 5′ end of exon 2 has been demonstrated (Wight *et al.* 1993). This may indicate the presence of *cis*-elements within intron 1.

Several regulatory genes which appear to be involved in regulation of the *plp* gene have been documented and include MyT1, a member of the zinc finger superfamily of transcription factors (Kim and Hudson 1992; Armstrong *et al.* 1995), Sp1 transcription factor and a brain enriched 66kD protein (Janz and Stoffel 1993) and the POU-domain transcription factor, SCIP (Collarini *et al.* 1992). Factors regulating embryonic expression of the *plp* gene are unknown although it has been suggested that early expression of "pattern forming" genes such as the *Pax* family or the *hedgehog* gene may induce expression of the *plp* gene in the ventral ventricular area of the spinal cord (Yu *et al.* 1994).

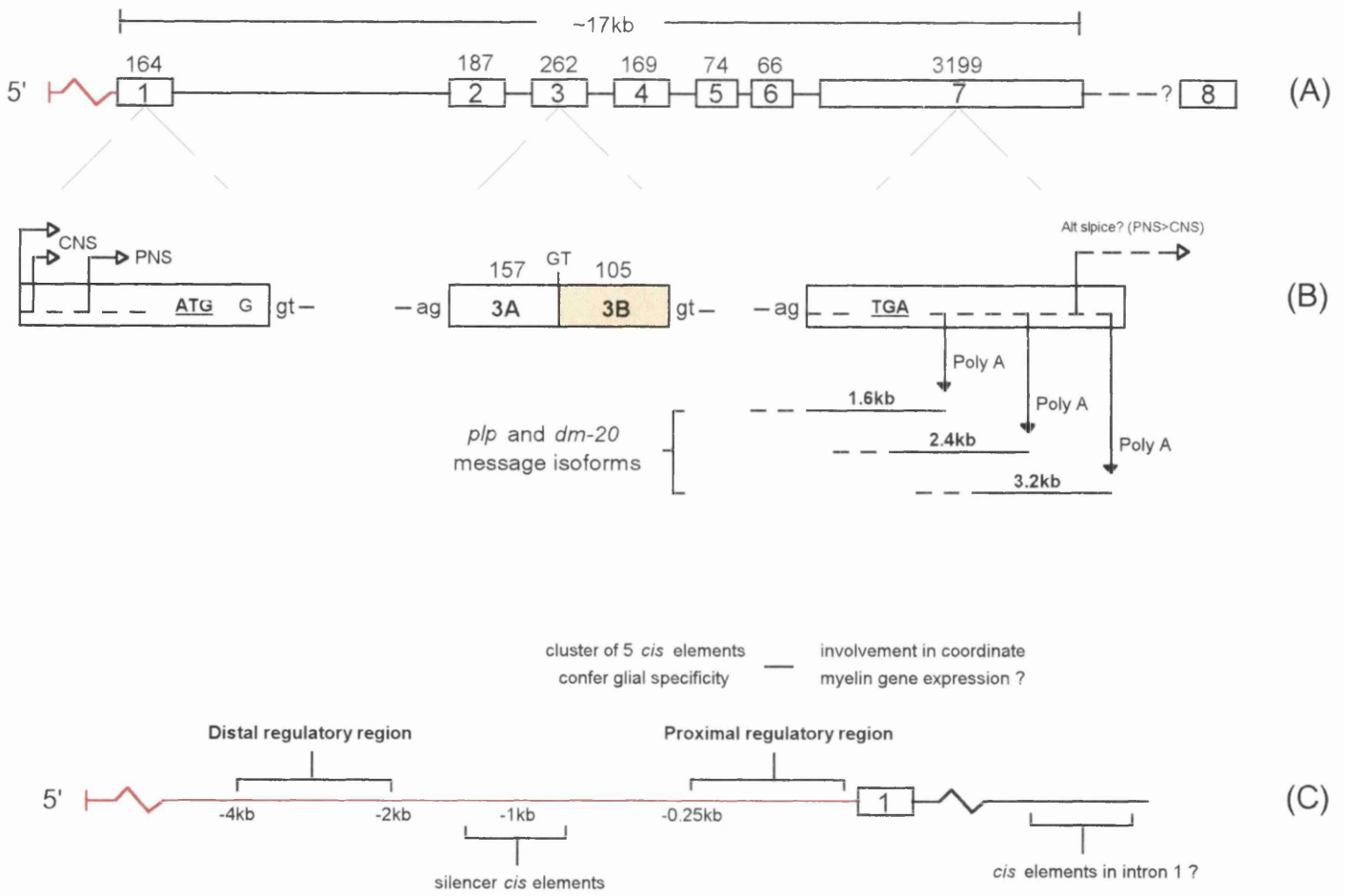


**Figure 1**. Organisation of the mouse *plp* gene. The highly conserved arrangement and sizes of the exons are depicted in (A). A ? is placed by exon 8 as this has only been reported in one study. Sequences controlling message isoform synthesis are shown in (B). Exon 3 contains the alternate splice site giving rise to the *dm-20* isoform in which exon 3B (shaded) is deleted from the final transcript. A putative regulatory map encompassing the 5′ non-coding region (red) and intron 1 is illustrated in (C).

## 1.3.2.Phylogeny

Compact myelin is formed in all vertebrates except *Agnatha* (lamprey, hagfish) (Waehneldt 1990). CNS myelin of bony (*Actinopterygii*) and cartilaginous (*Chondrichthyes*) fish carry several glycosylated components recognised by antibodies against the major mammalian PNS protein $P_0$. In contrast, unglycosylated PLP is the major CNS protein of all tetrapods (*Mammalia, Aves, Reptilia* and *Amphibia*) (Waehneldt *et al.* 1985). It is likely that the integral myelin proteins in the CNS of fish were replaced in amphibia and higher animals by proteolipid protein (Schliess and Stoffel 1991). Studies on cross-immunoreactivity with mammalian PLP antibodies indicated the spontaneous appearance of PLP-like protein approximately 400 million years ago, before the appearance of the tetrapods, in CNS myelin of *Sarcopterygii* fish (Lungfish (glycosylated) and Coelacanth (non-glycosylated)) (Waehneldt *et al.* 1986; Waehneldt and Malotka 1989). DM-20 is not detectable by SDS gel electrophoresis and immunoblotting in amphibia (Schliess and Stoffel 1991; Waehneldt *et al.* 1985) and neither cDNAs nor PCR product could be demonstrated in *Xenopus* brain (Nave *et al.* 1993). It has been suggested from peptide studies that DM-20 arose following a point mutation which generated the alternate DM-20 splice site in post amphibian tetrapods (Karthigasan *et al.* 1991; Schliess and Stoffel 1991); alternatively the DM-20 splice site may have been lost in amphibians and is just not immunodetectable in the lower vertebrates, although present.

The spontaneous appearance of PLP/DM-20 is now under question after the discovery of DM-20-like cDNA sequences in the *Elasmobranch* cartilaginous fishes *Squalus acanthias* (shark) and *Torpedo californica* (electric ray) (Kitagawa *et al.* 1993). DM proteins were similar but not identical between the two species, and three proteins termed DMα, DMβ and DMγ were described with DMα having the greatest similarity to mammalian DM-20 (62.7% identity, 80.5% similarity). DMα and DMγ are expressed in shark myelinated CNS tracts. Two DM-20-like proteins, termed M6a and M6b, have also been isolated from mouse (Yan *et al.* 1993); M6a is mainly neuronal in localisation but is also present on the apical surfaces of choroid plexus, renal tubules and olfactory epithelium and is similar to DMβ. M6b is found in both grey and white matter and has the greatest similarity to DMγ. M6 protein is glycosylated, and the DM-like proteins have the consensus sequence (NXS/T) for N-linked glycosylation. Neither the DM-like or M6 proteins contain the PLP specific insert and in contrast to the splice site mutation theory above, it has been suggested that DM-20 initially arose by a gene duplication of one of the DM-like genes (probably DMα) and that this was coincident with, or preceded the acquisition of, the PLP specific segment (Kitagawa *et al.* 1993).

Within the tetrapods, the PLP gene is conserved to an extraordinarily high degree. The cDNA sequence is known for rat (Milner *et al.* 1985), mouse (Macklin *et al.* 1987), human (Hudson *et al.* 1989b; Kronquist *et al.* 1987), rabbit (Tosic *et al.* 1994), dog (Nadon *et al.* 1990), frog and chicken (Nave *et al.* 1993; Schliess and Stoffel 1991). In addition, the

bovine protein sequence is known (Stoffel *et al.* 1983). Remarkably, the protein sequences are nearly identical (100% between rodents and human, and >98% including cow and dog), a phenomenon unprecedented for any other myelin protein. In non mammalians, such as the chicken and frog, conservation is still high at 95% and 70% respectively, with the majority of deviations present in the hydrophilic, non-transmembrane domains (Nave *et al.* 1993; Schliess and Stoffel 1991). Even at the nucleic acid level conservation is extremely high. In the 831 nucleotides of the protein coding regions only 11 differences between mouse and rat (Milner *et al.* 1985) and 25 between mouse and human (Diehl *et al.* 1986) have been demonstrated, and all of these are conservative. Upstream and downstream untranslated regions also show a high degree of conservation even extending into the 5′ flanking DNA sequences (Janz and Stoffel 1993; Kronquist *et al.* 1987; Nave and Lemke 1991; Macklin *et al.* 1987). Selective pressure on regulatory, coding and non-coding sequences of the *plp* gene is obviously extremely strong and *plp* may be one of the most conserved genes so far described.

## 1.3.3.Protein structure, function and synthesis

### Structure

Several suggestions have been made regarding the exact orientation and integration of the PLP protein in cell membranes (Hudson *et al.* 1989a; Laursen *et al.* 1984; Popot *et al.* 1991; Stoffel *et al.* 1984; Weimbs and Stoffel 1992) (Figure 3, Figure 4). The four highly hydrophobic domains are postulated to lie within the lipid bilayer as α helices with the surrounding hydrophilic areas protruding into either the intra or extra-cellular space. Proposed models have been based on combinations of theoretical, immunological, biochemical and biophysical data and by comparison to known transmembrane proteins, however some evidence has been contradictory and the true molecular arrangement remains unresolved. The major differences relate to the positioning of the N and C-terminals and the hydrophilic, highly charged DM-20-deleted portion (residues 116-150) either at the intracellular or extracellular face.

Most recent studies (Popot *et al.* 1991; Weimbs and Stoffel 1992; Weimbs and Stoffel 1994) suggest that both the N- and C-terminals lie on the cytoplasmic surface. Additionally, residues 103-116 have been localised at the major dense line (Sobel *et al.* 1994), which would predict that the adjacent DM-20 deleted segment is also likely to be on the cytoplasmic surface.

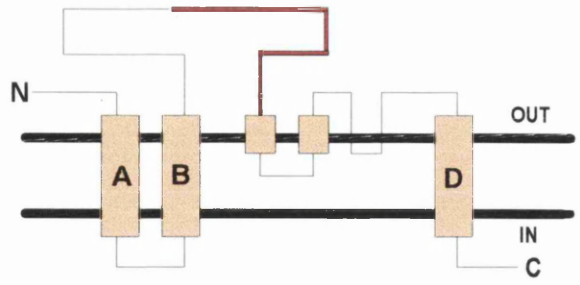


(a)

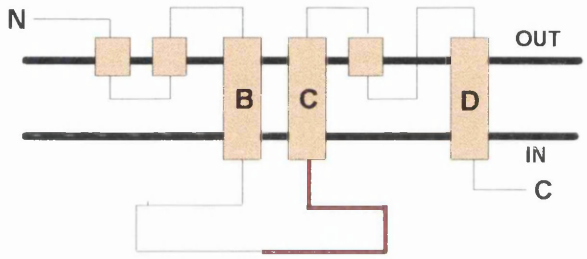


(b)

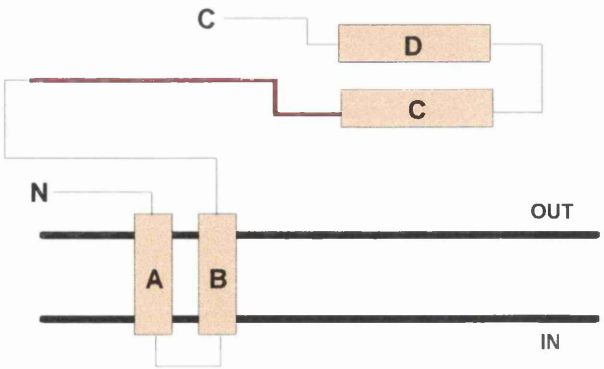


(c)

**Figure 3.** PLP/DM-20 membrane orientation models. **a)** Stoffel *et al.*, **b)** Laursen *et al.*, **c)** Hudson *et al.*

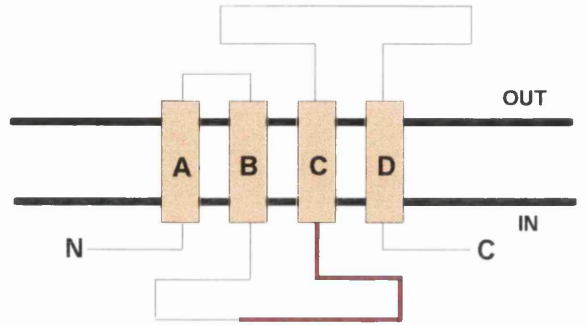


(a)

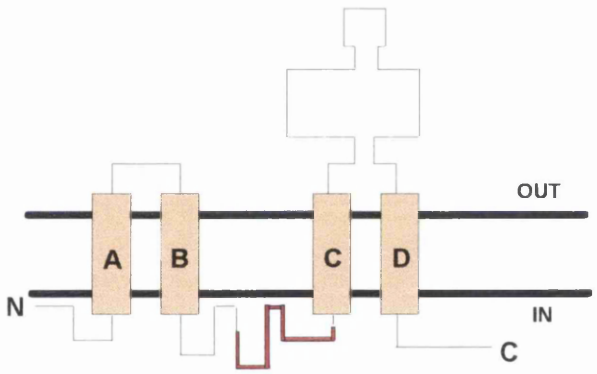


(b)

**Figure 4.** PLP/DM-20 membrane orientation models (cont.). **a)** Popot *et al.*, **b)** Weimbs and Stoffel (**OUT** = extracellular membrane face, **IN** = intracellular membrane face). Hydrophobic domains predicted to form transmembrane α helices are shown as shaded boxes. The residues deleted in DM-20 are shown as a thick red line. The latest models predict four trans-membrane domains with N and C termini, as well as the DM-20 deleted portion of the protein, positioned at the cytoplasmic face.

## Function

The high degree of conservation of the primary structure of PLP is suggestive of multiple critical protein-protein interactions. When looking at PLP/DM-20 in the more primitive tetrapods (Nave *et al.* 1993) or the DM family of proteins (Kitagawa *et al.* 1993; Yan *et al.* 1993) the hydrophobic transmembrane domains are the most highly conserved regions suggesting that the most important protein-protein interactions occur in the plane of the membrane, potentially in the formation of homo-oligomeric complexes (Nave *et al.* 1993). Many lines of evidence point to the two protein isomers of the *plp* gene having different functions. The predominant localisation of PLP in the compact myelin sheath and observed abnormalities of the intraperiod line in a PLP "knockout" mouse and several PLP-deficient mutants (Boison and Stoffel 1994; Boison *et al.* 1995; Duncan *et al.* 1987), suggests a role in maintenance of the regular periodicity of the compact sheath, possibly as an adhesive strut. It has been suggested that PLP may also be involved in generation of the major dense line as well as the intraperiod line (Duncan *et al.* 1987; Kitagawa *et al.* 1993). In contrast with *plp,* the *dm-20* isoform is also expressed at times, and in tissues where no obvious role in myelination could be present. *Dm-20* expression is present prior to *plp* during embryogenesis, well before myelination has begun (see 1.3.1.The *plp* gene). *Plp* gene expression is also present in CNS and PNS glia and cardiac myocytes where again, little correlation with myelination is evident (see 1.3.5.PLP in the peripheral nervous system). The uncoupling of hypomyelination and glial cell death (the two major phenotypic characteristics of *plp* mutants), in the rumpshaker *plp* mutant mouse (Schneider *et al.* 1992) (see 1.3.4.Mutations of the *plp* gene) strongly suggested a role for the DM-20 isomer in glial cell development. The $jp^{rsh}$ is the least severe of the *plp* mutants and is associated with normal levels of DM-20 protein. Interestingly, the equivalent mutation in humans (Kobayashi *et al.* 1994), and another mutation predicted to have normal levels of DM-20 (Saugier-Veber *et al.* 1994), are also associated with a less severe phenotype than other *plp* mutations. All these facts point towards a non-structural role for DM-20. In addition to the high degree of similarity present between different members of the DM family of proteins, similarities are also present to segments of channel forming regions of the nicotinic acetylcholine receptor and the glutamate receptor macromolecular complexes (Kitagawa *et al.* 1993). The idea that DM-20 originated from an ancestral gene encoding an "adhesive pore" forming protein is enticing. Indeed several studies have indicated that PLP may form pores in the membrane and be involved in ion transport (Diaz *et al.* 1990; Helynck *et al.* 1983; Lin and Lees 1982).

## Protein synthesis

*Plp* mRNA is translated on membrane bound ribosomes of the rough endoplasmic reticulum (RER) (Colman *et al.* 1982) and then packaged in the Golgi complex prior to its transport and incorporation into the myelin sheath (Nussbaum and Roussel 1983;

Townsend and Benjamins 1983). Immunostaining of transfected cell lines and cultured oligodendrocytes for PLP/DM-20 shows a punctate pattern corresponding to Golgi, cytoplasmic vesicles and endosomes (Dubois-Dalcq *et al.* 1986; Gow *et al.* 1994a; Sinoway *et al.* 1994; Timsit *et al.* 1992b). The protein is probably carried to the membrane by vesicles which use microtubule-dependent transport processes (Brown *et al.* 1993; Trapp 1990) and is probably co-transported with specific lipids (Pasquini *et al.* 1989). Transport from the RER to the membrane takes ~ 30min. (Colman *et al.* 1982). Some cell transfection studies suggest that both PLP and DM-20 need to be present to enable incorporation into the membrane, and interestingly increased staining for PLP/DM-20 at cell-cell contact boundaries (as seen with other "adhesive" proteins such as $P_0$) has been seen when PLP and DM-20 are present together (Sinoway *et al.* 1994) but not obvious when PLP or DM-20 alone are present (Gow *et al.* 1994a; Timsit *et al.* 1992b). The necessity for both PLP and DM-20 to achieve these cell-cell interactions is disputed by other studies (Montague *et al.* In press). PLP appears to form hexamers under certain conditions (Smith *et al.* 1984) and although direct evidence for PLP/PLP or PLP/DM-20 interactions has been elusive, some cell transfection studies suggest that PLP/DM-20 heteromeric interactions may occur (Sinoway *et al.* 1994).

Two modifications of the PLP/DM-20 protein occur post translationally; first the N-terminal methionine is removed leaving the final 276 residue protein (Milner *et al.* 1985), and secondly, the protein is covalently acylated, predominantly with palmitic, oleic and stearic acids. The acylation occurs non-enzymically (Ross and Braun 1988) and may occur within the myelin sheath. The lack of an amino terminal leader sequence (other than the single methionine which is removed) to target this transmembranous protein to the membrane would indicate that PLP is targeted using an internal signal. Studies using a PLP-LacZ fusion protein suggest that the first 13 amino acids may contain a myelin specific topogenic signal (Wight *et al.* 1993). The position of the acylated residues (thought to occur only on the cytoplasmic side of membranes) has been used to predict orientation of PLP in the membrane (Weimbs and Stoffel 1992) (see 1.3.3.Protein structure, function).

## 1.3.4.Mutations of the *plp* gene

The high evolutionary conservation of PLP is reflected in the severe phenotype of *plp* mutant animals. Mutations have been characterised in several species (Table 1) and several allelic forms are present in man and mice. The majority of detected mutations in all species are point mutations within the coding region causing single amino acid substitutions and most of these are present in the carboxy-terminal half of the protein (Gow *et al.* 1994b). The first and most extensively studied mutation was the jimpy (*jp*) mouse resulting from a point mutation within the 3′ acceptor splice site of intron 4. The resultant deletion of exon 5 and alteration in reading frame generates a message coding for a

truncated protein with an altered carboxy terminus (Nave *et al.* 1987a). The *plp* gene appears intolerant of almost any change, and even conservative amino acid substitutions, such as the $jp^{msd}$ mutation (Gencic and Hudson 1990; Macklin *et al.* 1991), result in gross phenotypic changes. Although there are differences in severity and age of onset between species and allelic forms the general phenotype is similar with hypomyelination, generalised tremors, seizures and early death, prior to adulthood, in hemizygous affected males. The degree of hypomyelination varies being very marked in the myelin deficient rat (*md-rat*) (Duncan *et al.* 1987) and jimpy mouse (*jp*) (Sidman *et al.* 1964) but less severe in the shaking pup (*sh-pup*) (Griffiths *et al.* 1981). Any myelin which is formed is usually disproportionately thin, poorly compacted and fails to immunostain for PLP protein. Abnormalities of the intraperiod line are common (Duncan *et al.* 1987; Duncan *et al.* 1989). A moderate to severe astrocytosis is seen and deficits in astrocyte cell cycle and metabolism have been reported (Knapp and Skoff 1993). In severely affected mutants, *plp* mRNA levels are < 5% of normal and protein is undetectable. There is also a profound effect on the other major myelin gene, MBP, where transcripts and protein levels are both decreased (Bourre *et al.* 1980) although compact myelin still immunostains strongly for MBP. Expression of other myelin protein genes such as MAG and CNP is also affected (Yanagisawa and Quarles 1986).

Interestingly, *plp* mutants such as *jp*, as well as being hypomyelinated, have reduced numbers of mature oligodendrocytes, probably due to their premature death (Knapp *et al.* 1986) prior to the stage at which they would be expected to produce PLP protein (Vermeesch *et al.* 1990). Increased mitotic rates of immature glia and distended RER have also been seen. This is not the case in other hypomyelinating, myelin protein mutants such as *shiverer* mice (MBP mutant) and quaking mouse (not determined) (Privat *et al.* 1979; Samorajski *et al.* 1970). An exception to this trend is seen in the $jp^{rsh}$ *plp* mutant (Schneider *et al.* 1992) where normal or increased numbers of oligodendrocytes are seen. Although hypomyelinated, these mice "recover" and have a normal lifespan. PLP protein levels are severely decreased, but the amount of the DM-20 isoprotein is normal (Mitchell *et al.* 1992). This is intriguing in that it uncouples the two major phenotypic characteristics of *plp* mutants, that is, hypomyelination and glial cell death, and suggests a connection between DM-20 and glial cell survival and development. An interesting parallel is seen in man in some cases of X-linked spastic paraplegia type 2A (SPG2), a much less severe allelic disorder than Pelizaeus-Merzbacher disease (PMD), associated with point mutations in exons 3B and 4. The mutation in exon 3B (Saugier-Veber *et al.* 1994) predictably would result in altered PLP but normal DM-20 protein; the exon 4 mutation (Ile186-Thr) (Kobayashi *et al.* 1994) is identical to the $jp^{rsh}$ mutation and again would presumably result in normal levels of DM-20 as in the mouse.

Female heterozygotes of the *plp* mutants are mosaics having oligodendrocytes expressing either the mutated or wild-type gene, due to X-inactivation. Phenotype varies considerably

between different mutants and even within animals with the same mutation. Small patches of amyelination/hypomyelination may be present, particularly in the optic nerve (Duncan *et al.* 1986; Duncan *et al.* 1993). The myelin defects may show some resolution with time as seen in heterozygotes of the *sh-pup* which may show a slight tremor in early life which disappears with age. (Bartlett and Skoff 1986). Theoretically 50% of oligodendrocytes should be affected, however the extent of dysmyelination is always considerably less than this and in some instances may be minimal. This is presumably due to increased proliferation of normal immature glia to compensate for the loss of mutant cells.

The phenotypic effects of the natural mutations may be the result of one or more factors. The absence or critical reduction of functionally active PLP and/or DM-20 may be the major factor. Amounts of protein present are always subjectively far lower than would be expected, even allowing for the marked reduction in transcripts. This suggests that the oligodendrocytes may have translational or post-translational mechanisms for minimising the accumulation of myelin proteins whenever myelin assembly is blocked. It has been demonstrated *in vivo* (Roussel *et al.* 1987) and *in vitro* (Gow *et al.* 1994b) that mutant PLP/DM-20 protein is arrested in its passage through the ER, and congestion of the secretory pathways with abnormal protein has been put forward as a possible cause of oligodendrocyte death in *plp* mutant animals (Gow *et al.* 1994b). Studies of PLP-transgenic *jp*/Y mice suggest that the *jp* allele may act in a dominant negative manner, such that aberrantly folded protein complexes with normal protein triggering proteolytic degradation (Schneider *et al.* 1995). It is also possible that *jp* PLP is, in a less specific way, toxic to oligodendrocytes, although the presence of a family with PMD due to complete deletion of the *plp* gene (Raskind *et al.* 1991) where no protein either toxic or otherwise could be present would argue against this. Details of glial cell numbers are however, not available in these cases, and the phenotype is much less severe than classical PMD.

An interesting comparison can be made between the *plp* gene and the peripheral myelin protein-22 (*PMP-22*) gene. PMP-22 is also a membrane spanning protein and has two isomers differing in their $5'$ untranslated region. One isoform is found in compact peripheral myelin and appears to be regulated like conventional myelin genes, while the other is present outside the nervous system, is not regulated like a myelin gene and arrests the growth of fibroblasts (Bosse *et al.* 1994). The *PMP-22* gene, on chromosomes 17 and 11 in man and mouse respectively, is the candidate gene for the hypertrophic neuropathies Charcot-Marie-Tooth disease type 1A (CMT-1A) and Dejerine-Sottas hypertrophic neuropathy (DS) in man and the trembler and trembler-J mutant mice. As with the *plp* gene, duplications, deletions and point mutations are all associated with varying clinical phenotypes; point mutations are found in trembler/trembler-J mice (Suter *et al.* 1992a; Suter *et al.* 1992b), CMT-1A (Patel and Lupski 1994) and DS (Roa *et al.* 1993). The majority of cases of CMT-1A are associated with a 1.5Mb duplication containing the *PMP-*

*22* gene (Patel and Lupski 1994) and a 1.4Mb deletion containing the *PMP-22* gene is most frequently responsible for hereditary neuropathy with liability to pressure palsy (tomaculous neuropathy) (Chance *et al.* 1993). Although there is no significant sequence similarity between PLP and PMP-22, interesting similarities are apparent. Both have two isomers, one highly integrated in the myelination process, the other probably involved in growth and development, and both are intolerant of either point mutation or alteration in gene dosage.

## Transgenic mice

The generation of PLP transgenic animals, initially to investigate the possibility of "rescuing" dysmyelinating mutants, has yielded some unexpected insights into the regulation of the *plp* gene. Lines of transgenic mice exhibiting increased *plp* and *dm-20* transcript levels due to the presence of transgenes have been found to develop a phenotype similar to the *jp* mutant (Kagawa *et al.* 1994; Readhead *et al.* 1994) In one line, hemizygous mice are clinically normal but have subtle hypomyelination, whilst homozygotes exhibit the classical tremoring phenotype and die at about 60 days. Oligodendrocyte numbers are normal and thin PLP+ sheaths are present. Cases of PMD due to duplication of the gene are also recognised (Cremers *et al.* 1987; Ellis and Malcolm 1994). Another transgenic model has been used to increase levels of *dm-20* under the regulation of the *plp* promoter (Johnson *et al.* 1995; Mastronardi *et al.* 1993) creating a demyelinating phenotype, possibly due to excess DM-20 preventing stabilisation of the myelin sheath. Attempts to "rescue" jimpy mutant mice using *plp* and/or *dm-20* transgenes have achieved partial success (Nadon *et al.* 1994; Schneider *et al.* 1995). However, normal levels of gene expression are not seen and the phenotype remains essentially unchanged, suggesting that the jimpy mutation exerts a dominant-negative effect. These "rescue" studies also suggest that presence of both PLP and DM-20 may be required for normal myelination.

*Plp* gene function is normally tightly regulated so that deregulation of expression, whether quantitative or qualitative results in major phenotypic effects. Decreased levels of functional PLP/DM-20 due to missense mutations, frameshifts and deletions or, alternatively, increased levels due to duplication or transgenic copies, result in dysmyelination in most instances and demyelination in the case of elevated levels of DM-20.

## Knockout mice

Whilst attempting to generate mice expressing only the *dm-20* isoform by the use of homologous recombination, two strains of mice totally deficient of both isoforms were produced (Boison and Stoffel 1994; Boison *et al.* 1995). Absence of transcripts was due to

the unexpected retention of a neo cassette, introduced for selection purposes in reverse orientation, within intron 3, in the mature message. Surprisingly, these mice did not develop the lethal phenotype associated with *plp* mutations and did not even show gross behavioural abnormalities. EM analysis identified abnormal, loosely wrapped myelin sheaths with a complete lack of an intraperiod line and lack of myelination of small diameter axons. Nerve conduction velocities were decreased and specialised tests identified neuromotor deficits. Another line of knockout mice have been produced (K.Nave unpublished) which also appear to have no gross phenotypic abnormalities and even fewer abnormalities on EM examination although intraperiod lines appear abnormal. These mice further confirm the function of PLP/DM-20 in maintaining the structural integrity of the myelin sheath, in particular the intraperiod line. Surprisingly, the total lack of these proteins, especially DM-20 does not seem to be necessary for survival of oligodendrocytes and it is possible that any such functions may be compensated by other proteins. These findings seem to add weight to the argument that loss of oligodendrocytes in the mutant animals may be due to abnormal conformations or toxic effects of mutant proteins, or deleterious effects on the integrated regulatory machinery of myelination. It does however seem somewhat surprising that the function of a gene as highly conserved as the *plp* gene can be removed with so little gross phenotypic effect. It is also interesting that the case of deletion of the *plp* gene in a human patient did not result in a normal phenotype, but the severe neurological syndrome of Pelizaeus-Merzbacher disease. The final conclusion must be that the situation is still highly confusing and far from being resolved.

| Species | Allele | Mutation |
|---|---|---|
| **Mouse** | *jp* | Missense (splice site), frameshift causing truncated C-terminal |
| | $jp^{msd}$ | Missense, exon 6 |
| | $jp^{rsh}$ | Missense, exon 4 |
| **Rat** | *md-rat* | Missense, exon 2 |
| **Dog** | *sh-pup* | Missense, exon 3A |
| **Rabbit** | *pt* | Missense, exon 2 |
| **Pig** | hypomyelinogenesis cong. ? | Not determined |
| **Human** | Pelizaeus-Merzbacher | Missense, exons 2,3,4,5 |
| | | Deletions; partial (ex. 3+4), total |
| | | Frameshifts, exons 4,7 |
| | | Duplication |
| | | Other (*) |
| | Spastic paraplegia (SPG2) | Missense, exon 3B |
| | | Missense, exon 4 (*rsh*) |

**Table 1.** Summary of mutations affecting the *plp* gene. (*) Cases of PMD have been described with no mutations or alterations of the structural gene. These may represent mutations within regulatory regions.

## 1.3.5.PLP in the peripheral nervous system

The specificity of PLP to the CNS was first questioned with the demonstration of transcripts and protein in Schwann cells in the PNS (Griffiths *et al.* 1989; Puckett *et al.* 1987), although most studies have found that protein is not present in the compact myelin sheath (Ono *et al.* 1990; Puckett *et al.* 1987). Early embryonic expression of the *plp* gene, thought to be predominantly *dm-20* has been demonstrated by several groups. *Plp/lacZ* transgene product has been demonstrated in spinal nerves, dorsal root ganglia and olfactory bulbs at E15 in the mouse at a greater intensity than in the CNS (Wight *et al.* 1993). DM-20 protein has been demonstrated as early as E13 in spinal ganglia and nerves (P Dickinson unpublished) and ISH studies have shown expression in cranial, spinal and autonomic ganglia and nerves and olfactory blastema as early as E10 (E12.5 for the olfactory blastema) (Timsit *et al.* 1992a; Timsit *et al.* 1995; Yu *et al.* 1994) (P Dickinson unpublished). DM-20 has been defined as the major transcript and protein in post-natal sciatic nerve and cranial sympathetic trunk (Agrawal and Agrawal 1991; Griffiths *et al.* 1995a; Pham-Dinh *et al.* 1991) and its predominance in the embryonic PNS has been inferred by the use of differential immunostaining and ISH (Griffiths *et al.* 1995a).

The *plp* gene is expressed in both myelin-forming and non-myelin-forming Schwann cells with the predominance of DM-20 being even greater in the latter (Griffiths *et al.* 1995a). Both isoproteins have a cytoplasmic distribution, however PLP seems to be predominantly located in the perinuclear region of myelinated internodes whereas DM-20 is found in non-myelin-forming Schwann cells, satellite cells, the olfactory nerve layer and paranodes (paranodal cytoplasm and lateral loops), Schmidt-Lantermann incisures and to a lesser degree the perinuclear area of internodes (Griffiths *et al.* 1995a).

The reason(s) for the differences between CNS and PNS localisation is unknown and could be due to several factors influencing *plp* gene expression in oligodendrocytes and Schwann cells. Use of the alternative initiation site (Kamholz *et al.* 1992), differences in the PLP/DM-20 ratio, differences in lipid composition or disputed differences with respect to lack of post-translational acylation of the protein (Agrawal and Agrawal 1991; Tetzloff and Bizzozero 1993) may affect the ability of the protein to be inserted into the compact myelin sheath. Interestingly, PLP/DM-20 protein appears to be present in the compact PNS myelin of transgenic mice carrying extra copies of the wild type *plp* gene (Griffiths *et al.* 1995b; Readhead *et al.* 1994) (Anderson and Griffiths unpublished). No information is available on the relative amounts of PLP and DM-20 in these animals which might explain this finding. PLP/DM-20 immunostaining has also been described in myelin-like figures in the PNS of $P_0$ knockout mice (Giese *et al.* 1992).

The pattern of PLP/DM-20 localisation in the PNS is very unusual for a myelin protein. Major myelin proteins such as $P_0$ and MBP are present in the myelin sheath and those such as MAG which are located in uncompacted regions of myelin-forming Schwann cells are not found in non-myelin forming Schwann cells or satellite cells (Trapp and Quarles 1982;

Trapp and Quarles 1984), unlike PLP/DM-20. In myelinating Schwann cells, expression of the *plp* gene appears to be uncoupled from myelination (Gupta *et al.* 1991; Stahl *et al.* 1990), although modest increases in transcript levels have been reported during myelination (Kamholz *et al.* 1992). Presence of DM-20 in non-myelin-forming Schwann cells, satellite cells and the unmyelinated olfactory nerve layer is also presumably unrelated to myelin formation. As with the developing oligodendrocyte (see 1.5.THE O-2A LINEAGE) in the CNS, the myelin-forming Schwann cell develops from a precursor cell and begins expressing various markers in a regulated progression beginning with NGF-receptor and then S100 at about E15 and later O4, GalC and finally myelin proteins such as MBP, MAG and $P_0$ postnatally (Jessen and Mirsky 1991). Mature non-myelin-forming Schwann cells express a different set of protein markers such as GFAP and NGF-receptor and N-CAM. S-100 and O4 are common to both types of mature Schwann cell (Jessen and Mirsky 1991). Developing Schwann cell precursors are highly mitotic (Stewart *et al.* 1993), as are the O-2A oligodendrocyte progenitors, and expression of myelin protein genes is usually associated with the post mitotic mature glial cell. It is therefore interesting that the *plp* gene is very active before E15 in these dividing Schwann cell precursors. Following axotomy, myelin genes such as $P_0$ are profoundly down-regulated, however levels of *plp* gene transcripts remain relatively unchanged (Gupta *et al.* 1991). All these features suggest that the function and regulation of the *plp* gene in the PNS are different from the CNS and from other typical myelin proteins in the PNS. However, an interesting parallel can be drawn with early embryonic expression of *dm-20* in the brain and spinal cord, (see 1.3.1.The *plp* gene) and the early expression in the PNS.). As DM-20 is the major PNS isoform it is probable that these anomalies may reflect functions of DM-20 different from those of PLP.

## 1.4.THE OLFACTORY BULB

The olfactory bulb is a highly specialised region of the CNS acting as a relay centre for olfactory nerve axons and has a defined laminar structure (Figure 5). The outer olfactory nerve layer (ONL) is composed of the olfactory nerves and their supporting glia (Doucette 1984; Doucette 1989). Deep to the ONL lies the glomerular layer. The glomeruli represent anatomical and functional entities in which the central endings of the olfactory axons synapse with the dendrites of periglomerular, tufted and mitral cells (Pinching and Powell 1971a; Pinching and Powell 1971b; Valverde and Lopez-Mascaraque 1991). Whilst the periglomerular cells provide lateral communication between the glomeruli, the myelinated axons of the mitral and tufted cells form the olfactory tract and convey olfactory information to several regions of the brain. Tufted cells are found in the external plexiform layer and mitral cells in the deeper inner plexiform and mitral cell layers (Pinching and Powell 1971a). Another neuronal cell type, the anaxonic granule cell, is also found in these deeper layers, predominantly in the granule cell layer and is thought to be involved in lateral communication and summation of impulses. The olfactory system is an exceptional area of the CNS for several reasons. Neurones of the olfactory epithelium are produced throughout the entire life of the animal (Graziadei and Monti Graziadei 1979) and their axons are able to grow from the PNS to reach their target cells in the olfactory bulb (OB) of the CNS. The ability of the OB to support neuronal outgrowth is thought to be attributable, in part, to the glial cells that reside mainly in the ONL, which may provide signalling and guidance to the olfactory sensory neurones (Doucette 1984). Two types of glial cell have been described in the ONL, the astrocyte and a highly specialised glial cell which ensheathes the olfactory nerves, the olfactory nerve ensheathing cell (ONEC) (Doucette 1984; Doucette 1989). ONECs are also found in the outermost part of the adjacent glomerular layer, where they are situated at the interstices separating the glomeruli but never entering into them (Pinching and Powell 1971b; Valverde and Lopez-Mascaraque 1991). The ONECs appear to share properties of both Schwann cells and astrocytes (Barnett *et al.* 1993; Doucette 1984; Doucette 1990) (S. Barnett personal communication). Recent studies using clonal cell lines transformed with SV40 large T antigen and cell-sorted ONECs suggest that there may be two sub-divisions of the ONEC cells into astrocyte-like and Schwann cell-like cells which have a common origin (S. Barnett personal communication).

ONECs originate from the olfactory placode (future nasal epithelium), along with the olfactory neurones, and are not of neural tube or neural crest origin (Barnett *et al.* 1993; Valverde *et al.* 1992). The olfactory bulb primordium forms from an evagination of the telencephalon and the "migratory mass" of ONECs and axons forms a cap over the developing OB which will become the ONL (Doucette 1989; Doucette 1990; Valverde *et al.* 1992). The ONECs have an exclusive role of forming the glia limitans at the PNS-CNS transitional zone of the olfactory nerve (Doucette 1991). Myelinated fibres are never seen

in the olfactory nerve (De Lorenzo 1957; Gasser 1956), although a small number of myelinated fibres may travel with the nerve and it has been suggested that ONECs may ensheathe some of these myelinated fibres (Doucette 1990). It has also been demonstrated that ONECs can myelinate peripheral axons in culture (Devon and Doucette 1992). Oligodendrocytes are present in the deeper layers of the olfactory bulb (Valverde and Lopez-Mascaraque 1991) and are responsible for myelination of dendritic segments and cell bodies of mitral and tufted cells, and also the mitral and tufted cell axons which run in the granule cell layer eventually forming the olfactory tract.

*In vivo* the ONL can be divided into areas using several antigenic markers (S. Barnett personal communication), however the whole of the ONL will immunostain for O4, vimentin and neural cell adhesion molecule (N-CAM) and all but the outermost layer stains with S-100. The ONL is negative for GalC staining. Expression of markers in cell sorted cultures (Barnett *et al.* 1993) shows variation with both media and time and does not seem to parallel *in vivo* development exactly (for example, O4 staining is lost in culture), however cells retain markers such as S-100, N-CAM and vimentin and remain GalC- (S. Barnett personal communication).

Expression of the *plp* gene in the OB has not been studied in detail. *Plp* expression was detected initially in the post-natal mouse at P9 by ISH (Shiota *et al.* 1989) although the location is not given and may correspond to expression in oligodendrocytes rather than ONECs, and at P1 by northern analysis (Kanfer *et al.* 1989). A recent study (Griffiths *et al.* 1995a) demonstrated the presence of both protein and transcripts localised to the ONL at P5 and suggested that this was predominantly the *dm-20* isoform. During embryogenesis PLP/LacZ fusion protein is present at E14.5 in transgenic mice (Wight *et al.* 1993) and transcripts, presumed to be *dm-20*, are present in the olfactory blastema as early as E12.5 (Timsit *et al.* 1995). Expression of the *plp* gene, predominantly in the form of the *dm-20* isoform, in the non-myelinated ONL both during embryogenesis and during post-natal life may represent another example of the alternative, non-myelin-related function(s) of this protein.

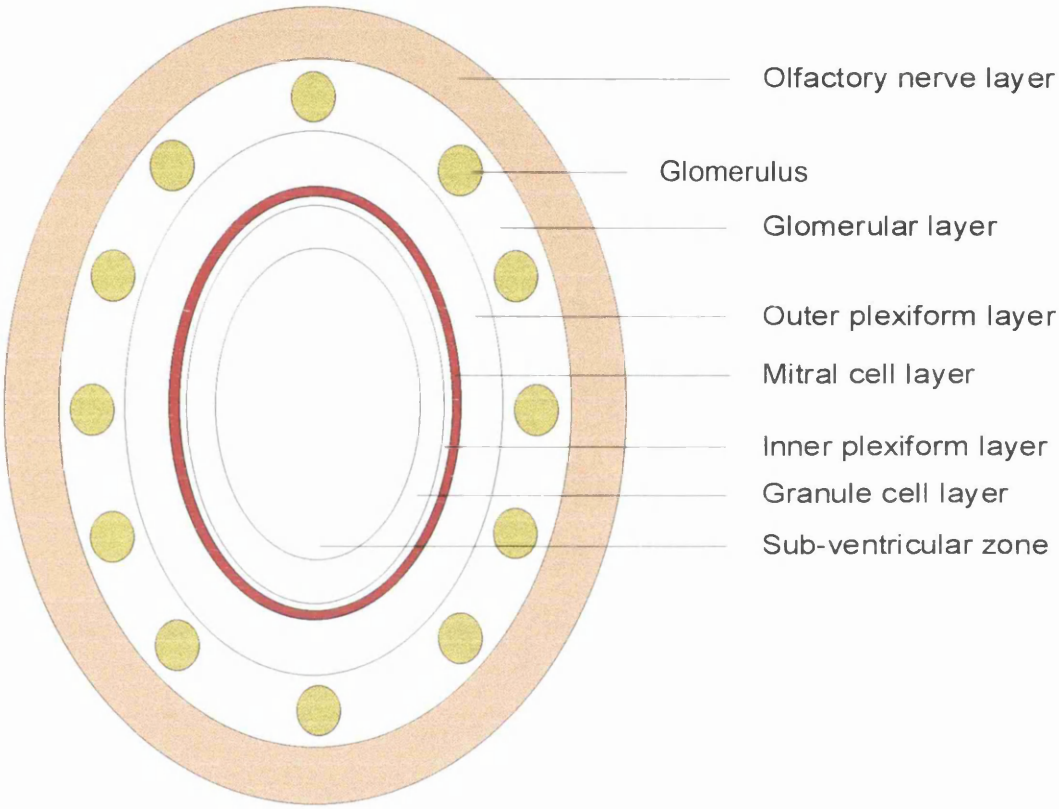


**Figure 5.** Diagramatic representation of the olfactory bulb (coronal section). Non-myelinated olfactory nerve fibres enter the olfactory nerve layer and synapse with mitral and tufted cell dendrites in the glomeruli. Myelinated mitral and tufted cell axons travel in the granule cell layer and project centrally in the olfactory tract. The direction of these axons is perpendicular to the plane of section.

# 1.5.THE O-2A LINEAGE

Oligodendrocyte precursors are thought to originate as neuroectodermal cells of the subventricular zones which migrate and mature into post-mitotic myelin-producing oligodendrocytes. Much of the oligodendrocyte developmental lineage has been elucidated from studies of oligodendrocytes in culture and based on this work three major macroglial cell types were identified in culture; the type-1 astrocyte, the type-2 astrocyte and the oligodendrocyte (Miller *et al.* 1985; Raff *et al.* 1983; Raff 1989). These cells develop from two different precursors, the type-1 astrocyte from an undetermined precursor and the oligodendrocyte and type-2 astrocyte from a highly motile (Small *et al.* 1987) progenitor called the O-2A progenitor (Raff *et al.* 1983). The O-2A progenitor migrates, divides and differentiates into an oligodendrocyte or type-2 astrocyte depending on environmental signals (Raff *et al.* 1983; Raff 1989). In the absence of foetal calf serum (FCS) O-2A progenitors give rise to oligodendrocytes and in the presence of 10% FCS to type-2 astrocytes. Type-1 astrocytes secrete platelet derived growth factor (PDGF) which stimulates the proliferation of O-2A progenitors and prevents them differentiating prematurely into oligodendrocytes (Noble *et al.* 1988; Richardson *et al.* 1988). Type 1 astrocytes can be distinguished from type 2 astrocytes by the fact that they do not stain with A2B5 but do stain with rat neural antigen 2 (Ran-2). Type 2 astrocytes are A2B5+/Ran-2- (Raff *et al.* 1984a). There is some controversy regarding the ability of O-2A progenitors to generate type-2 astrocytes *in vivo*, and the current consensus would regard the O-2A progenitor as essentially producing oligodendrocytes under normal conditions (Franklin and Blakemore 1995).

The developmental profile of the O-2A progenitor can be characterised by the sequential appearance of developmental markers, identified by a panel of cell specific antibodies (Figure 6). The earliest precursor cell recognised (termed the preprogenitor) immunostains for the intermediate filament protein vimentin (vim) (Gonye *et al.* 1994; Hardy and Reynolds 1991) before developing into a bipolar O-2A progenitor staining for one or more of the gangliosides recognised by the antibody A2B5 (Einsenbarth *et al.* 1979; Raff *et al.* 1983) or the single ganglioside $G_{D3}$ (LB1) (Levi *et al.* 1987). (A2B5 will also stain neurones and astrocytes (Einsenbarth *et al.* 1979; Schnitzer and Schachner 1982) and $G_{D3}$ will also stain microglia and reactive astrocytes (Wolswijk 1994). These vim+/A2B5+/$G_{D3}$+ cells represent the O-2A progenitor and are bipotential, (in culture) developing into either glial fibrillary acidic protein (GFAP) + type 2 astrocytes or oligodendrocytes (vim, $G_{D3}$ and A2B5 staining are lost as the O-2A matures). The cell then progresses to the multipolar, post migratory proliferative proligodendroblast which may still be bipotential. These cells additionally stain with O4/A007 Ab (Sommer and Schachner 1981) which recognise proligodendroblast antigen (POA) (Bansal *et al.* 1992) (O4/A007 also stains Schwann cells (Mirsky *et al.* 1990) ). The cell now starts to express

galactolipids and stains with O4/A007 now recognising sulphatide and seminolipid followed by Ranscht monoclonal antibody (R-mAb) (Ranscht *et al.* 1982) which recognises sulphatide, seminolipid and galactocerebroside (GalC) (Pfeiffer *et al.* 1990) and then the O1 Ab (Sommer and Schachner 1981) which recognises GalC specifically and is taken as the indication of a cell committed to the oligodendrocyte lineage (Raff *et al.* 1978). Schwann cells also stain for GalC on their surface but this is lost in culture (Ranscht *et al.* 1982). This immature oligodendrocyte also stains for CNP at this time and goes on to become a mature oligodendrocyte with the regulated appearance of terminal markers (such as MBP, MAG, DM-20, O10, PLP and O11) and the synthesis of myelin membrane (Dubois-Dalcq *et al.* 1986; Fanarraga *et al.* 1993; Kuhlmann-Krieg *et al.* 1988). Appearance of DM-20 occurs before PLP with both isoforms having been previously reported late in oligodendrocyte development, after the appearance of O1, CNP and MBP (Fanarraga *et al.* 1993). Cultured O-2A progenitors are capable of reversing the differentiation process, even 2 days after becoming GFAP+ type 2 astrocytes to become GalC+/GFAP- oligodendrocytes (Raff *et al.* 1984b).

There is evidence to suggest that the O-2A progenitor may also give rise to a unipolar O-2A$^{ADULT}$ progenitor (O4+/GalC-) which may have stem cell-like properties in the adult CNS (Noble *et al.* 1989).

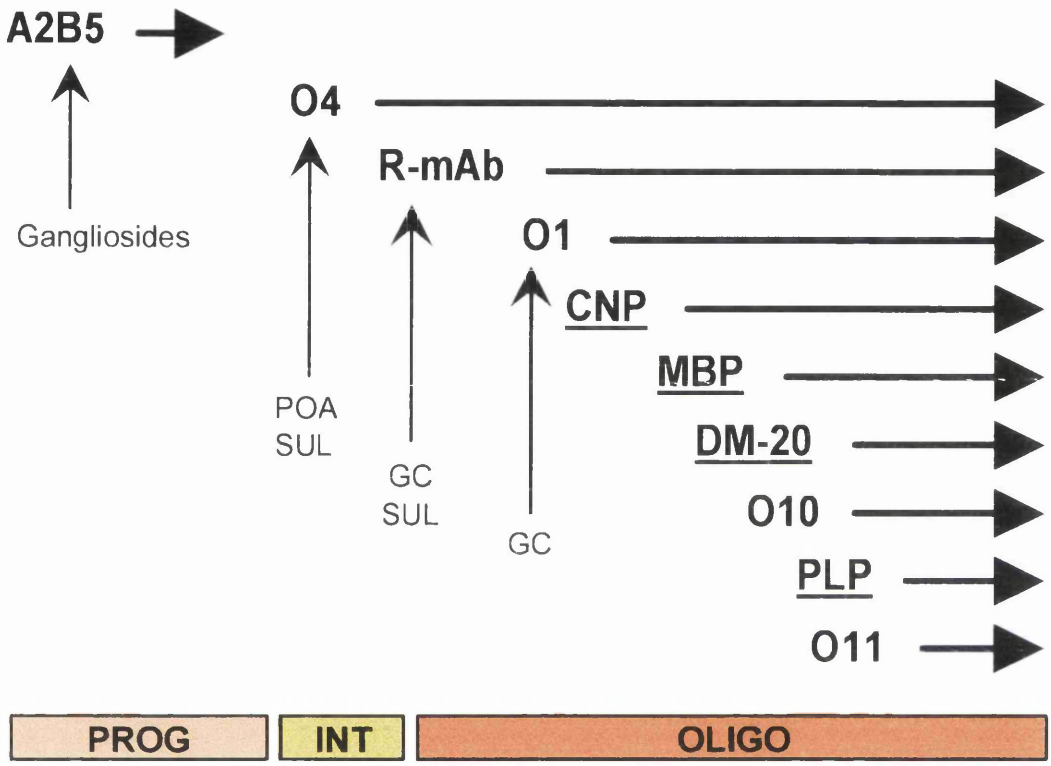


**Figure 6.** Representation of the sequence of oligodendrocyte differentiation in the mouse. Progenitors (PROG) develop through an intermediate stage (INT) to the committed oligodendrocyte (OLIGO). Stages of differentiation are defined by specific antibodies against surface molecules or cytoplasmic antigens (underlined). Horizontal arrows represent duration of expression and vertical arrows represent antigens recognised by the antibodies. CNP, 2',3'-cyclic nucleotide 3'-phosphodiesterase; GC, galactocerebroside; MBP, myelin basic protein; PLP, proteolipid protein; POA, proligodendroblast antigen; SUL, sulphatide.

# 1.6.MYELINOGENESIS

Myelination within the CNS is a highly heterogeneous process. Not only do different regions myelinate at different times and rates, but different tracts within these areas also show considerable variation. Early studies showed that myelination occurs in an orderly sequence (Flechsig 1894; Langworthy 1929; Tilney and Casamajor 1924; Windle *et al.* 1934) and numerous microscopic, biological, biochemical and molecular biological techniques have been used subsequently to expand this work.

According to Flechsig (1894) the first myelinated fibres are found in the spinal cord. Myelination then spreads into the medulla, pons, midbrain and finally into the telencephalon (within the cortex, projection areas myelinate before association areas). Light and EM microscopy in several species such as man (Langworthy 1933), possum (Langworthy 1928), rat (Banik and Smith 1977; Tilney 1933) and mouse (Uzman and Rumley 1958) and more recent ISH studies using myelin specific probes against *plp* and *mbp* in the mouse (Shiota *et al.* 1989; Verity and Campagnoni 1988) have corroborated this general caudal to rostral sequence of brain myelination.

The pattern of myelination in the optic nerve is particularly interesting; In the rat, O-2A progenitor cells first appear in the optic nerve at ~ E16 and migrate along the nerve from the chiasmal end towards the retina with an equal dispersion of cells by P5-P9 (Small *et al.* 1987). However myelination even within the optic nerve is itself heterogeneous beginning at several different sites along the nerve by P6 and progressing in a general rostral to caudal direction from retina to the chiasm (Black *et al.* 1982; Colello *et al.* 1995; Hildebrand and Waxman 1984; Skoff *et al.* 1980; Tennekoon *et al.* 1977). The situation is further complicated if different species, such as the rabbit, are also studied where myelination appears to be much more homogenous in nature (Skoff *et al.* 1980).

Myelination is first seen in the cervical region of the spinal cord and has been shown to progress in a rostral to caudal direction in man (Langworthy 1933; Lucas Keene and Hewer 1931), possum (Langworthy 1928), dog (Fox *et al.* 1967), cat (Langworthy 1929), rat (Tilney 1933) by microscopic examination and by ISH in the rat (Schwab and Schnell 1989). Within the spinal cord there is a set pattern of myelination of tracts at any one level, with the ventral columns being myelinated first followed by the cuneate, ventrolateral, gracile, and later by the rubrospinal and corticospinal tracts (Baron *et al.* 1993; Fox *et al.* 1967; Langworthy 1928; Langworthy 1929; Lucas Keene and Hewer 1931; Matthews and Duncan 1971; Tilney 1933). Hildebrand and Skoglund (1971) although agreeing with a general rostral to caudal gradient states that hindlimb dorsal column afferent fibres (gracile tract) myelinate earlier in the lumbar region than the cervical; that is, fibres myelinate from their cell body distally, a theory supported by Langworthy (Langworthy 1933). However, an immunocytochemical study looking at the presence of oligodendrocyte markers MBP and O1 demonstrated a rostral to caudal gradient in both descending and ascending tracts (Schwab and Schnell 1989).

Other general trends include the myelination of motor areas and motor nerve roots before sensory (Langworthy 1928; Langworthy 1929; Yakovlev and Lecours 1967) and PNS before CNS. Interesting parallels can be made between myelination, phylogeny and ontogeny. Generally speaking, the phylogenetically older tracts and areas such as the vestibulospinal, tectospinal, reticulospinal tracts (ventral columns) and brainstem myelinate earlier than the phylogenetically more advanced areas such as the cortex and fine motor tracts such as the corticospinal (pyramidal) and rubrospinal tracts. Ontogenetically, the fore limbs develop ahead of the hind limbs which is paralleled by the earlier myelination of the cervical cord relative to the lumbar and the cuneate tract (forelimb sensory) prior to the gracile (hindlimb sensory).

Onset and duration of myelination varies enormously between species; myelin sheaths can be demonstrated in rat ventral columns by electron microscopy just before birth at E19 and only at P12 in the corpus callosum (Bjartmar *et al.* 1994) and most myelination is completed by 2 months. In the cat the same tracts begin myelinating 4 weeks before and 3 weeks after birth respectively and are still doing so by 7 months (Remahl and Hildebrand 1982). In humans myelin is initially present in the cord by the fourth or fifth month of foetal life and myelination continues until puberty (Langworthy 1933) and probably very much later than this in the neocortex.

Even within the framework of general observations stated above the process of myelination is remarkably complex. Myelin does not make its appearance in all parts of the CNS at the same time, nor simultaneously in all parts of an individual fibre and there appears to be pulses or waves of rapid myelination (Langworthy 1933) preceded by periods of oligodendrocyte proliferation (Bensted *et al.* 1957; Matthews and Duncan 1971; Samorajski and Friede 1968; Schonbach *et al.* 1968; Skoff *et al.* 1976a; Skoff *et al.* 1976b). Even after myelination has commenced, rates of progression vary and one system may be surpassed by another in which the process commenced much later (Langworthy 1933).

Following the work of Flechsig (1894) several authors have attempted to correlate myelination with the acquisition of specific reflexes indicating functionality of the tracts involved (Langworthy 1928; Langworthy 1929; Langworthy 1933; Tilney and Casamajor 1924; Tilney 1933; Windle *et al.* 1934). In 1916 Kappers hypothesised that "...myelinisation of a nerve fibre occurs at a time when impulses first begin to travel along the fibre." (Kappers 1916). Almost 80 years later following studies on transected optic nerves, Barres and Raff (1993) suggested that "...axonal electrical activity normally controls the production and/or the release of the growth factors that are responsible for proliferation of oligodendrocyte precursor cells...", the cells responsible for myelination.

## 1.7.AIM OF THESIS

Proteolipid protein is the major protein constituent of CNS myelin and abnormalities of *plp* gene expression are associated with severe dysmyelinating phenotypes in man and several animal species. The *plp* gene encodes two isoproteins, PLP and DM-20, the latter having a deletion of 35 amino acids. PLP is postulated to play a structural role in maintaining the double intraperiod line of the myelin sheath, whilst DM-20 may have a non-structural role which is not directly associated with the myelination. Many workers have studied expression of the *plp* gene in terms of transcriptional output or protein levels, often looking at relatively large, heterogeneous areas of myelinating CNS tissue. Less information is available regarding the relative expression of the two isoforms and how this is related to the local myelinating environment. It was therefore the aim of this thesis to address this area of study looking at more defined, homogeneous areas of the CNS during myelination with particular reference to the developmental patterns of expression of the *plp* and *dm-20* isoforms. The ventral columns of the spinal cord and mid-optic nerve were chosen as well defined, easily accessible areas of the CNS known to have different ages of onset of myelination (~ P1 and P7 respectively). Given the possible non-myelinating role of DM-20 it was also decided to study *plp* gene expression in tissues where *plp/dm-20* message had been demonstrated but no obvious connection with myelination was present; such areas included the embryonic spinal cord and the PNS.

Experimental design required the use of a technique which was both highly sensitive, and capable of discriminating between the two *plp* isoforms. Reverse transcription-polymerase chain reaction (RT-PCR) technology provided both the means of quantifying the relative amounts of the *plp* and *dm-20* isomers, and also the degree of sensitivity required when analysing low levels of transcripts. Limiting message was due to both the small amounts of tissue available when studying specific myelinating areas, and low levels of message present in tissues prior to myelination. Although the use of RT-PCR is an indirect method of measuring *plp* gene expression, direct methods such as northern blotting and even transcript mapping were not found to be sensitive enough to be appropriate alternatives. Use of this indirect method did however necessitate calibration of the RT-PCR protocol prior to collection of data, and the appropriate use of positive, negative and internal controls. It was envisaged, with the use of this extremely powerful molecular technique, together with routine immunocytochemical and histological techniques, to gain a more detailed appreciation of the developmental and spatial expression of the *plp* gene.

# CHAPTER 2. MATERIALS AND METHODS

# 2.1.TISSUE FIXATION AND PROCESSING

## 2.1.1.Fixation

### Fixatives

#### Buffered neutral formaldehyde (BNF), (4%)

Tissues fixed in BNF were paraffin-embedded and sections taken for routine haematoxylin and eosin (H and E) staining, immunocytochemistry and *in situ* hybridisation.
1 litre of fixative:

| | |
|---|---|
| 40% Formaldehyde | 100ml |
| Tap water | 900ml |
| $NaH_2PO_4$ | 4g/l |
| $K_2HPO_4$ | 8g/l |

#### Strong fixative (paraformaldehyde/glutaraldehyde 2%/5%)

Tissues fixed in strong fix were resin-embedded and sections taken for methylene blue/azure II staining, immunocytochemistry and electron microscopy.
500ml of fixative:

8% Paraformaldehyde 250ml

*(20g paraformaldehyde + 250ml distilled water (DW); heat to 65$^0$C; add 1M NaOH till solution clears; cool to 4$^0$C)*

25% Glutaraldehyde 100ml

Make up to 500ml with 0.08M isotonic cacodylate buffer

*(Sodium cacodylate 16.05g, NaCl 3.8g, $CaCl_2$ 0.055g, $MgCl_2$ 0.102g; Add DW to 100ml: pH to 7.2-7.3)*

| | |
|---|---|
| $CaCl_2$ | 250mg |

Filter in fume hood, adjust to pH 7.2

#### Carnoy's fixative

Carnoy's fixed tissue was collected for RNA extraction and subsequent RT-PCR.
100ml of fixative:

| | |
|---|---|
| Absolute alcohol | 60ml |
| Chloroform | 30ml |
| Glacial acetic acid | 10ml |

## Techniques

### Immersion

a) *Tissue culture cover slips:*

After routine surface immunostaining, coverslips were fixed in methanol at -20$^0$C for 10min., washed in distilled water and dried prior to mounting. Coverslips to be processed for *in situ* hybridisation (ISH) alone or for ISH after immunostaining for surface markers were immersion fixed in 4% paraformaldehyde for 20min., rinsed twice in PBS and stored at 4$^0$C in 70% ethanol. Coverslips to be processed for immunostaining for cytoplasmic markers by the technique of Gow *et al.* (1994a) were immersion fixed in 2% paraformaldehyde in Dulbecco's modified Eagle medium (DMEM) for 30min.

b) *Cryosections:*

Cryosections were immersion fixed in 2% paraformaldehyde in PBS for 20min. when immunostaining for cytoplasmic markers and in 2% paraformaldehyde in PBS for 5min. when immunostaining for the surface marker O4.

### Intra-cardiac perfusion

All perfusions were carried out in a fume hood. Post-natal animals and embryos as young as E14 were perfused transcardially with either BNF, strong fix or Carnoy's fix. Animals were killed by halothane or carbon dioxide inhalation and pinned in dorsal recumbency. After exposure of the heart *via* a thoracotomy, the right auricle was incised and perfusion initiated through the left ventricle using 23-27 gauge needles depending on the size of the animal. E14 and E16 embryos were perfused through fine, pulled glass Pasteur pipettes. The animals were first exsanguinated by perfusion with 0.85% NaCl followed by between 5-120ml fixative with fixation being assessed by rigidity. Animals were stored at 4$^0$C in fixative moisturised containers for 1hr. after which time the required tissue was dissected and stored at 4$^0$C in the same fixative until processed. Embryos younger than E14 were decapitated and immersion fixed in the appropriate fixative.

# 2.1.2.Processing

## Paraffin processing

Tissue for paraffin wax embedding was processed using a Shandon Elliot automatic tissue processor (Histokinette) and was passed through the following dehydration solutions:

| | | |
|---|---|---|
| 1) | 70% methylated spirit | 2hr. |
| 2) | 70% methylated spirit / 5% phenol | 2hr. |

| | | |
|---|---|---|
| 3) | 90% methylated spirit / 5% phenol | 2hr. |
| 4) | Methylated spirit | 2hr. |
| 5) | Ethanol / 5% phenol | 1hr. |
| 6) | 1% celloidin in methyl benzoate | 4hr. |
| 7) | Xylene | 1hr. (x3) |
| 8) | Paraffin wax | 4-6hr. |

Tissues were blocked out at $60^0$C in fresh paraffin wax.
Celloidin was obtained from Merk "Necoloidine"$^{(R)}$ as an 8% solution, treated as a 100% solution when made up with methyl benzoate.

## Resin processing

Samples were processed for araldite resin embedding using a Lynx$^{TM}$ el microscopy tissue processor (Leica). Samples were passed through the following solutions:

| | | | |
|---|---|---|---|
| 1) | Isotonic cacodylate buffer | $4^0$C | 50min. |
| 2) | 1% osmium tetroxide in cac. buffer | room temp | 2hr. |
| 3) | Isotonic cacodylate buffer | $4^0$C | 30min. |
| 4) | 50% alcohol | $4^0$C | 5min. |
| | 50% alcohol | $4^0$C | 10min. |
| 5) | 70% alcohol | $4^0$C | 5min. |
| | 70% alcohol | $4^0$C | 10min. |
| 6) | 80% alcohol | $4^0$C | 5min. |
| | 80% alcohol | $4^0$C | 10min. |
| 7) | 90% alcohol | $4^0$C | 5min. |
| | 90% alcohol | $4^0$C | 10min. |
| 8) | 100% alcohol | $4^0$C | 20min. (x2) |
| 9) | Propylene oxide | room temp | 15min. (x2) |
| 10) | 1:3, resin:propylene oxide | room temp | 13hr. |
| 11) | 1:2, resin:propylene oxide | room temp | 6hr. |
| 12) | 1:1, resin:propylene oxide | room temp | 18hr. |
| 13) | Resin | $30^0$C | 4hr. |

Processed samples were embedded in resin filled rubber moulds and left to polymerise overnight in a $60^0$C oven.

Resin composition:

30g Araldite CY212 (resin)
25.2g Dodecanyl succinic anhydride (DDSA) (hardener)

1.2ml 2,4,6-tri-dimethylaminomethyl-phenol (DMP 30) (accelerator)
1.0ml Di-butyl phthalate (plasticiser)

## Cryo-preservation

Tissue was cryo-preserved by snap freezing samples embedded in "Tissue-Tek" OCT compound (Miles inc.). Samples were suspended in OCT in small foil boats and held in isopentane cooled in liquid nitrogen. After freezing the foil was removed and the solid OCT embedded sample double wrapped in "Sealon film" (Fuji) and stored at -20$^0$C.

## Sections

### Paraffin-embedded tissue

Paraffin embedded tissue sections were cut on a Biocut 2035 microtome (Leica) at 6μm for ISH and routine staining and left overnight in a 60$^0$C oven.

### Cryo-preserved tissue

OCT embedded cryosections were cut on an OTF cryostat (Bright instrument company) at 15μm for ISH and immunocytochemistry and stored at -20$^0$C until use.

### Resin sections

Sections for light microscopy were cut at 1μm on a Reichert-Jung Ultracut E ultratome and placed on plain sulphuric acid treated slides (see 2.3.IN *SITU* HYBRIDISATION).

### Ultra-thin sections

Sections for electron microscopy were cut at 70nm on the same ultratome and mounted on 200 mesh-3.06mm diameter copper grids.

## Staining techniques

### Light microscopy

a) *Haematoxylin and eosin (paraffin sections):*

Sections were passed through the following solutions:

| | | |
|---|---|---|
| 1) | Histoclear | 2min. |
| 2) | Absolute alcohol | 2min. |
| 3) | Methylated spirit | 2min. |
| 4) | Water | 2min. |
| 5) | Iodine | 2min. |

| | | |
|---|---|---|
| 6) | Water | 1min. |
| 7) | Sodium thiosulphate | 1min. |
| 8) | Water | 1min. |
| 9) | Mayer's haematoxylin | 10min. |
| 10) | 1% acid alcohol | 3 dips |
| 11) | Water | 2min. |
| 12) | Scots tap water | 1min. |
| 13) | Water | 1min. |
| 14) | Methylated spirit | 10sec. |
| 15) | Saturated alcoholic eosin | 2min. |
| 16) | Methylated spirit | 1min. (dehydration start) |
| 17) | Absolute alcohol | 2min. (x2) |
| 18) | Histoclear | 2min. (x2) |
| 19) | Xylene | 1min. |

The initial hydration steps (1-4) were omitted with unfixed material. Sections were mounted in DPX mountant (BDH).
Mayer's haematoxylin was made up as follows: 1.0g haematoxylin, 50.0g potassium alum and 0.2g sodium iodate in 1L water, brought to boiling point and left overnight before adding 1.0g citric acid and 50.0g chloral hydrate.
Scots tap water was made up as follows: 3.5g sodium bicarbonate and 20.0g magnesium sulphate in 1L water.

b) *Haematoxylin:*

ISH sections were counterstained with haematoxylin after autoradiography as follows:

| | | |
|---|---|---|
| 1) | Water | 2min. |
| 2) | Mayer's haematoxylin | 30sec. |
| 3) | Water | 2min. |
| 4) | Scots water | 15sec. |

Sections were dehydrated and mounted as above.

d) *Methylene blue/azure II (resin sections):*

Slides were placed on a $60^0$C hot plate flooded with stain for 10-30sec. and rinsed in running tap water.
(Methylene blue/azure II: 1.0% methylene blue, 1.0% azure II, 1.0% borax in distilled water.)

e) *4',6-diamidino-2-phenylindole (DAPI):*

Immunostained cryosections were counterstained with DAPI nuclear stain (6μg/ml) by flooding the section for 1min. and rinsing in distilled water.

**Electron microscopy**

Ultra thin sections were stained by covering grids with a saturated solution of uranyl acetate in 50% ethanol for 5-15min. at room temperature, before rinsing in 50% and 75% ethanol, distilled water (x2) and air drying. Grids were then stained with Reynold's lead citrate for 5-10min. inside a NaOH moisturised chamber and washed in 1M NaOH solution (x3) and distilled water (x5).

(Reynold's lead citrate: 1.33g lead nitrate, 1.76g sodium citrate each dissolved in 15ml. water; mix together and shake vigorously for 1min. then occasionally for 30min. Clear with 8.0ml. 1M NaOH and make up to 50ml. with water; final pH 12.0).

# 2.2.GENETIC MANIPULATION

## 2.2.1.Core techniques

### Ethanol precipitation

Nucleic acids were routinely precipitated in the presence of 0.3M sodium acetate (NaAc) pH 5.2 and 3 vol. ice cold ethanol. Amounts less than 1μg were precipitated overnight at -70$^0$C. Larger amounts were precipitated at -20$^0$C or -70$^0$C for not less than 2hr. and 1 hr. respectively. RNA riboprobes were also precipitated in the presence of 0.75M ammonium acetate ($NH_4Ac$) or 0.4M lithium chloride (LiCl). Samples were centrifuged at 4$^0$C for 15-30min. at 12,000g and the supernatant removed. RNA and DNA pellets were washed with 75% ethanol/di-ethyl pyrocarbonate treated sterile distilled water (DEPC SDW) (see 2.2.2.Analysis of transcripts) and 70% ethanol/SDW respectively, either air dried for 10-20min. or vacuum dried for 2-3min. and reconstituted in the appropriate volume of either DEPC SDW or SDW respectively.

### Chloroform extraction

Mineral oil was removed from PCR reactions by the addition of 2 vol. chloroform. The mixture was vortexed and centrifuged at 12,000g for 2min. before removal of the upper aqueous layer containing the nucleic acid.

### Phenol:chloroform extraction

Deproteinisation of nucleic acids was performed using phenol:chloroform:isoamyl alcohol (25:24:1) extraction followed by ethanol precipitation. A phenol:chloroform mix was used since deproteinisation is more efficient when two different organic solvents are used. An equal volume of phenol:chloroform was added to the nucleic acid sample which was mixed to an emulsion and centrifuged at 12,000g for 2min. The aqueous phase was removed and nucleic acids precipitated as described above. Phenol:chloroform was prepared as follows:

1) Melt phenol at 68$^0$C.
2) Add hydroxyquinoline to a final conc. of 0.1% (antioxidant, RNase inhibitor, chelates metal ions, colours organic phase yellow).
3) Saturate to raise pH >7.8 by repeated exposure to 0.5M Tris Cl (pH 8.0) using a separating funnel and agitation (DNA partitions into the organic phase at acid pH).
4) Add an equal volume of chloroform:isoamyl alcohol (24:1) and store under 0.1M Tris Cl (pH 8.0) in a light tight bottle at 4$^0$C (Chloroform denatures protein and facilitates separation of the organic and aqueous phases. Isoamyl alcohol reduces foaming.).

## Enzymatic manipulations

### Restriction enzymes

Restriction enzymes were supplied by "Gibco BRL", "Promega", and "New England Biolabs" and used according to manufacturer's instructions.

### Modification enzymes

a) *Klenow:*

DNA polymerase I large (Klenow) fragment (Promega) was used to fill in 3′ ends of DNA fragments. Up to 1μg of DNA was treated in the presence of between 1-4U Klenow enzyme, 2mM dNTPs, 5mM Tris-HCl, pH 7.2, 10mM $MgSO_4$ and 0.1mM dithiothrietol (DTT). The mixture was incubated for 30min. at room temperature followed by inactivation of the enzyme by heating at 65$^0$C for 10min. Product was purified using a Qiaex gel extraction kit (Qiagen) as described below to remove unincorporated dNTPs which could interfere with subsequent ligation reactions.

b) *Alkaline Phosphatase:*

Vectors were dephosphorylated (CIP treated) prior to insert ligation using calf intestinal alkaline phosphatase (CIAP) (Gibco BRL). 10μg of linearised vector was dephosphorylated in the presence of 50mM Tris-HCl pH 8.5 and 0.1mM EDTA using 0.1U CIAP at 37$^0$C for 30min. followed by a further 30min. after the addition of another 0.1U CIAP. The enzyme was inactivated by heating at 75$^0$C for 15min. followed by two phenol:chloroform extractions (see 2.2.1.Core techniques). The product was ethanol precipitated and reconstituted at 100μg/ml. Parallel reactions in the absence of CIAP were run in all cases to allow assessment of dephosphorylation efficiency during ligation reactions.

c) *Ligase:*

Ligation reactions were catalysed by T4 DNA ligase (Gibco BRL) at 12$^0$C overnight in a 10μl volume in the presence of 0.25U enzyme, 0.05mM Tris-HCl pH 7.6, 10mM $MgCl_2$, 1mM ATP, 1mM DTT, 25% (w/v) polyethylene glycol-800 and between 10-25μg/ml CIAP treated linearised vector at a 1:1 molar ratio with respect to the insert to be ligated. Both sticky and blunt end ligations were incubated as described above. Reactions containing 2.5:1 and 5:1 ratios of vector to insert and insert to vector were also performed as well as the following control reactions:

| | | |
|---|---|---|
| 1) | Native vector + ligase. | (To assess transformation efficiency. Ligase is not required but is included since it will decrease transformation efficiency.) |
| 2) | Linearised vector (non CIP) - ligase. | (To assess efficiency of digestion of vector.) |
| 3) | Linearised vector (non CIP) + ligase. | (To assess ligation efficiency) |
| 4) | Linearised vector (CIP) + ligase. | (To assess CIP efficiency) |

## DNA fragment isolation

DNA fragments were isolated using a Qiaex gel extraction kit (Qiagen) according to manufacturer's instructions. Gel slices containing the fragment were pre-washed in Tris buffer pH 7.0 to lower the sample pH as binding efficiency of DNA to the Qiaex decreases rapidly above pH 7.5. The method utilises the property of nucleic acids binding to silicagel particles in the presence of high concentrations of chaotropic salts such as NaI, $NaClO_4$ and GuSCN. Fragments were resolved on both regular TAE agarose gels up to 2% concentration and on TBE "Metaphor$^{TM}$" gels (Flowgen) up to 5% concentration. Yields were generally around 50% and were calculated by comparison of aliquots of isolated fragment with parallel fragment digests of known amounts.

## Nucleic acid electrophoresis

### Agarose gels

Routine electrophoresis of both DNA and RNA was performed using 1-2% regular agarose gels using ultra pure electrophoresis grade agarose (Gibco BRL). Gels were cast by melting the agarose in the presence of Tris acetate EDTA (TAE) buffer with a final concentration of 0.04M Tris acetate, 0.001M EDTA and 0.5µg/ml ethidium bromide and run in the same buffer. Samples were loaded with 6x TAE gel loading buffer (6x TAE; 30% glycerol (Sigma); 0.25% bromophenol blue (BDH chemicals Ltd.); 0.25% xylene cyanole FF (Sigma) ). Gels were viewed using a "Fotoprep I" ultraviolet transilluminator (Fotodyne Inc.) and photographed using a Polaroid MP4 land camera (Polaroid), a T2201 transilluminator (Sigma), a Wratten 22A filter (Kodak) and Polaroid 667 (ASA 3000) film.

### Metaphor gels

Resolution of small DNA fragments (< 100bp) and separation of fragments differing by as little as 10 base pairs (bp) was achieved using " Metaphor$^{TM}$" agarose gels (Flowgen).

"Metaphor" is an intermediate melting temperature (<75$^0$C) agarose with twice the resolution capacity of the finest sieving agarose products. Metaphor gels have a similar resolution capacity to polyacrylamide gels in resolving small fragments (~ 20-1000bp), whilst being much less toxic to handle. Gels of between 2-5% were used and were prepared and run in Tris borate EDTA buffer (TBE) to give smaller gel pore size and higher resolution. Final buffer concentration was 0.09M Tris borate, 0.002M EDTA and 0.5μg/ml ethidium bromide. Gel loading buffer was the same as for agarose gels.

## Microbiological manipulations

### Bacterial media

a) *Luria-Bertani medium (LB medium):*

| | | |
|---|---|---|
| 1 Litre | Tryptone | 10g |
| | Yeast extract | 5g |
| | NaCl | 10g |

Dissolve in distilled water and adjust pH to 7.0 using ~ 0.2ml 5N NaOH. Sterilise by autoclaving for 20min. at 15lb/sq. in.
Bacteria containing plasmids conferring ampicillin or tetracycline resistance were grown in LB containing 100μg/ml ampicillin or 50μg/ml tetracycline respectively.

b) *SOC medium:*

| | | |
|---|---|---|
| 1 Litre | Tryptone | 20g |
| | Yeast extract | 5g |
| | NaCl | 0.5g |

Dissolve in distilled water, add 10ml of 250mM KCl and adjust pH to 7.0 using ~ 0.2ml 5N NaOH. Sterilise by autoclaving for 20min. at 15lb/sq. in. Allow to cool to less than 60$^0$C and add 20ml of filter sterilised 1M glucose solution.

c) *M9 minimal medium:*

| | | |
|---|---|---|
| 250ml | $Na_2HPO_4.7H_2O$ | 1.5g |
| | $KH_2PO_4$ | 0.75g |
| | NaCl | 0.125g |
| | $NH_4Cl$ | 0.25g |

Make up to 238ml with distilled water and pH to 7.4 with NaOH. Sterilise by autoclaving for 15min. at 15lb/sq. in. Cool to ~50$^0$C and add:

| | |
|---|---|
| 1M $MgSO_4$ | 64g |
| 1M $CaCl_2$ | 15g |
| 20% glucose (filter sterilised) | 2.5g |
| Thiamine (10mg/ml, filter sterilised) | 5.0g |

d) *LB agar plates:*

LB agarose plates were prepared at a concentration of 1.2% by the addition of 12g agar/L of LB prior to autoclaving. The mix was allowed to cool to 50$^0$C before pouring (approx. 30ml/90mm plate) at which time any thermolabile substances such as antibiotics were added. Ampicillin (NBL) was added to media and plates at a concentration of 100μg/ml. Tetracycline (NBL) was added at a concentration of 50μg/ml. Both medium and plates were stored at 4$^0$C and plates were removed from storage 2hrs. before use to prevent "sweating" and smearing.

e) *M9 agar plates:*

M9 agar plates were prepared at a concentration of 1.2% by the addition of 3g agar to the M9 media prior to autoclaving. The mix was cooled to 50$^0$C prior to addition of glucose, thiamine and additional salts.

**Competent cell preparation**

Competent cells were prepared from JM101 Escherichia coli bacteria (supE, thi, Δ(lac-proAB), [F', traD36, proAB, lacI9ZΔM15]) (Pharmacia) maintained on M9 thiamine agarose plates as single colony cultures. Cultures were replated every 6-8 weeks.

1) Inoculate a single colony into 10ml L broth and incubate overnight at 37$^0$C and 200 rpm. in an orbital incubator.
2) Inoculate 1ml of the culture into 100ml L broth and incubate under the above conditions for ~ 1.5-2hrs. until the optical density (600nm) ($OD_{600}$) of the culture is between 0.2-0.3. This ensures that the number of viable cells does not exceed $10^8$ cells/ml.
3) Aseptically transfer the cells into 3x 40ml, sterile, ice cold, polypropylene tubes

(Becton Dickinson) and incubate on ice for 20min. All subsequent steps should be carried out aseptically

4) Recover the cells by centrifugation at 5000rpm. for 5min. at $4^0$C (JA-20 rotor) and remove the media from the pellet .

5) Gently reconstitute the pellets in 50ml (total vol.) of ice cold, filter sterilised (Flowpore 0.45μm filter (Biomedicals Ltd.))100mM $MgCl_2$ and recover the cells again as above.

6) Gently reconstitute the pellets in 50ml (total vol.) of ice cold, filter sterilised 100mM $CaCl_2$ and incubate on ice with occasional gentle agitation for 60min.

7) Recover cells as above and reconstitute in 10ml ice cold filter sterilised 100mM $CaCl_2$ with 15% glycerol.

8) Aliquot into 1.5ml ependorfs, snap freeze in liquid nitrogen and store at -$70^0$C. Allow 24hrs. before using for transformations.

**Transformations**

Transformations were performed in sterile 40ml polypropylene tubes pre-chilled on ice. Between 0.05-25ng of DNA was aliquoted and made up to a final volume of 100μl with Tris EDTA buffer (TE) pH 8.0 (10mM Tris Cl pH 8.0/1mM EDTA pH 8.0). Competent cells were thawed by hand. A 100μl aliquot was added to the DNA, swirled gently and incubated on ice for 30min. The competent culture was then heat-shocked at $42^0$C for 45sec. and rapidly transferred to ice for a further 2min. The cultures were incubated at $37^0$C and 100rpm. for 1hr. in an orbital incubator after the addition of 800μl SOC medium, and duplicate 200μl aliquots were plated out onto LB agar plates using a sterile bent glass rod. Plates were left at room temperature until the liquid had been absorbed, inverted and incubated at $37^0$C overnight.

**Plasmid preparations**

a) *Minipreps:*

Total amounts of plasmid DNA < 10μg were isolated from bacterial cells using the Wizard™ minipreps DNA purification system (Promega). This is based on the alkaline lysis procedure (Birnboim and Doly 1979) with lysis of bacteria using sodium dodecyl sulphate (SDS) and NaOH (SDS denatures bacterial proteins, and NaOH denatures chromosomal and plasmid DNA). Neutralisation with potassium acetate causes the covalently closed plasmid DNA to reanneal rapidly whilst most chromosomal DNA and bacterial proteins precipitate with the SDS and form a complex with the potassium which is removed by centrifugation. Plasmid DNA is further purified by passage through a

proprietary chromatography column before elution with Tris EDTA (TE) buffer. Yields of up to 10μg were obtained from 3ml overnight cultures.

b) *Maxipreps:*

Large scale preparation of plasmid DNA from 200ml overnight cultures followed the protocol above using the WizardTM maxiprep DNA purification system with yields of up to 1mg DNA.

Plasmids were stored as both purified DNA at -20$^0$C and as bacterial culture glycerol stocks (800μl culture + 200μl sterile glycerol) at -70$^0$C.

## 2.2.2.Analysis of transcripts

### RNA Extraction

#### Fresh Tissue

RNA was isolated from tissue using RNAzol$^{TM}$ B (Biotech Laboratories, Inc.) following the manufacturer's instructions. The method is a modification of the single step procedure of Chomczynski and Sacchi (1987) and utilises the complexing of RNA with guanidinium and water molecules in the aqueous phase from which DNA and proteins are excluded.
Plastic-ware and apparatus were soaked overnight in a sterile 0.1% solution of di-ethyl pyrocarbonate (DEPC) in distilled water, autoclaved for 15min. and oven dried prior to use.
Tissue samples were frozen in liquid nitrogen after collection. Tissue samples greater than 0.1g were homogenised in liquid nitrogen with a mortar and pestle followed by a Dounce homogeniser in the presence of the required amount of RNAzol (1-2ml/100mg tissue). Small tissue samples were triturated through decreasing needle sizes (21 gauge to 27 gauge) using 1ml RNAzol and a 2ml syringe. One tenth of the total volume of chloroform was added to the homogenate and vortexed for 15 seconds before incubation on ice for 15 minutes. The sample was centrifuged at 4$^0$C for 15min. at 12,000g and the upper clear aqueous phase removed and retained. RNA was precipitated using an equal volume of isopropanol. Samples with expected yields of over 1μg were left for 15min. on ice before centrifuging at 4$^0$C for 15min. at 12,000g. Samples with lower expected yields were precipitated overnight at 4$^0$C. Pellets were washed with 800μl 75% ethanol/DEPC-treated sterile distilled water (SDW) and dried under vacuum for 2-3min. The RNA pellet was reconstituted in 0.1% DEPC-treated SDW and RNA concentration assessed either by absorbence spectrophotometry at 260nm and 280nm UV, gel comparison with aliquots of RNA of known concentration or colourimetrically using a DNA Dipstick$^{TM}$ (Invitrogen).

**Fixed Tissue**

Tissues fixed using Carnoy's fixative were treated in the same manner as fresh tissue apart from liquid nitrogen freezing which was not required.

## cDNA Preparation

First strand cDNAs were synthesised from 2μg of total RNA given availability. RNA was initially denatured at $65^0$C for 5min. and quenched on ice. Reactions proceeded in the presence of 3μg random primers (Gibco BRL), 0.5mM deoxynucleotides, 10mM dithiothrietol and 20 U RNasin$^R$ (Promega) ribonuclease inhibitor for 30min. at $37^0$C and 60 min. at $42^0$C using 400U Moloney murine leukaemia virus (M-MLV) reverse transcriptase (Gibco BRL) in the manufacturer's buffer. Reactions were terminated with 2.5μl 500mM EDTA. The product was ethanol precipitated (see 2.2.1.Core techniques) and reconstituted in SDW at 25ng/μl.

## Reverse transcription polymerase chain reaction (RT-PCR)

*Plp* and *dm-20* RT-PCR products were amplified using a "Perkin Elmer" DNA thermal cycler from 50ng cDNA using a forward primer in exon 2 and a reverse primer in exon 4 spanning exon 3 (Table 2). In the presence of both *plp* and *dm-20* cDNAs two products of 506 and 401 base pairs, respectively, were generated (Figure 7). Cyclophilin products were generated in parallel with *plp/dm-20* products when semi-quantitative information was required about the expression of the *plp* or $P_0$ genes. Cyclophilin is an ubiquitous constitutively expressed protein (Danielson *et al.* 1988) and generation of RT-PCR product could therefore be used as an internal control to ensure equal loading of cDNA between samples. Cyclophilin product of 300bp was generated using the primers described below (Table 2). Major peripheral myelin protein $P_0$ RT-PCR product was generated using the primers described below (Table 2) giving a final product of 210bp. Reactions were performed in 0.5ml eppendorfs in the presence of 2.5U Taq DNA polymerase (Promega) in the manufacturer's reaction buffer, 0.2mM dNTPs, either 0.3μM each cyclophilin/$P_0$ primer or 0.3μM PLP forward primer and 0.2μM PLP reverse primer and between 1.5-4.5mM $MgCl_2$. Reagents were overlaid with 50 μl mineral oil (Sigma).

Between 2-5ng of plasmid containing the appropriate cDNA insert were used as target for positive internal controls; pC4 (PLP), pC11 (DM-20), p1B15 (Cyclophilin), $pP_0$ ($P_0$).

The PCR program consisted of:

| | | |
|---|---|---|
| **1) Initial denaturation** | $94^0$C | 1min. 30sec. |
| **2) Step cycle** (25-39 cycles) | | |
| Annealing | $55^0$C | 45 sec. |
| Extension | $72^0$C | 1 min. |
| Denaturation | $94^0$C | 45 sec. |
| **3) Final cycle** | | |
| Annealing | $55^0$C | 1 min. |
| Extension | $72^0$C | 5 min. |
| **4) Soak** (storage) | $4^0$C | |

PCR products were extracted from the mineral oil either by direct removal of the lower aqueous layer or by chloroform extraction (see 2.2.1.Core techniques).

| RT-PCR Product | Forward primer | Reverse primer | Product length |
|---|---|---|---|
| ***plp/dm-20*** | 5′ GCTCTCACTGGTACAGAA 3′ | 5′ TACATTCTGGCATCAGCGCAGAGACTGC 3′ | *plp*/506bp + *dm-20*/401bp |
| ***cylcophilin*** | 5′ ACCCCACCGTGTTCTTCGAC 3′ | 5′ CATTTGCCATGGACAAGATG 3′ | 300bp |
| $P_0$ | 5′ CCAGTGAATGGGTCTCAGAT 3′ | 5′ TGCCGTTGTCACTGTAGTCT 3′ | 210bp |

**Table 2.** Summary of RT-PCR primers and lengths of generated products.

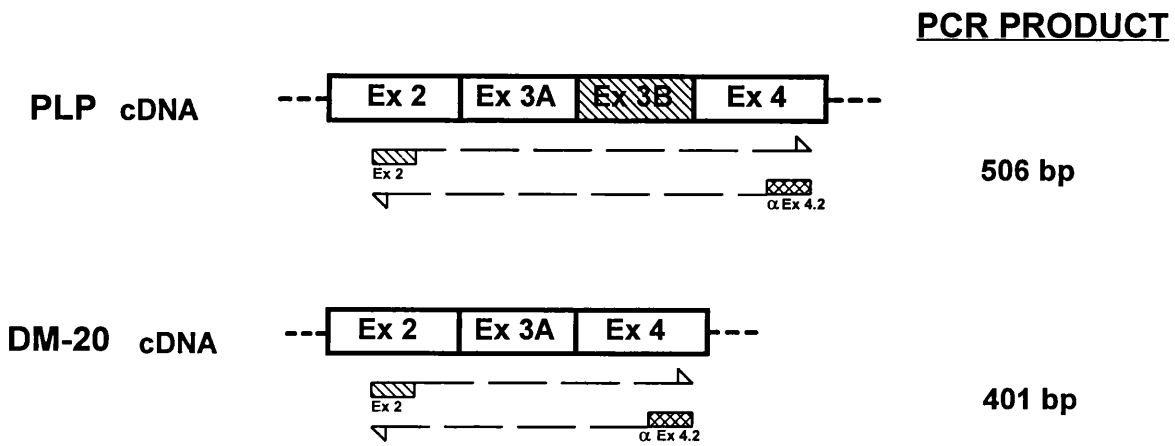


**Figure 7.** The use of RT-PCR technology to identify *plp* and *dm-20* transcripts. By designing PCR primers placed either side of exon 3B, *plp* and *dm-20* products of different lengths are generated. *Dm-20* product will be shorter by 105bp, thus allowing the two products to be resolved during gel electrophoresis.

## 2.2.3.Southern blotting (pPLP-3B probe specificity confirmation)

### Gel preparation

DNA was run on standard 2% agarose gels, to achieve adequate resolution of *plp/dm-20* PCR/RT-PCR products, with appropriate DNA size markers. Gels were photographed with a ruler alongside to allow later identification of bands on the transfer membrane. The gel was rinsed in distilled water, placed in denaturing solution (0.5M NaOH/1.5M NaCl) in a plastic dish and shaken slowly on a platform shaker for 15min. The rinse and denaturation were repeated. The gel was then rinsed and shaken twice in neutralisation solution (3M NaCl/0.5M Tris pH 7.4) for 30min. to lower the pH to below 9.0, above which DNA binding to membranes is poor.

### Transfer

DNA was transferred by upward capillary action using a high-salt transfer buffer (20x standard sodium citrate (SSC); 3M NaCl/0.3M trisodium citrate) onto "Hybond$^{TM}$-N+" nylon membranes (Amersham) cut to the same size as the gel. A solid support was placed in a tray containing 20x SSC and wicks made from Whatman 3MM paper (Whatman International Ltd.) soaked in buffer were placed over the support trailing into the buffer, 3 lengthways and 3 breadthways. The gel was placed on top and the surrounding paper sealed with "Sealon film" (Fuji) to ensure only vertical capillary transfer. Positioned above this were; the transfer membrane which had been previously soaked in SDW followed by 6x SSC; 3 pieces of 3MM cut to gel size, soaked in 20x SSC; 3 pieces of 3MM cut to gel size, unsoaked; paper towels cut to gel size to a height of ~ 4cm; a sheet of glass and a weight to hold everything in place. Transfer was carried out overnight ensuring that the 20x SSC reservoir did not run dry. Efficiency of transfer was assessed by viewing the gel and filter using a UV transilluminator. The filter was rinsed in 6x SSC, air dried and the DNA immobilised on the filter by UV crosslinking using an XL-100 UV crosslinker (Spectronics corporation).

### DNA radiolabelling

Random primed $^{32}$P labelled DNA probes were generated from pPLP-3B plasmid using the "High prime" labelling kit (Boehringer Mannheim). *Plp*-specific insert was liberated from the plasmid by an *Eco* RI/*Hin* dIII digest, gel isolated and quantified as described above. 50ng of insert was reconstituted in 11µl SDW, denatured in a boiling water bath for 10min. and quenched on ice. This was used as template in a 20µl reaction containing 4µl "High Prime" solution and 5µl (50µCi) $^{32}$P dCTP, 3000 Ci/mMol, aqueous solution. The mixture was incubated for 10min. at 37$^{0}$C and the reaction stopped by the addition of 2µl 0.2M EDTA (pH 8.0). Labelled DNA was separated from unincorporated $^{32}$P-labelled

nucleotides by elution from "Sephadex Nick" columns (Pharmacia Biotech) according to the manufacturer's instructions. Specific activity of probes was estimated using a mini-monitor and found to be in agreement with predicted values (~$1x10^8$-$1x10^9$ cpm/μg).

## Prehybridisation

Filters were prehybridised in heat sealed plastic bags using 0.1ml/$cm^2$ "Rapid-hyb" buffer (Amersham). Buffer was pre-heated to $65^0$C and prehybridisation was carried out in a shaking water bath for a minimum of 1hr.

## Hybridisation

Approximately 2ng/ml of labelled probe was added to the prehybridisation solution after separate mixing in a 1ml aliquot to prevent concentrated probe being added directly to the membrane. After ensuring even mixing and distribution, hybridisation was allowed to proceed with shaking at $65^0$C overnight.

## Washing

Washes to remove non-specifically bound probe were as follows:

| | | | |
|---|---|---|---|
| 1) | 2x SSC, 0.1% (w/v) SDS | 30min. | room temp. |
| 2) | 2x SSC, 0.1% (w/v) SDS | 30min. | $65^0$C |
| 3) | 1.0-0.1x SSC, 0.1% (w/v) SDS | 15min. x2 | $65^0$C |
| 4) | 0.1x SSC, 0.1% (w/v) SDS | 15min. x2 | $65^0$C |

Reduction in background levels of probe was moitored using a mini-monitor and the stringency and length of washes increased as appropriate.

## Development

Hybridised filters were allowed to air dry and placed in heat-sealed plastic bags. Autoradiography was performed using Cronex 10S X-ray film (DuPont) with Kodak "X-Omatic" regular intensifying screens for the appropriate times.

# 2.3.*IN SITU* HYBRIDISATION

## 2.3.1.Riboprobes

### $^{35}$S riboprobes

Both sense and antisense $^{35}$S probes were generated which would recognise *plp* and *dm*-20 (PLP-1) or only *plp* transcripts (PLP-3B) using the SP6/T7 Transcription kit (Boehringer Mannheim). PLP-1 probes were generated from a 0.8kb cDNA containing mainly coding region cloned into pGEM 4 (Promega), (Milner *et al.* 1985). PLP-3B probes were generated from an 81bp cDNA fragment in exon 3B subcloned into pGEM 3Z (Promega), (see 3.1.SUBCLONING OF THE MOUSE *plp* SPECIFIC SEQUENCE). Plasmids were linearised using the appropriate restriction enzyme (see below), confirmed by analytical gel analysis, ethanol precipitated and reconstituted at 500µg/ml. All restriction enzymes were chosen to generate 5′ overhangs as 3′ overhangs may cause aberrant transcript generation.

| **Plasmid** | **Digest** | **Promoter** | **Sense/αSense** |
|---|---|---|---|
| pPLP-1 | *Bam* HI | T7 | α Sense |
| pPLP-1 | *Hin* dIII | SP6 | Sense |
| pPLP-3B | *Eco* RI | SP6 | α Sense |
| pPLP-3B | *Xba* I | T7 | Sense |

A 20µl labelling reaction contained the following:

1-2µg linearised DNA, 1.0µl each of nucleotides (ATP, GTP, UTP (10mM in Tris buffer)), 5.0µl (50µCi) $^{35}$S αCTP (specific activity 37TBq/mM; < 1000 Ci/mM; Amersham), 2.0µl 10x transcription buffer, 1.0µl RNAse inhibitor (20 units/µl) and DEPC SDW to 20µl. The mixture was incubated at 37$^0$C for 30min. after the addition of 1.0µl either T7 or SP6 RNA polymerase (20 units/µl). An additional 1.0µl enzyme was then added and the incubation repeated. Template was digested with the addition of 2.0µl RNAse free DNAse(10 units/µl) incubated at 37$^0$C for 15min. The product was phenol chloroform extracted and a back extraction performed after the addition of a further 22µl DEPC SDW. The RNA was precipitated with 7.5M $NH_4Ac$, a 5.0µl aliquot removed prior to centrifugation and placed in 5.0ml "Ecoscint" (National Diagnostics) labelled A. RNA pellets were reconstituted in 100µl DEPC SDW and 5.0µl of this, labelled B and 5.0µl of the supernatant, labelled C were added separately to 5ml Ecoscint. The riboprobe was reprecipitated overnight with 3M NaAc.

Ecoscint vials were counted on a Beckman LS 1801 scintillation counter.

| | |
|---|---|
| Vial A represented | Total amount of isotope. |
| Vial B represented | Amount of incorporated isotope. |
| Vial C represented | Amount of unincorporated isotope. |

Percentage isotope incorporation was calculated as a ratio of B/A. Isotope incorporated into RNA was calculated by a standard formula and the riboprobe reconstituted in 0.01M dithiothreitol at a concentration of 1.0ng/μl/kb. Probe was stored at -20$^0$C and used within 6-8 weeks.

## Digoxigenin riboprobes

Digoxigenin probes were generated using the DIG RNA Labelling kit (SP6/T7) (Boehringer Mannheim). Although $^{35}$S-labelled probes provided greater sensitivity, digoxigenin-labelled riboprobes offered the advantages of safer handling and greater stability. Digoxigenin-labelled probes are stable for more than 1 year, whereas $^{35}$S-labelled probes must be used within 6-8 weeks. A 20μl labelling reaction contained the following:

1μg linearised DNA, 1.0μl NTPs (10mM ATP, CTP, GTP, 6.5mM UTP, 3.5mM DIG-11-UTP, pH 7.5), 2.0μl 10x transcription buffer, 1.0μl RNAse inhibitor (20 units/μl) and DEPC SDW to 20μl. The mixture was incubated at 37$^0$C for 1hr. after the addition of 1.0μl either T7 or SP6 RNA polymerase (20 units/μl). An additional 1.0μl of enzyme was added and the incubation repeated. Template was removed with the addition of 2.0μl RNAse free DNAse (10 units/μl) incubated at 37$^0$C for 15min. The reaction was terminated with 2.0μl 0.2M EDTA and precipitated with 4M LiCl (see above). RNA pellets were reconstituted in 100μl DEPC SDW + 1.0μl RNAse inhibitor and incubated at 37$^0$C for 30min. before storing at -20$^0$C.

Incorporation of digoxigenin was checked using an alkaline phosphatase conjugated anti-digoxigenin antibody and dig-labelled pSPT18-neo (100μg/ml) as a positive control. Serial 50% dilutions of control and probe were dotted onto Hybond$^{TM}$-N nylon hybridisation transfer membrane (Amersham), air dried and immobilised by crosslinking (see 2.2.3.Southern blotting (pPLP-3B probe specificity confirmation)). Filters were incubated in sealed polythene bags (Pifco) at room temperature on a platform shaker with; 20ml maleate buffer (0.1M maleic acid, 0.15M NaCl, pH 7.5) for 1min.; 20ml blocking reagent (1% w/v in maleate buffer; Boehringer Mannheim) for 30min.; 10ml anti DIG-AP, Fab fragments (2.0μl (0.75U/μl); Boehringer Mannheim, in 10ml TBS buffer (0.1M Tris HCl, 0.15M NaCl, pH 7.5)) for 30min.; 2x 20ml TBS buffer for 15min. and 10ml substrate (45μl 4-nitroblue tetra-zolium chloride(NBT); 100mg/ml; (Boehringer Mannheim), + 35μl 5-bromo-4-chloro-3-indoyl-phosphate (X-phosphate, BCIP); 50mg/ml; (Boehringer Mannheim) + 10ml substrate buffer (0.1M Tris HCl, 0.1M NaCl, 0.05M $MgCl_2$, pH 9.5) ).

Incubation with the substrate was without shaking and blue reaction product was generally visible after 1-5min. after which time filters were rinsed in DW and air dried.

## 2.3.2.ISH Protocol

The basic procedure was as described by Cox *et al.* (1984) and modified by Wilkinson *et al.* (1987). Pre-treatment involves several steps which increase the accessibility of the target (mRNA) to the probe whilst maintaining morphological preservation of the tissue. Proteinase K treatment removes protein bound to the target whilst acetylation (Hayashi 1978) decreases non-specific binding due to electrostatic interactions between probe and basic proteins. Hybridisation of riboprobe to the target is performed under low stringency conditions favouring hybrid formation and washing removes unbound probe giving acceptable background. An RNase step is included to remove single stranded RNA.

### Apparatus/Tissue preparation

To minimise RNase activity, all glassware and slides were soaked in 6.0% sulphuric acid, 6.0% potassium dichromate overnight; rinsed for 2-4hr. in tap water; rinsed in distilled water; immersed in 0.01% DEPC SDW overnight, and oven-dried at $60^0$C and baked at $180^0$C for 4hr. loosely wrapped in foil. Eppendorfs and pipette tips were DEPC-treated as described previously(see 2.2.2.Analysis of transcripts).

Coverslips used to cover sections during hybridisation were siliconised to decrease probe binding. They were soaked in 1M HCl for 30min.; washed in distilled water 3 times; air dried; immersed in Repelcot$^{TM}$ (BDH) for 20min.; rinsed in distilled water and baked at $130^0$C for 90min.

3-aminopropyltriethoxy-silane (APES) (Sigma) coated slides were prepared as follows. Slides were washed as above, soaked in Decon 90 (Decon Lab. Ltd.) (5% solution) overnight, washed well and oven dried wrapped in foil. In a fume hood slides were soaked in, 0.25% APES in methylated spirit for 2min. and 0.01% DEPC SDW for 2min. prior to oven drying wrapped in foil. Slides were stored at room temperature.

Chrome alum/gelatin coated slides were prepared as follows. A 1% (w/v) gelatin, 0.1%(w/v) chrome alum, 0.01% DEPC solution was made by dissolving the gelatin in boiling DW, cooling, adding the chrome alum, filtering through 3MM paper and adding the DEPC. Slides were coated in three separate solutions for 2min. each, oven dried wrapped in foil and stored at room temperature.

*In situ* hybridisation was performed on cultured cells grown on poly-L-lysine coated coverslips (see2.6.TISSUE CULTURE), 6μm tissue sections from BNF perfused tissue (see 2.1.1.Fixation) on APES coated slides or 15μm tissue sections from unfixed cryo-preserved tissue (see 2.1.1.Fixation) on gelatin coated slides. Tissue culture coverslips

were fixed onto RNase free slides using Loctite glassbond (Loctite UK.) prior to processing.

## Pre-treatment

Slides were passed through the following solutions:

| | | | |
|---|---|---|---|
| 1) | Xylene | 10min. | (paraffin-embedded sections only) |
| 2) | Absolute alcohol | 5min. | (paraffin-embedded sections only) |
| 3) | Methylated spirit | 5min. | (paraffin-embedded sections only) |
| 4) | 0.85% saline | 5min. | |
| 5) | Phosphate buffered saline (PBS) | 5min. | |
| 6) | 4% paraformaldehyde (in PBS) | 20min. | |
| 7) | PBS x2 | 5min. | |

(PBS- 137mM NaCl/2.8mM KCl/1.5mM $KH_2PO_4$/8mM $Na_2HPO_4$)

Sections were then covered with a 0.002% solution of proteinase K in 0 05M Tris-HCl (pH 7.6); 0.005M EDTA for 7.5min., washed in PBS for 5min. and the proteinase K inactivated by fixation in 4% paraformaldehyde for 5min. Slides were placed in 0.1M triethanolamine + 625µl acetic anhydride in a fume hood with magnetic stirrer for 10min. with a further 625µl acetic anhydride added after 5min. Finally slides were passed through:

| | | |
|---|---|---|
| 1) | PBS | 5min. |
| 2) | 0.85% saline | 5min. |
| 3) | Methylated spirit | 5min. |
| 4) | Absolute alcohol (x2) | 5min. |

Slides were then air dried for 1hr.
(Proteinase K treatment was omitted with cryo-sections and tissue culture coverslips.)

## Hybridisation

Total volume of probe required was calculated depending on number and size of sections (brain sections ~ 6µl; spinal cord sections ~ 3µl) and dilution factor of the probe. Generally PLP-1 was used at 1:10 and PLP-3B at 1:2-5. Dilutions were made in hybridisation buffer:

50% formamide
10% dextran sulphate
1x Denhardt's
20mM Tris-HCl (pH 8.0)
0.3M NaCl

5mM EDTA
10mM $NaH_2PO_4$ (pH 8.0)
0.5mg/ml yeast tRNA

Hybridisation buffer was stored at -20$^0$C and 1% 1M dithiothrietol (DTT) diluted with DEPC SDW was added to the final probe/buffer mixture. Probe was denatured at 80$^0$C for 2min., quenched on ice and aliquoted onto the sections which were covered with siliconised coverslips (see above). Slides were placed horizontally in a slide holding box containing tissue soaked in 50% formamide/5x SSC. The box was sealed with tape, placed inside 3 vacuum sealed bags and immersed in a 50$^0$C waterbath for overnight hybridisation.

## Washing

Post-hybridisation treatment consisted of:

1) Washes:

| | | | | |
|---|---|---|---|---|
| a) | Wash 1 | 5x SSC/0.01M DTT | 50$^0$C | 30min. |
| b) | Wash 2 | 2x SSC in 50% formamide/ 0. 1M DDT | 65$^0$C | 20min. |
| c) | Wash 3 | 0.5M NaCl/0.005M EDTA/ 0.01M Tris-HCl (pH 7.5) | 37$^0$C | 10min. (x3) |
| d) | RNAse A | 0.02mg/ml in Wash 3 | 37$^0$C | 30min. |
| e) | Wash 3 | | 37$^0$C | 15min. |
| f) | Wash 2 | | 65$^0$C | 20min. |
| g) | Wash 4 | 2x SSC | Room T$^0$ | 15min. |
| h) | Wash 5 | 0.1x SSC | Room T$^0$ | 15min. |

2) Dehydration:

| | | |
|---|---|---|
| D 1 | 75ml ethanol, 162.5ml water, 12.5ml 6M ammonium acetate | 30sec. |
| D 2 | 150ml ethanol, 87.5ml water, 12.5ml 6M ammonium acetate | 30sec. |
| D 3 | 200ml ethanol, 37.5ml water, 12.5ml 6M ammonium acetate | 30sec. |
| D 4 | 237.5ml ethanol, 12.5ml 6M ammonium acetate | 30sec. |

Slides were finally dehydrated through absolute alcohol for 2min. (x2) and air dried.

## Autoradiography

Slides were exposed against Cronex (DuPont) medical screen film inside a radiographic cassette at room temperature overnight. Intensity of developed image determined subsequent exposure times. Slides were dipped in a solution of Ilford K5 emulsion in a 1:1

ratio with distilled water containing 1.0% glycerol, at 42$^0$C. Slides were air dried for 4-6hr. and stored at 4$^0$C in light tight boxes containing a sachet of silica gel for the required exposure time. Exposure times were generally between 1-7 days.

## Digoxigenin (modifications)

Digoxigenin *in situ* protocol was identical to $^{35}$S protocol up to washing with the omission of DTT from the hybridisation buffer.

Washes:

| | | | | |
|---|---|---|---|---|
| 1) | Wash 1 | 2x SSC | 50$^0$C | 2.5hr. |
| 2) | Wash 2 | 2x SSC in 50% formamide | 50$^0$C | 1.5hr. |
| 3) | Wash 3 | 0.1x SSC | room temp | 30min. |
| 4) | Wash 4 | Tris pH7.5 | room temp | 15min. |

At room temperature, slides were then blocked with Tris pH7.5/10% foetal calf serum for 15min., incubated with anti DIG-AP (1:500) (see 2.3.1.Riboprobes) for 1hr., washed in Tris pH7.5 for 30min. and incubated with the substrate (see 2.3.1.Riboprobes) overnight.

Slides were wet mounted with 90% glycerol in PBS.

## Tissue culture (modifications)

After fixation in 4% paraformaldehyde (pre-treatment step 6) tissue culture coverslips were treated as for tissue sections, with the omission of the Proteinase K treatment. If coverslips had been immunostained previously, hybridisation time was reduced to 3.5hr. instead of overnight to reduce degradation of the fluorescent signal. Washes not at room temperature were also reduced by half apart from the RNase treatment.

# 2.4.IMMUNOCYTOCHEMISTRY

## 2.4.1.Tissue sections

### Peroxidase anti-peroxidase

#### Paraffin embedded tissue

Sections were initially hydrated:

| | | |
|---|---|---|
| 1) | Xylene | 2min. |
| 2) | Absolute alcohol | 2min. |
| 3) | Methylated spirit | 2min. |
| 4) | Water | 2min. |
| 5) | Iodine | 1min. |
| 6) | Water | 2min. |
| 7) | 5% sodium thiosulphate | 1min. |
| 8) | Water | 2min. |

Endogenous peroxidase activity was blocked by immersing the slides in 3% hydrogen peroxide in absolute alcohol for 30min., then washed in running water for 30min. Non-specific binding sites were blocked with 10% normal goat serum in PBS for 2hr. and the sections blotted dry. Sections were incubated at $4^0$C overnight with the primary antibody diluted in 1% normal goat serum in PBS.

Sections were warmed to room temperature, washed in 6 changes of PBS over 30min., and the secondary antibody (link) diluted in 1% normal goat serum in PBS added for 1hr. Sections were washed with 6 changes of PBS over 20min., and covered with the PAP complex diluted in 1% normal goat serum in PBS for 30min. Sections were washed with 6 changes of PBS over 20min., placed in 0.2M phosphate buffer (~ 80% $Na_2HPO_4$, ~ 20% $KH_2PO_4$ added to achieve pH 7.4) for 1min. and transferred for 20min. to a filtered solution of 50mg 3,4,3',4',-tetraminobiphenyl hydrochloride (DAB) in 50ml distilled water made up to 100ml with 0.2M phosphate buffer. 330µl 30% aqueous hydrogen peroxide was added to the DAB solution and the colour allowed to develop over 3-5min. Sections were washed in 0.2M phosphate buffer for 2min. and running water for 5min.

#### Resin embedded tissue

Resin was removed from the sections prior to hydrogen peroxide treatment by submerging the slides in sodium ethoxide solution (50% ripened sodium ethoxide solution in absolute alcohol). Removal was checked microscopically after 30min. and the sections washed 6 times in absolute alcohol and submerged in running water for 30min. Hydrogen peroxide

(3%) was made up in absolute alcohol for the resin-embedded slides. After endogenous peroxidase blocking, slides were treated as above.

Primary antibodies, their associated links and PAP complexes with dilutions and sources are detailed in Table 3

## Immunofluorescence

### Cryosections

Cryosections (15μm) were stained by single or double immunofluorescence. To demonstrate myelin proteins (PLP/DM-20, PLP, MBP) or neurofilaments (NF) the fixation and permeabilisation technique of Gow *et al.* ( 1994a) was used:

Sections were thawed and covered with Tris buffered saline (TBS) pH7.5 (25mM Tris pH7.5, 136mM NaCl, 2.6mM KCl) for 10min. Sections were fixed in 4% paraformaldehyde in PBS for 30min. and washed in PBS for 20min. (x2). Sections were permeabilised with 0.1% saponin (Sigma) in PBS for 30min. in a humidity chamber and excess solution removed with a tissue. Blocking buffer was applied for at least 30min. again in a humidity chamber. Blocking buffer consisted of:

2% bovine serum albumin (BSA/Fraction V ) (BDH)
0.1% porcine skin gelatin/type A (Sigma)
2% normal goat serum (NGS) (Scottish antibody production unit)
0.02% biotin (Sigma) (omit if using biotinylated secondary antibody)
0.1% saponin (Sigma)

Excess solution was removed with a tissue and the primary antibody applied overnight at $4^0$C in a humidity chamber. Antibody was diluted in the same blocking buffer but with 0.02% saponin. Sections were washed with PBS for 20min. (x3) and the secondary antibody, diluted as above, applied for 30min. at room temp. Sections were washed in PBS for 5min. (x2), water for 5min., and mounted in Citifluor antifade mountant (UKC Chem Lab).
To demonstrate the surface protein marker O4, sections were fixed in 2% paraformaldehyde in PBS for 5min., washed and the primary antibody applied for 1hr. at room temperature..

# 2.4.2.Tissue culture

## Immunofluorescence

Dissociated cell cultures were stained by single or double immunofluorescence. All primary and secondary antibodies were diluted with buffered staining solution (4% donor

calf serum, 0.05% azide in HEPES made up in Hank's buffered salt solution, $Ca^{2+}$, $Mg^{2+}$ free (HBSS) ). All incubations were carried out in closed staining trays.

For surface markers, coverslips were incubated with ~ 20µl of the primary antibody for 20min at room temp, washed 3 times in staining solution before the addition of ~ 20ml of the secondary antibody for 20min. followed by a further 3 washes. The procedure was repeated for double surface immunostaining.

For immunostaining with cytoplasmic markers after a surface marker, the surface stained cells were washed twice in buffered DMEM and fixed with 2% paraformaldehyde in DMEM for 30min. at room temperature. From that point the Gow's method was used as described above. Coverslips were mounted in Citifluor antifade mountant (UKC Chem Lab).

Immunostained coverslips for ISH or $^{3}H$ thymidine studies were fixed as appropriate and attached to slides as described previously (see 2.3.2.ISH Protocol). After ISH processing slides were dipped and developed as previously described (see 2.3.2.ISH Protocol) prior to sealing in Citifluor media under an additional coverslip.

All primary and secondary antibodies, with dilutions and sources are detailed in Table 4.

## PAP Immunostaining

| PRIMARY ANTIBODY | DILUTION | SOURCE | PAP COMPLEX | SOURCE | LINK |
|---|---|---|---|---|---|
| anti-MBP (polyclonal) | 1:400 | Dr.J.M.Matthieu, (Lausanne, Switzerland) | anti-Rabbit (1:400) | ICN | Goat-anti-Rabbit (1:10) |
| anti-PLP/DM-20 (PLP-CT) (amino acids 271-276) | 1:600 | Prof.N.P. Groome, (Oxford) | anti-Rabbit (1:400) | ICN | Goat-anti-Rabbit (1:10) |

**Table 1**. Antibodies, dilutions, sources and links used in PAP immunostaining.

## Fluorescent Immunostaining

| PRIMARY ANTIBODY | DILUTION | SOURCE | SECONDARY ANTIBODY | DILUTION | SOURCE |
|---|---|---|---|---|---|
| anti-PLP/DM-20 (PLP-CT) (a.a 271-276) | 1:600 | Prof.N.P. Groome, (Oxford, UK) | Goat-anti-Rabbit-IgG FITC/TxR | 1:80/1:200 | S. Biotech |
| anti-PLP specific (a.a 117-129) | 1:600 | Dr.J.C.Nussbaum, (Strasbourg, France) | Goat-anti-Rabbit-IgG FITC/TxR | 1:80/1:200 | S. Biotech |
| anti-MBP (monoclonal) | 1:400 | Prof.N.P. Groome, (Oxford, UK) | Goat-anti-Rat-IgG-FITC | 1:50-60 | S. Biotech |
| anti-A2B5,O4,O1 | 1:3 | Dr.I. Sommer, (Glasgow, UK) | Goat-anti-Mouse-IgM-TxR | 1:50 | S. Biotech |
| Ranscht (RmAb) | 1:3 | Dr.I. Sommer, (Glasgow, UK) | Goat-anti-Mouse $IgG_3$-TxR | 1:100 | S. Biotech |
| anti-GFAP (monoclonal) | 1:1000 | Sigma | Goat-anti-Mouse-$IgG_1$-TxR | 1:80 | S. Biotech |
| anti-Neurofilaments (SMI-31) | 1:1,500 | Affiniti | Goat-anti-Mouse-$IgG_1$-TxR | 1:80 | S. Biotech |
| anti-Neurofilaments (NF2H3) | 1:15,000 | DSHB | Goat-anti-Mouse-IgG-TxR | 1:50 | S. Biotech |
| anti-β Tubulin III | 1:200 | Sigma | Goat-anti-Mouse-IgG-TxR | 1:50 | S. Biotech |
| anti-S100 (monoclonal) | 1:300 | Affiniti | Goat-anti-Mouse-$IgG_1$-TxR | 1:80 | S. Biotech |

**Table 2.** Antibodies, dilutions, sources and secondary antibodies used in immunofluorescence

# 2.5.MORPHOMETRY

## 2.5.1.Glial cell quantification

All cell counting was performed on 1μm resin embedded sections, stained with methylene blue/azure II. Cells in selected areas (see below) were counted using a 6.3X eyepiece lens, a 100X oil immersion lens and a 100 square graticule (Graticules Ltd.). A minimum of 600 squares were counted for each area. Total cell counts included precursor cells, oligodendrocytes, astrocytes and microglia. Endothelial cells were not counted. Cells were only counted when an intact nucleus could be seen. Longitudinal sections taken at right angles to the counting sections allowed estimation of maximum and mean glial nuclear length. The length of 50 cells in the appropriate field were counted. Where multiple sections were needed, serial sections were cut at a separation greater than the maximum glial cell length. Areas of sections were calculated from Polaroid light microscopy images with appropriate calibration standards using Sigma Scan™/Image image measurement software (Jandel Scientific Software) and a Summa Sketch III graphics tablet (Summagraphics). Corrected total glial cell counts and glial cell densities were calculated using Abercrombie's formula as discussed by Sturrock (1983). Three animals were counted for each area and data was plotted using Graphpad Prism software (Graphpad Software Inc.).

| | **Area counted** | **Section** |
|---|---|---|
| a) | Spinal cord ventral columns | Transverse/proximal cervical intumescence |
| | | Transverse/mid thoracic cord |
| | | Transverse/proximal lumbar intumescence |
| b) | Optic nerve | Transverse/mid optic nerve |

# 2.6.TISSUE CULTURE

## 2.6.1.Tissue preparation

### Spinal cords

The method used is that described by Fanarraga *et al.* (1993). Spinal cords were dissected from embryos into HBSS medium and nerve roots, ganglia and meninges completely removed. Tissue was minced with a No.10 scalpel blade, transferred to a sterile centrifuge tube with ~ 900µl collagenase solution and incubated at $37^0$C for 30-45min.
The tube was centrifuged at 1000 rpm. for 3min. at room temperature and the supernatant removed. 1ml. of 0.05% trypsin/0.02% EDTA solution was added to the pellet and incubated at $37^0$C for 30min followed by 1ml SD solution for 2min. to stop enzymatic activity and prevent cell clumping. The suspension was centrifuged at 1000 rpm. for 3min. at room temperature, the supernatant removed and the cells mechanically dissociated by trituration in warm HBSS through decreasing gauge needles (21G, 23G, 25G, and 27G).
The suspension was centrifuged at 1000rpm. for 10min. at room temperature and the pellet reconstituted in ~ 200µl 50% HBSS/50% Bottenstein and Sato medium (Bottenstein and Sato 1979) + 0.4% foetal calf serum (FCS). Cell density was calculated using a Levy counting chamber with a Neubauer ruling and cell numbers adjusted to 3-4,000,000/ml with the same medium. Cells were plated at 60-80,000 (~ 20µl) per 13mm poly-L-lysine coated coverslip placed inside Linbro 24 well plates (Flow Laboratories) and incubated at $37^0$C/5% $CO_2$ until cells attached (10-30min.). Cultures were fed with 600µl Bottenstein Sato 0.4% FCS and maintained at $37^0$C/5% $CO_2$ for up to 48hr. All solutions were prewarmed to $37^0$C prior to use.

### Spinal roots and ganglia

Spinal roots and ganglia dissected from the spinal cords were cultured as described above.

### Olfactory bulbs

Olfactory bulbs were dissected from P1 mice into L15 medium and the meninges removed. Cultures were performed as described above with the following exceptions. Collagenase solution was diluted 1:1 with L15 and incubated for 1hr and trypsin/EDTA treatment was omitted. Cultures were resuspended and fed with Dulbecco's modified Eagle medium (DMEM)/10% FCS rather than SATO medium.

## 2.6.2.Thymidine incorporation

In some studies, 3μCi $^{3}H$ thymidine (Amersham) per 0.5ml. medium was added to embryonic day 12 (E12) cultures for 1hr. immediately after plating. Fresh medium was then added for survival times of 1, 24 or 48hr. after radiolabelling.

## 2.6.3.Solutions

1) Hanks' balanced salt solution (HBSS):

$Ca^{2+}$, $Mg^{2+}$ free solution (Sigma) to prevent enzyme inactivation.

2) Collagenase:

50mg/ml stock solution/~200 units/mg collagenase (Couper biomedical) in HBSS. 200μl aliquots stored at -20$^{0}$C and diluted 1:3 with HBSS

3) Trypsin/EDTA:

0.1% trypsin (Flow laboratories) solution in HBSS, 0.04% EDTA (Flow laboratories) in HBSS. 0.5ml. aliquots stored at -20$^{0}$C mixed 1:1 for use.

4) SD solution:

0.52mg/ml soybean trypsin inhibitor (SD) (Sigma)
0.04mg/ml bovine pancreas DNAse (Sigma)
3mg/ml factor V bovine serum albumin (Sigma)

Made up in L15/HBSS, 1ml. aliquots stored at -20$^{0}$C.

5) Bottenstein Sato media:

| | |
|---|---|
| 1g/l | glucose |
| 2mM | glutamine (Sigma) |
| 10μg/ml | insulin (bovine/27.3 U/mg) (Sigma) |
| 100μg/ml | transferrin (human) (Sigma) |
| 0.0286% | BSA-pathocyte (ICN) |
| 0.2μM | progesterone (Sigma) |
| 0.1mM | putrescine (Sigma) |
| 0.45μM | thyroxine (Sigma) |
| 0.224μM | selenite (Sigma) |
| 0.5μM | tri-iodo-thyronine (Sigma) |

Made up in DMEM, 30ml aliquots stored at -20$^{0}$C.

## Poly-L lysine coverslips

Coverslips were coated with poly-L-lysine to encourage cell adhesion (Mazia *et al.* 1975) and were prepared as follows:

1) Wash in 70% alcohol
2) Rinse in distilled water
3) Soak in 1M nitric acid overnight
4) Rinse in distilled water
5) Rinse in absolute alcohol
6) Separate individually and air dry on filter paper
7) Autoclave (20min. 15lb/sq. in)
8) Immerse in poly-L-lysine (100μg/ml in SDW) (Sigma) for 30min.
9) Rinse in SDW x2
10) Air dry

Coverslips were stored at room temperature prior to poly-L-lysine treatment, or at $-20^{0}$C after treatment. After autoclaving, all procedures were performed in a tissue culture hood.

# CHAPTER 3. RESULTS

# 3.1.SUBCLONING OF THE MOUSE *plp* SPECIFIC SEQUENCE

## 3.1.1.Background

At the level of immunodetection or ISH performed on tissue sections or cells, only PLP protein or transcripts can be individually identified by the use of antibodies or probes directed against the exon 3B region of the protein or transcript. Since DM-20 differs from PLP only by the deletion of the 35 amino acids (105 base pairs) coded by exon 3B it is not possible to generate DM-20 specific antibodies or probes. The presence of DM-20 may be inferred by differential methods if a difference is seen using an antibody/probe recognising PLP and DM-20 or a PLP specific antibody/probe. This approach must be treated with some caution as other factors such as different avidity or affinity of antisera or differing availability of the target antigens could also affect differential staining during immunocytochemistry. Likewise during ISH there may be variation in activity and hybridisation kinetics of specific and non-specific probes.

Identification of *dm-20* transcripts on northern blots has been performed using a probe that is complementary to the exon 3A/4 junctional region. Although both the exon 3A and exon 4 sequences are present in *plp* RNA, it is only in *dm-20* RNA that they are contiguous. This method relies on using stringent hybridisation and washing conditions which will favour hybridisation to *dm-20* transcripts (Ikenaka *et al.* 1988; LeVine *et al.* 1990). A similar strategy has been employed for immunostaining by generating antibodies to a variety of junctional peptides bridging the exon 3A/4 boundary. As yet this approach has proved unsuccessful *in vivo* (N. Groome, unpublished).

An anti-C-terminal antiserum raised against residues 271-276 reacting with both PLP and DM-20 and a PLP specific antiserum raised against amino acids 117-129 were available for use and have been described elsewhere (Fanarraga *et al.* 1993). A plasmid containing *plp* sequence for the generation of riboprobes hybridising to both *plp* and *dm-20* transcripts (PLP-1) (Griffiths *et al.* 1989) was also available, however it was judged advantageous to produce a *plp* specific riboprobe vector for use in differential ISH studies as described above.

## 3.1.2.Experimental strategy

A 2.2kb *Bam HI* restriction fragment containing the complete coding sequence plus some $5^{/}$ and $3^{/}$ untranslated region (UTR) was obtained from the low copy number, Okayama/Berg fragment plasmid pC4 (Nave *et al.* 1986). The fragment was gel isolated from a 1% standard agarose gel using a Qiaex extraction kit (see 2.2.1.Core techniques). The fragment was ligated into the high copy number vector pBluescript II (Stratagene) following *Bam* HI digestion and CIP treatment of the plasmid (see 2.2.1.Core techniques). Transformation of JM101 competent cells and plasmid mini/maxi-preps were performed as

described in methods (see 2.2.1.Core techniques) and insertion confirmed by liberation of the fragment following *Bam* HI digestion. This plasmid was termed pBluescript-PLP.
A *Sau* 96I/*Bfa* I, 81 bp fragment from exon 3B was isolated from pBluescript PLP and subcloned into pGEM 3z (Promega) according to the following strategy:

1) 40μg pBluescript-PLP was digested with *Bfa* I and a 413 bp *Bfa* I fragment containing the desired sequence was gel isolated from a 2% TBE Metaphor gel and Qiaex extraction kit (Figure 8).
2) 2.5μg *Bfa* I fragment was digested with *Sau* 96I to liberate the desired sequence, and with *Hae* II to digest a fragment of similar size to maximise resolution. (Figure 9). The sequence was isolated from a 5% TBE Metaphor gel as above.

The fragment was Klenow treated to produce flush ends and blunt ligated into the pGEM 3z plasmid vector following *Sma* I digestion and CIP treatment of the plasmid (see 2.2.1.Core techniques). The plasmid was termed pPLP-3B. Transformation of competent JM101 cells and plasmid mini/maxi-preps were performed as described in 2.2.1.Core techniques, and presence of insert was confirmed by release of fragment and presence of an insert specific *Bsr* BI restriction site on diagnostic digests (Figure 10, Figure 11).
Fragment orientation was deduced from *Eco* RI/*Hin* dIII/*Bsr* BI, *Eco* RI/*Bsr* BI and *Hin* dIII/*Bsr* BI restriction digests exploiting the asymmetric position of the *Bsr* BI site in the fragment (Figure 12, Figure 13). Both digests indicated $3' \rightarrow 5'$ orientation. Generation of sense probes would therefore be possible using the SP6 promoter after linearising the plasmid with *Eco* RI and antisense probes using the T7 promoter following *Xba* I digestion.

Operational specificity of the pPLP-3B probe was confirmed by Southern blotting of PCR product generated from *plp* specific (pC4) and *dm-20* specific (pC11) plasmids and from a 15 day old wild type brain cDNA library (Figure 14). Generation of $^{32}P$ random labelled probe using the "High Prime" DNA labelling kit (Boehringer Mannheim), blotting and hybridisation were as previously described (see 2.2.3.Southern blotting (pPLP-3B probe specificity confirmation)). The autoradiograph was exposed for 5 hours and additional film was overexposed for 24 hours to confirm absence of significant hybridisation to *dm-20* RT-PCR product.

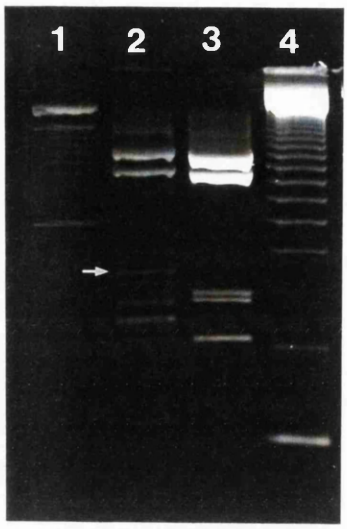


**(a)**

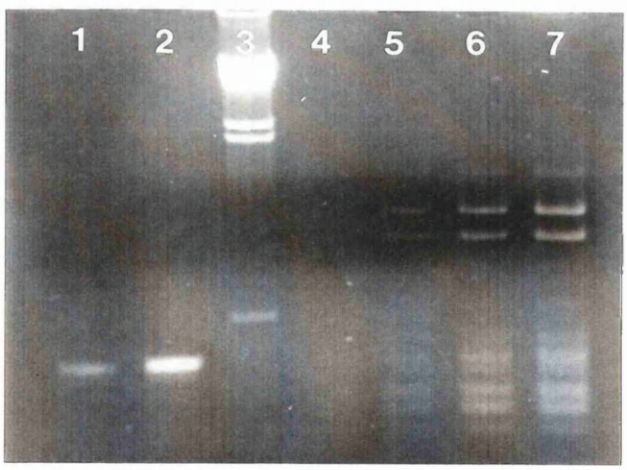


**(b)**

**Figure 8.** **a)** *Bfa* I digest of pBluescript-PLP. Lane **1** 100 bp calibration ladder; Lane **2** pBluescript-PLP/*Bfa* I digest; Lane **3** pBluescript II/*Bfa* I digest; Lane **4** 123 bp calibration ladder. The 413 bp *Bfa* I fragment containing the insert is arrowed. **b)** Qiaex isolated *Bfa* I fragment (lanes **1** and **2**), Lane **3** λ *Hin* dIII marker; Lanes **4-7** fragment quantification standards comprising pBluescript-PLP/*Bfa* I digests of known amounts.

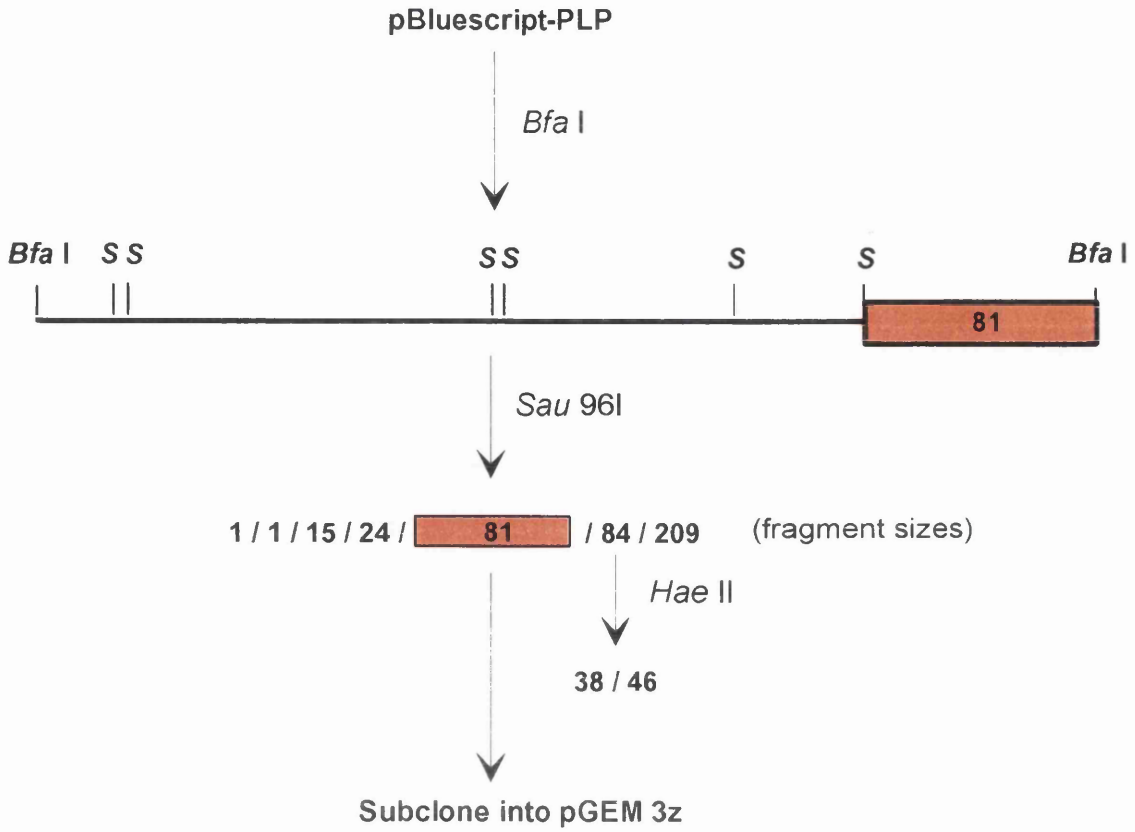


**(a)**

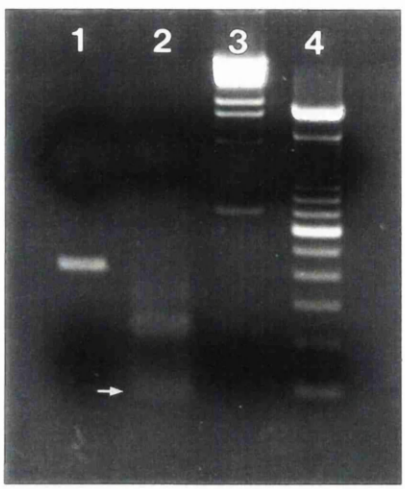


**(b)**

**Figure 9. a)** Schematic diagram of subcloning strategy for *plp* specific probe. S= *Sau* 96I restriction sites. **b)** *Sau* 96I/*Hae* II digestion of initial *Bfa* I fragment; Lane **1** *Bfa* I fragment; Lane **2** *Sau* 96I/*Hae* II digest; Lane **3** λ/*Bst* EII marker; Lane **4** 100 bp calibration ladder. Final 81bp fragment to be isolated is arrowed.

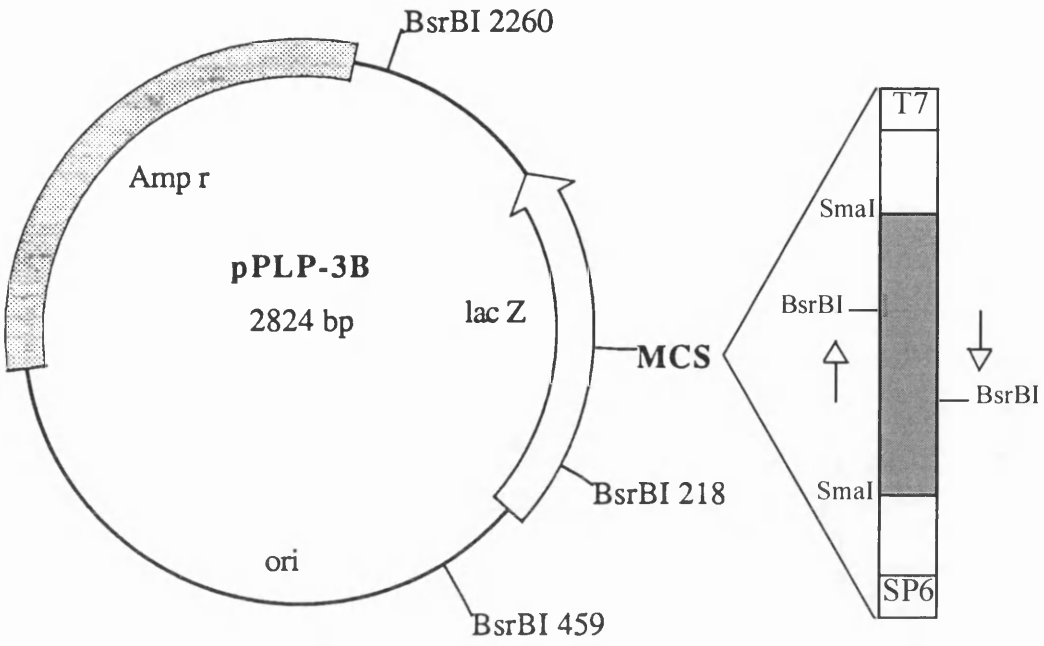


## *Bsr* BI restriction profile

| pGEM 3z | pPLP-3B (insert 5′-3′) | pPLP-3B (insert 3′-5′) |
|---|---|---|
| 241/**701**/1801 | **144**/241/**638**/1801 | **165**/241/**617**/1801 |

**Figure 10.** pPLP-3B plasmid map showing *Bsr* BI restriction sites. Position of insert in the multiple cloning site (MCS) is shown as a shaded area. Diagnostic *Bsr* BI restriction profile is shown below. Differing fragment sizes are shown in bold.

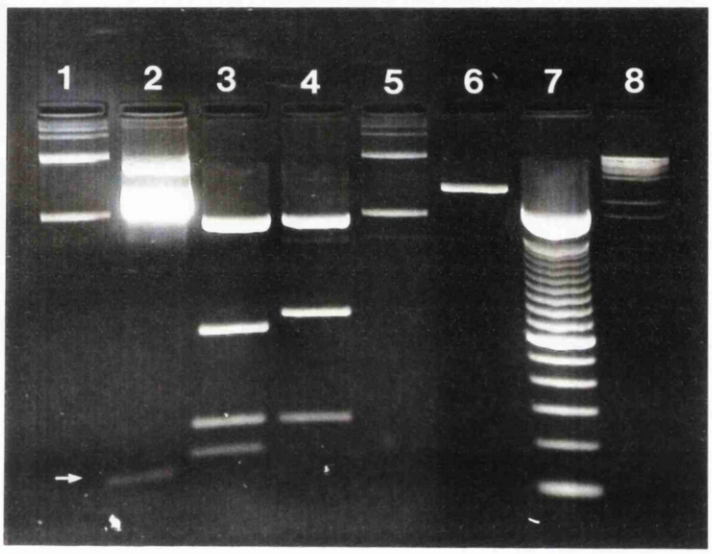


**Figure 11.** pPLP-3B/*Bsr* BI digest; Lane **1** undigested pPLP-3B, Lane **2** pPLP-3B/*Eco* RI/*Pst* I digest showing liberated insert (arrow), Lane **3** pPLP-3B/*Bsr* BI digest, Lane **4** pGEM 3z/*Bsr* BI digest, Lane **5** undigested pGEM 3z, Lane **6** pGEM 3z/*Eco* RI digest, Lane **7** 100 bp calibration ladder, Lane **8** λ/*Bst* EII marker.

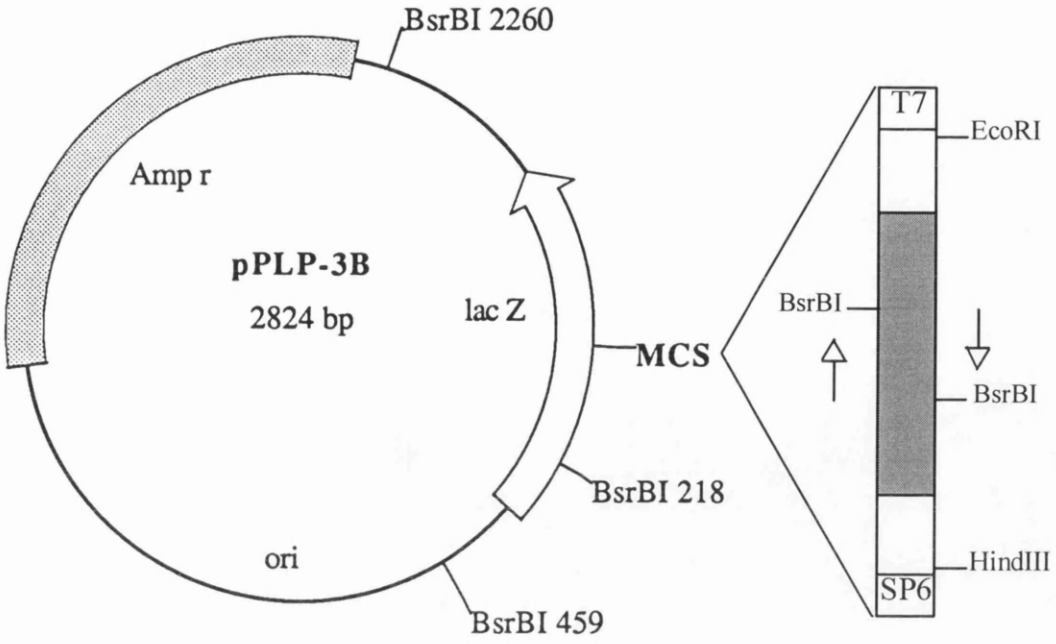


## *Eco* RI/*Hin* dIII/*Bsr* BI restriction profile

| pPLP-3B (insert 5′-3′) | pPLP-3B (insert 3′-5′) |
|---|---|
| **68**/**69**/76/241/569/1801 | **48**/76/**89**/241/569/1801 |

## *Eco* RI/*Bsr* BI restriction profile

| pPLP-3B (insert 5′-3′) | pPLP-3B (insert 3′-5′) |
|---|---|
| **69**/**144**/241/569/1801 | **48**/**165**/241/569/1801 |

## *Hin* dIII/*Bsr* BI restriction profile

| pPLP-3B (insert 5′-3′) | pPLP-3B (insert 3′-5′) |
|---|---|
| **68**/76/241/**638**/1801 | 76/**89**/241/**617**/1801 |

**Figure 12.** pPLP-3B plasmid map showing *Bsr* BI, *Eco* RI *and Hin* dIII restriction sites. Diagnostic *Bsr* BI/*Eco* RI/*Hin* dIII restriction profiles to determine insert orientation are shown below. Differing fragment sizes are shown in bold.

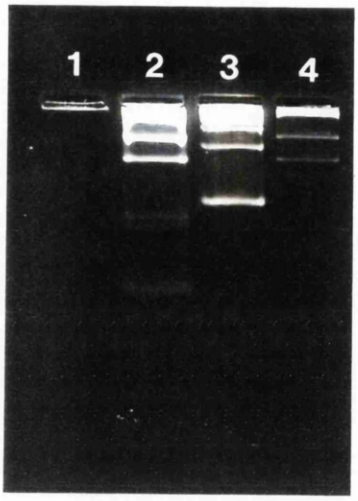


(a)

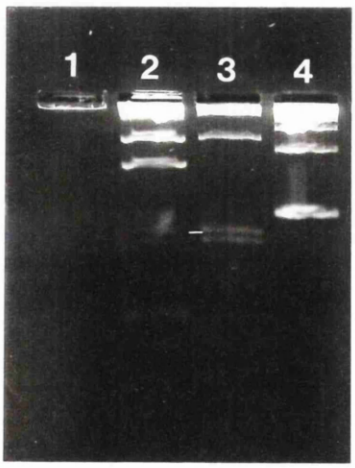


(b)

**Figure 13.** pPLP-3B insert orientation digests. **a)** *Eco* RI/*Hin* dIII/*Bsr* BI digest; Lane **1** undigested pPLP-3B, Lane **2** pPLP-3B/*Eco* RI/*Hin* dIII/*Bsr* BI digest, Lane **3** 100 bp calibration ladder, Lane **4** pPLP-3B/*Bsr* BI digest. **b)** *Eco* RI/*Bsr* BI and *Hin* dIII/*Bsr* BI digests; Lane **1** undigested pPLP-3B, Lane **2** pPLP-3B *Eco* RI/*Bsr* BI digest, Lane **3** pPLP-3B *Hin* dIII/*Bsr* BI digest, Lane **4** 100 bp calibration ladder.

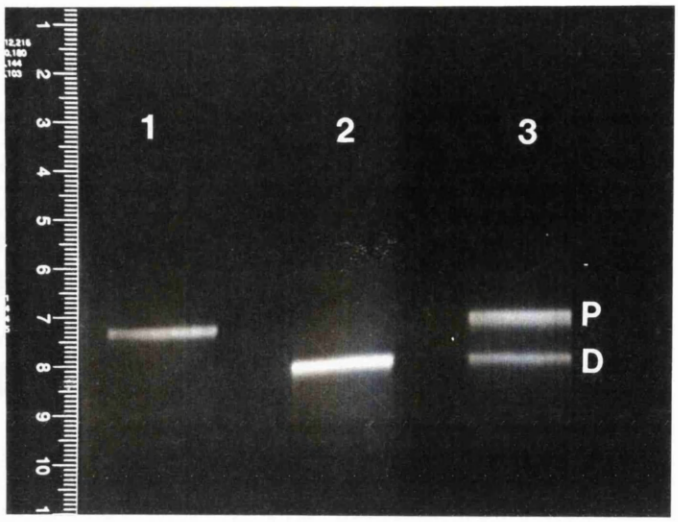


(a)


(b)

**Figure 14.** pPLP-3B $^{32}$P Southern blot (5 hour exposure). **a)** Gel prior to blotting; Lane **1** pC4 (*plp*) PCR product, Lane **2** pC11 (*dm-20*) PCR product, Lane **3** 15 day mouse brain RT-PCR product. *plp* product (**P**), *dm-20* product (**D**). **b)** Southern blot autoradiograph; PLP-3B labelled probe is hybridised with pC4 (*plp*) PCR product (**P**) and with the upper *plp* band of the 15 day brain RT-PCR product. No significant hybridisation to either pC11 (*dm-20*) product (**D**), or the lower *dm-20* band of the 15 day brain product is seen.

# 3.2.*Plp* GENE EXPRESSION STUDIES

## 3.2.1.*Plp/dm-20* transcript ratio studies

### Introduction and aims

In general terms, the level of total *plp* transcripts defined by dot or northern blotting appears to parallel myelination within a particular region (Gardinier *et al.* 1986; LeVine *et al.* 1990; Naismith *et al.* 1985; Sorg *et al.* 1987). It has also been shown using RT-PCR that *dm-20* is the only isoform expressed in the embryonic rodent brain and that *plp* becomes the dominant transcript during post-natal life (Ikenaka *et al.* 1992; Timsit *et al.* 1992a). All these studies however have used bulk tissue samples, at the best limiting tissue to gross areas such as the cerebrum or hindbrain. As discussed in the introduction the myelination state of specific tracts within these gross areas will be highly varied thus making it difficult to make comments in relation to myelination status other than in general terms. The change in *plp/dm-20* transcript ratio is interesting, given the probable different roles of the two subsequent isoproteins, and in order to study the precise relationship between transcript ratio and state of myelination and gliogenesis, more discreet areas with a more uniform state of myelination should be chosen.

Initial studies were performed on bulk mouse spinal cord and brain samples to give an appreciation of times of onset of expression and general trends in transcript ratios. Specific areas of the CNS were then chosen which were known to have different times of onset of myelination. The ventral columns of the spinal cord is the first area of the CNS to myelinate beginning around birth (Bjartmar *et al.* 1994) and could further be divided into cervical, thoracic and lumbar regions since myelination proceeds temporally in a rostral to caudal direction in the spinal cord (Schwab and Schnell 1989; Tilney 1933). The optic nerve begins myelinating approximately 6-7 days later and this was chosen as an example of a later myelinating area. In an attempt to eliminate some of the heterogeneity in myelination present even within the optic nerve as a whole (Skoff *et al.* 1980), the study was limited to the mid third portion of the nerve. The main aim of the study was to determine whether changes in *plp/dm-20* transcript ratios were associated with age of the animal or "age" of myelination. We hypothesised that changes in the ratio would be associated with myelination status and would therefore occur at different chronological times in areas with different times of onset of myelination. As well as demonstration of myelin sheaths by light microscopy and at the earliest time points by electron microscopy, other markers of myelination such as *plp/dm-20* expression in oligodendrocytes on ISH, appearance of PLP/DM-20 protein as demonstrated by immunocytochemistry and changes in glial cell densities were also studied.

## PCR calibration

RT-PCR is an invaluable technique for the analysis of gene expression using mRNA/cDNA hybrids as template for PCR amplification. This is particularly useful when analysing low abundance mRNAs such as *plp/dm-20* transcripts in the embryo, or when limiting amounts of material are available such as spinal cord ventral columns or mid third optic nerves.

Such a powerful technique is however not without its problems. The exponential nature of PCR amplification means that initially small artefacts may generate significant false positive results. Contamination of reactions with target DNA either in the form of previously amplified material, or positive control template is a significant operational problem. Contamination can be minimised by the use of dedicated laboratory equipment, filter pipette tips and ultraviolet irradiation of equipment and reagents (excluding primers and target). Set up and analysis of PCR reactions should be performed in separate, dedicated areas and all PCR runs should include negative controls consisting of all reagents minus target.

In addition to looking at *plp/dm-20* transcript ratios, relative transcriptional activity over a series of ages was studied in whole spinal cord and mid third optic nerve. Conventional methods of studying spatio-temporal expression of genes such as northern blotting and transcript mapping have the disadvantage of requiring relatively large amounts of mRNA as starting material. Semi-quantitative RT-PCR allows for the indirect analysis of much smaller amounts of mRNA and is therefore particularly useful when looking at expression of genes such as *plp,* when mRNA is present in low abundance. Semi-quantitative RT-PCR as a means of measuring transcriptional activity has its disadvantages; it is an indirect measurement of transcriptional activity (through the intermediate step of an mRNA/cDNA hybrid), unlike northern blotting or transcript mapping; secondly, the possibility of generating false positive results is higher as is the possibility of underestimating transcriptional activity due to exhaustion of the system or the plateau effect. Reactions will plateau when amplification is no longer exponential. This will occur relatively sooner for samples with higher target concentrations leading to an underestimation of transcript levels. The same problem may occur within a sample when looking at the relative ratio of two isoforms such as *plp* and *dm-20* and is most likely to be a problem where transcriptional activity is very high. As with direct methods of measuring transcriptional activity, it is necessary to ensure processing of equivalent amounts of the tissues being compared during RT-PCR analysis. This is achieved by the amplification of an internal control target in parallel with the target being studied. Ideally this control target will be derived from a constitutively expressed gene such as cyclophilin.

Semi-quantitative RT-PCR was considered to be the only practical way of studying *plp/dm-20* transcript ratios and activity during embryonic and early post natal life due to the low abundance of transcripts. The limitations of the system as described above mean

that data generated should be interpreted in terms of general trends as opposed to finite values.

**Transcript ratio**

Before analysing data it was essential to confirm that under the specific range of PCR conditions to be employed, the ratio of *plp/dm-20* RT-PCR product was a true reflection of the initial *plp/dm-20* transcript ratio. Several factors could potentially lead to anomalous results; differences in efficiency of primer annealing, presence of exonuclease activity, susceptibility to template reannealing and time to reach plateau (the time at which amplification is no longer exponential) could all potentially result in altered product ratios. Two plasmids, pC4 and pC11 containing *plp* and *dm-20* specific cDNAs respectively, were quantified spectrophotometrically and linearised with *Sal* I. The relative concentrations were further confirmed by standard agarose gel analysis (Figure 15). Varying ratios of the linearised plasmids (4:1,1:1,1:4) were used as target in PCR reactions between 10 and 40 cycles. Product ratio was analysed using standard agarose gels (Figure 16). A 4:1 target ratio was also used with variation in magnesium concentration (1.5mM-4.5mM) at a constant 25 cycles to check for product ratio variation with magnesium concentration (Figure 15).
The following conclusions were drawn:

Under the standard PCR conditions used (see 2.2.2.Analysis of transcripts):

**1**) Fidelity of *plp/dm-20* product ratio to *plp/dm-20* plasmid input ratio appeared to be high even up to 40 cycles, although slight drift with apparent favouring of *dm-20* product was occasionally seen at the highest cycle numbers.

**2**) Fidelity of *plp/dm-20* product ratio to *plp/dm-20* plasmid input ratio appeared to be high with variations in magnesium concentration at cycle numbers less than 40.

It was therefore decided to employ a cycle number of less than 40, and that when high cycle numbers were used (for sensitivity purposes), the ratios would be confirmed at lower cycle numbers.

**RT-PCR product**

Recent investigations have demonstrated the likelihood of a DM-20-like family of proteins (Kitagawa *et al.* 1993; Yan *et al.* 1993). It was therefore considered necessary to ensure that the PCR product generated was from genuine *plp/dm-20* transcripts. Evidence to support this was threefold:

1) Products generated were of the correct size (*plp*-506/*dm-20*-401) as predicted from *plp* sequence data (Figure 7).
2) Computer-assisted analysis of primers and known mouse *dm-20*-like sequences (M6a/M6b) demonstrated insufficient sequence identity for the generation of stable hybrids at the PCR annealing temperatures used. Even excepting this fact, products generated would not have been of a similar length to those predicted for *plp/dm-20*.
3) *Plp* and *dm-20* RT-PCR products were gel isolated and diagnostic digests performed using 6 restriction enzymes known to have one or more recognition sequences within the predicted fragment. Despite the presence of partial digestion with 3 of the 12 enzymes, all restriction profiles were in agreement with those from predicted sequence data. (Figure 17, Figure 18).

The presence of high molecular weight RT-PCR bands when using *plp* primers has been reported (Ikenaka *et al.* 1992; Timsit *et al.* 1992a) and was also noted in the present studies (e.g. Figure 22). Whether these products represent RT-PCR artefacts or novel transcripts is yet to be resolved, however their presence was noted when pC4 plasmid was used as template which would suggest that RT-PCR artefact is the more likely explanation.

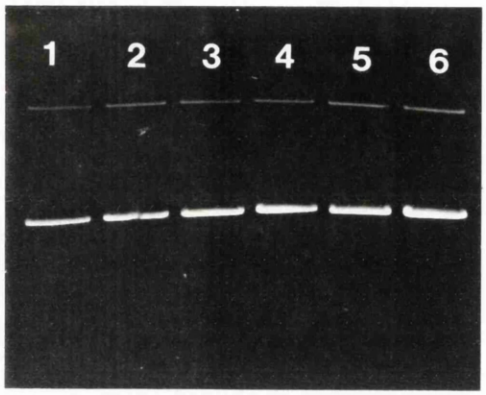


(a)

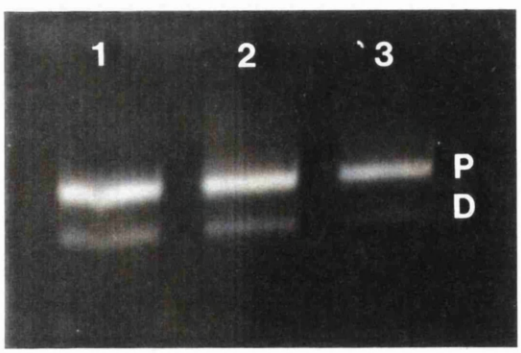


(b)

**Figure 15.** PCR calibration of input/output *plp/dm-20* ratio. **a)** Quantification of plasmid target: Upper bands; Lanes **1-3** and **5-6** pC11/*Sal* I 12.25ng, 18.75ng, 25ng, 31.25ng, 37.5ng; Lane **4** pC4/*Sal* I 25ng. Lower bands; Lanes **1-3** and **5-6** pC11/*Sal* I 50ng, 75ng, 100ng, 125ng, 150ng; Lane **4** pC4/*Sal* I 100ng. **b)** Magnesium assay confirming fidelity of *plp/dm-20* product ratio; Lanes **1-3** pC4/pC11 target ratio 4:1, Mg concentrations 1.5mM, 3.0mM, 4.5mM. *Plp* product (**P**), *dm-20* product (**D**).

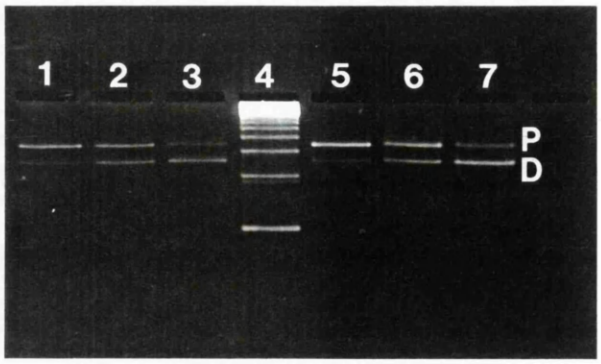


**(a)**

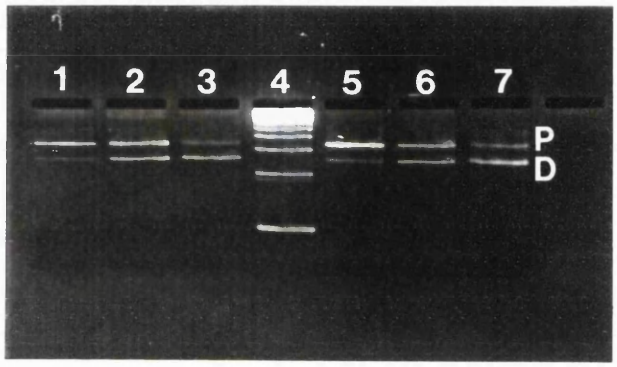


**(b)**

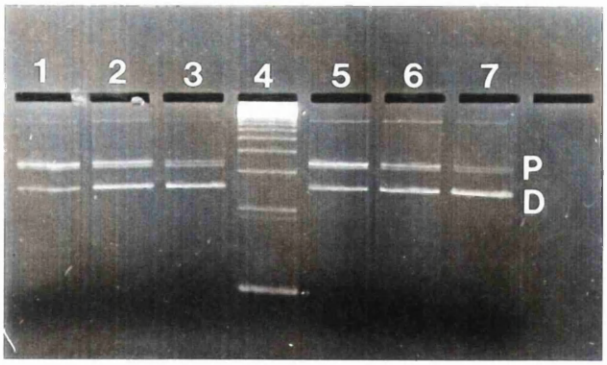


**(c)**

**Figure 16.** PCR calibration of input/output *plp/dm-20* ratio (cont.). *Plp* and *dm-20* PCR product from 10, 15, 20, 25, 30 and 40 cycle reactions. **a)** 10 and 15 cycles, **b)** 20 and 25 cycles, **c)** 30 and 40 cycles. Lanes **1-3** 4:1, 1:1, 1:4 pC4/pC11 target ratios; Lane **4** 123 bp calibration ladder; Lanes **5-7** 4:1, 1:1, 1:4 pC4/pC11 target ratios. Fidelity of input to output ratios is maintained over the cycle range. *Plp* product (P), *dm-20* product (**D**).

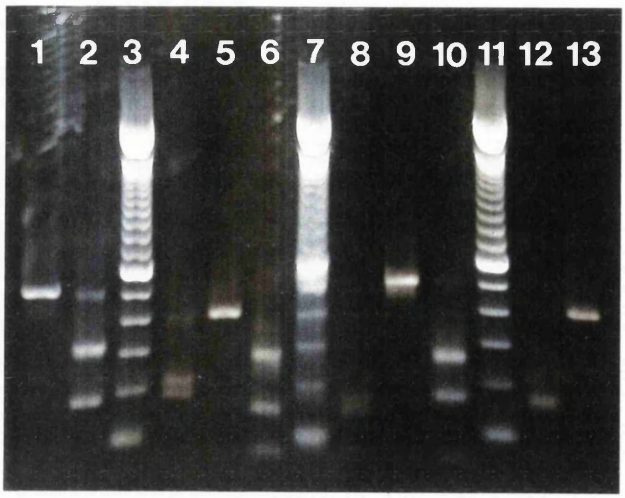


**Predicted *plp/dm-20* RT-PCR product restriction profiles**

| Restriction enzyme | *plp* | *dm-20* |
|---|---|---|
| *Bgl* II | 181/324 | 181/220 |
| *Dde* I | 74/148/283 | 74/148/179 |
| *Hha* I | 16/57/171/261 | 16/57/156/171 |

**Figure 17.** Restriction analysis of *plp/dm-20* RT-PCR products. Lanes **1,9** undigested *plp* product, Lanes **5,13** undigested *dm-20* product, Lanes **3,7,11** 100bp DNA calibration ladder, Lane **2** *plp*/*Bgl* II digest, Lane **4** *dm-20*/*Bgl* II digest Lane **6** *plp*/*Dde* I digest, Lane **8** *dm-20*/*Dde* I digest, Lane **10** *plp*/*Hha* I digest, Lane **12** *dm-20*/*Hha* I digest. Predicted restriction profiles are shown below.

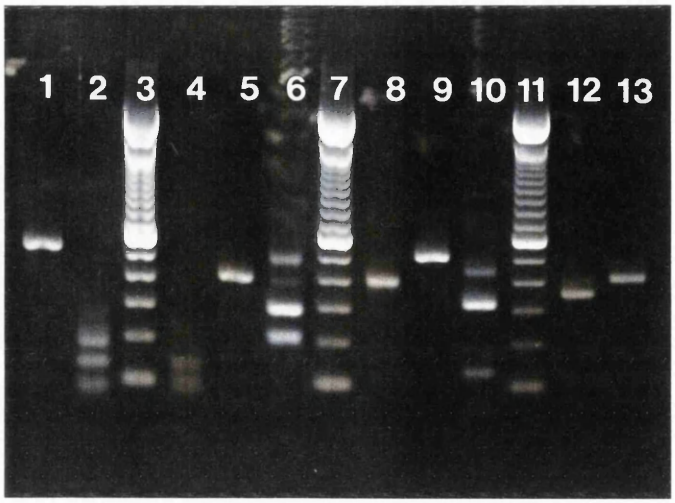


**Predicted *plp/dm-20* RT-PCR product restriction profiles**

| **Restriction enzyme** | ***plp*** | ***dm-20*** |
|---|---|---|
| *Sau* 96I | 1/24/78/84/133/185 | 1/78/84/105/133 |
| *Bsr* BI | 212/293 | 401 (undigested) |
| *Bfa* I | 51/133/321 | 51/350 |

**Figure 18.** Restriction analysis of *plp/dm-20* RT-PCR products (cont.). Lanes **1,9** undigested *plp* product, Lanes **5,13** undigested *dm-20* product, Lanes **3,7,11** 100bp DNA calibration ladder. Lane **2** *plp/Sau* 96I digest, Lane **4** *dm-20/Sau* 96I digest Lane **6** *plp/Bsr* BI digest, Lane **8** *dm-20/Bsr* BI digest, Lane **10** *plp/Bfa* I digest, Lane **12** *dm-20/Bfa* I digest. Predicted restriction profiles are shown below.

## Materials and methods

Studies were performed on C3H/HeH x 101H mice at the following ages; embryonic day 12 (E12), 14, 16, 18, and post-natal day 1 (P1), 5, 10, 15, 20 and 25. Intermediate ages were studied if considered necessary. The stage of embryonic development was timed from the appearance of cervical plugs after timed matings and also from crown/rump measurements in older embryos and somite counts of younger embryos. Mice were time mated for 3 hours each morning and animals with plugs were recorded as E0. Post-natal animals were recorded as post-natal day 1 (P1) on the day of birth.

Bulk brain and spinal cord samples for RT-PCR analysis (E12-P20) were dissected free of meninges, nerve roots and ganglia and processed as described in methods (see 2.2.2.Analysis of transcripts). To allow more accurate dissection, spinal cord ventral columns (E18-P20) were collected from 2 thin slices of Carnoy's-fixed material taken from proximal cervical intumescence, mid thoracic cord and proximal lumbar intumescence. Mid third optic nerve (P1-P20) was collected from both fresh and Carnoy's-fixed material. All samples collected from fixed tissue were subsequently processed as for fresh material. Semi-quantitative analysis of transcripts was performed on whole spinal cord and fresh mid third optic nerve using cyclophilin primers as an internal control. Densitometric analysis of the ethidium bromide stained signals was determined from Polaroid negative images using a Chromoscan 3 densitometer (Joyce Lobel). *Plp* and *dm-20* values were corrected for variation in gel loading. Standardised incremental aliquots of one cyclophilin RT-PCR product were assayed against test samples to determine if readings were within the linear range of the densitometer.

ISH studies were performed on paraffin sections of post-natal mice with $^{35}S$ and digoxigenin-labelled riboprobes recognising *plp* and *dm-20* transcripts (PLP-1) (see 2.3.IN *SITU* HYBRIDISATION). Some sections were counterstained with haematoxylin, and $^{35}S$ sections were viewed in both bright and darkfield illumination. Glial cell quantification was performed as described in methods on 1μm resin embedded sections (see 2.5.1.Glial cell quantification). The peroxidase anti-peroxidase method was used to demonstrate PLP/DM-20 protein (C-terminal antiserum) and MBP in post-natal mice on 1μm resin embedded sections (see2.4.IMMUNOCYTOCHEMISTRY).

## Results

### RT-PCR

1) Bulk brain/spinal cord:

Both *plp* and *dm-20* product were detected at all ages studied from E12-P20 in the spinal cord and E13-P20 in the brain using 39 cycles (Figure 19). In both brain and spinal cord three distinct phases could be identified in terms of *plp/dm-20* product ratio, however the

temporal progression varied between the two samples. In the spinal cord, *dm-20* was the predominant product from E12 to E18 with a shift to an approximate equimolar relationship between E18 and P1. From P1 onward *plp* was the predominant isoform. In the brain equimolar amounts of product were not present until P5 with *plp* becoming predominant from P10 onward.
Semi-quantitative analysis of spinal cord product demonstrated marked up-regulation of the *plp* gene around P1 at about the same time that *plp* was becoming the predominant transcript (Figure 20). Both *plp* and *dm-20* transcripts appear to be up-regulated with *plp* transcript levels increasing to a much greater degree. *Plp/dm-20* product ratio as assessed by densitometric analysis increased from approximately 0.5 at E12 to 3.5 at P20 (Figure 20).

2) Spinal cord ventral columns:

Product ratios for Carnoy's-fixed spinal cord ventral columns generally paralleled those seen in the bulk spinal cord samples. At E18 *dm-20* was the predominant product but from P1 onward, *plp* predominated (Figure 21). No obvious difference could be seen in *plp/dm-20* ratios between cervical, thoracic and lumbar areas at the same age (Figure 21).

3a) Mid third optic nerves:

Analysis of mid third optic nerves was performed on two sample types; Carnoy's-fixed material, to allow direct comparison with the ventral spinal columns, and unfixed material . Quality of RNA extracted from unfixed tissue was considerably better than that from fixed tissue as assessed by standard agarose gel analysis. Since the small amounts of transcript available precluded spectrophotometric analysis, this better quality allowed more accurate gel quantification and subsequent semi-quantitative RT-PCR analysis. Analysis of unfixed tissue also served to check for the possibility of alterations in transcript ratio due to Carnoy's fixation.
The profile of *plp/dm-20* product ratios was the same for both fixed and non-fixed samples and varied in several respects from that seen in the spinal cord at the same age (Figure 22): RT-PCR products were demonstrated at all ages studied, however the change from *dm-20* to *plp* predominance occurred between P5 and P7, approximately 6-7 days later than the spinal cord. Marked up-regulation of the gene was seen at the same time as the change in product ratio (Figure 23). At ages where *dm-20* predominated (P1 and P5) levels of *plp* product were very low (undetectable for fresh samples) even when compared to E12 spinal cord samples. Consequently, the change from *dm-20* to *plp* dominance was more abrupt in the mid third optic nerve than in the spinal cord (Figure 22). *Plp/dm-20* product ratio as assessed by densitometric analysis increased from 0 (totally *dm-20*) at P1 to 2.5 at P15 (Figure 23).

3b) Whole optic nerves:

RT-PCR analysis of whole optic nerves from a separate study revealed a difference in *plp/dm-20* ratio compared to mid third optic nerve samples at P1 and P5. Although *dm-20* was still the major isoform present, the level of *plp* product was considerably greater than for mid optic nerves and was approaching equivalence (Figure 24).

**Immunocytochemistry**

Results of immunostaining with PLP-CT or MBP antibodies were essentially identical for all areas studied in the postnatal mouse at P1, 5, 10, 15, and 20, with both antibodies staining the myelin sheaths.

a) spinal cords:

At P1 (Figure 25, Figure 26) at the level of the proximal cervical intumescence, a few myelin sheaths were present and immunostained for PLP/DM-20 and MBP in the ventral columns and cuneate tract of the dorsal column. An occasional sheath was also seen in the lateral column. No immunostained sheaths were present in the gracile or corticospinal tracts of the dorsal column. At the level of the mid thoracic cord, a few sheaths stained in the ventral and lateral columns, but staining of sheaths was absent from the dorsal columns. At the level of the proximal lumbar intumescence the few positive staining sheaths were restricted to the ventral columns.
Increasing numbers of PLP positive sheaths were seen at older ages (Figure 27). By P5, numerous positive staining sheaths were present at all cord levels. Cervical and thoracic cords were very similar, still with fewer positive sheaths in the gracile and corticospinal tracts. There were generally fewer positive sheaths in all areas of the lumbar cord. By P10, similar staining is seen in cervical, thoracic and lumbar areas. Gracile and corticospinal tracts are still less intensely stained. The distribution of positive staining sheaths is fairly homogenous throughout all the white matter tracts at all cord levels by P20.

b) Mid optic nerves:

No positive staining sheaths were present at P1 or P5 (Figure 28). At P10 numerous sheaths immunostaining for both PLP/DM-20 and MBP were present and the number of these increased at P15 and P20 (Figure 28).

## ISH

a) spinal cords:

At P1, numerous strongly positive cells were present predominantly in the ventral and ventro-lateral white matter with occasional cells present in the dorsal columns (Figure 30). The number of positive cells and signal intensity per cell decreased slightly passing in a rostral to caudal direction. This gradient was still visible at P5 (Figure 29), although there was now considerably more signal, especially in the dorsal columns, and occasional expressing cells were present in the grey matter. From P10 to P20 both number of cells and strength of expression increased with little difference between cord levels by P10. By P20 numerous positive cells were present in the grey matter, however the majority of *plp/dm-20* positive cells were found in the white matter tracts (Figure 30).

b) Mid optic nerves:

No positive cells were detected in either P1 or P5 mid optic nerves. By P10 numerous positive cells were present (Figure 31), and numbers of positive cells and intensity of signal increased up to P20 (Figure 31). On longitudinal optic nerve sections one or two positive cells were present in the optic chiasm by P2 (Figure 32). By P5 several positive cells were present along the length of the nerve, but were concentrated towards the chiasmal end (Figure 32) and by P7 numerous positive cells were fairly evenly distributed along the nerve, apart from the optic nerve head which was always devoid of positive cells (Figure 32).

## Glial cell counts

Three data points were collected for each area measured. Whilst this may limit statistical analysis of results, general trends in glial cell density with age or area may be commented upon.

The developmental profiles of glial cell densities at cervical, thoracic and lumbar levels of the spinal cord were essentially very similar. Values were at a maximum at P1 or P5 with the general trend of decreasing values from P1 onwards. No obvious peak in glial cell density was apparent after P1 (Figure 33, Figure 34, Figure 35). Although variation in glial cell densities of mid optic nerves was relatively large, especially at the earlier time points, the trend appears different from that seen in the spinal cord. A peak in cell density is seen at P5 with values decreasing at later time points (Figure 34, Figure 35).

When comparing glial cell densities at different levels of the spinal cord at the same age, no obvious rostro-caudal trend in values was apparent. (Figure 36, Figure 37, Figure 38).

## Discussion

The predominance of the *dm-20* isoform of the *plp* gene during embryogenesis, which was apparent in the RT-PCR data for bulk spinal cords, brains and spinal cord ventral columns in this study, is in good agreement with the previously published data (Ikenaka *et al.* 1992; Timsit *et al.* 1992a). The presence of *plp* product in the present study, although it was always present as the minor isoform during embryogenesis, is at variance with these reports, in which the selective expression of *dm-20* alone is particularly noted. This difference could be due to one of three reasons; the product generated in the present study is due to RT-PCR contamination; the product is not authentic *plp* product, or the sensitivity of the present study is greater than previous studies thus revealing levels of *plp* product previously below the level of detection. Steps taken to eliminate RT-PCR contamination have been described above, and all negative control reactions, in the absence of target generated no PCR product. Generation of the predicted product lengths and comprehensive restriction enzyme analysis of the RT-PCR products, as described in the results above, show that both the *plp* and *dm-20* products are generated from authentic *plp/dm-20* transcripts. Ikenaka's study (1992) utilised a PCR amplification of 45 cycles followed by Southern blotting and probing with $^{32}P$ labelled oligonucleotide probes. One would expect this approach to be more sensitive than the 39 cycle RT-PCR employed in the present study, however *plp* product was detected only at P2 in brain after prolonged exposure and not at all in post-natal sciatic nerve. Using the current protocol *plp* product is easily demonstrable in these two tissues after a RT-PCR of only 30 cycles, and *plp* product has been demonstrated by RT-PCR in previous studies of post-natal sciatic nerve (Pham-Dinh *et al.* 1991). Additionally, PLP specific protein has been demonstrated in post-natal sciatic nerve by several groups (Agrawal and Agrawal 1991; Griffiths *et al.* 1995a; Tetzloff and Bizzozero 1993), from which one can infer that the transcript must also be present. It therefore seems likely that if the protocol employed by Ikenaka is unable to detect *plp* transcripts in post-natal sciatic nerve it will also be unable to detect it in embryonic brain, when the amounts present are considerably lower. The protocol of Timsit *et. al.* (1992) used a standard 33 cycle RT-PCR reaction and also failed to demonstrate *plp* product in embryonic brain. Sensitivity and efficiency of RT-PCR reactions may vary considerably depending on numerous variables such as target concentration and quality, magnesium concentration, cycle profile and design of primers. Both of the previous studies utilised primers in exons 1 and 7 which generated *plp* product of over 800bp. The present study used primers in exons 2 and 4 generating a much smaller product of around 500bp. As well as the possibility of decreased overall sensitivity, it must also be noted that neither of the previous studies demonstrated the fidelity of *plp/dm-20* input to output ratios with their particular RT-PCR protocols, as has been described for the current protocol. It is possible that the particular RT-PCR conditions used favoured amplification of the *dm-20* product, thus selectively decreasing sensitivity of detection of the *plp* transcripts. The

demonstration of *plp*-specific transcripts and PLP-specific protein in embryonic spinal cord sections by ISH and immunostaining during the present study, is further evidence of the authenticity of this *plp* specific RT-PCR product (see 3.2.2.Embryonic expression studies).

*Plp/dm-20* product ratios for spinal cord ventral columns were similar to those seen in bulk spinal cords down to the earliest age studied, E18, at which time a moderate predominance of *dm-20* was seen. The use of Carnoy's fixed tissue does not appear to have affected the RT-PCR efficiency adversely even though the quality of RNA extracted from the fixed tissue was poorer than that from fresh tissue; standard agarose gel analysis revealed degradation of RNA from fixed tissue, evident as smearing and loss of the 28S and 18S ribosomal RNA bands. Due to the relatively small size of the product being generated during the RT-PCR reaction, moderate degradation of the target RNA is not a major problem. When looking at *plp/dm-20* ratios, the assumption is made that any degradation and resultant decrease in product will affect *plp* and *dm-20* transcripts equally. This assumption appears to be validated by the similar *plp/dm-20* ratios obtained when using Carnoy's-fixed and fresh tissue from mid-third optic nerves.

It was evident from both the immunostaining and ISH studies that the ventral columns of the spinal cord were the first areas to acquire myelin sheaths and exhibit positive *plp/dm-20* ISH signal. This is in good agreement with previous studies (see 1.6.MYELINOGENESIS). No difference however was seen in the *plp/dm-20* ratios when comparing whole spinal cord and ventral column RT-PCR products. Likewise the well documented rostral to caudal gradient of myelination (see 1.6.MYELINOGENESIS) which was demonstrated at P1 and even at P5 quite clearly by the ISH and immunostaining, was not reflected in a similar gradient of ventral column *plp/dm-20* ratios at these levels. If the initial hypothesis that changes in *plp/dm-20* ratios should mirror changes in myelination status, one would have expected to see a greater *plp* predominance in the ventral column samples relative to the whole cord and in the cervical ventral column samples relative to thoracic or lumbar, since these areas are relatively more advanced in terms of myelination. Either the hypothesis is incorrect or the difference in myelination between the comparative areas is not great enough to demonstrate a significant difference in *plp/dm-20* ratios. Although myelination in the cord is highly heterogeneous, gross differences between cervical and lumbar cord or between general areas at the same level appear to resolve over a period of approximately 1 to 2 days, and certainly less than 5 days. To distinguish between these two possibilities it is necessary to compare areas with a much greater difference in time of onset of myelination, such as the ventral columns and the mid third optic nerve where a difference of at least 6 days is seen.

As stated above, similar results were obtained with Carnoy's-fixed and fresh mid third optic nerves. Dominance of *dm-20* product, almost to the exclusion of *plp,* was seen post-natally up to P5, with a change to *plp* predominance at the next time point studied (P10 for Carnoy's-fixed and P7 for fresh tissue). This change over in ratio correlates well with the

appearance of PLP/DM-20+ sheaths on immunostaining and *plp/dm-20* ISH signal on mid-optic nerve transverse sections, both being found only at P10, the next time point studied after P5. It therefore seems apparent that change in *plp/dm-20* ratio from *dm-20* to *plp* predominance is correlated with the appearance of myelin sheaths in a particular myelinating area. Correlation of *plp/dm-20* ratio changes with appearance of positive ISH signal is not as obvious. Even though a significant increase in *plp/dm-20*-positive cells is seen in the spinal cord at P1 as myelin sheaths are appearing, positive cells are present well before this time. Expression of the *plp* gene in these cells (see 3.2.2.Embryonic expression studies), may well not be directly related to myelin sheath formation itself. Although no ISH signal was seen on P5 transverse mid optic nerve sections, signal was present in several cells on P5 longitudinal nerve sections. These positive cells probably represent immature oligodendrocytes similar to those found in the embryonic cord, rather than actively myelinating cells since myelin sheaths have not been demonstrated at this age. Analysis of increased numbers of mid optic nerve sections would probably have revealed occasional ISH-positive cells. Product ratio in whole optic nerve samples at P1 and P5 were still *dm-20* predominant, however there was considerably more *plp* product. This may well reflect the heterogeneous nature of myelination described in the optic nerve suggesting more advanced myelination in either the proximal or distal-third of the nerve, or both. Analysis of product ratio in all three portions of the nerve would allow clarification of this point. A more heterogeneous population of myelinating cells in the whole optic nerve compared to the mid third optic nerve would also explain the more gradual change from *dm-20* to *plp* predominance seen in these samples, similar to that seen in the spinal cord. Colello *et al.* (1995) describe a gradient of *plp* expressing cells from the chiasmal to retinal end of the rat optic nerve between P2 and P7 which is similar to that seen in the present work. The gradient of myelination at P7, however, was in the opposite direction. The gradient of *plp* expression would correlate well with the more gradual change in *plp/dm-20* ratio seen in the whole optic nerves, and it would be interesting to see if a gradient of *plp* dominance also existed similar to that seen for myelination in the study of Colello *et al.*(1995).

Increases in glial cell density have been shown to occur in the CNS just prior to the onset of myelination in a specific area (Bensted *et al.* 1957; Matthews and Duncan 1971; Samorajski and Friede 1968; Schonbach *et al.* 1968), although the exact profile seems to vary from area to area (Matthews and Duncan 1971; Schonbach *et al.* 1968). The profile and glial cell densities seen in the spinal cord are in good agreement with previous work (Fanarraga 1993; Matthews and Duncan 1971). The presumed peak in glial cell density is likely to occur prior to or around birth in the ventral columns as myelination has already begun at P1. The later peak in cell density seen in the optic nerve is also in agreement with previous studies (Vaughn 1969), and seems to be correlated with the later appearance of myelin and the later change in *plp/dm-20* product ratio in this area. The similarity seen

between glial cell density at different cord levels at the same age is also reflected in the *plp/dm-20* product ratios. It seems that changes in glial cell density and *plp/dm-20* transcript ratios are less precise temporal markers than the appearance of stainable myelin sheaths since it is only with the latter that a rostral to caudal gradient is seen.

The third parameter which appears to be correlated with appearance of myelin and change in transcript ratio at around P1 in the spinal cord and P7 in the optic nerve is a marked up-regulation of the *plp* gene. The up-regulation seen in the spinal cord is in good agreement with the appearance of *plp/dm-20* signal on northern blots of mouse brain RNA at P2-P3 found in two previous studies (Gardinier *et al.* 1986; Sorg *et al.* 1987). The lack of signal earlier than P2 on northern analysis is presumably due to a combination of the slightly later myelination of the brain as a whole, relative to the spinal cord, and the lower sensitivity of this technique compared to RT-PCR. A study using rat cerebra or hindbrain, demonstrated northern signal increasing from P0 in the hindbrain and P4 in the cerebra (LeVine *et al.* 1990). The hindbrain myelinates earlier than the cerebra in accordance with the general caudal to rostral gradient in the brain and is similar in time of onset to the spinal cord. Approximately ten-fold increases in total transcripts were seen in spinal cords between E18 and P20 and in mid optic nerves between P5 and P15. It must be emphasised again however that the semi-quantitative RT-PCR data is not being presented to define absolute values of up-regulation or total transcription rates, but more as an indication of time points where marked changes in both *plp/dm-20* product ratio and *plp* gene expression are seen. Absolute values of transcripts as discussed previously are probably higher than is apparent and more stringent controls would be necessary before statements could be made regarding any such figures. Such stringent controls were not considered necessary in the present context.

Analysis of *plp/dm-20* RT-PCR product ratios for whole brain samples also reveals a more gradual, and later appearance of *plp* predominance compared to whole spinal cord. The later onset of *plp* predominance would be expected, given the later myelination of the brain relative to the spinal cord (Langworthy 1928; Langworthy 1933; Windle *et al.* 1934; Zgorzalewicz *et al.* 1974). It has been demonstrated that trigeminal ganglia express *dm-20* very strongly in the embryonic and post-natal mouse, as is the case with spinal ganglia (Timsit *et al.* 1992a; Timsit *et al.* 1995). However, it is not possible to remove this source of *dm-20* transcripts from bulk brain samples as it is for spinal ganglia from spinal cord samples, and this may help to maintain *dm-20* dominance in bulk brain samples. *Dm-20* transcripts from cranial ganglia plus the greater heterogeneity present in the myelinating brain would also account for the more gradual transition to *plp* predominance seen in the bulk brain samples.

In summary, the change in *plp/dm-20* transcript ratio from *dm-20* to *plp* predominance during development of the mouse CNS appears to be correlated with the onset of

myelination and not with chronological age of the developing CNS as a whole. Onset of myelination was assessed by appearance of myelin sheaths and associated changes in glial cell densities, and expression of the *plp* gene. The change in transcript ratio is accompanied by a marked up-regulation of the *plp* gene with an increase in both *plp* and *dm-20* transcripts. The precise mechanisms controlling this up-regulation and change in transcript ratio are poorly understood and will be discussed more fully in the final discussion.

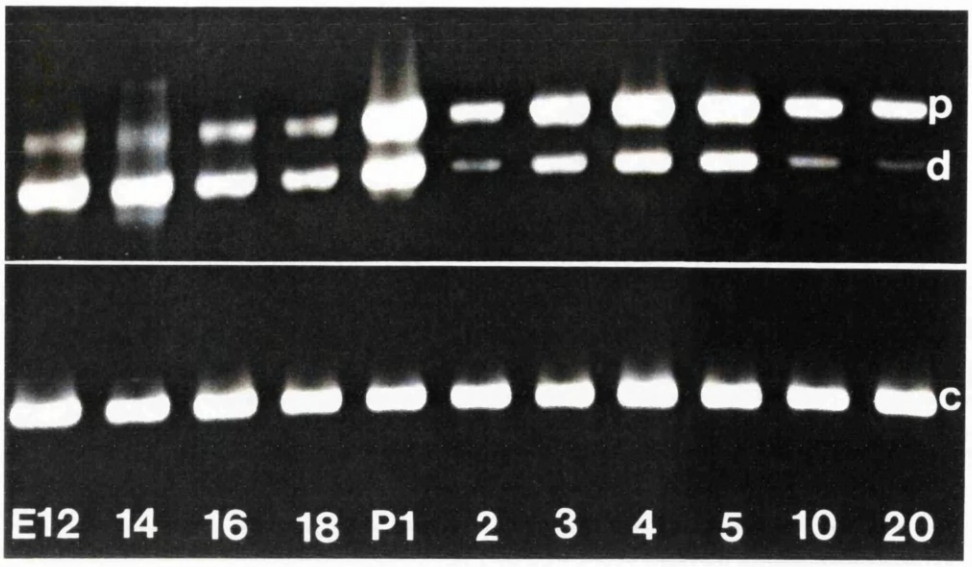


(a)

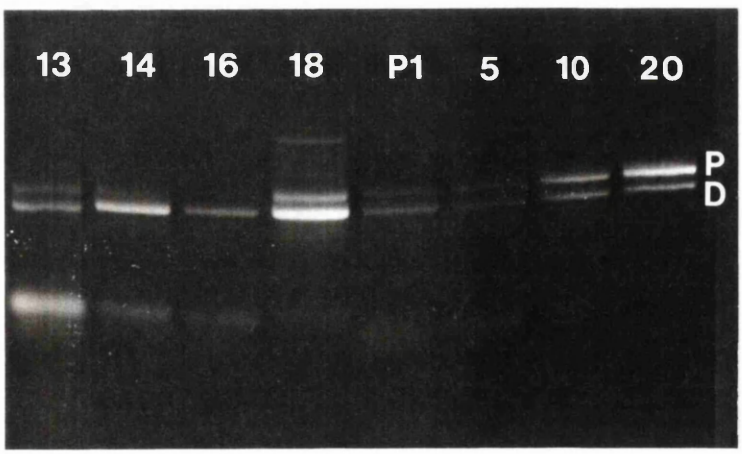


(b)

**Figure 19.** RT-PCR product from whole mouse spinal cord and brain. **a)** spinal cord; *plp* product (**p**) and *dm-20* product (**d**) are seen at all ages from E12-P20. Cyclophilin product (**c**) used as an internal control is shown below. The change in predominance from *dm-20* during embryogenesis to *plp* in post-natal life is illustrated. **b)** brain; predominance of *plp* lags temporally behind the spinal cord and is not seen until after P5

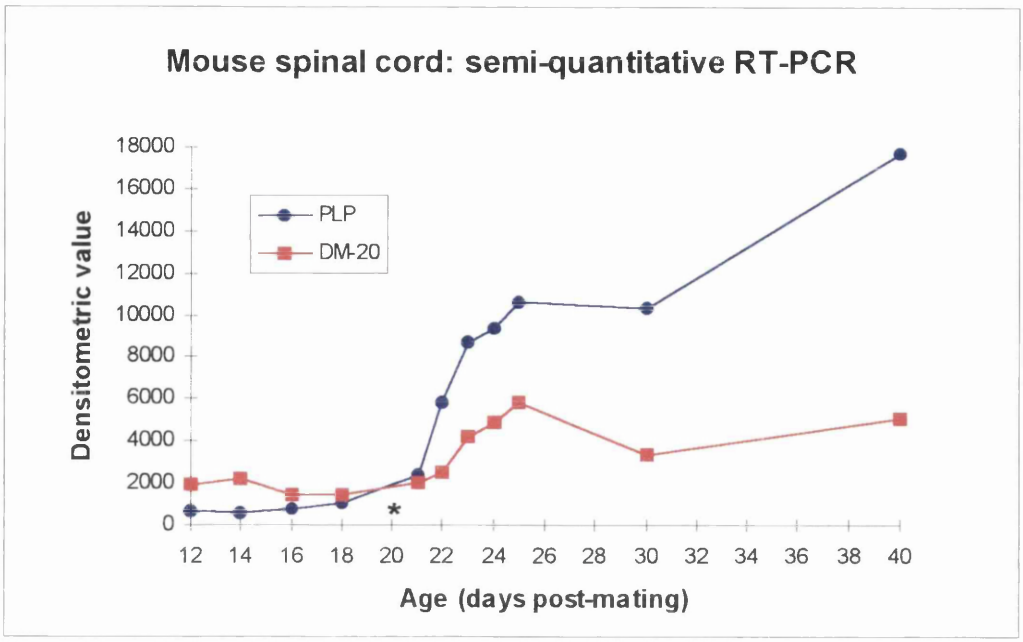


**(a)**

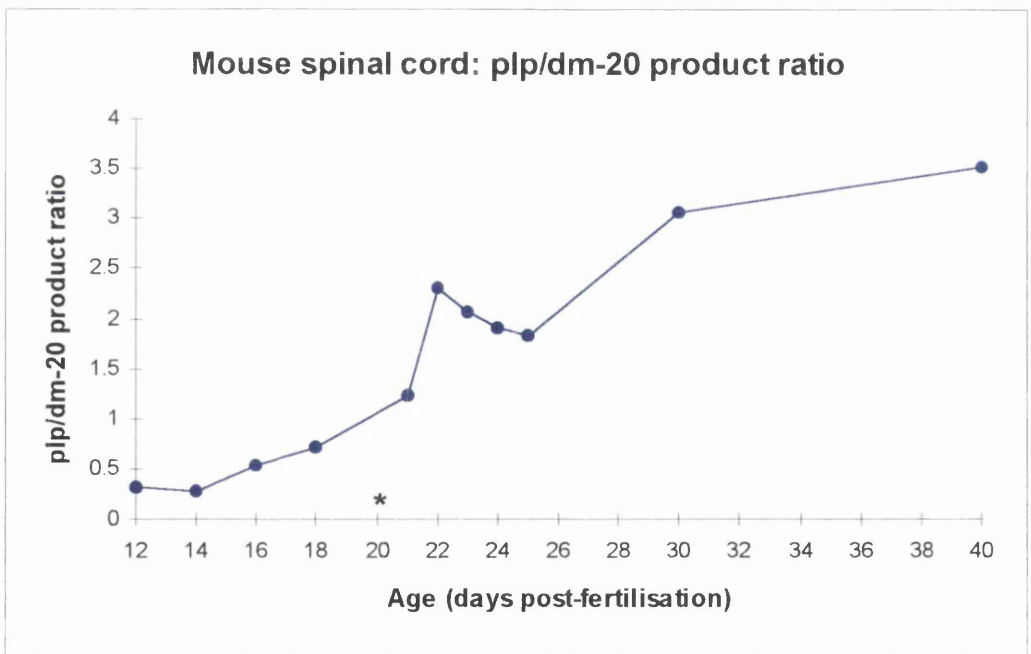


**(b)**

**Figure 20.** Spinal cord semi-quantitative RT-PCR analysis. **a)** Densitometric analysis of RT-PCR products illustrates marked up-regulation of the *plp* gene coinciding with the change to *plp* predominance around P1. **b)** Increasing *plp* predominance in post-natal life is seen as *plp/dm-20* product ratios greater than 1 rising to 3.5 by P20. Gestation length is approximately 20 days in the strain of mice studied and approximate time of birth is marked on the graphs (*).

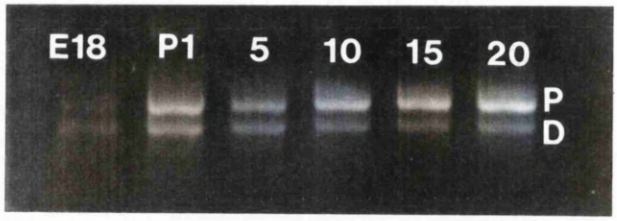


**(a)**

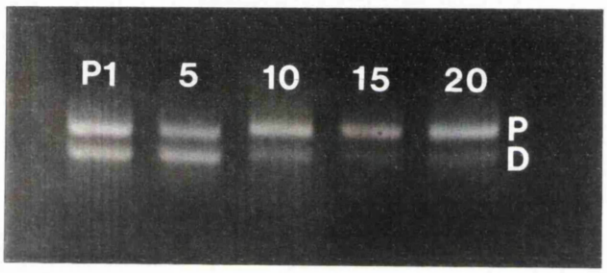


**(b)**

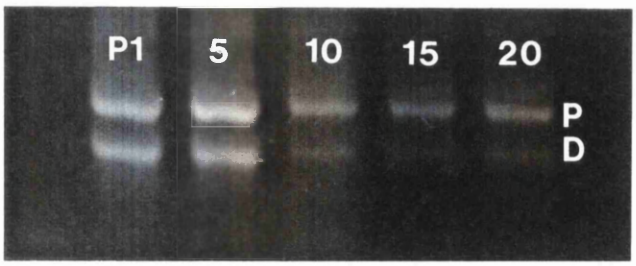


**(c)**

**Figure 21.** RT-PCR product from spinal cord ventral columns. **a)** cervical; **b)** thoracic; **c)** lumbar. No significant differences can be seen between samples of the same age at different spinal cord levels. *Plp* product (**P**), *dm-20* product (**D**).

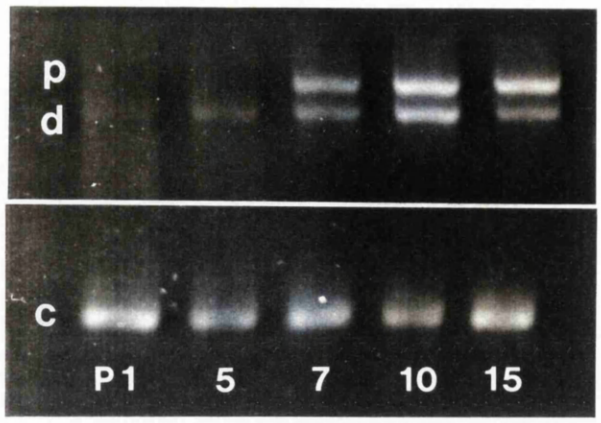


**(a)**

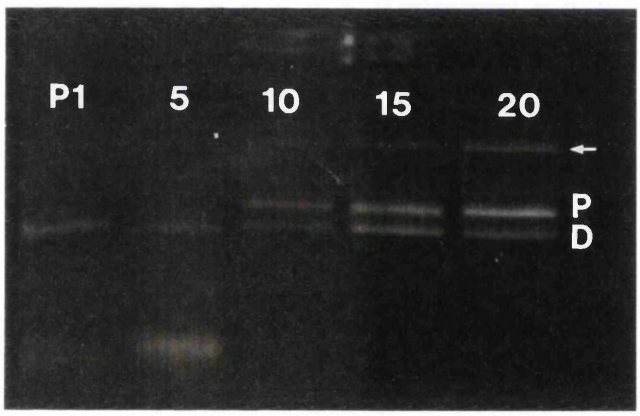


**(b)**

**Figure 22.** RT-PCR products from mid third optic nerves. **a)** Fresh tissue; *dm-20* product (**d**) predominates until P7 when *plp* (**p**) is the major isoform present. Cyclophilin product (**c**), used as an internal control is shown below. **b)** Carnoy's fixed tissue; developmental profile is the same as for fresh tissue. *Plp* product is almost totally absent before P7 at times when *dm-20* predominates. A larger product which is probably a PCR artefact is present at the older ages (arrow).

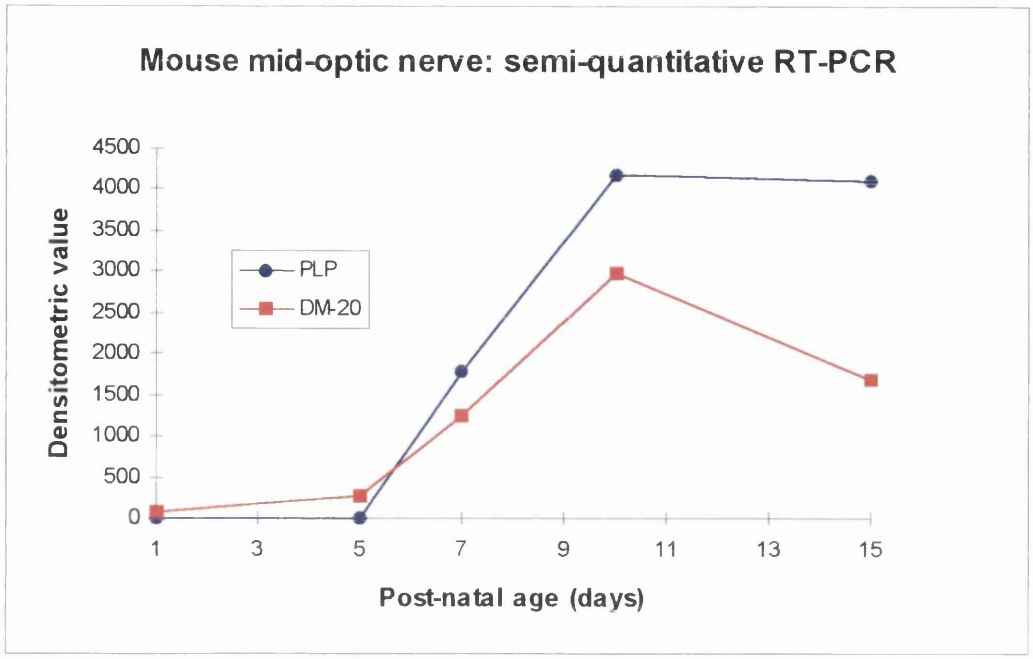


(a)

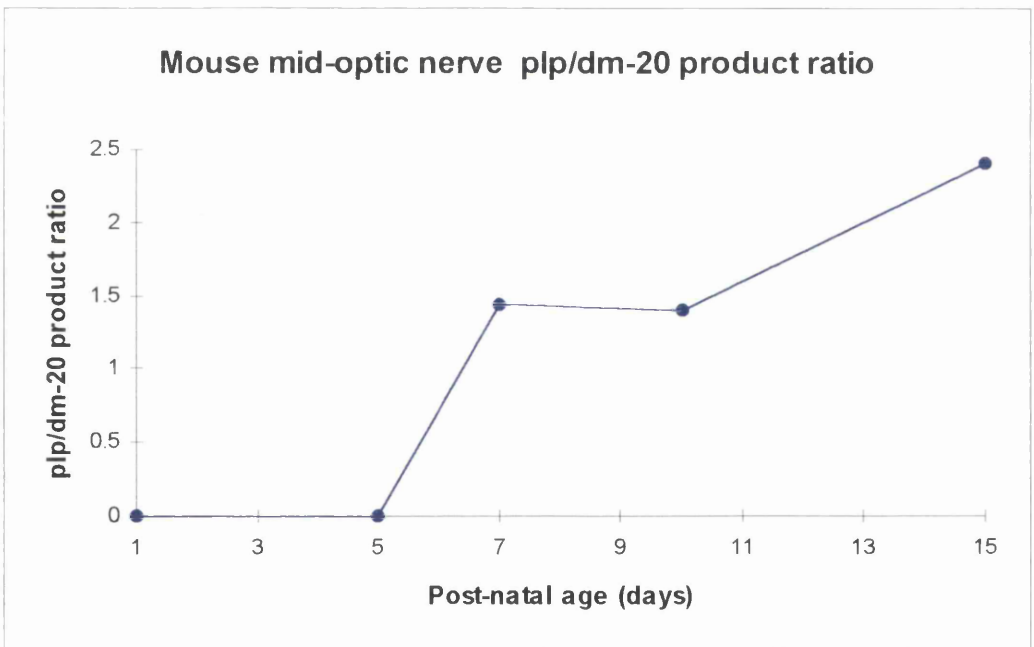


(b)

**Figure 23.** Mid third optic nerve semi-quantitative RT-PCR analysis. **a)** Densitometric analysis of RT-PCR product illustrates marked up-regulation of the *plp* gene coinciding with a change to *plp* predominance around P7. **b)** *Plp/dm-20* ratios greater than 1 are seen later in the mid third optic nerve (P7) than in the spinal cord (P1).

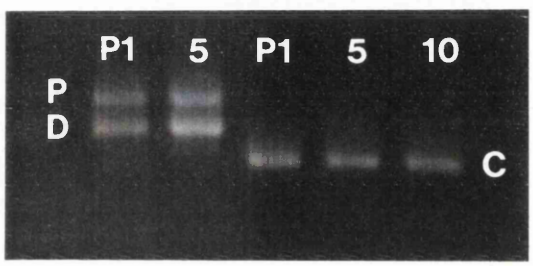


**Figure 24.** Whole optic nerve RT-PCR product. Levels of *plp* product (**P**) are considerably higher at P1 and P5 in whole optic nerves compared to mid third optic nerves. Cyclophilin product (**C**) used as an internal control is shown for P1 (whole ON), P5 (whole ON) and P10 (mid third ON).

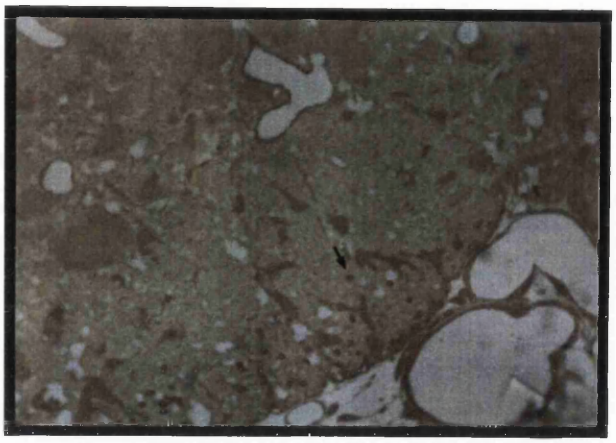

(a)

(b) (c)

**Figure 25.** PLP/DM-20 immunostaining of P1 spinal cords (ventral columns). **a)** Cervical cord, **b)** thoracic cord, **c)** lumbar cord. At this early stage of myelination the rostral to caudal gradient (cervical to lumbar) of myelination is apparent with many more PLP staining sheaths (arrows) in the cervical cord compared to the lumbar cord. The ventral columns are the first area of the spinal cord to acquire myelin sheaths.

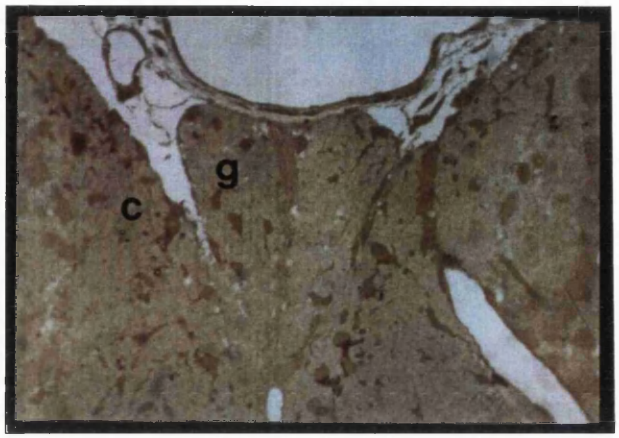


(a)


(b) (c)

**Figure 26.** PLP/DM-20 immunostaining of P1 spinal cords (dorsal columns). **a)** Cervical cord, **b)** thoracic cord, **c)** lumbar cord. PLP positive staining sheaths are present only in the cervical cord and only in the cuneate tract (**c**). The later myelinating gracile tract (**g**) and corticospinal tract (**ct**) have yet to acquire myelin at any level. The rostral to caudal gradient is again evident, as is the earlier myelination of different tracts at the same age and spinal cord level.

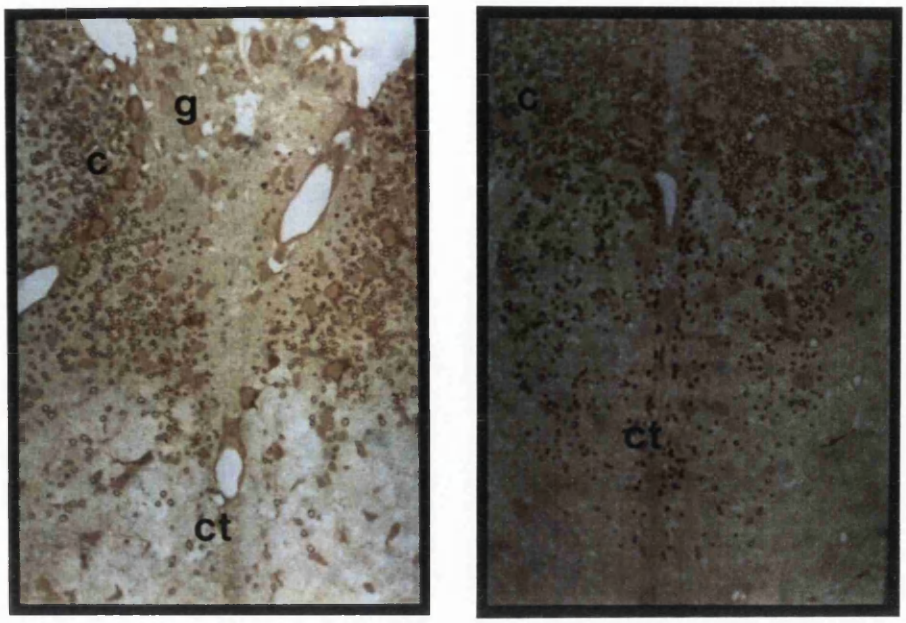


(a) (b)


(c)

**Figure 27.** PLP/DM-20 immunostaining of P5, P10 and P20 cervical spinal cords (dorsal columns). **a)** P5, **b)** P10, **c)** P20. (cuneate tract=**c**, gracile tract=**g**, corticospinal tract=**ct**). Increasing numbers of PLP positive sheaths are seen at older ages and the rostral to caudal gradient is no longer obvious. However, the later myelination of the gracile and corticospinal tracts is still evident. By P20 the degree of myelination is more homogenous in all tracts.

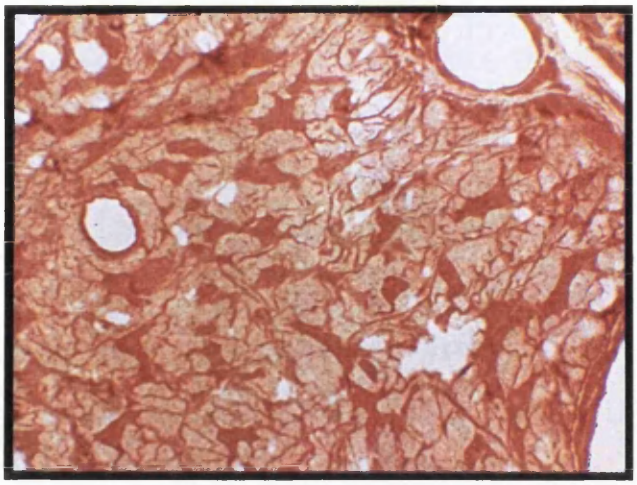

(a)

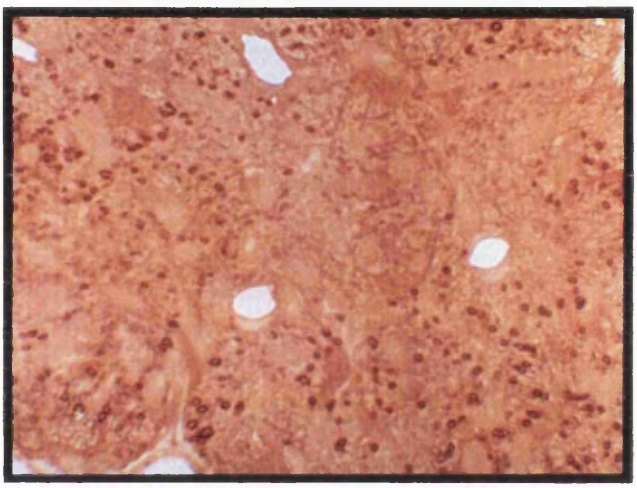

(b)

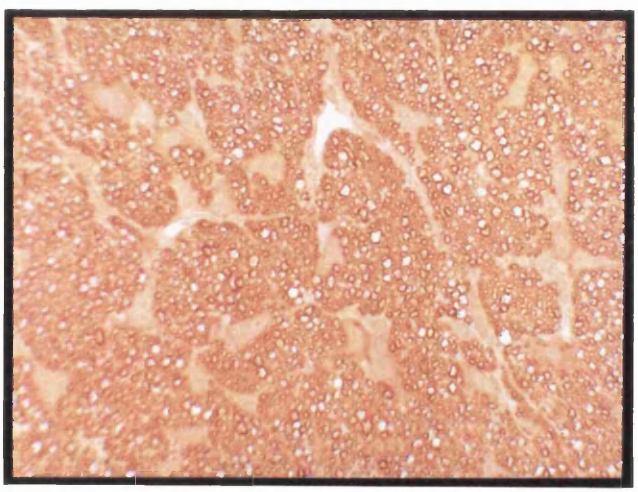

(c)

**Figure 28.** PLP/DM-20 immunostaining of P5, P10 and P20 mid optic nerves. ( **a)** P5, **b)** P10, **c)** P20. Positive staining sheaths are found in increasing numbers from P10 onwards.

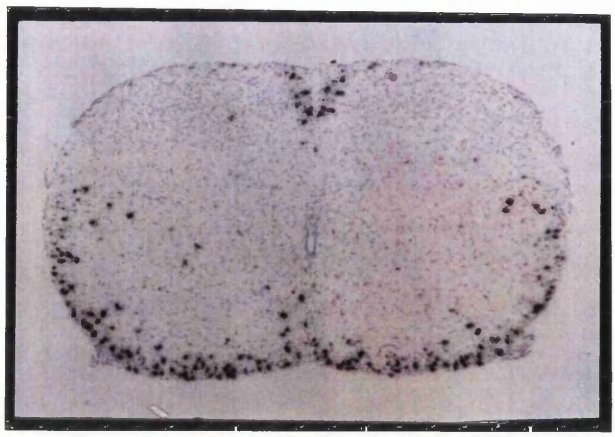

**(a)**

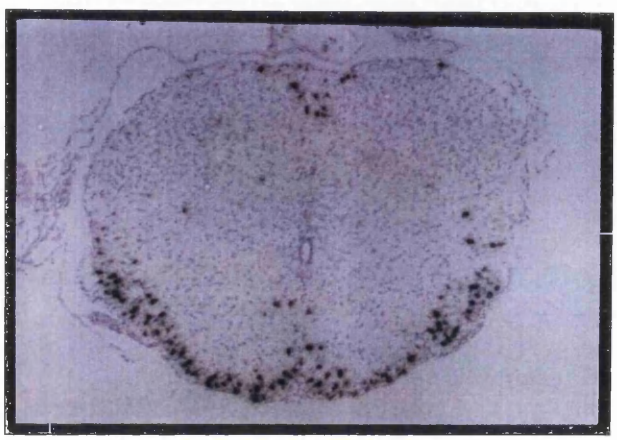

**(b)**

**(c)**

**Figure 29.** Post-natal mouse spinal cords; *plp/dm-20* ISH ($^{35}$S-PLP-1). **a)** P5 cervical, **b)** P5 thoracic cord, **c)** P5 lumbar cord. The rostral to caudal gradient of myelination in the spinal cord can still be seen at P5 with fewer positive cells present in lumbar cord sections relative to cervical cord.

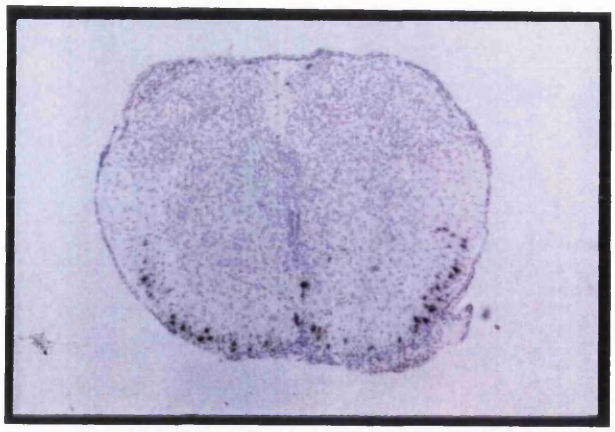

**(a)**

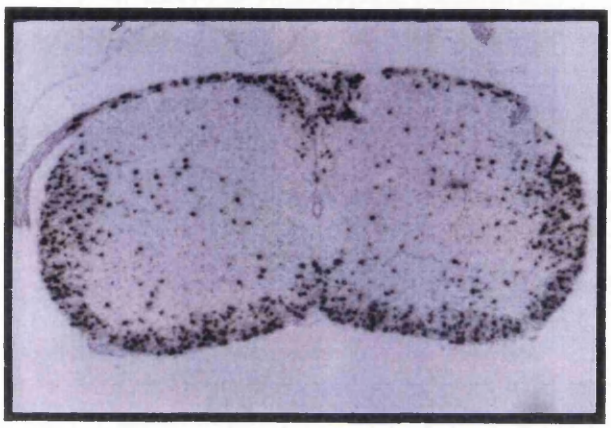

**(b)**

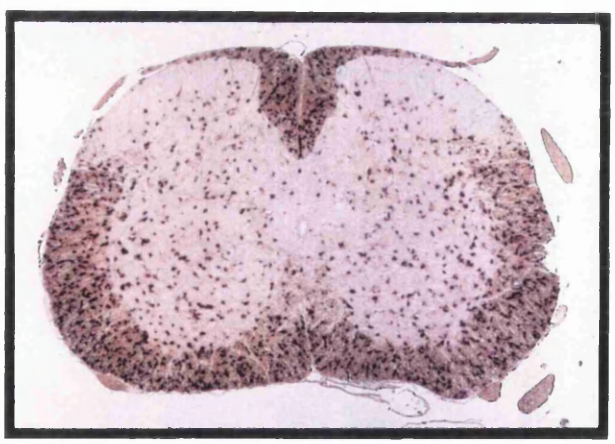

**(c)**

**Figure 30.** Post-natal mouse spinal cords; *plp/dm-20* ISH (PLP-1). **a)** P1 cervical cord, **b)** P10 cervical cord, **c)** P20 cervical cord. $^{35}S$ labelled riboprobes are shown except on the P20 section where a digoxigenin labelled riboprobe has been used. From P1 to P20, *plp/dm-20* expressing cells are found with increasing frequency throughout the white matter. By P20 numerous positive cells are also found within the grey matter.

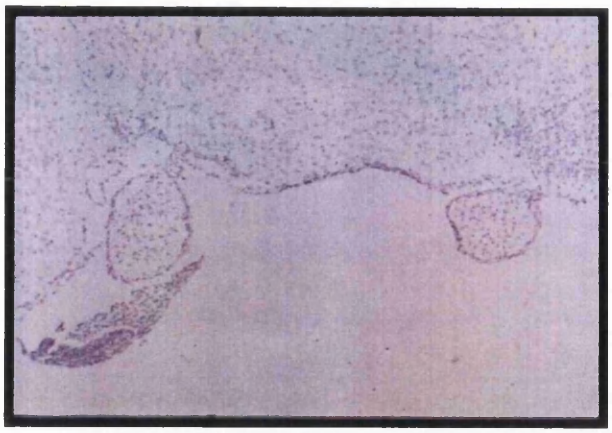

(a)

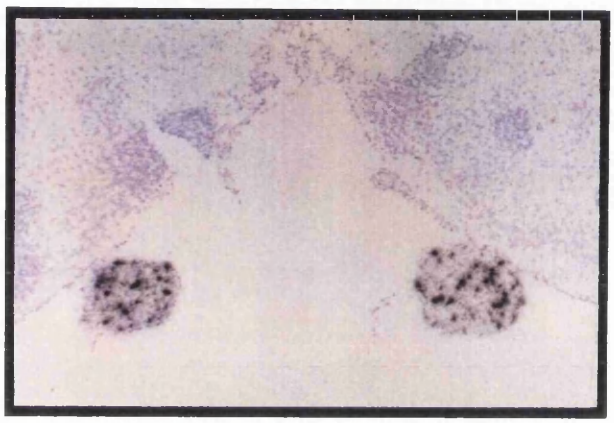

(b)

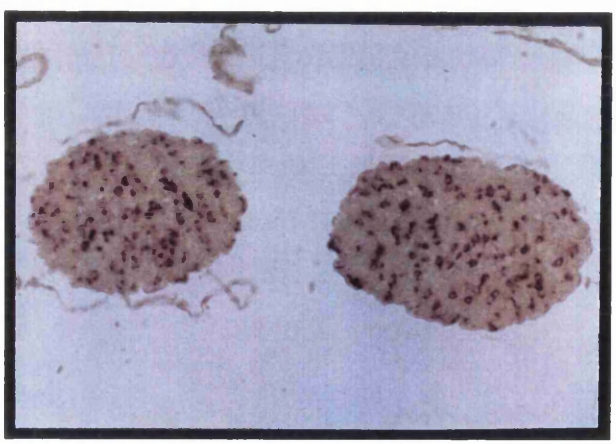

(c)

**Figure 31.** Post-natal mouse mid optic nerve; *plp/dm-20* ISH (PLP-1). **a)** P5 mid optic nerve, **b)** P10 mid optic nerve, **c)** P20 mid optic nerve. $^{35}$S PLP-1 riboprobes are shown except on the P20 section where a digoxigenin PLP-1 riboprobe has been used. *Plp/dm-20* expressing cells are absent from P5 sections, but are present by P10 and increase in number between P10 and P20.

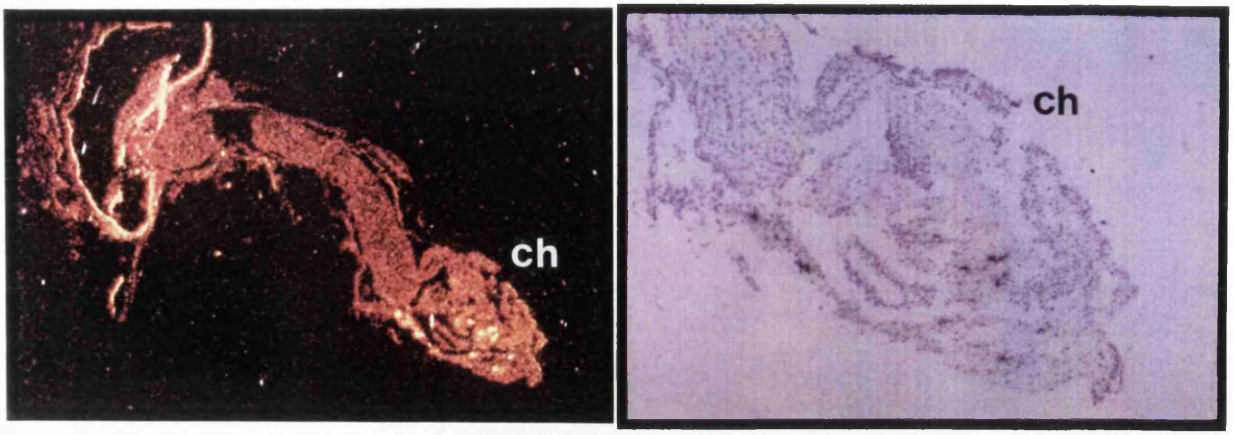


(a)

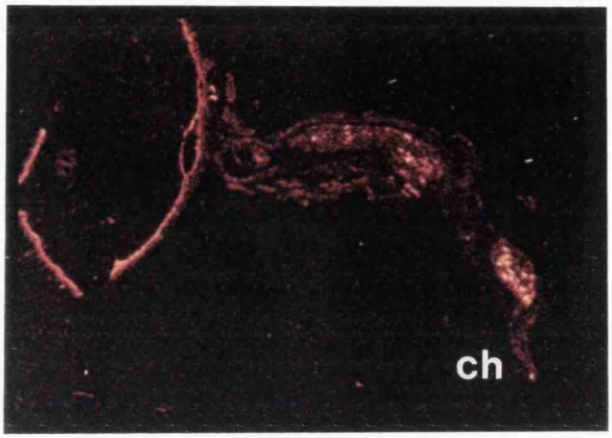


(b)

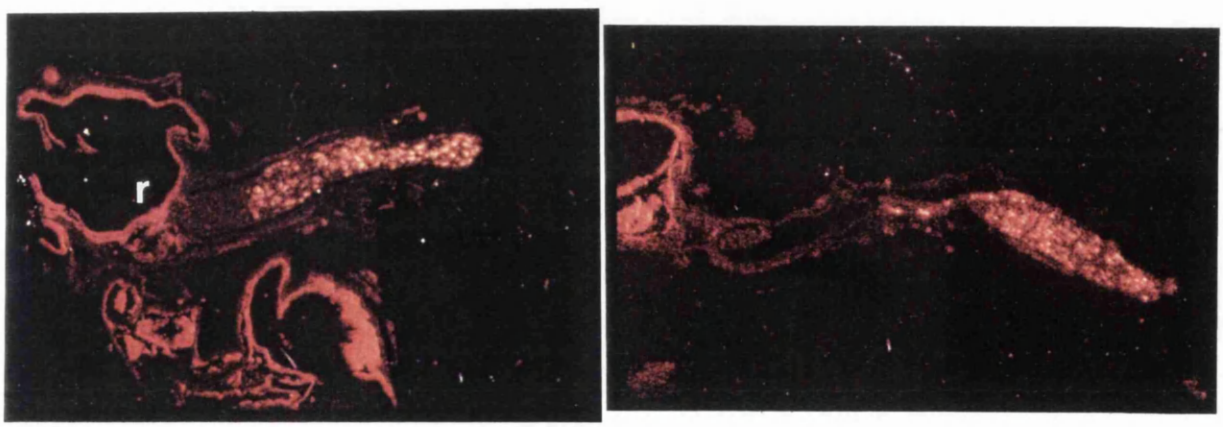


(c)

**Figure 32.** Post-natal mouse longitudinal optic nerve *plp/dm-20* ISH ($^{35}$S-PLP-1). **a)** P2 optic nerve, **b)** P5 optic nerve, **c)** P7 optic nerve. *Plp/dm-20* expressing cells are first apparent in the optic chiasm (**ch**) of the P2 nerve. By P5 positive cells are found sporadically along the whole nerve and by P7, numerous strongly expressing cells are present. The absence of positive cells from the optic nerve head at the retinal end of the optic nerve (**r**) is illustrated.

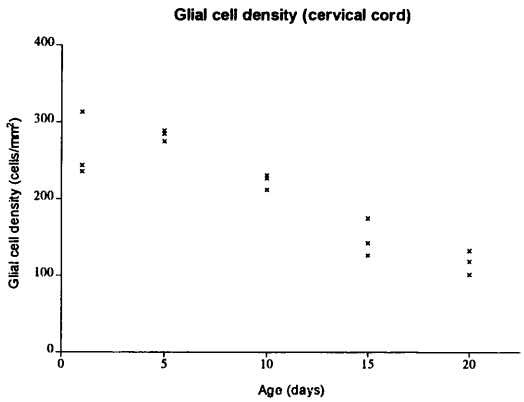


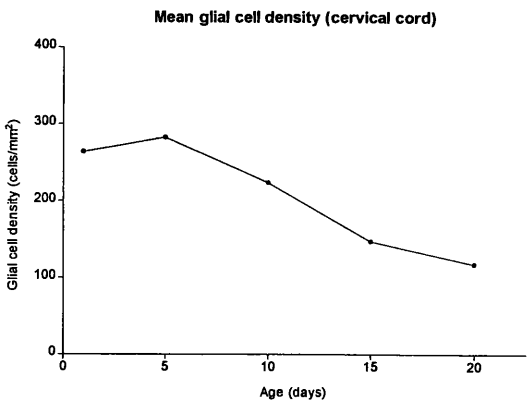


**(a)**

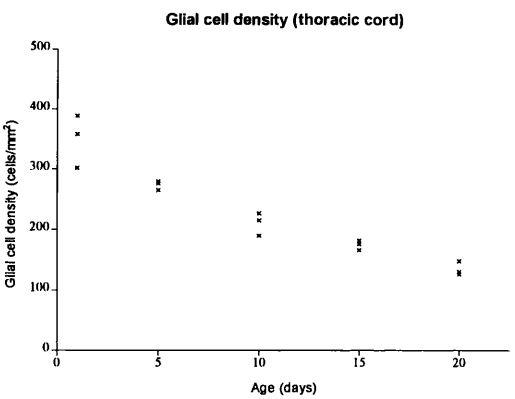


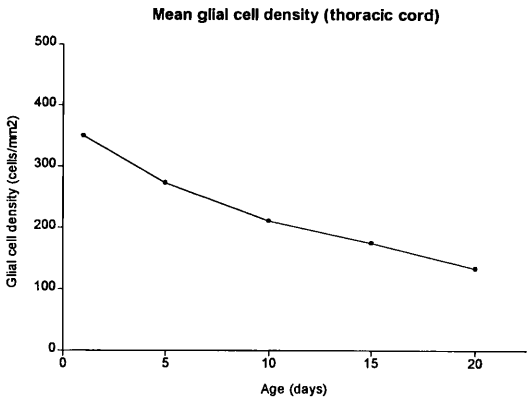


**(b)**

**Figure 33.** Glial cell density, cervical and thoracic cord ventral columns. **a)** cervical cord, **b)** thoracic cord. All data points are plotted on the left hand graphs and mean values on the right.

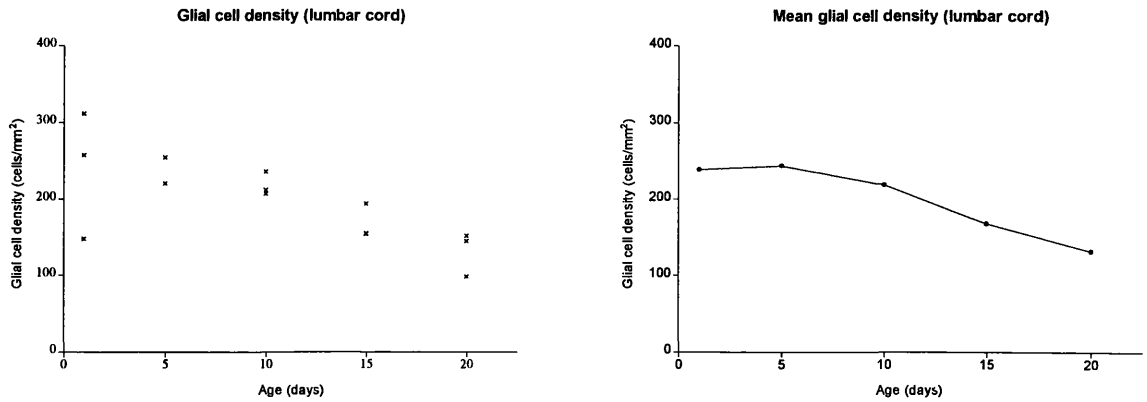


**(a)**

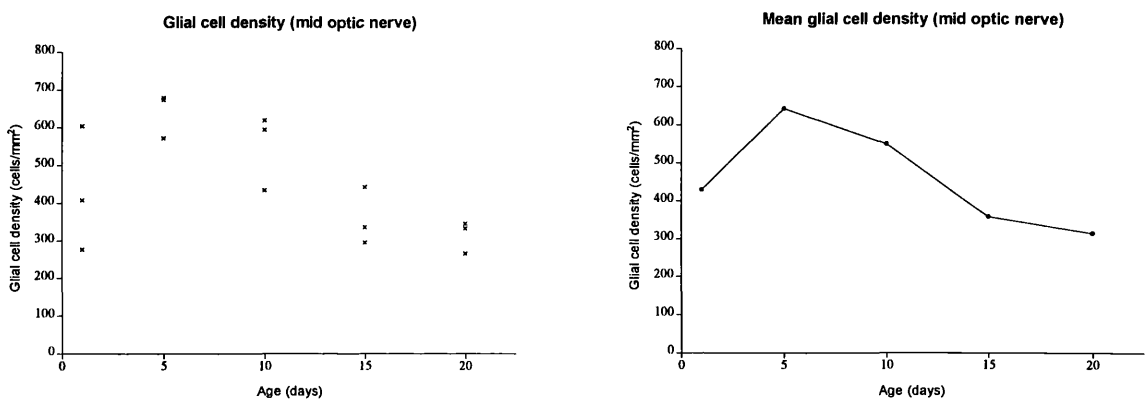


**(b)**

**Figure 34.** Glial cell density, lumbar cord ventral columns and mid optic nerve. **a)** lumbar cord, **b)** mid optic nerve. All data points are plotted on the left hand graphs and mean values on the right.

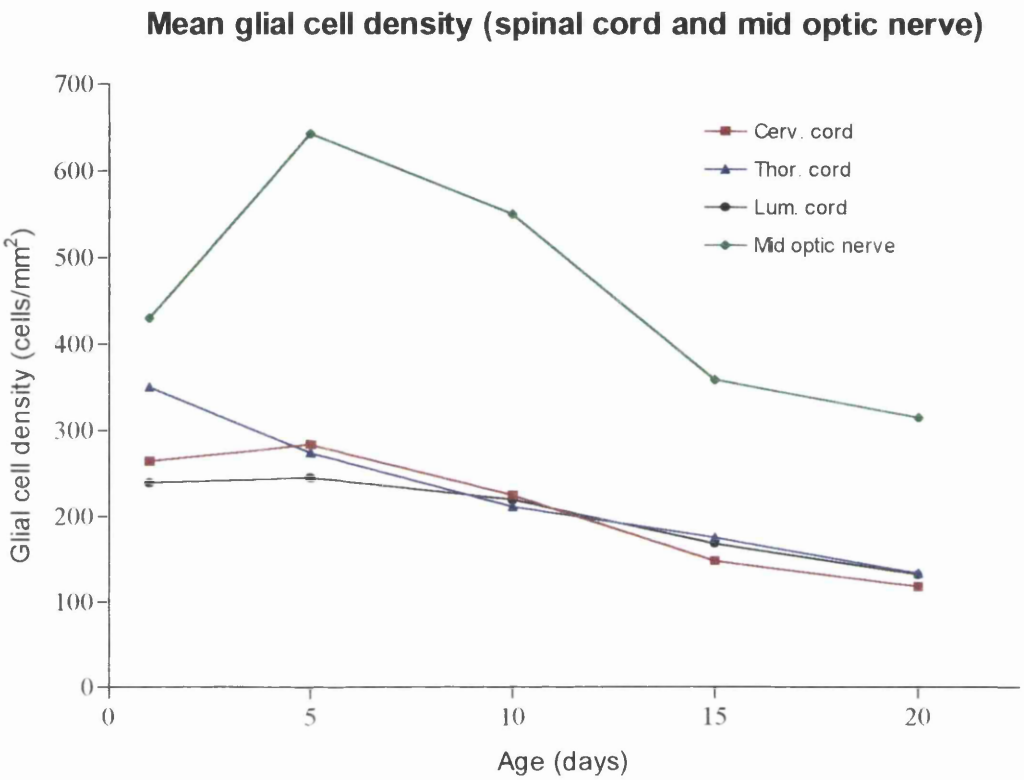


**Figure 35.** Glial cell density, spinal cord all levels and mid optic nerve. Glial cell density at all levels of the spinal cord exhibits a decreasing trend from P1 onwards. Mid optic nerve glial cell density appears to peak around P5 with a decreasing trend from P5 onwards. This later peak of glial cell density is consistent with the later onset of myelination and up-regulation of the *plp* gene seen in the optic nerve compared to the spinal cord.

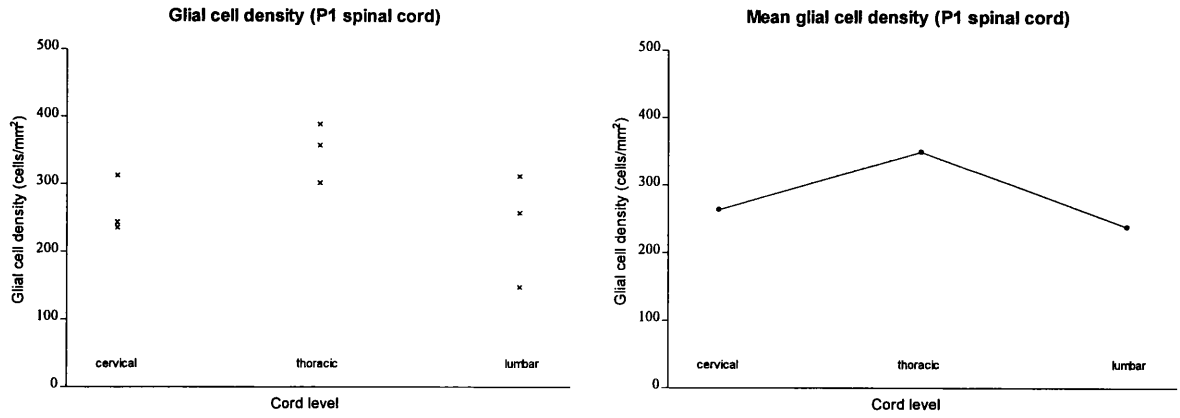


(a)

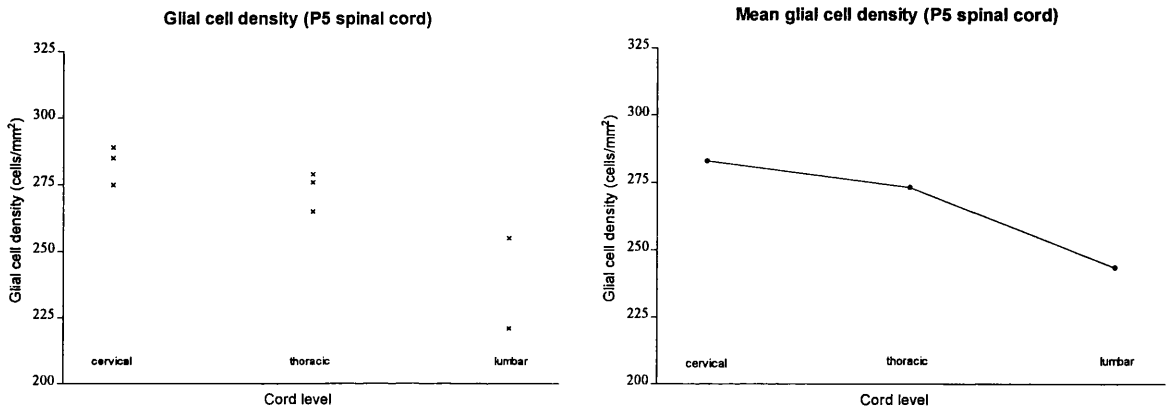


(b)

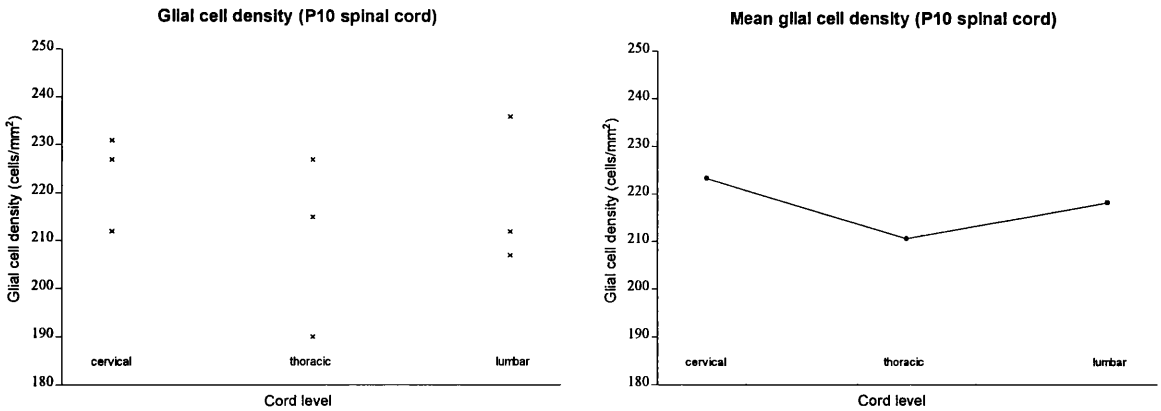


(c)

**Figure 36.** Glial cell densities, spinal cord rostral to caudal gradient. **a)** P1, **b)** P5, **c)** P10. All data points are plotted on the left-hand graphs and mean values on the right.

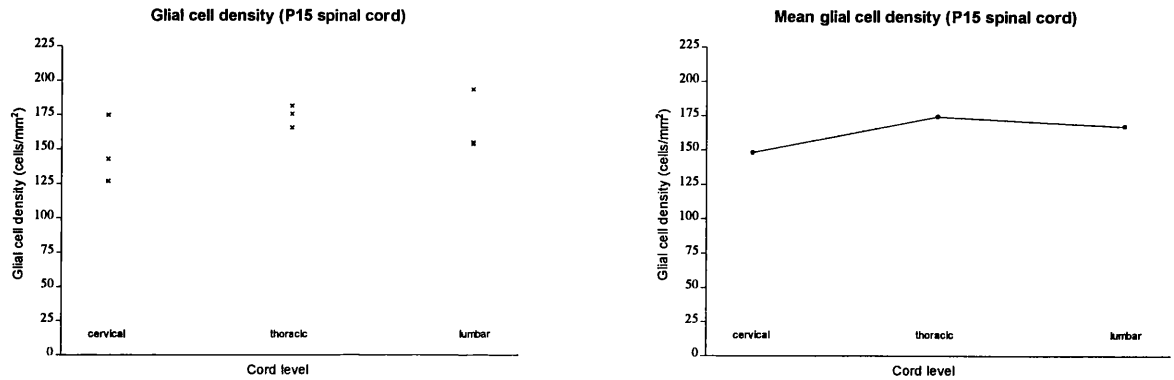


**(a)**

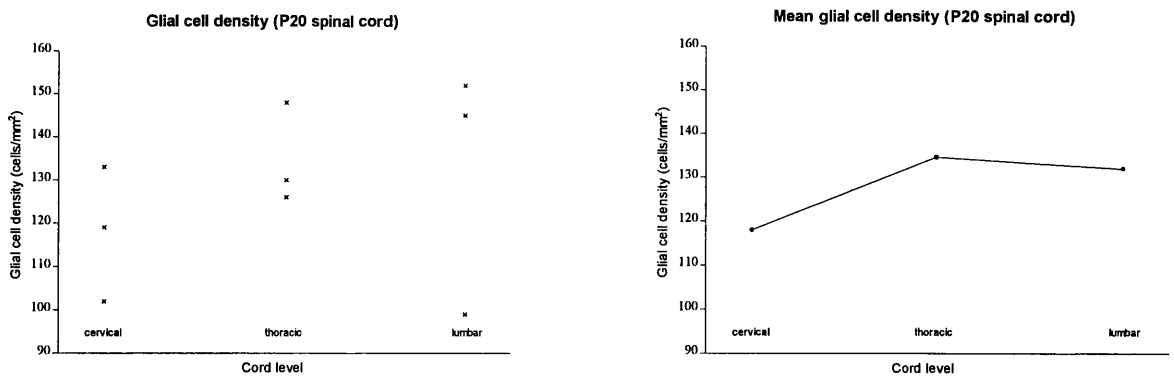


**(b)**

**Figure 37.** Glial cell density, spinal cord rostral to caudal gradient (cont.). **a)** P15, **b)** P20. All data points are plotted on the left hand graphs and mean values on the right.

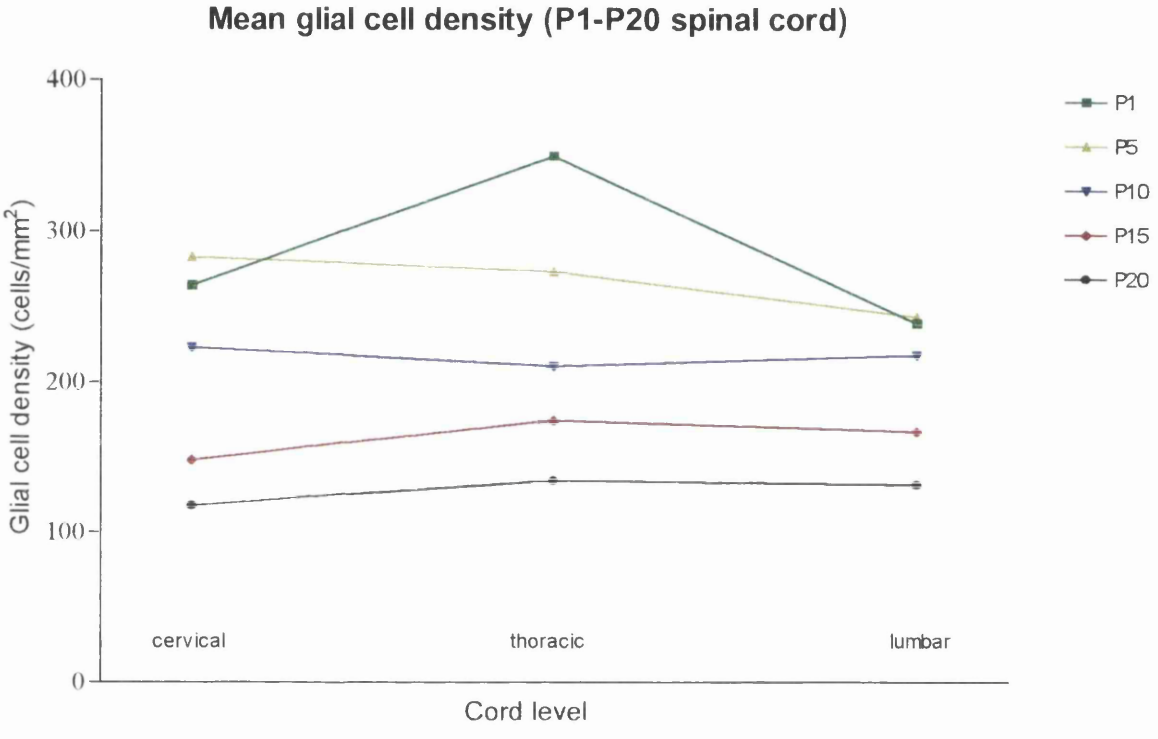


**Figure 38.** Glial cell density, spinal cord rostral to caudal gradient (summary). No significant or consistent trends are apparent when comparing mean glial cell density from rostral (cervical) to caudal (lumbar) levels of the spinal cord. The decrease in mean glial cell density with age is also apparent at cervical, thoracic and lumbar levels.

## 3.2.2.Embryonic expression studies

### Introduction and aims

Induced, high levels of expression of the *plp* gene is conventionally associated with mature post-mitotic oligodendrocytes and the production and maintenance of myelin sheaths. Demonstration of *dm-20* transcripts in rodent brain by mid gestation (Ikenaka *et al.* 1992; Timsit *et al.* 1992a) well before the onset of myelination was therefore both surprising and intriguing in terms of a possible alternative non-structural role for DM-20 protein. Subsequent ISH studies have localised *plp/dm-20* expressing cells in the brain and spinal cord of mice (Timsit *et al.* 1995) and rats (Yu *et al.* 1994) during this developmental period.

In the rat spinal cord, transcripts were localised to a column of cells either side of mid-line just above the floor plate at E12, whereas in the mouse the positive cells were slightly more dorsal and identified at E14.5. In the rat expression appeared to be transient at E12 and was only detected again at E18 in ventral white matter. In contrast in the mouse, positive cells progressively colonised the white matter areas of the cord throughout late embryogenesis. This variation may be related to the two species but additionally the two reports ascribed the positive cells to different cell types. In the mouse they were predicted to be oligodendrocyte precursors (Timsit *et al.* 1995) while a possible neuronal basis was considered in the rat (Yu *et al.* 1994). This latter suggestion was based on a more ventral localisation of the *plp/dm-20* transcripts relative to those for platelet-derived growth factor α receptor (PDGF-αR) and 2',3'-cyclic nucleotide 3'-phosphodiesterase (CNP), presumed markers for the early oligodendrocyte lineage. The cells expressing the *plp* gene have not therefore been unequivocally linked to a cell lineage, nor has a gene product been demonstrated. The purpose of the study on embryonic expression of the *plp* gene in the mouse was 1) to clarify discrepancies in previous publications regarding the initial localisation of cells expressing *plp/dm-20* transcripts; 2) to determine if there is detectable product; 3) to define whether these cells can be categorically linked to the O-2A lineage.

### Materials and methods

Studies were performed on mice aged E12 to P1 with stage of development timed as described previously (see 3.2.1.Plp/dm-20 transcript ratio studies). ISH to localise *plp/dm-20* expressing cells was performed with $^{35}$S-labelled riboprobes recognising *plp* and *dm-20* transcripts (PLP-1) or only *plp* transcripts (PLP-3B). ISH was performed on cervical, thoracic and lumbar spinal cord on both paraffin sections and cryosections (see 2.3.2.ISH Protocol). Animals E14 or older were transcardially perfused and younger animals immersion fixed using BNF prior to paraffin processing. Complete spinal columns or whole embryos were snap frozen unfixed in OCT for cryostat sections (see 2.1.TISSUE FIXATION AND PROCESSING). Some sections were counterstained with haematoxylin

and examined in bright and darkfield illumination, with or without coloured filters. To visualise the signal relative to normal architecture the bright and darkfield images were either double exposed or digitised and merged using appropriate software.

Cervical and thoracic spinal cord cryosections (15μm) were immunostained by single or double immunofluorescence. To demonstrate myelin proteins or neurofilaments, Gow's technique was used (see 2.4.1.Tissue sections). To stain for O4, sections were fixed for 5 min. in 2% paraformaldehyde followed by primary antibody for 1 hour at room temperature.

In order to increase the probability of detecting PLP-CT+ cells and to allow their characterisation, dissociated cell cultures were prepared from E12-E16 spinal cords, spinal ganglia and roots (see 2.6.1.Tissue preparation). Cells were cultured for 2 hours to give an indication of their *in vivo* status prior to either double immunostaining for myelin proteins and markers for various cell lineages or combined immunostaining/ISH. Some cultures were maintained for 24 or 48 hours so that development of the PLP expressing cells could be studied. Immunostaining for surface markers, myelin proteins and neurofilaments, combined immunostaining/ISH and $^{3}$H thymidine incorporation studies were performed as described in methods (see 2.4.2.Tissue culture and 2.6.2.Thymidine incorporation).

$^{3}$H thymidine incorporation was also studied in E14 spinal cord cryosections following intra-peritoneal injection of 5μCi $^{3}$H thymidine/gram body weight into a time mated pregnant mouse 2 hours prior to killing and embedding of the embryos. Cryosections were counterstained with haematoxylin and processed for autoradiography as described in methods (see 2.3.2.ISH Protocol). $^{3}$H Thymidine incorporation was used as a mitotic marker to determine whether cells immunostaining with the PLP-CT antibody were capable of mitosis and to visualise the position of dividing cells in the E14 spinal cord.

## Results

### ISH

*Plp/dm-20* transcripts were detected initially in the E13 cervical cord of one embryo in one cell per transverse section located in the ventricular layer approximately 2/3 down the dorsal/ventral length of the central canal and one or two cells outwith the canal. The position in the dorso-ventral axis was immediately ventral to the *sulcus limitans* of the neural canal. By E14 (Figure 39) approximately two to three positive cells per section were usual in the cervical cord of all embryos in an identical position to E13 while thoracic segments contained one cell and none were present in lumbar sections. In serial 15μm sections approximately every third section of cervical and thoracic cord contained positive cells. By E16 several additional positive cells were located immediately lateral to the floor plate and reaching to the surface of the marginal layer (Figure 39). Very occasional expressing cells were present in the medial aspects of the mantle layer. At E18 positive

cells were identified around the pial surface of the ventral and lateral marginal layer, in the dorsal columns and occasionally through the mantle layer (Figure 40). The positive cells immediately ventral to the canal (the site of initial embryonic expression) were now much less prominent. By P1 numerous expressing cells were present throughout the white matter and less frequently in grey matter (Figure 40).

RT-PCR data presented above (see 3.2.1.*Plp/dm-20* transcript ratio studies) strongly suggested that the *dm-20* isoform was predominantly responsible for the signal detected by ISH. The non-specific PLP-1 probe recognises both *plp* and *dm-20* transcripts and it is not possible to label *dm-20* transcripts specifically in tissue sections. Their presence however can be inferred by differential labelling with a *plp*-specific probe. A *plp* specific probe (PLP-3B, see 3.1.SUBCLONING OF THE MOUSE *plp* SPECIFIC SEQUENCE) was therefore used to label alternate tissue sections. No signal was detected with the PLP-3B probe at any level until E16 when occasional cells were present adjacent to the central canal and floor plate. The pattern of expression subsequently followed that identified with the PLP-1 probe but with fewer positive cells until the postnatal period.

Satellite cells in ganglia and cells in nerve roots and peripheral spinal nerves hybridised strongly with the PLP-1 probe at all ages (Figure 39) but not with the PLP-3B probe.

**Immunocytochemistry**

Reactivity to the PLP-CT antibody was not detected at E13 but was present at E14 in the cervical segments in one, or occasionally two, cells per transverse section located in an identical position to that described for ISH (Figure 41). Subsequently the developmental pattern of cells reacting to the PLP-CT antibody mirrored that found in the hybridisation studies (Figure 41, Figure 42). The developmental pattern was identical at cervical, thoracic and lumbar regions with approximately a 1 day sequential difference moving caudally between the 3 regions. Between E14 and E16 the PLP-CT antibody stained the lumen of the central canal and, more faintly, the area of the floor plate (Figure 41). This pattern was not seen with other polyclonal antibodies such as the PLP-specific antibody, nor with normal rabbit serum, and was abolished by pre-incubation with the specific C-terminal peptide.

No protein was detected with the PLP-specific antibody before E17 when positive cells were located around the floor plate; subsequent staining mirrored that with the PLP-CT antibody. Co-labelling studies showed that MBP was not detectable in the PLP-CT+ cells until E16.5/17.

Satellite cells in ganglia and cells in nerve roots and peripheral spinal nerves stained strongly with the PLP-CT antibody at E13 and older, but not with the PLP-specific

antibody. Spinal roots and ganglia failed to stain with O4 at E13 and E14 but were positive at E18.

**Dissociated cell culture**

Initially E14 and older embryonic cultures were studied. As would be expected from immunostaining of cryostat sections PLP-CT+ cells were found, in increasing numbers, at all ages from E14 onwards. The majority of these cells co-stained with A2B5, O4 or RmAb and in older embryos (E16+), MBP, suggesting that they were from the O-2A lineage. Cultures also contained numerous neurones labelling with A2B5 and SMI-31 (neurofilament) antibodies.

At E12, numerous small A2B5+ cells were present; O4+ cells were obvious though less frequent; very occasional RmAb+ cells were seen but O8+ cells were not detected. Cells immunostaining with the PLP-CT antibody (Figure 43) or hybridising with the PLP-1 probe (Figure 44) were detected at a frequency of approximately 1 to 3 per coverslip (60-80,000 cells/coverslip) at E12 and 10 to 20 positive cells at E13. Small clumps of positive cells were also seen. Cells staining with PLP-CT or hybridising with the PLP-1 probe labelled with A2B5 or O4 and occasionally RmAb. Not all cells staining for A2B5 or O4 or RmAb co-labelled for PLP-CT or hybridised with the PLP-1 probe, and at 2 hours, and to a lesser degree at 24 and 48 hours after culture of E12 cords, cells were identified labelling with the PLP-CT antibody or PLP-1 probe, but negative for A2B5, O4 or RmAb. After 24 hours in culture, multiprocess oligodendrocytes labelling with O4 and RmAb were detected, which became more numerous by 48 hours. Some of these cells co-labelled with PLP-CT antibody (Figure 43). No cells from E12 spinal cords immunostained with MBP or PLP-specific antibodies up to 48 hours in culture. Although numerous PLP-CT+ cells were present in dissociated cultures of spinal roots and ganglia, no PLP-CT+/O4+ or PLP-CT+/RmAb+ cells were seen.

**$^{3}$H thymidine incorporation**

Pulse labelled, dissociated cells were immunostained with PLP-CT and a recognised O-2A lineage marker, either 1, 24 or 48 hours after removal of thymidine. In E12 dissociated spinal cord cultures one hour after labelling, PLP-CT+ cells were present which had incorporated thymidine, many of which were co-labelled with A2B5 (Figure 45). One RmAb+ cell was seen but no O4+ cells. After up to 48 hours in culture, multiprocess PLP-CT+/O4+ and PLP-CT+/RmAb+ cells were identified, which had incorporated thymidine during the 1 hour pulse (Figure 45).

Numerous cells which had incorporated thymidine in the E14 embryos could be seen throughout the body structures. Within the developing spinal cord positive cells were seen much less frequently. Several positive cells per section were present, mostly in the outer mantle area, predominantly ventrally. Occasional positive cells were seen in the marginal

zone. In all sections studied a few positive cells were present in the ventral ventricular area corresponding to the location of the PLP-1+/PLP-CT+ cells seen in ISH and immunostaining studies (Figure 46).

## Discussion

The above results demonstrate that the *plp* gene is expressed in a very discrete region of the ventricular layer of the embryonic spinal cord, located immediately ventral to the future central canal, at E13 and probably at E12. Between E14 and birth, cells expressing the *plp* gene appear to progress ventrally via the borders of the floor plate to reach the pial surface between E16 and E18. At E18 similar cells are also found in the lateral and to a lesser extent, dorsal columns. Full length protein product is present in these cells, the majority of which can be identified as belonging to the O-2A lineage.

Presence of *plp* transcripts in the mouse embryo (as discussed in 3.2.1.Plp/dm-20 transcript ratio studies) has been demonstrated previously, and indeed it has been suggested that *dm-20* is exclusively expressed in the embryo (Ikenaka *et al.* 1992; Timsit *et al.* 1992a). The validity of the RT-PCR findings is strengthened by the demonstration of *plp*-specific transcripts by ISH at E16 and PLP-specific immunostaining at E17 and E18. It is clear however from the above results that at all embryonic ages *dm-20* is the predominant message. *Dm-20* transcripts have been demonstrated previously in the mouse or rat spinal cord (Timsit *et al.* 1995; Yu *et al.* 1994) but this is the first demonstration of the presence of protein. As the PLP-CT antibody is directed against the C-terminal portion of the protein it would indicate that a full length, and therefore functional product is present. Demonstration of product implies that the presence of transcripts is not likely to be due to non-regulated transcription and that the presence of DM-20 in the embryonic spinal cord is likely to have real functional significance.

The apparent orderly spread of PLP-CT+ cells and eventual co-expression of the myelin proteins MBP and PLP strongly suggest that they are derived from the O-2A lineage. Freshly dissociated cells from E12 spinal cords and older which are positive for *dm-20* transcripts and protein co-stain with known markers of the O-2A lineage:

1) A2B5, a marker for some O-2A progenitors in the mouse (Raff *et al.* 1983). A2B5 does label other cell types such as neurones and type 2 astrocytes (Einsenbarth *et al.* 1979; Schnitzer and Schachner 1982), however no evidence was found that DM-20+ cells co-stained with the neuronal marker SMI-31 (neurofilaments) and E12 spinal cords did not stain for the astrocytic marker GFAP.

2) O4 and RmAb, markers of the proligodendroblast and immature oligodendrocyte respectively. Perinatal and postnatal Schwann cells also bind O4 and RmAb. In rat, Schwann cells acquire O4 staining at E16/17 and Gal C (also recognised by RmAb) at E18/19 (Jessen and Mirsky 1991; Mirsky *et al.* 1990), but neither was detected at E14 (Jessen *et al.* 1994). Although all efforts were made to prevent contamination of spinal

cord cultures with PNS material it was necessary to exclude this possible contamination as a source of the PLP-CT+/O4+ or PLP-CT+/RmAb+ cells. This was done on the basis that O4 staining of ganglia and spinal roots was present on cryostats only at E17 and older, and that no PLP-CT+/O4+ or PLP-CT+/RmAb+ cells were present in E12/13 spinal root and ganglia dissociated cultures prepared using material removed during the establishment of the spinal cord cultures of the same age.

After 24 to 48 hours in culture, cells with typical oligodendrocyte morphology and positive for Gal C, some of which co-stained for PLP-CT, were detectable.

Some of the cells expressing *dm-20* transcripts or staining for PLP-CT could not be co-stained with A2B5, O4 or RmAb, nor with SMI-31. These may represent; 1) earlier precursor cells, known to exist (Gonye *et al.* 1994; Hardy and Reynolds 1991; Nakafuku and Nakamura 1995), for which there are as yet no defining markers; 2) O-2A cells which are staining for DM-20 but are unlabelled by A2B5 or O4 due to the discontinuity between loss of A2B5 and gain of O4 in the mouse. In the rat the earlier A2B5 marker is overlapped by O4 which is then followed by RmAb. This overlap does not occur in the mouse thus giving rise to some cells unlabelled by either A2B5 or O4 (Fanaragga *et al.* 1995). It is possible that some of the positive cells may represent early neuronal precursors not expressing neurofilaments, but neither the present results nor those of other groups using neuronal markers such as TuJ1 (Timsit *et al.* 1995) would support this.

Mouse E12 spinal cord cultures at 2 to 48 hours, contained O4+ and RmAb+ cells which did not co-express PLP-CT. These cells may represent; 1) sub-populations of O-2A lineage cells exhibiting differences in the timing and level of *dm-20* expression relative to cell differentiation, perhaps regulated by their immediate environment; 2) biphasic expression in individual cells. Early O-2A progenitors may express *dm-20* with a partial down-regulation of the gene in the intermediate proligodendroblast stage accounting for the O4+/DM-20- cells, to be followed by a further period of *dm-20/plp* expression as the GalC+ oligodendrocyte matures. The absence of a biphasic expression profile in the RT-PCR data reflects the fact that the generation and differentiation of all O-2A lineage cells is not synchronous so that bulk samples from whole spinal cords will contain increasing numbers of cells at various stages of development.

It is known that O-2A progenitors are motile *in vitro* (Small *et al.* 1987), and probably *in vivo* although precursor cells may also contribute to the dispersion of the lineage (Gonye *et al.* 1994). Progenitors and proligodendroblasts are known to be proliferative and divide in response to various mitogens (Gard and Pfeiffer 1990; Hardy and Reynolds 1991; Barres and Raff 1994). On the other hand, oligodendrocytes expressing myelin proteins are classically non-motile (Small *et al.* 1987), post-mitotic cells (Gard and Pfeiffer 1990; Hardy and Reynolds 1991). If the PLP-CT+ cells present in the embryonic cord are O-2A progenitors, we would therefore expect them to be both motile and capable of cell division. The studies suggest indirectly that the PLP-CT+ cells are likely to be motile. This is based

on the sequentially progressive distribution of labelled cells in tissue sections, suggestive of migration. The thymidine incorporation in dissociated cultures show that PLP-CT+ cells undergo mitosis and subsequently develop into oligodendrocytes. The presence of thymidine-labelled cells in the same location as PLP-CT+ and PLP-1+ cells in the E14 embryo sections is consistent with the *in vitro* thymidine labelling, however it is not possible to ascribe these cells to a particular lineage based on thymidine labelling alone. The majority of radiolabelled cells in the E14 cord cryosections probably represent glial precursors as most neurogenesis in the spinal cord is essentially complete by E14 in the mouse (Nornes and Carry 1978; Sims and Vaughn 1979). The majority of glial proliferation, however, has still to occur (Gilmore 1971). The above data challenge previous perceptions relating to myelin gene expression during oligodendrocyte development indicating the DM-20 isoform is present in progenitors, much earlier than previously recognised, and not just in the more mature, post-mitotic oligodendrocyte.

The results also support the proposition that oligodendrocytes originate in a discrete region of the ventral spinal cord (Noll and Miller 1993; Timsit *et al.* 1995; Warf *et al.* 1991; Yu *et al.* 1994). The location of DM-20+ cells in this study is in agreement with the findings of Timsit *et al.* (1995) in the mouse rather than those of Yu *et al.* (1994) in the rat. It may be that DM-20 labels different cell types in the rat or that the same cell types originate in slightly different locations. The transient nature of *plp* gene expression seen in the rat relative to the mouse is harder to explain. In the rat, other markers such as CNP and PDGFα receptor have been used to define O-2A progenitors in the embryonic spinal cord (Pringle and Richardson 1993; Yu *et al.* 1994). The pattern of expression seen with these markers is somewhat different from that seen with DM-20 in the mouse. Positive cells tend to be more numerous and more widely distributed throughout the grey and white matter. If the CNP+, PDGFαR+ cells are all O-2A progenitors it is possible that not all these cells express *dm-20*, or that they do so in a more transient manner, possibly influenced more by local environment. Cells present in white matter areas may express *dm-20* whilst those migrating through grey matter areas may lack expression although still exhibiting other O-2A markers such as CNP and PDGFαR. Changes in antigenic profile in precursor cells whilst migrating through grey matter areas have been reported previously in studies on oligodendrocyte differentiation in rat brain (LeVine and Goldman 1988). Rapid changes in both morphology and loss of ability to bind anti-$G_{D3}$ antibody were seen when cells entered the grey matter. Presumably, local environment must play an important role in determining cell morphology and expression of markers such as $G_{D3}$ and possibly, therefore, PLP/DM-20. It is also possible that not all CNP+, PDGFαR+ cells are destined to become oligodendrocytes or that oligodendrocytes may be derived from more than one distinct lineage. PDGFαR expression is seen at earlier times in the rat spinal cord, probably in developing interneurones (Pringle and Richardson 1993). CNP appears to mark two populations of cells, strongly staining cells with a distribution similar to that seen with

*dm-20*, and diffusely staining cells with a more widespread distribution (Yu *et al.* 1994). The appearance of *plp/dm-20*+ cells in the dorsal columns at E18 raises questions about the possible migration pathways of the oligodendrocyte precursor cells. It is possible that precursors may migrate ventrally and then laterally to colonise the ventral and ventro-lateral columns or, alternatively, cells may " take the shortest route" migrating in a radial manner. This would be consistent with previous studies which have demonstrated that immature spinal cord oligodendrocyte precursors in the developing white matter have a striking radial orientation (Choi *et al.* 1983; Hirano and Goldman 1988). Migration of cells to the dorsal columns, however, would logically occur in a dorsal direction, a theory supported by studies of oligodendrocyte precursors in embryonic chicken spinal cord (Ono *et al.* 1995). No *plp/dm-20*+ "migrating" cells are seen in the intermediate grey matter between E14 and appearance of *plp/dm-20*+ cells in the dorsal columns at E18. It is possible that expression in oligodendrocyte precursors and oligodendrocytes once they have reached the white matter areas is controlled by different factors than those influencing early expression in the germinal areas of the ventricular zone during earlier embryogenesis. * There is currently much speculation regarding the factors involved in inducing specific cells in the ventricular zone to develop into particular lineages and express associated genes. Expression or activation of transcription factors, DNA-binding proteins which exercise control over transcription of genes is likely to be of critical importance. Genes encoding these proteins are involved in rostro-caudal positioning (*Hox* genes), dorso/ventral positioning (*Pax* genes) and also may be involved in the determination of cell fate (for review see Lemke (1993)). It has recently been demonstrated that expression of the *plp* gene itself is sufficient for, and directly associated with, secretion of a factor which influences oligodendrocyte development (Nakao *et al.* 1995). Culture supernatants from *plp* expressing cell lines were shown to increase oligodendrocyte numbers when added to primary glial cell cultures from embryonic brain. Whether *plp/dm-20* expression is one of the initial committing steps towards the oligodendrocyte lineage, and what the factors initiating this early *plp* expression are, remain as yet, unanswered questions. The notochord and floor plate are known to exert a strong influence on the development of the embryonic cord (Yamada *et al.* 1991) and substances produced by the floor plate, such as retinoids (Noll and Miller 1994), PDGF-A (Orr-Urtreger and Lonai 1992) and products of the hedgehog gene family (Martí *et al.* 1995), are possible influencing factors. Indeed it has recently been shown in the chick embryo that floor plate or notochord explants can influence oligodendrocyte differentiation *in vitro* (Trousse *et al.* 1995). The close

---

* Using isotopic/isochronic grafts of chick and quail neural tube, Cameron-Curry and Le Douarin (1995) have demonstrated that oligodendrocytes are also generated from dorsal neural tube and that extensive ventrodorsal and dorsoventral migrations of oligodendroblasts occurs.

association of *plp* expressing cells with the floor plate, as observed in the present study would also raise the question as to whether the floor plate may exert a chemotactant influence on these cells.

It may be possible to further confirm that the oligodendrocyte lineage is the source of early embryonic expression of the *plp* gene by a combination of either ISH or immunostaining of thick vibratome tissue sections with PLP/DM-20 markers followed by EM examination of ultra-structural morphology of labelled cells. Such an approach has been used by Ono *et al.* (1995) to study early O4+ cells in chicken spinal cord, another proposed marker of the oligodendrocyte lineage. These authors demonstrated O4+ cells were present in the ventricular zone, in a similar position to *dm-20*+ cells seen in the rat, and that they had many characteristics associated with ventricular cells. Indeed the O4+ cells were essentially identical to their surrounding neighbours. It may therefore be necessary to look at cells which are further along the differentiation pathway, around E16 in the mouse, before typical morphology associated with the oligodendrocyte lineage or possibly other lineages becomes apparent. The major problem with this approach is the assumption that one can infer developmental changes by examining a series of static images. The cells expressing *plp/dm-20* at E16 or older ages may not be the same cells as those seen at E14 adjacent to the central canal, nor may they be derived from these cells. This is especially pertinent given the apparent transient nature of expression seen in these cells in the rat (Yu *et al.* 1994). The limitation of only being able to view a specific cell at one particular time point is the root of this problem. Demonstrating that expression of the *plp* gene is biphasic is difficult using different cells at single time points, but may be accomplished by double immunostaining for PLP/DM-20 and a series of sequential O-2A markers such as GD3, A2B5, O4, RmAb. This will still be difficult given the very small number of expressing cells in the embryonic cord. Optic nerve cultures contain considerably more DM-20+ progenitors, and their use may overcome this problem. Similar problems of studying single time points arise when trying to follow migration and expression of these early PLP/DM-20+ cells. Ideally, it would be desirable to be able to label and view positive cells both *in vivo* and *in vitro*, possibly in cord explant cultures, using a non-invasive technique. This would allow assessment of expression in the same cell over a defined period. One approach to this would be the generation of transgenic mice expressing PLP fusion proteins consisting of PLP plus a marker protein such as Lac-Z or Green fluorescent protein (GFP) (Chalfie *et al.* 1994; Prasher *et al.* 1992). A PLP/Lac-Z transgenic mouse with apparently normal temporal and spatial expression of the PLP-fusion protein has been reported (Wight *et al.* 1993). GFP exhibits inherent fluorescence under UV illumination and appears to exert no toxic effects in eukaryotic systems. A PLP/GFP transgenic mouse similar to the PLP/Lac-Z mouse, with normal expression and targeting, would allow non-invasive monitoring of *plp* expression in the embryo in real time. This may prove a useful tool in unravelling some of these remaining questions.

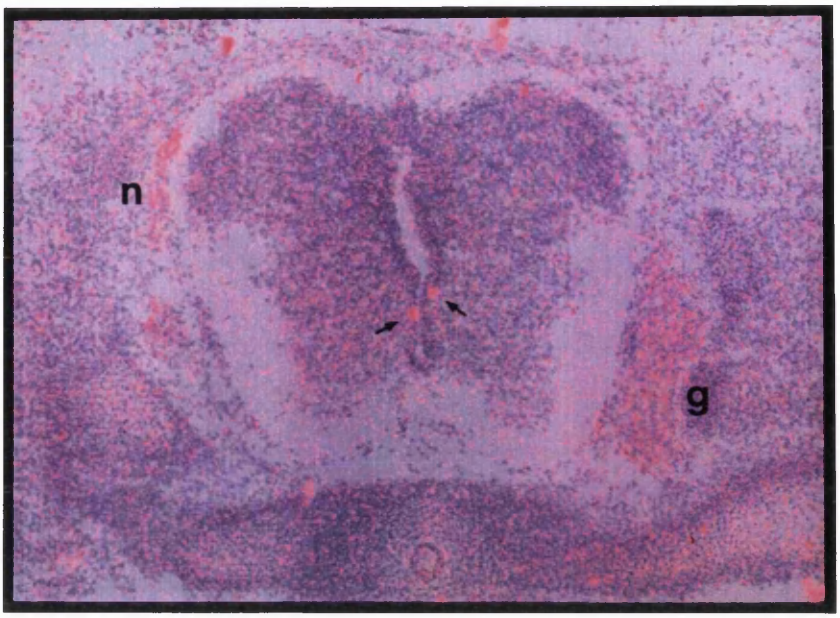


**(a)**

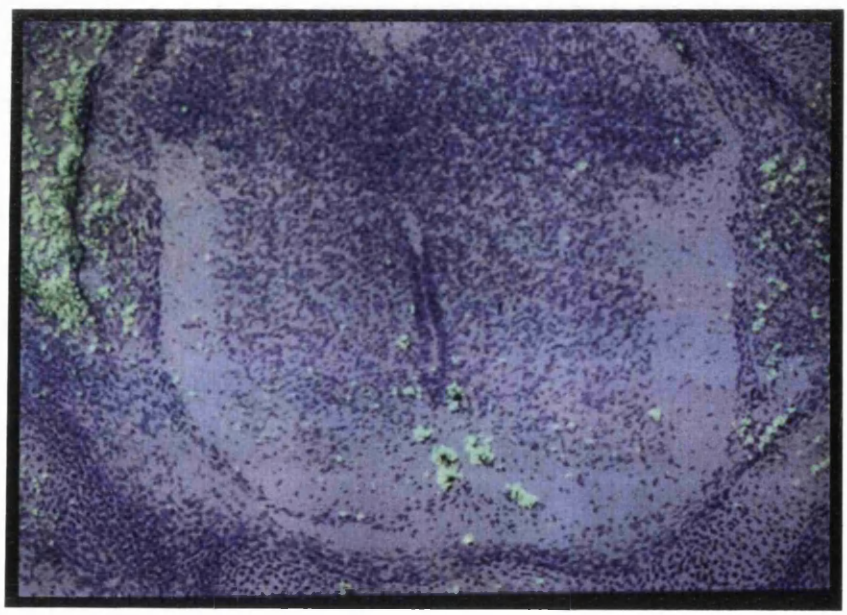

**(b)**

**Figure 39.** Embryonic spinal cord ISH (PLP-1 probe recognising *plp* and *dm-20*). Hybridisation signal has been photographed in darkfield using either a red filter and then double exposed with the brightfield image or with a green filter, digitised and merged with the brightfield image using software. **a)** E14 Positive cells are present in a discrete region of the ventricular zone (arrows), spinal ganglia (**g**) and nerve roots (**n**). **b**) E16 Positive cells are now seen adjacent to the floor plate.

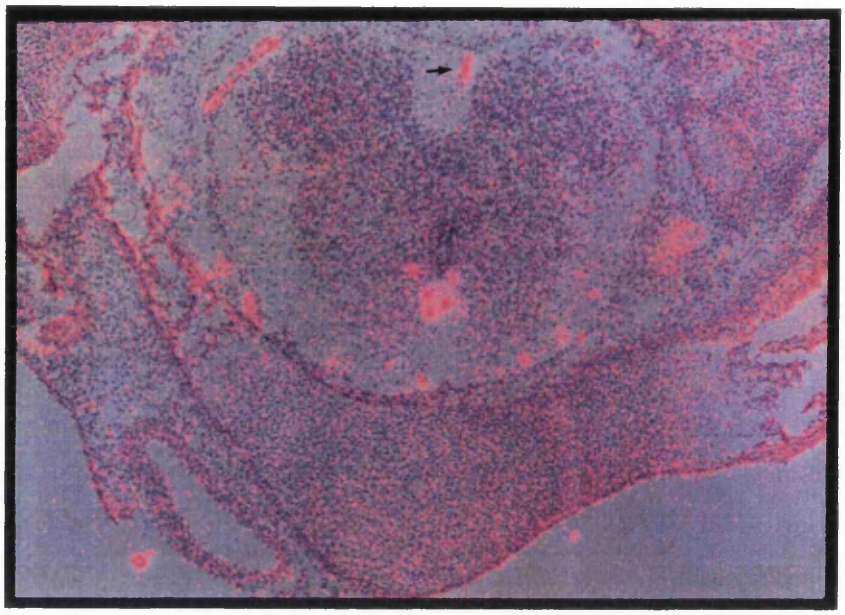

(a)

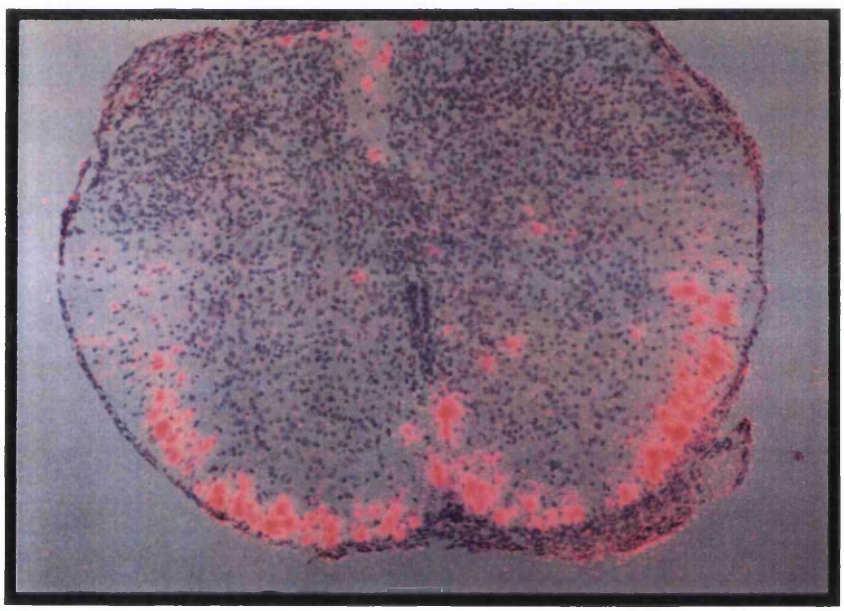

(b)

**Figure 40.** Embryonic spinal cord ISH (PLP-1) (cont.). **a**) E18 Positive cells are now more widespread in the ventral marginal zone with occasional positive cells in the dorsal columns (arrow). **b**) P1 Numerous strongly positive cells are now present throughout the white matter with occasional positive cells present in the grey matter.

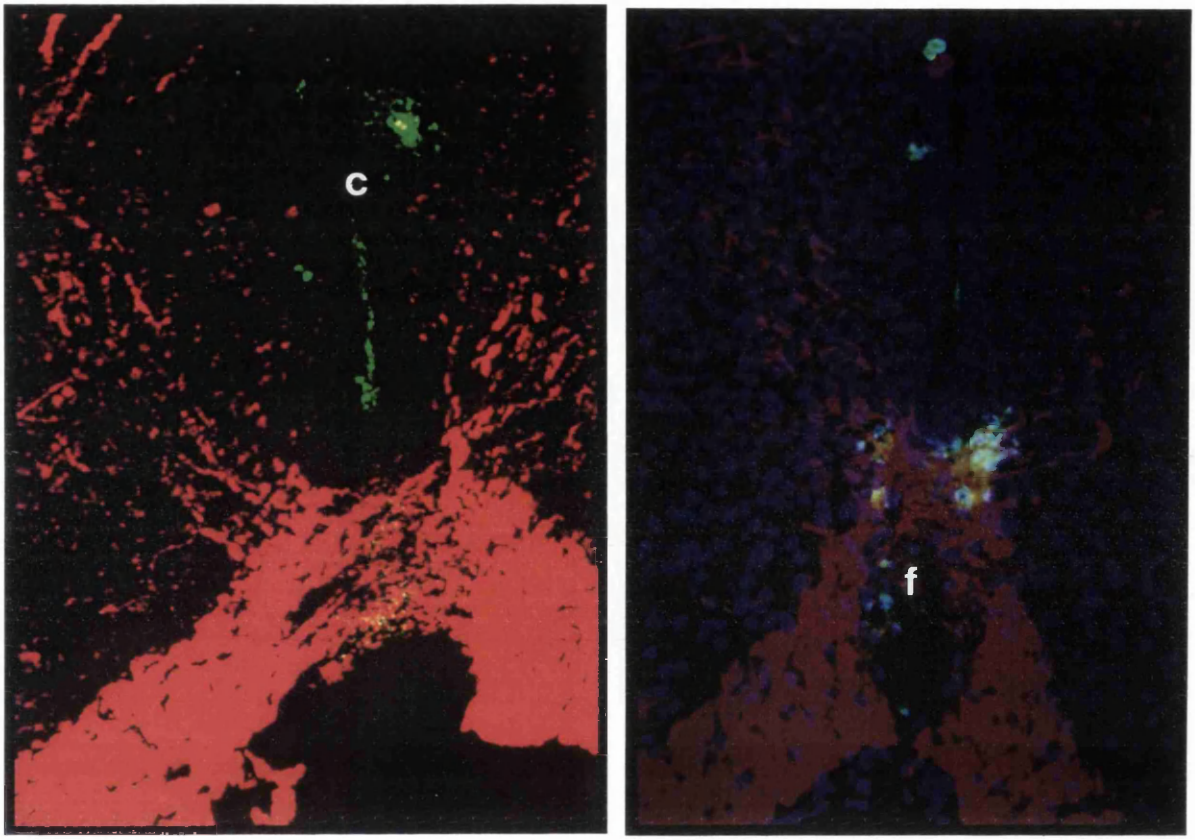


(a) (b)

**Figure 41.** Embryonic spinal cord immunostaining. PLP-CT antibody (green), neurofilament antibody (SMI-31), detecting axons (red). **a)** E14 One or two positive cells are present adjacent to the central canal (**c**). The luminal surface of the canal and the floor plate area (appearing as yellow) are also stained with PLP-CT. **b)** E16 Cells are present below the central canal and around the floor plate (**f**). The yellow appearance of some cells is due to superimposition of cells and axons , not co-localisation. Nuclei are stained with DAPI (blue).


(a)

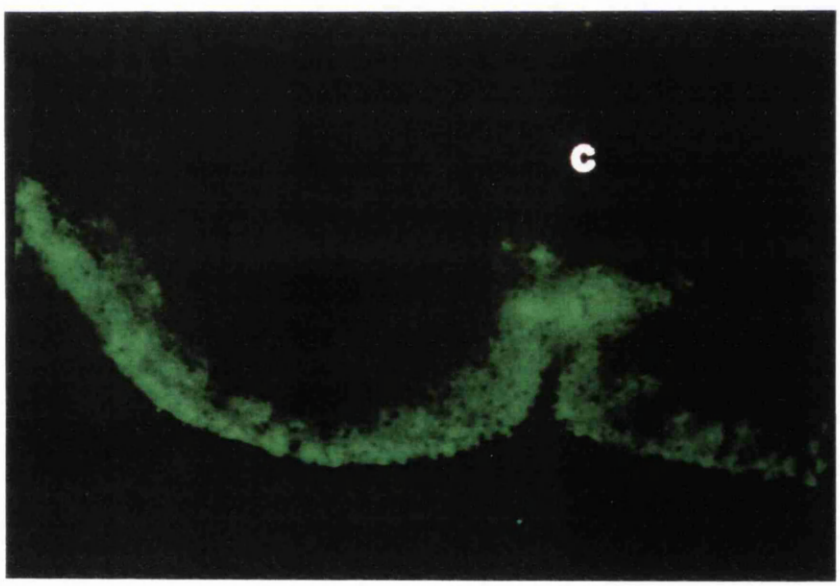


(b)

**Figure 42.** Embryonic spinal cord immunostaining PLP-CT antibody (cont.). **a)** E16 floor plate region (**f**) in more detail; positive cells can be seen in close association with the lateral borders of the floor plate. **b)** By P1 intense staining is now present throughout the white matter (central canal = **c** ).

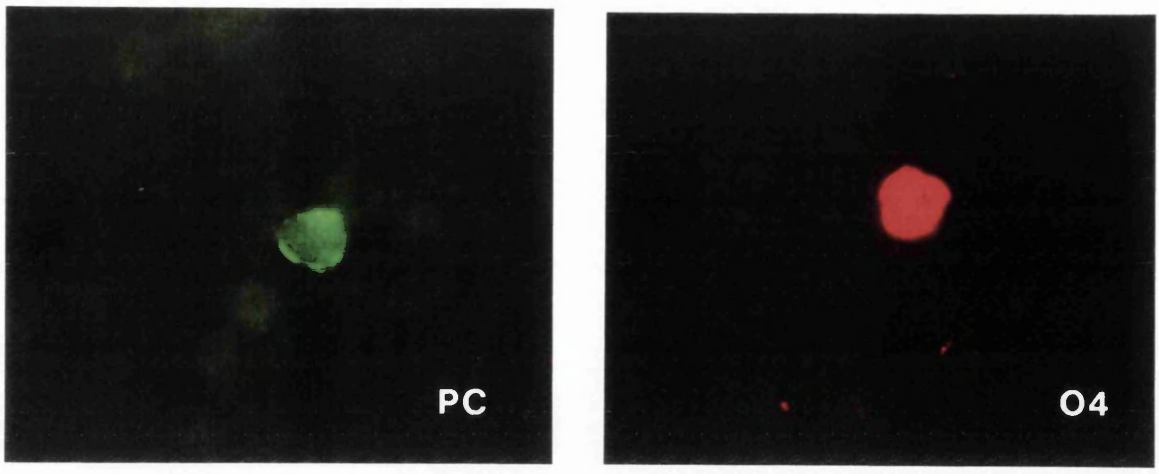


(a)

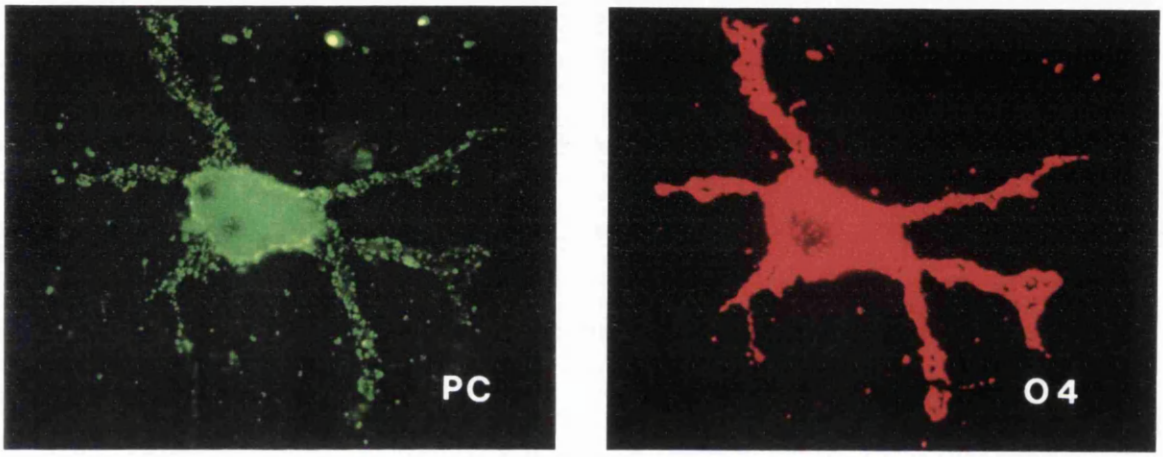


(b)

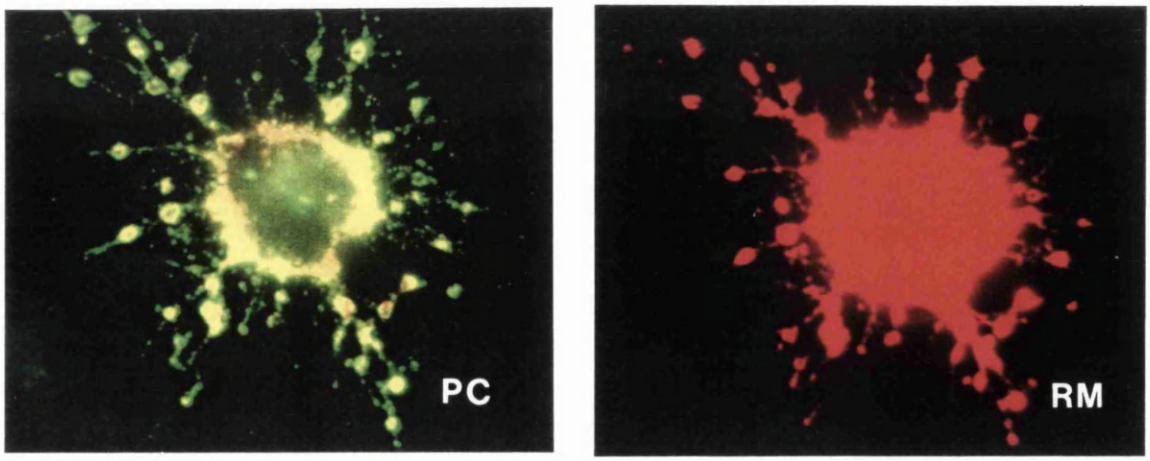


(c)

**Figure 43.** E12 spinal cord dissociated cell culture. **a**) 2 hours, **b**) 24 hours, **c**) 48 hours in culture. Cells can be seen co-immunostaining with PLP-CT (**PC**) and O4 or RmAb (**RM**), markers of the O-2A lineage. With time in culture, the development of a multipolar morphology typical of developing oligodendrocytes is evident.

(a)

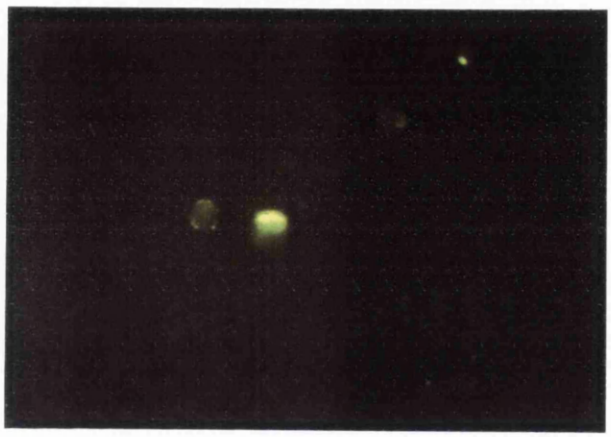

(b)

(c)

**Figure 44.** E13 spinal cord dissociated culture, combined ISH/immunostaining. Cells were cultured for 2 hours before immunostaining with **a)** A2B5, **b)** RmAb, and then hybridised for **c)** PLP-1. Co-localisation of hybridisation signal (arrow) with markers of the O-2A lineage is demonstrated.

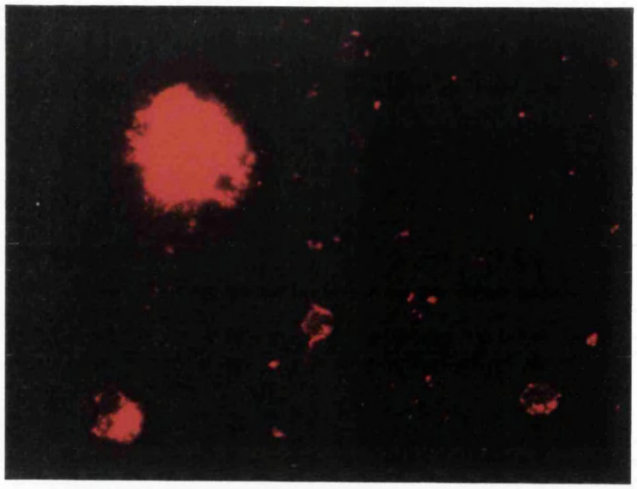

(a)

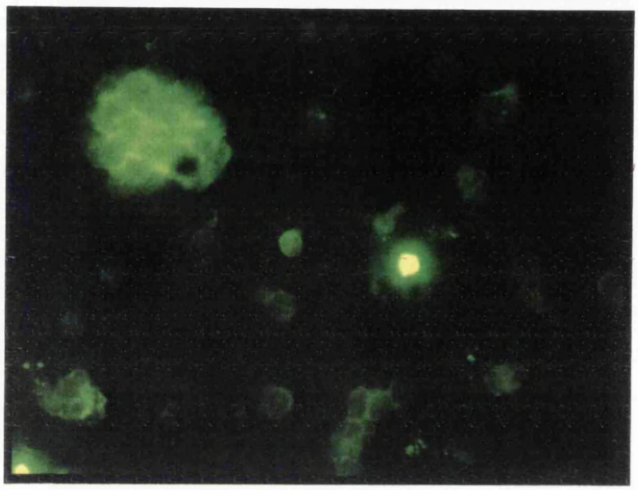

(b)

(c)

**Figure 45.** Thymidine incorporation, E12 dissociated spinal cord culture. Two hour total culture time after 1 hour $^{3}H$ thymidine labelling; **a**) A2B5, **b)** PLP-CT, **c)** $^{3}H$ thymidine. Co-immunostaining with the O-2A lineage marker A2B5 and PLP-CT demonstrates a clump of A2B5+/PLP-CT+ cells at 2 hours, one of which has incorporated radiolabel (arrow).

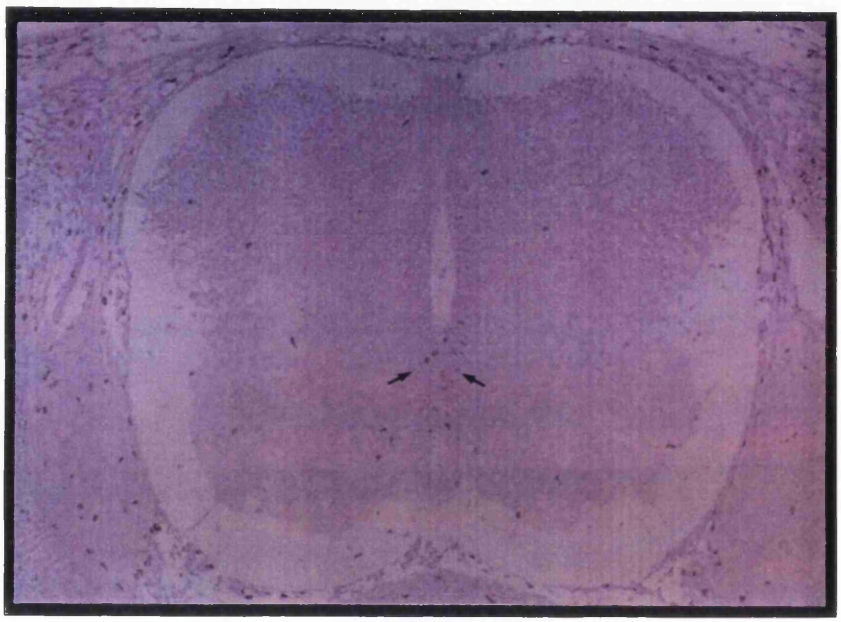

**Figure 46.** E14 embryo spinal cord, *in situ* $^{3}$H thymidine labelling. Numerous labelled cells are present throughout the body of the embryo with fewer labelled cells in the spinal cord. Within the cord, positive cells can be seen in the ventral ventricular area (arrows).

## 3.2.3.PNS studies

### Introduction and aims

The expression of the *plp* gene in the peripheral nervous system has been well documented for several years (Ono *et al.* 1990; Puckett *et al.* 1987; Stahl *et al.* 1990). It is known that in the normal animal PLP/DM-20 protein is not incorporated into the myelin sheath (Ono *et al.* 1990; Puckett *et al.* 1987) and that DM-20 is the predominant isoform (Pham-Dinh *et al.* 1991). Unlike myelin proteins which are incorporated into PNS myelin ($P_0$, PMP-22, MBP), it has been shown that *plp/dm-20* expression does not parallel the myelination process, as it does in the CNS (Gupta *et al.* 1991; Stahl *et al.* 1990), although a modest increase concomitant with increasing numbers of Schwann cells may be seen (Kamholz *et al.* 1992). However, there is little information relating to possible changes in *plp/dm-20* ratios during this developmental period. It has also been demonstrated that the effect of nerve section or crush injury on *plp* gene expression is minimal compared to the dramatic down-regulation seen with other PNS myelin proteins such as $P_0$ or PMP-22 (Gupta *et al.* 1991; Kamholz *et al.* 1992). Again, little information is available regarding the possible effects on *plp/dm-20* transcript ratios following axotomy or crush injury of peripheral nerve. It was therefore decided to use RT-PCR to study the relative developmental pattern of expression of the *plp* and *dm-20* isoforms in the PNS and also to determine whether transection of peripheral nerve would have any effect on *plp/dm-20* transcript ratio.

### Materials and methods

Developmental studies were performed using sciatic nerves from P1, 5, 10, 15, and 20 C3H/HeH X 101H mice. Cervical sympathetic trunks (CST) and cranial cervical ganglia (CCG) and sciatic nerve were collected from adult Sprague-Dawley rats. Rats were used as a source of CST material due to the limiting amounts of tissue obtainable from mice. Transection studies were performed on distal segments of transected sciatic nerve from adult mice 1 and 3 weeks post-transection. Six transected and six contralateral non-transected sciatic nerves from age matched littermates were processed for RT-PCR as previously described using cyclophilin as an internal control, and $P_0$ as a positive control for down-regulation (see 2.2.2.Analysis of transcripts). As a comparative study, *plp/dm-20* transcript ratio was studied in transected and non-transected adult rat optic nerves 3 weeks post-transection. Both sciatic and optic nerve transections were performed under halothane/oxygen general anaesthesia using an induction chamber and mask. Access to the sciatic nerve was *via* a lateral approach separating the vastus and biceps muscles. Access to the optic nerve was achieved *via* an incision over the dorso-lateral aspect of the bony orbit and blunt dissection between the eyeball and the bony orbit. Skin wounds were closed with Michel clips (International market supply).

## Results

### Developmental profile

Both *plp* and *dm-20* products were identified in the sciatic nerve at all ages studied. *Dm-20* was always the predominant product and there was no observable alteration in product ratio over the period from P1 to P20 (Figure 47). Both products were also present in rat CST, CCG and sciatic nerve. When CST and sciatic nerve were compared, the relative abundance of the *dm-20* product was greater in the CST with the *plp* isoform being a minor signal in both (Figure 47).

### Sciatic nerve transection

Three weeks after transection of mouse sciatic nerve, semi-quantitative RT-PCR analysis of distal nerve segments identified a marked decrease in $P_0$ mRNA in the transected nerve compared to the contralateral non-transected nerve (Figure 48). Using *plp/dm-20* primers a similar product ratio to the one seen in the mouse developmental profile was observed in the non-transected nerve with marked predominance of *dm-20* product. No significant change in amount of *dm-20* product was seen in the transected nerve, however *plp* product was significantly less in the transected nerve (Figure 48). This would suggest that there was selective down-regulation of the *plp* isoform. The experiment was repeated with analysis of transcripts 1 week post-transection with results similar to those of the 3 week post-transection study (Figure 48).

Effects of transection of the rat optic nerve is similar to that seen in mouse sciatic nerve with *dm-20* product levels remaining unchanged, and *plp* levels decreasing (Figure 49). *Plp* however is the major isoform present at all times as would be expected in the CNS.

## Discussion

Upon transection of a peripheral nerve, down-regulation of myelin genes coding for proteins incorporated into the PNS myelin sheath such, as $P_0$, PMP-22 and MBP, is well documented (De Leon *et al.* 1991; Gupta *et al.* 1991; Kamholz *et al.* 1992; LeBlanc *et al.* 1987; Snipes *et al.* 1992; Trapp *et al.* 1988). It has been suggested that maintenance of Schwann cell expression of these genes is highly dependent on axonal contact, and regulation occurs primarily at the level of transcription. Similar studies into *plp/dm-20* expression following either transection or crush injury of sciatic nerve demonstrated that down regulation may be relatively small, possibly as little as 30% as compared to >90% for $P_0$ (Gupta *et al.* 1991) following transection. These findings together with the apparent uncoupling of the *plp* gene from the co-ordinate expression seen in other PNS myelin genes, has lead to the conclusion that unlike the major myelin proteins in the PNS, *plp* gene expression is not under strict axonal control.

No apparent developmental change in *plp/dm-20* ratio was seen in this study, unlike the

CNS where the dramatic *plp/dm-20* ratio change appears to be a feature of co-ordinate gene expression during myelination (see 3.2.1.Plp/dm-20 transcript ratio studies). This would imply that not only is total transcriptional activity not correlated with myelination in the PNS, as has been demonstrated previously (Gupta *et al.* 1991; Stahl *et al.* 1990), but also that regulation of transcript ratios appears to be unaffected by the onset of myelination. Myelination of mouse sciatic nerve commences around birth (Fraher 1972; Winter *et al.* 1982) and probably slightly before. The current study did not look at embryonic sciatic nerves. However given the constancy in ratio seen during the earliest post-natal period, it is unlikely that any gross changes will be seen in late embryonic nerves. This may imply that either the *plp* gene does not have a critical role in PNS myelination, as might be supported by the lack of abnormalities in the PNS of *plp* mutant animals, or any role that it does play does not require predominance of the *plp* isoform. Abnormalities in the PNS of *plp* mutant animals may exist, but may be subtle and require demonstration at EM level. It is also possible that the markedly reduced lifespan of these severely affected mutants is too short for structural changes to develop. A further consideration is that the function of DM-20 may be duplicated by other molecules unaffected by mutations of the *plp* gene so that no phenotypic effect is evident, a theory supported by the surprisingly normal phenotype reported in *plp* transgenic "knockout" mice (Boison and Stoffel 1994) (K.Nave unpublished). It is interesting to note that levels of *dm-20* product were found to be higher in CST relative to sciatic nerve. The CST contains predominantly unmyelinated fibres compared to the mixed population found in the sciatic nerve and this increased *dm-20* product level possibly reflects a high abundance of *dm-20* transcripts in non-myelin-forming Schwann cells.

It has been suggested that the difference between *plp* gene expression in the PNS and the co-ordinate expression seen during myelination in the CNS may be due differences in the *trans*-acting factors involved in the regulation of transcription in the Schwann cell and oligodendrocyte (Kamholz *et al.* 1992). Consistent with this notion is the fact that most transcripts in the PNS are initiated from the more proximal of two start sites, possibly responsible for maintenance expression, while in the CNS the distal site is used, which may be responsible for inducible transcription as is seen during CNS myelination. Interestingly, it appears that steady state transcription in the CNS may also involve transcription from this proximal start site (Scherer *et al.* 1992). A recent study has shown that the two PLP isoproteins are targeted to different locations in the Schwann cell cytoplasm, with the less abundant PLP being found only in the perinuclear cytoplasm of myelin forming Schwann cells, and DM-20 being found predominantly at the paranodes, Schmidt-Lantermann incisures and in non-myelin-forming Schwann cells (Griffiths *et al.* 1995a). This may imply that the two proteins have different functions in the PNS (as is postulated in the CNS). Given this apparent uncoupling of targeting of the two isoforms it is interesting that regulation of the two isoforms at the transcript level also appears to be

under differing controls. Although levels of *plp* transcripts in the PNS are low, PLP specific product has been demonstrated (Griffiths *et al.* 1995a) and the down-regulation seen upon nerve transection would imply that expression of *plp* is influenced by axonal factors. Whether this results from loss of positive regulatory influences, activity of silencer elements known to exist (Berndt *et al.* 1992; Cambi and Kamholz 1994; Nave and Lemke 1991) or variation in transcript splicing remains to be seen. *Dm-20* transcript levels on the other hand do not seem to be affected by nerve transection either in the PNS or CNS. As *dm-20* is by far the predominant isoform in the PNS, this may explain why only minimal down-regulation of total transcripts is seen on northern and dot blots after nerve transection/crush, as the two isoforms cannot be distinguished using these techniques. Down-regulation of myelin genes in the CNS following optic nerve transection is not as severe as that seen in the PNS but can be up to 50% by 10 days post transection (Kidd *et al.* 1990; McPhilemy *et al.* 1990; Scherer *et al.* 1992). The down-regulation seen with the RT-PCR after 3 weeks is in good agreement with these studies and interestingly, as in the PNS, appears to show that loss of axonal influences are responsible for down-regulation of *plp* transcripts, but have little effect on *dm-20* transcript levels. Optic nerve transections were performed on rats due to size limitations and familiarity with the procedure in this species. An interesting observation in the PNS was that although overall levels of transcript were little altered, it was not possible to demonstrate immunostaining in the distal segment of the 3 week transected nerves using the PLP-CT antibody. However, PLP/DM-20 protein was present in the Schwann cell cytoplasm of the degenerating nerve 1 week post-transection. This would imply additional post-transcriptional control of PLP/DM-20 protein levels, or at least of DM-20 protein, in the PNS since no such decrease in transcript is demonstrated by RT-PCR. Lack of staining of PLP specific protein is presumably attributable to the transcriptional down-regulation similar to that seen with other major PNS myelin proteins such as $P_0$ and MBP. Post-transcriptional control of PLP/DM-20 has been demonstrated *in vitro* by Kamholz *et al.* (1992). Loss of immunostaining for $P_0$ and PLP/DM-20 in primary rat Schwann cell cultures was demonstrated over a 1 week period, after which time, addition of high concentrations of dibutryl 2', 3' cyclic AMP produced a marked increase in $P_0$ and PLP/DM-20 immunoreactive cells. However, whereas steady state levels of $P_0$ mRNA increased after addition of cyclic AMP, levels of *plp* message remained the same, suggesting post-transcriptional regulation of PLP/DM-20.

Based on previous studies suggesting a dual role for the *plp* gene, the specific targeting of the two isoforms in the Schwann cell and the relative abundance of DM-20, it seems likely that DM-20 may well have a non-structural role to play in Schwann cells. The evidence that regulation of transcript levels of the two *plp* isoforms may be under the influence of different factors adds weight to this theory. Additional corroboration of the RT-PCR data will be needed, preferably by a direct method such as transcript mapping along with

western analysis of protein levels in the intact and transected nerves, although limiting amounts of tissue may well pose considerable problems. Differences between Schwann cells and oligodendrocytes in transcript regulation and targeting of the final protein is intriguing and poorly understood. Studies using transgenic mice carrying extra copies of the *plp* gene (Readhead *et al.* 1994) or mice expressing *plp* or *dm-20* cDNA transgenes (Nadon *et al.* 1994) on various mutant and wild type backgrounds (Anderson and Griffiths unpublished data) have demonstrated incorporation of PLP protein into the myelin sheath in some but not all cases. If the control of *plp* and *dm-20* is indeed influenced by different factors and the two proteins perform different functions, effects of one or both of the transcripts in these transgenic animals may provide further insight into this largely unresolved area of study.

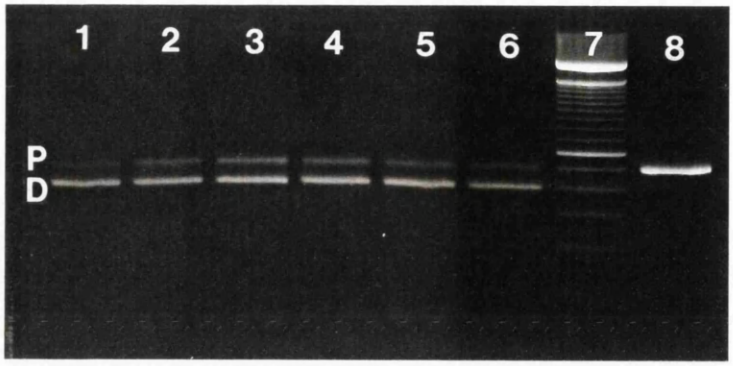


**(a)**

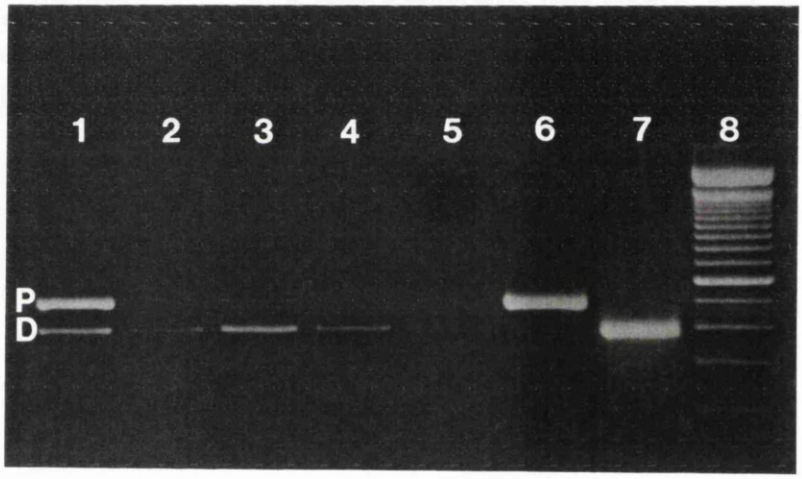


**(b)**

**Figure 47.** PNS *plp/dm-20* RT-PCR products. **a**) Developmental profile: Lane **1** adult rat CCG, Lanes **2-6** mouse sciatic nerves aged P1, 5, 10, 15, 20 respectively, Lane **7** 100bp DNA calibration ladder, Lane **8** pC4 (*plp*) control. Predominance of *dm-20* product (**D**) at all ages is demonstrated. *Plp* product (**P**). There is no apparent change in *plp/dm-20* product ratio between P1 and P20, during which time peak myelination in the sciatic nerve is occurring. **b**) Adult rat CST: Lane **1** adult rat brain, Lane **2** adult rat CST, Lane **3-5** adult rat sciatic nerve, decreasing product loading, Lane **6** pC4 (*plp*) control, Lane **7** pC11 (*dm-20*) control, Lane **8** 100bp DNA calibration ladder. The difference between *plp/dm-20* ratio in the *plp* predominant CNS and *dm-20* predominant PNS is illustrated. *Dm-20* accounts for virtually all the signal in the CST which contains almost exclusively non-myelin-forming Schwann cells. A relatively greater *plp* signal is present in the sciatic nerve which contains a higher proportion of myelin-forming Schwann cells.

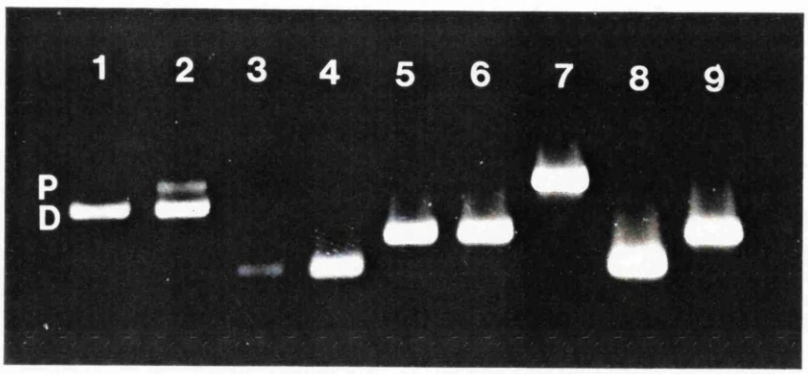


(a)

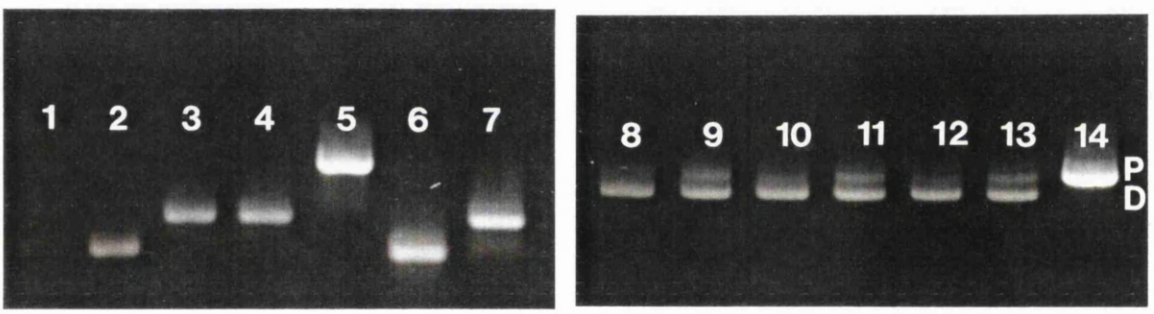


(b)

**Figure 48.** Adult mouse sciatic nerve transections, semi-quantitative RT-PCR. **a)** 3 weeks post-transection: Lane **1** transected nerve (*plp/dm-20*), Lane 2 intact nerve (*plp/dm-20*) Lane **3** transected nerve ($P_0$), Lane **4** intact nerve ($P_0$), Lane **5** transected nerve (*cycl*), Lane **6** intact nerve (*cycl*), Lane **7** pC4 (*plp*) control, Lane **8** $pP_0$ ($P_0$) control, Lane **9** p1B15 (*cycl*) control. **b)** 1 week post-transection: Lane **1** transected nerve ($P_0$), Lane **2** intact nerve ($P_0$), Lane **3** transected nerve (*cycl*), Lane **4** intact nerve (*cycl*), Lane **5** pC4 (*plp*) control, Lane **6** $pP_0$ ($P_0$) control, Lane **7** p1B15 (*cycl*) control, Lanes **8,10,12** transected nerve (*plp/dm-20*) (PCR Mg conc. 1.5/3.0/4.5mM), Lanes **9,11,13** intact nerve (*plp/dm-20*) (PCR Mg conc. 1.5/3.0/4.5mM), Lane **14** pC4 (*plp*)control. Marked down-regulation of $P_0$ is seen in transected sciatic nerves. Levels of *dm-20* product (**D**) appear relatively unaltered whereas *plp* product (**P**) is considerably reduced.

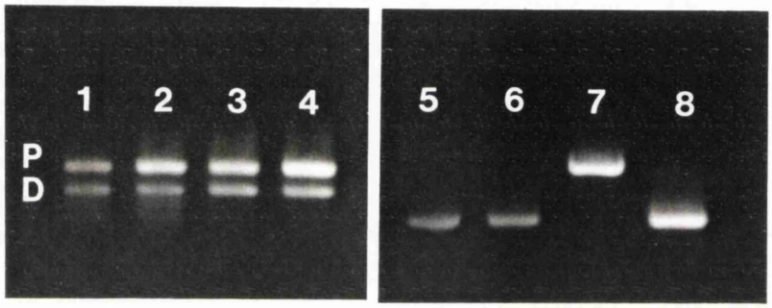


**Figure 49.** Adult rat optic nerve transection, semi-quantitative RT-PCR. Lanes **1,3** transected nerve (*plp/dm-20*) (PCR Mg conc. 3.0/4.5mM), Lanes **2,4** intact nerve (*plp/dm-20*) (PCR Mg conc. 3.0/4.5mM), Lane **5** transected nerve (*cycl*), Lane **6** intact nerve (*cycl*), Lane **7** pC4 (*plp*) control, Lane **8** p1B15 (*cycl*) control. 3 weeks post-transection, levels of *plp* product (**P**) are decreased in the transected nerve whereas *dm-20* product levels (**D**) remain unchanged.

## 3.2.4.Olfactory bulb studies

### Introduction and aims

During the study of the *plp* gene in the post-natal mouse, the presence of ISH signal and PLP/DM-20 immunostaining was noted in the olfactory nerve layer (ONL) of the olfactory bulb (OB). Presence of *plp/dm-20* transcripts has been noted previously in the OB in the post-natal mouse as early as P1 using ISH and P9 using northern analysis (Kanfer *et al.* 1989; Shiota *et al.* 1989) but no specific location could be determined for the source of the expressing cells. Subsequent to our initial observations, PLP/LacZ fusion protein has been demonstrated in the olfactory bulb at E14.5 in transgenic mice (Wight *et al.* 1993) and *plp/dm-20* transcripts by ISH in the mouse olfactory blastema by E12.5 (Timsit *et al.* 1995). It was assumed that ISH signal present in embryonic olfactory bulbs was due to *dm-20* expression. No information was available regarding precise localisation of *plp* expressing cells, their developmental profile or relative amounts of *plp* and *dm-20* transcript and product. To gain a better understanding of the expression of the *plp* gene in the mouse OB a more detailed ISH and immunocytochemical study of this area was undertaken. *Plp* gene expression was studied from late embryogenesis (E14) through to adult mice (P40).

### Materials and methods

Olfactory bulbs, attached to brain to facilitate orientation, were collected from C3H/HeH X 101H mice aged between E14 and P40. Tissue for immunocytochemistry was removed unfixed for freezing. Samples were embedded in OCT compound and snap frozen as previously described (see 2.1.2.Processing). Frozen tissue was also used for ISH and additional samples were fixed in BNF for paraffin-wax embedding.

ISH was performed using the PLP-1 probe recognising both *plp* and *dm-20* transcripts and the PLP-3B probe recognising *plp* transcripts specifically. Sections were counterstained with haematoxylin and viewed under brightfield, darkfield and combined brightfield and darkfield illumination. Immunostaining was performed with the PLP-CT antibody recognising both PLP and DM-20 and a PLP specific antibody, using Gow's technique, as previously described (see 2.4.1.Tissue sections). Sections were also stained using the DAPI technique to highlight cell nuclei.

In order to confirm the cell lineage responsible for *plp* gene expression, dissociated cell cultures were prepared from mouse P1 olfactory bulbs. Cultures were grown for 2 hours to give an indication of their *in vivo* status prior to immunostaining with PLP-CT and a number of other cell lineage markers. These included O4, O1, GFAP, S-100, SMI-31, NF2H3 and TuJ1. Purified P7 rat ONECs were obtained by fluorescence-activated cell sorting (FACS) as described by Barnett *et al.* (1993) and were kindly provided by Dr. S.C.

Barnett. These cells were also immunostained using the PLP-CT antibody.

## Results

### ISH

Using the PLP-1 probe, recognising both *plp* and *dm-20* transcripts, signal was detected in the ONL of the OB at all ages studied (Figure 51, Figure 52, Figure 53). Little variation in signal intensity was seen throughout this period. Signal was apparent as a diffuse circular region lying at the outer surface of the OB adjacent to the glomerular layer on coronal sections (Figure 50, Figure 51). The area of positive cells tended to be thickest medially, especially with more rostral sections. From P10 onwards positive cells were present in the deeper layers of the bulb with a more distinct signal typical of *plp*-expressing oligodendrocytes in the CNS (Figure 50, Figure 52). These cells were initially located in the granule cell layer with a few strongly positive cells present in the sub-ventricular zone in more caudal sections, and extending peripherally into the external plexiform and glomerular layers at older ages (Figure 50). Strongly positive cells were not found amongst the diffusely hybridising cells in the ONL.

No similar diffuse signal was seen in the ONL using the *plp*-specific PLP-3B probe at any of the ages, even when exposure times were increased 50% relative to the PLP-1 probe (Figure 54). From P10 onwards the presence of cells positive for the PLP-3B probe in the deeper layers of the bulb mirrored that found with the PLP-1 probe (Figure 54).

### Immunocytochemistry

Using the PLP-CT antibody recognising both PLP and DM-20 proteins, faint and somewhat patchy immunoreactivity was detected in the ONL at E14. By E16 the intensity had increased and a complete peripheral band corresponding to the ONL was now visible (Figure 55). Immunostaining remained strong until after P10; by P25 the intensity was reduced and was considerably less intense by P40 (Figure 56). At P5 and P7 no immunoreactivity was detected in deeper layers of the bulb. By P10 reactivity was present in the granule cell layer. Initially staining was patchy and incomplete, localised to the more lateral aspect of the bulb, but then spread at older ages to the whole granule layer encircling the sub-ventricular zone and formed a dense layer of reactivity in the mitral cell layer immediately peripheral to the granule cell layer. Radial spokes of staining projected from the outer granule cell layer to the glomerular layer (Figure 56). Concurrent with the increase in extent and intensity of staining in the deeper layers of the OB, the reaction in the ONL became less intense.

No immunoreactivity was seen in the ONL using the PLP-specific antibody at any of the

ages studied. From P10 onwards reactivity was similar to that found with the PLP-CT antibody.

**Dissociated cell culture**

Purified P7 rat ONECs were FACS sorted as O4+/GC- cells. The cells were further characterised using the PLP-CT antibody within 24hr. of sorting. The vast majority of these cells (approximately 94%) were PLP-CT+ (Figure 57). Approximately 4% of cells were O4+/PLP-CT- and approximately 2% were PLP-CT+/O4-.

Dissociated mouse P1 olfactory bulb cultures were immunostained with PLP-CT and a number of other markers. Approximately 10-15% of cells in the cultures were PLP-CT+. Numerous A2B5+ cells and several GC+ and GFAP+ cells were present but no co-localisation with PLP-CT antibody was present. Approximately 75% of PLP-CT+ cells also immunostained with antibodies against O4 and S-100 (Figure 58). No cells immunostained with a PLP-specific antibody. Very few cells immunostained with the neuronal anti-neurofilament antibodies SMI-31 and NF2H3, however numerous cells were strongly stained using the TuJ1 neurone specific β tubulin III antibody. No co-localisation with the PLP-CT antibody was present with any of these neuronal markers.

## Discussion

The detection of *plp* transcripts in the post-natal mouse olfactory bulb using ISH or northern blotting is not in itself surprising. Myelinated axons are known to originate from secondary olfactory pathway neurones in the mitral cell layer and travel along the length of the OB, predominantly in the granule cell layer, eventually forming the olfactory tract. These myelinated axons passing through the granule cell layer are not the axons of the granule cells themselves as these are one of the few anaxonic neurones in the CNS (Price and Powell 1970). Ensheathment of these axons will be accomplished by oligodendrocytes, and it is these cells which will give rise to the distinct signal and strong immunostaining seen in the deeper layers of the OB following ISH and immunostaining with *plp/dm-20* probes and antibodies. The absence of detectable transcripts or protein before P10 would imply that myelination is commencing at around this time in the mouse OB. This is confirmed by the observations of Jacobson (1963) and Tilney (1933) who described the presence of "stainable" myelin in the olfactory tract of the rat at 10 and 14 days respectively. The presence of both *plp* and *dm-20* transcripts and protein in these cells is the same as would be found in any actively myelinating oligodendrocyte in the CNS. Occasional strongly expressing cells which were present in the external plexiform and glomerular layers are likely to be oligodendrocytes responsible for myelination of the dendrites and cell bodies of mitral, tufted and periglomerular cells (Valverde and Lopez-Mascaraque 1991).

The presence of *plp/dm-20* transcripts and protein in the ONL is considerably more

interesting for several reasons. Although occasional myelinated fibres may course with the olfactory nerve on its way to the OB, the olfactory nerve itself is unmyelinated as is the ONL (De Lorenzo 1957; Gasser 1956). *Plp* expression is first seen in the deeper layers of the bulb around the time of myelination (P10). Expression is present in the ONL, however, during embryogenesis, by E14 in the present study. Timsit *et al.* (1995) demonstrated *plp* ISH signal in the olfactory blastema and olfactory tracts at E12.5 and in the olfactory epithelium at E14.5. Clearly the expression of the *plp* gene in the ONL is unlikely to be associated with myelination directly as signal is present in an area where no myelin sheaths are formed, and is present during embryogenesis, probably 10-15 days before myelin is present in any part of the olfactory bulb. Although ISH and immunostaining are not easily quantifiable, there does appear to be a discrepancy between the apparent maintenance of a strong ISH signal at least until P30, whereas immunostaining becomes noticeably weaker by P25. The reason for this is unknown and may represent a change in the availability of the antigen at older ages or a true decrease in the amount of protein present. If the latter is the case it may indicate that control of product levels is occurring, at least in part, at a post-transcriptional level. Although it is not possible to detect *dm-20* transcripts and protein directly on tissue sections, the positive signal and staining in the ONL at all ages using non-specific *plp/dm-20* probe and antibody and the lack of signal and staining using *plp*-specific probe and antibody, would strongly suggest that *dm-20* is the sole or major isoform expressed in the ONL at all ages. Appearance of *plp*-specific signal at P10 in the deeper layers of the bulb, around the time of myelination, suggest that the earlier lack of signal is genuine, or due to levels of *plp*-specific transcript and protein below the levels of detection, rather than failure of the techniques. The diffuse signal seen in the ONL is reminiscent of that seen in non-myelin-forming Schwann cells in the PNS, indeed there are many similarities between expression of the *plp* gene in the PNS and the ONL. The pattern of expression in the ONL, in areas and at times when no myelin is present, strongly suggests a non-structural role for the *plp* gene in this situation and, as in the PNS, this is associated with a predominance and possibly in the case of the ONL, exclusivity of the DM-20 isoform. Although the olfactory bulb as a whole lies within the meninges of the CNS it is somewhat misleading to view the ONL as CNS tissue as it originated from the olfactory placode and migrated to cover the developing OB during embryogenesis. As such, it is not of neural tube origin, nor for that matter of neural crest origin (the origin of PNS tissue) and the glial cell which originates from this source, the olfactory nerve ensheathing cell (ONEC) should be regarded as a novel glial cell-type.

Of the two glial cells which have been described in the ONL, the astrocyte and the ONEC (Doucette 1984; Doucette 1989), it is most probable that the cells expressing the *plp* gene were the latter. Evidence supporting the ONECs being the source of *plp* expressing cells in the olfactory bulb is as follows; 1) During embryogenesis and at post-natal ages less than 10 days, PLP immunostaining and ISH signal is restricted to the ONL. Although

expression of the *plp* gene in ONECs has not been reported in detail previously, it has not been demonstrated convincingly that PLP or its message are present in astrocytes. ONECs exhibit some characteristics of Schwann cells (Doucette 1990; Norgren *et al.* 1992) a cell type known to express the *plp* gene, and it has been demonstrated that ONECs can elaborate myelin sheaths *in vitro* and express another myelin protein, MBP (Devon and Doucette 1992). It therefore seems likely that the ONEC rather than the astrocyte is the cell responsible for *plp* gene expression in the ONL. 2) Almost all O4+/GC- cell sorted ONECs from P7 rats, which have been shown previously not to be astrocytic or oligodendroglial in phenotype (Barnett *et al.* 1993), immunostained for PLP/DM-20. 3) Dissociated cell cultures from P1 mouse olfactory bulbs demonstrated PLP-CT+ cells, the majority of which co-stained with markers such as O4 and S-100 which are characteristic of ONECs (Barnett *et al.* 1993) (S.Barnett personal communication). Although O4 and to a lesser extent S-100 staining is also found in cells of the oligodendrocyte lineage, no co-localisation of PLP-CT+ cells with other oligodendrocyte lineage markers such as A2B5 or GC was present. It is possible that some of the PLP-CT+ cells in these cultures may belong to other cell lineages, possibly of neuronal origin. However, no co-localisation of PLP-CT+ cells with neuronal markers NF2H3, SMI-31 (anti-neurofilaments), TuJ1 (anti-β tubulin III) or A2B5 was present

Much evidence now points to a non-structural role for the DM-20 isoprotein in both the CNS and PNS, but progress in elucidating this role has been slow. Techniques to generate purified ONEC cultures have been described (Barnett *et al.* 1993), and immortalised ONEC cell lines have been generated (S.Barnett personal communication). The study of *plp* gene expression in this glial cell type may provide the background, free of the confusing factors of myelin and the PLP isoprotein, against which a specific function of DM-20 may be elucidated.

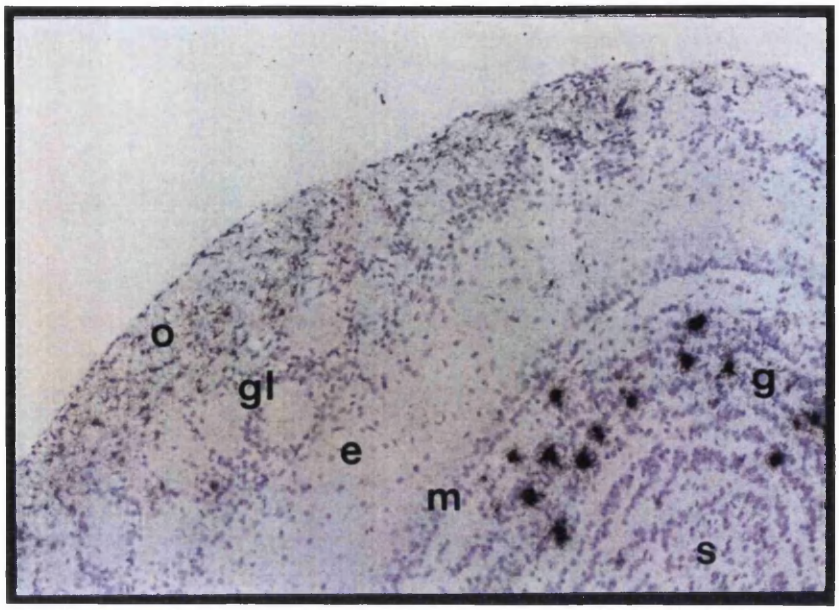


**(a)**

**(b)**

**Figure 50.** Olfactory bulb *plp/dm-20* ISH (PLP-1 probe). Coronal section of 15 day mouse olfactory bulb (OB): **a)** brightfield illumination, **b)** combined bright/darkfield illumination. The laminar structure of the OB is clearly seen (**o**-olfactory nerve layer, **gl**-glomerular layer, **e**-external plexiform layer, **m**-mitral cell layer, **g**-granule cell layer, **s**-sub-ventricular zone). Strongly positive cells, most probably oligodendrocytes, are seen in the granule cell layer in **a)**. Darkfield illumination, **b)** additionally reveals more diffuse staining in the olfactory nerve layer and occasional positive cells in the external plexiform layer.

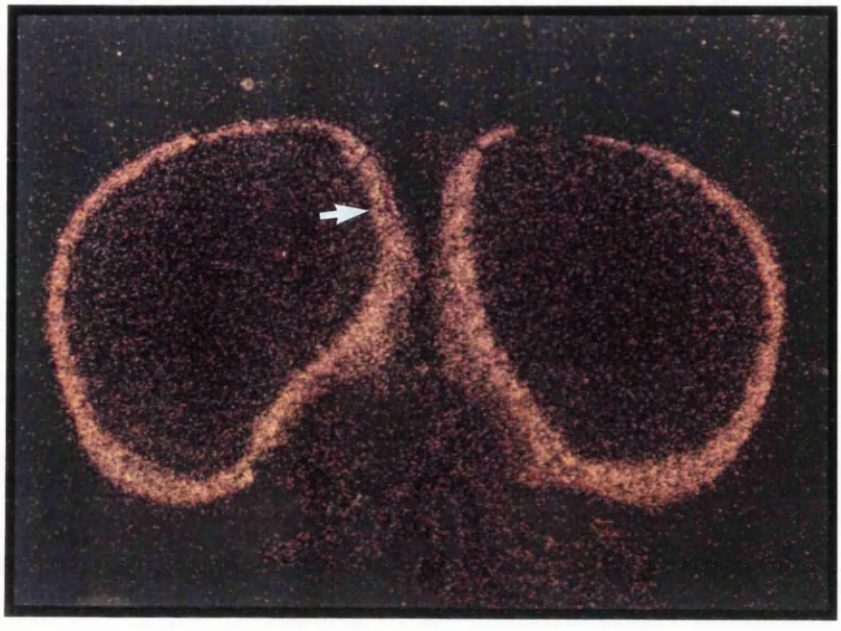

**(a)**

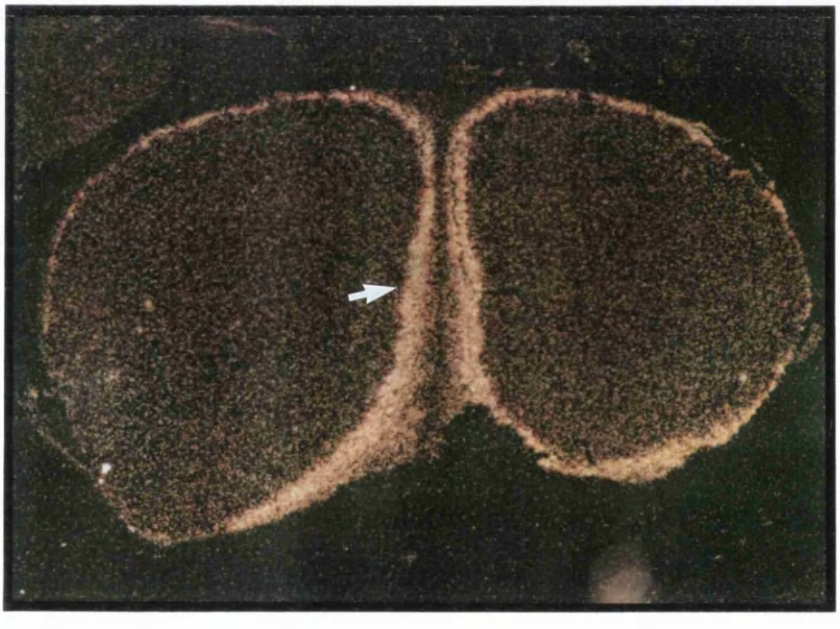

**(b)**

**Figure 51.** Post-natal olfactory bulb ISH, *plp/dm-20* developmental profile. **a)** P1 (dark/brightfield), **b)** P5 (darkfield). Diffuse signal is evident in the olfactory nerve layer under darkfield illumination at both ages (arrow). No signal is seen in the deeper layers of the bulb. The PLP-1 probe hybridises both *plp* and *dm-20* transcripts, however signal in the olfactory nerve layer can be demonstrated to be exclusively *dm-20* and is likely to be present in the olfactory nerve ensheathing cells.

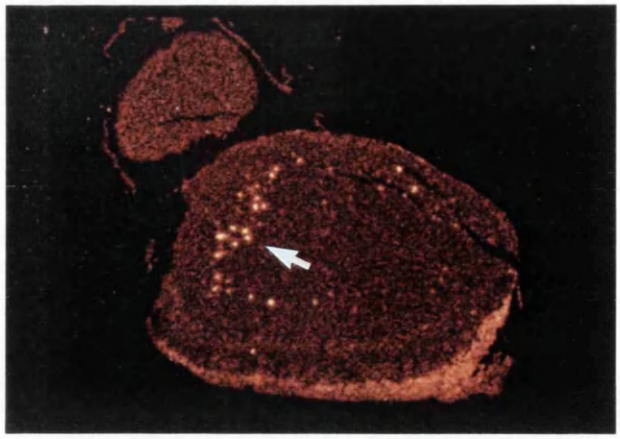

(a)

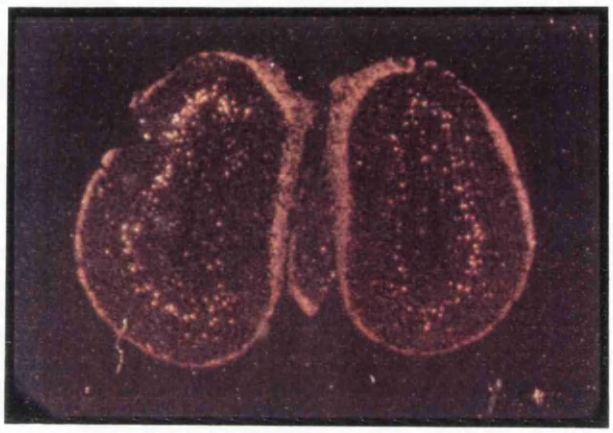

(b)

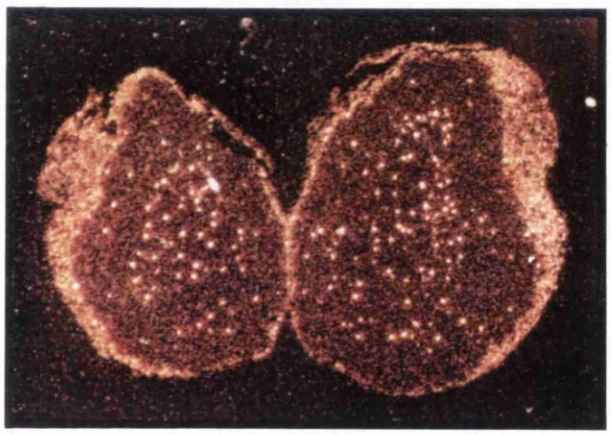

(c)

**Figure 52.** Post-natal olfactory bulb ISH, *plp/dm-20* developmental profile. **a)** P10 (darkfield), **b)** P15 (dark/brightfield), **c)** P30 (darkfield). Strong diffuse signal is found consistently in the olfactory nerve layer at all ages. Strong, focal staining in the deeper layers (arrow) is apparent from P10 onwards, and coincides with the onset of myelination of axons in the deeper layers of the bulb. This focal staining is similar to that seen in oligodendrocytes in other areas of the CNS.

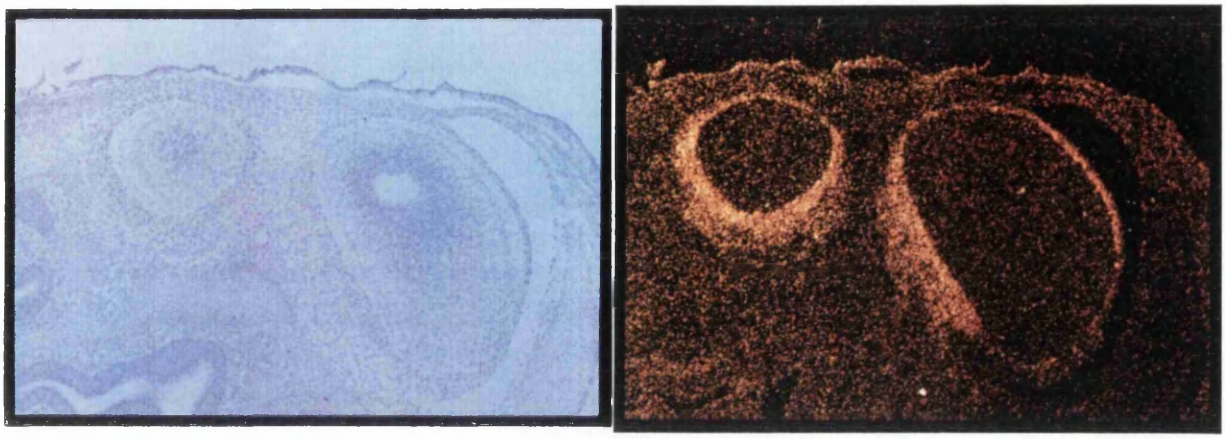

**(a)**

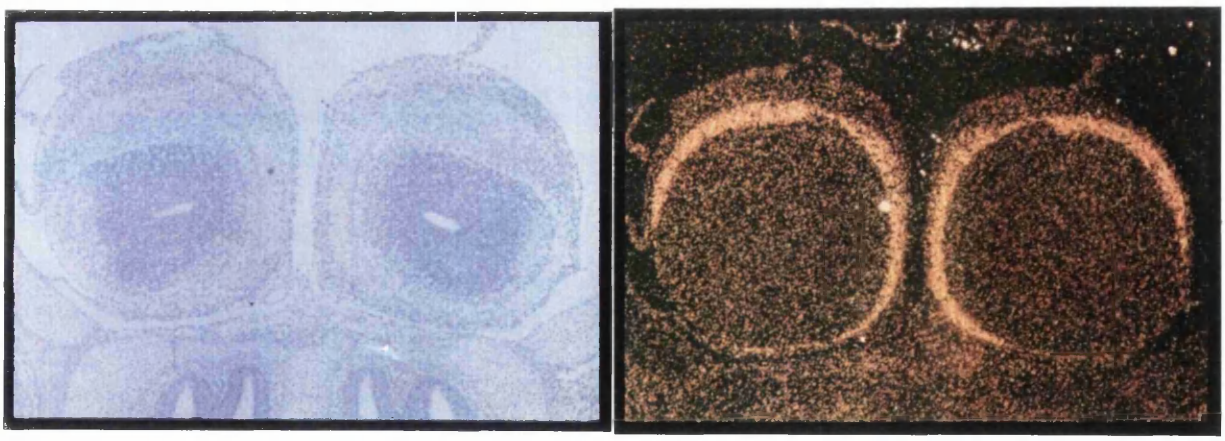

**(b)**

**Figure 53.** Embryonic olfactory bulb, ISH *plp/dm-20*. **a)** E16 bright and darkfield images, **b)** E18 bright and darkfield images. Signal in the olfactory nerve layer is as strong in the embryonic as the post-natal olfactory bulb. No signal is present in the deeper layers of the bulb.

**(a)**

**(b)**

**Figure 54.** Olfactory bulb ISH, *plp*-specific probe (PLP-3B). **a)** P15, **b)** P30; Although focal signal is present in the deeper layers of the bulb, no diffuse signal is evident in the olfactory nerve layer. This implies that signal in the olfactory nerve layer is predominantly, or possibly exclusively, *dm-20*.

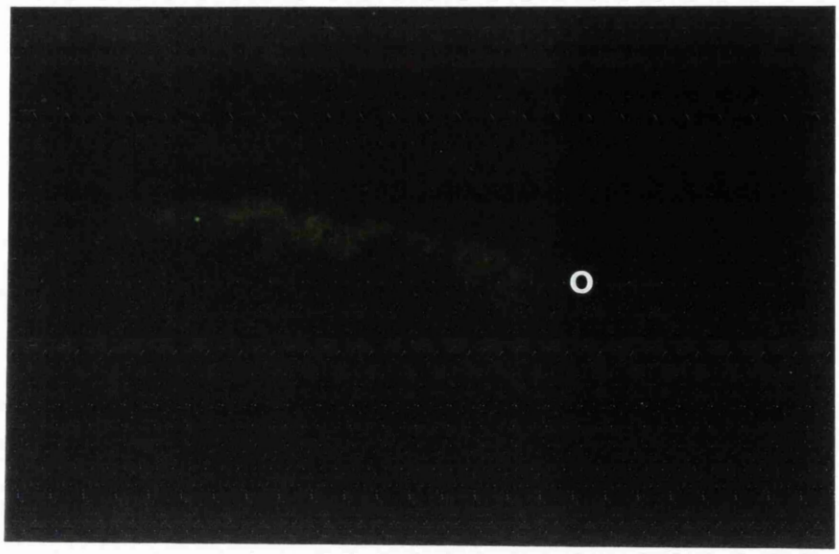


**(a)**

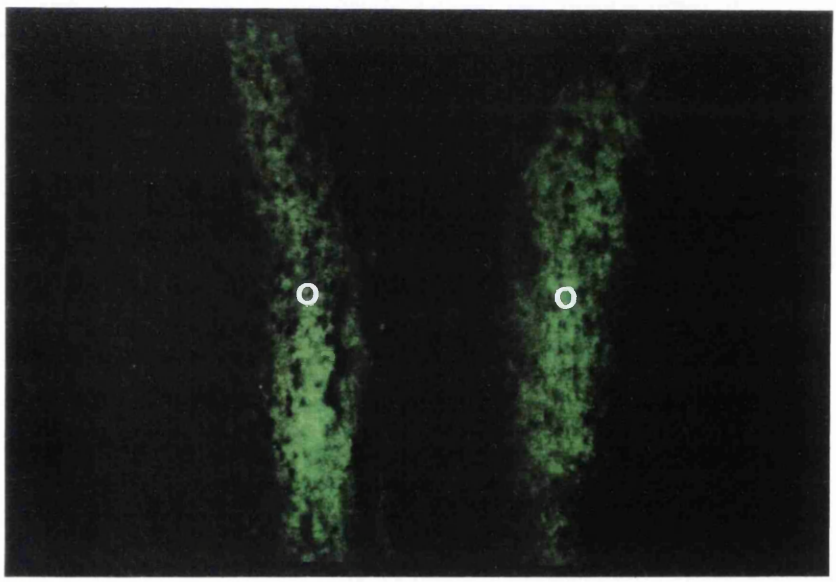


**(b)**

**Figure 55.** Olfactory bulb immunostaining, PLP/DM-20 (PLP-CT). **a)** E16, **b)** P5. Strong immunostaining in the olfactory nerve layer (**o**) with an antibody recognising PLP and DM-20 can be seen at E16 and P5. This staining represents the DM-20 isoprotein as no similar signal is seen using a PLP-specific antibody.

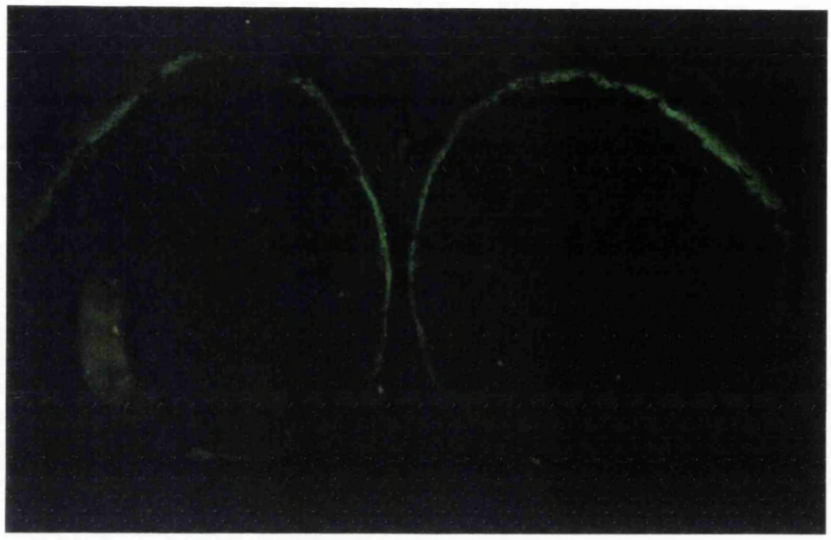

(a)

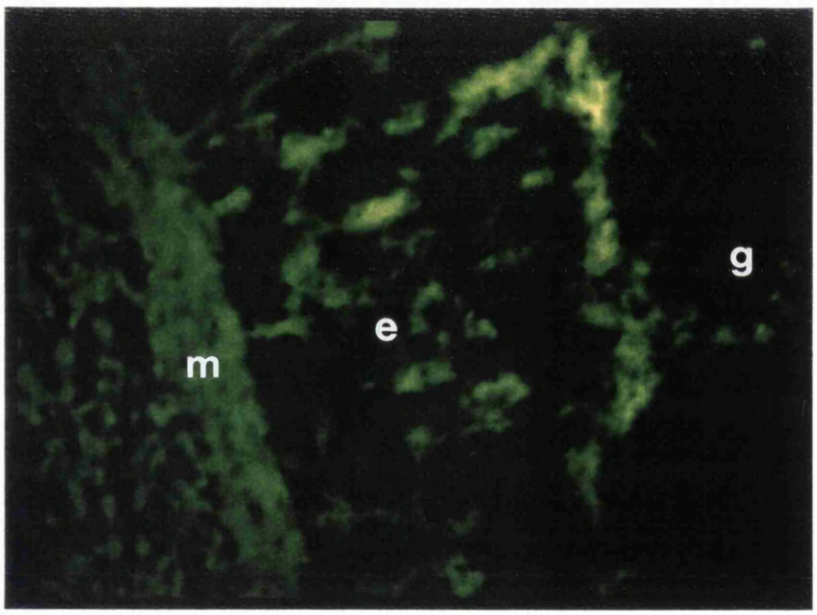


(b)

**Figure 56.** Olfactory bulb immunostaining, PLP/DM-20 (PLP-CT). **a)** P7, **b)** P40. Strong immunostaining is still present in the whole of the olfactory nerve layer at P7; staining is still not present in the deeper layers at this age. By P40 staining in the olfactory nerve layer is considerably weaker whilst intense staining is present in the deeper layers (**gl**-glomerular layer, **e**-external plexiform layer, **m**-mitral cell layer). Staining at this age is very similar using a PLP-specific antibody, with the exception of absence of any reactivity in the olfactory nerve layer.

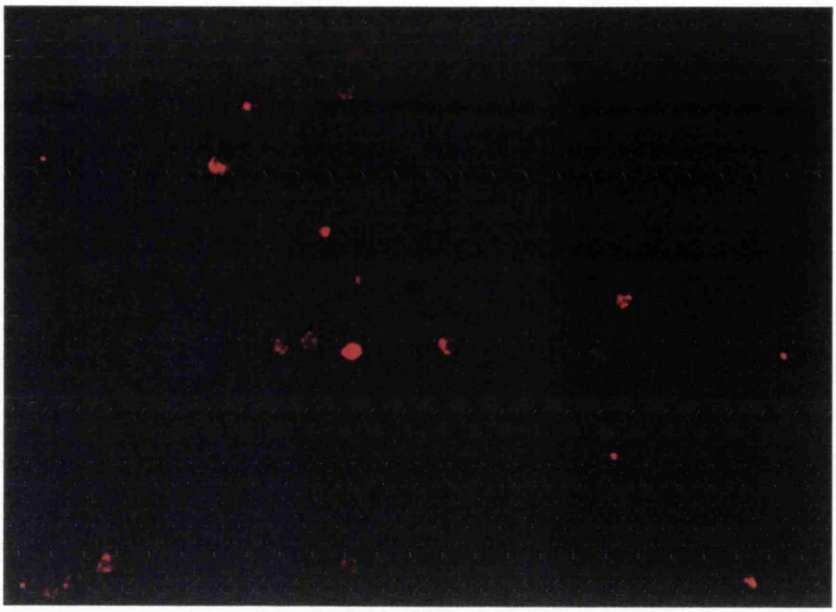

(a)

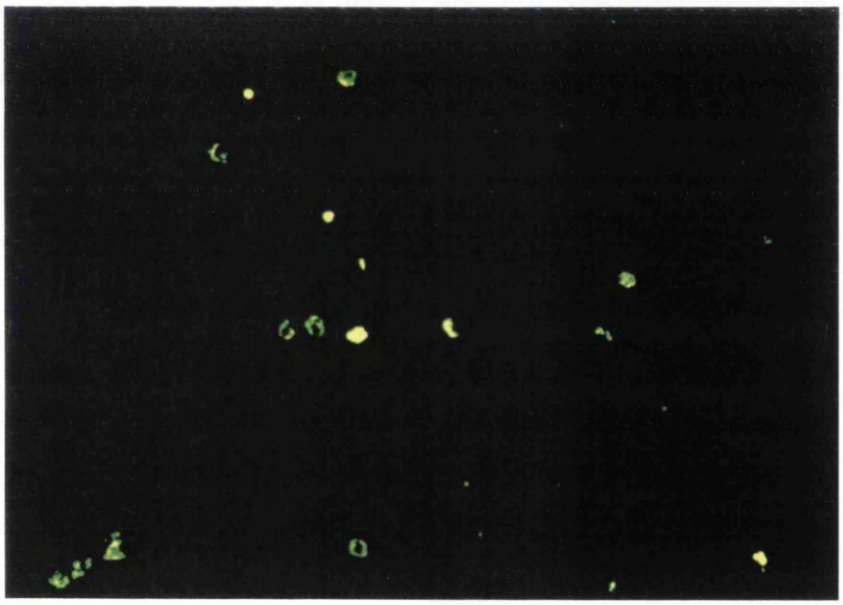

(b)

**Figure 57.** Rat P7 O4+/GC- cell sorted ONECs immunostained with PLP-CT antibody. **a)** O4 immunostaining, **b)** PLP-CT immunostaining. Almost all O4+ sorted cells co-stain with the PLP-CT antibody.

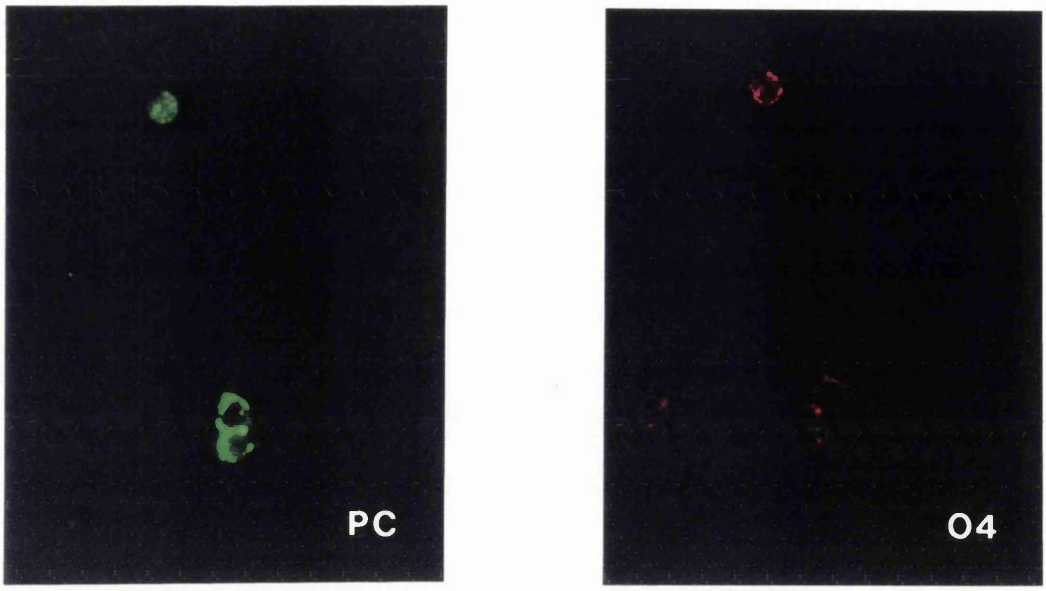


(a)

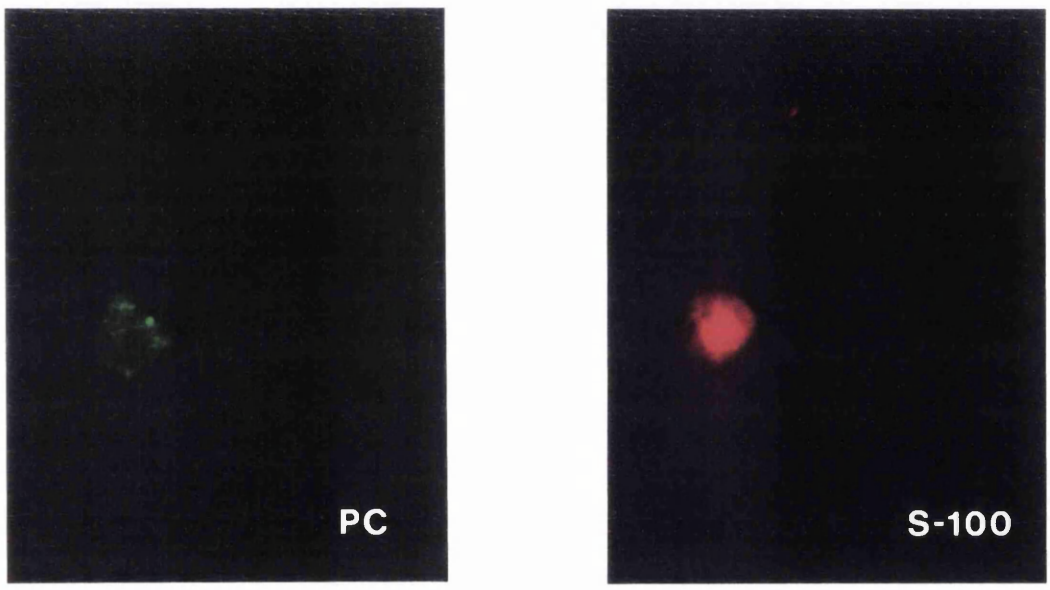


(b)

**Figure 58.** Mouse P1 dissociated olfactory bulb cultures (2 hours). Cells can be seen co-immunostaining for PLP-CT (**PC**) and **a)** the cell surface marker O4 or **b)** the cytoplasmic marker S-100. Both of these markers are characteristic of the olfactory nerve ensheathing cell.

## 3.3.GENERAL DISCUSSION

It is now over forty years since myelin proteolipid protein was first reported (Folch and Lees 1951). It is a sobering thought that despite the considerable advances in research technology during this period, and the numerous groups working in the area, we still do not actually know the true function of one or possibly both of the isoforms of the *plp* gene. Particularly in the case of DM-20, it is very difficult to interpret the large amount of experimental data now available without the baseline of a known function.

At the commencement of the present studies, the amount of information regarding the more widespread effects of the *plp* gene in the nervous system was relatively small. Studies of the $jp^{rsh}$ mutant (Schneider *et al.* 1992) had added considerable weight to the theory of dual roles for the two isoproteins of the *plp* gene although few examples of the non-myelinating role of DM-20 were documented. The ventral origin of oligodendrocytes in the spinal cord had been demonstrated using *in vitro* techniques (Warf *et al.* 1991), however, associated markers for these early precursor cells had still to be demonstrated. Expression of the *plp* gene was considered to be essentially a post-natal event in rodents with expression limited spatially to the oligodendrocyte and to a lesser extent the Schwann cell where expression appeared to be deregulated. The results presented in the current studies have added to the considerable body of information generated over the intervening period, and unsurprisingly in this highly complex area, generated new areas of interest. The use of RT-PCR technology has allowed the indirect analysis of the two isoforms of the *plp* gene and confirmed the marked up-regulation and transcript ratio changes which occur at the onset of myelination in the CNS. The lack of such changes in the PNS was not surprising, given the apparent uncoupling of *plp* gene expression from myelination in this tissue. However, the apparent separate regulatory control of the two isoforms apparent in the nerve transection studies has raised some intriguing questions. Studies on *plp* gene expression during embryogenesis have clearly demonstrated the presence of *dm-20* transcripts and protein and linked the expressing cells to the oligodendrocyte lineage. Whilst reinforcing previous evidence for the ventral origin of oligodendrocyte precursors in the developing spinal cord, this work also challenges some of the previous perceptions related to myelin gene expression in the developing oligodendrocyte, in particular, the idea of *plp* expression being restricted to the mature myelinating oligodendrocyte. The somewhat serendipitous finding of almost exclusive expression of the *dm-20* isoform in the olfactory nerve ensheathing cells of the olfactory bulb is an additional example of expression of the *plp* gene, in particular the *dm-20* isoform, in a "non-myelin environment". This provides additional evidence of a non-myelin role for DM-20 and indicates a possible area for future study to define this aspect.

Structural abnormalities of the compact myelin sheath in the absence of normal PLP, together with the physical localisation of the protein, give a strong indication that PLP and possibly DM-20 probably function as structural proteins. Evidence from the rumpshaker

mutation in mouse, its recently reported homologue in man, and the discovery of the DM family of proteins argue strongly in favour of a non-myelin role for DM-20. Several aspects of the presented work add further evidence to support this theory. Expression of *dm-20* at times and in tissues where an obvious link with myelination is absent is suggestive of a non-myelin role for this isoform. The present study clearly demonstrates the predominant expression of *dm-20* during embryogenesis of the spinal cord. *Dm-20* transcripts have been reported previously (Ikenaka *et al.* 1992; Timsit *et al.* 1992a), but this is the first time that product has been demonstrated. The presence of a protein product increases the likelihood that DM-20 does have a functional role and is not just a vestigial protein with non-regulated transcription occurring incidentally in cells prior to the up-regulation of the *plp* isoform during myelination. Nevertheless, it is possible that DM-20 may be a redundant protein; certainly, apart from the structural abnormalities in the myelin sheath, the otherwise normal appearance of *plp* knockout mice would support this (Boison and Stoffel 1994). It is also possible that DM-20 function is compensated for in these mice by another protein. Such compensation may not be induced in the *plp* mutant animals due to the continued presence of PLP/DM-20 protein, albeit abnormal. If DM-20 is vestigial or easily replaceable, why then do we see such lethal phenotypes in *plp* mutant animals, and such a high degree of conservation of the *plp* gene? Selection may be acting solely on the PLP isoform. If the appropriation of the *plp* specific sequence and the associated structural function was a late evolutionary development, the presence of compensatory mechanisms for loss of PLP function would seem less likely thus increasing selection pressure. Alternatively, selection may not be acting to maintain the function of an essential protein at all, but to prevent the appearance of deleterious proteins which would naturally be absent from knockout mice. In the case of a Pelizaeus-Merzbacher patient with a deletion of the *plp* gene, the clinical phenotype is similar to patients with point mutations of the gene (Juurlink and Hertz 1991). This would argue against a toxic protein theory since no protein can be present, and would argue for an important role for the products of the gene, seemingly contradicting the evidence from the knockout mice.

The present work has demonstrated DM-20 protein in the embryonic cord and identified the majority of expressing cells as precursors of the oligodendrocyte lineage, cells destined to express strongly the *plp* gene once myelination has commenced. The presence of DM-20 protein in the olfactory nerve ensheathing cells of the olfactory nerve layer not only demonstrates DM-20 in an environment devoid of myelin, but also in a cell type which is not destined to produce myelin at all *in vivo*. In this respect this is similar to the presence of DM-20 in non-myelin-forming Schwann cells in the PNS (Griffiths *et al.* 1995a). Without actually elucidating a function for DM-20, demonstrating the presence of functional protein in these non-myelin environments and cell types is some of the strongest circumstantial evidence available indicating a function for the DM-20 isoprotein unconnected with myelination.

Factors affecting regulation of the *plp* gene may give an insight into its functional significance. Results from semi-quantitative RT-PCR analysis of spinal cord and mid-optic nerve indicate that the dramatic up-regulation and change in *plp/dm-20* transcript ratio, from *dm-20* to *plp* predominance, correlates well with the onset of myelination. Although a rise in *dm-20* transcripts is seen, the majority of the increased total transcript level, and therefore the reason for the change in *plp/dm-20* transcript ratio, is attributable to increase of the *plp* isoform. The moderate rise in *dm-20* transcripts may well be due to increased transcriptional activity in general rather than a specific, targeted up-regulation of this isoform. This would imply that the function of PLP is more closely linked to myelination than that of DM-20. The mechanisms controlling the relative amounts of *plp* and *dm-20* transcripts and protein are unknown and may be dependent on several factors acting at different levels of gene expression. Differences in these regulatory mechanisms when comparing *plp* and *dm-20*, add further weight to the argument separating the end functions of the two isoproteins. Regulation of the *plp* gene, certainly in actively myelinating cells in the CNS, appears to occur mainly at the level of transcription, and probably at the level of rate of transcript initiation. The majority of transcripts in the PNS, where *dm-20* is predominant, are initiated from the more proximal (position −130) of the two major transcript initiation sites. In the actively myelinating CNS most transcripts are initiated from a more distal site (position −160), whereas in the mature CNS after peak transcription has occurred proximally initiated transcripts predominate as in the PNS (Kamholz *et al.* 1992; Scherer *et al.* 1992). It has been suggested that the proximal site (PNS and mature CNS) may be used during maintenance expression and is not inducible, while the distal site is responsible for the rapid, inducible increase of *plp* message during myelination. Induction may be due to transiently expressed factors or to utilisation of the distal site once the proximal site is "saturated". This certainly could explain differences in total transcript levels, however, it is less clear how alternative splicing may be affected. One could hypothesise that subsequent splicing of the primary transcript may be influenced by differing sequences present in the initiation region. This seems unlikely given that both PNS and mature CNS transcripts are predominantly initiated from the same site, yet have *plp/dm-20* ratios which are *dm-20* predominant and *plp* predominant respectively. Generation of PCR primers complementary to the two transcript initiation sites, with a common primer downstream of exon 3 would allow semi-quantitative analysis of the relationship between choice of transcript initiation site and subsequent levels of *plp* and *dm-20* transcripts. This could be further applied to nerve transection studies to determine if a relationship exists between choice of initiation site and selective down-regulation of the *plp* isoform.

Post-transcriptional regulation is the most likely mechanism for controlling relative levels of *plp/dm-20* transcripts. There is no strong evidence to suggest that stability of the different transcripts plays a significant role, however this is a possibility. Assuming that

both mRNA species are equally stable *in vivo*, the variations in transcript ratio must be due to selective utilisation of one or other of the alternate 5′ splice sites in exon 3, selection of the distal site resulting in the generation of *dm-20* transcripts. There is no obvious difference in homology of the alternate 5′ splice sites compared to the consensus sequence:

| % conserved | 70 | 60 | 80 | | 100 | 100 | 95 | 70 |
|---|---|---|---|---|---|---|---|---|
| **Consensus** | **A/C** | **A** | **G** | **↓** | **g** | **t** | **a/g** | **a** |
| PLP | A | A | G | ↓ | g | t | g | a |
| DM-20 | A | C | G | ↓ | G | T | A | A |

Favouring of one splice site due to greater homology to the consensus sequence therefore seems unlikely. Additionally, this could not explain the predominance of different transcripts in different tissues. It is more likely that other factors confer differential specificity. Assembly of the spliceosome onto the nascent pre-mRNA is mediated by RNA/RNA interactions between small nuclear RNAs (snRNAs), in particular the U1 snRNA, and the pre-mRNA. Numerous proteins are also involved, some of which are complexed to the snRNAs (forming small nuclear RNA protein complexes (snRNPs)). Other proteins, such as the SR protein family, which are required for constitutive splicing, have also been implicated in the function of specifying alternate splice site selection with specific SR proteins allowing for the preferential use of different 5′ splice sites within the same precursor (Zahler and Roth 1995). Whether or not control of *dm-20* and *plp* transcript levels at this or other levels is truly integrated, or under separate controls, remains to be resolved. Based on the evidence of the sciatic and optic nerve transections it certainly appears that axonally related factors play a role in determining *plp* transcript level but have little or no effect on *dm-20*. Whether this difference is expressed as a function of transcriptional control, decreased *plp* transcript stability or an alteration in the splice site selection procedure is as yet unclear. It appears that predominance of the *plp* isoform is limited to the myelinating oligodendrocyte, as demonstrated in the post-natal spinal cord and optic nerve. In all other situations, such as oligodendrocyte precursors , ONECs, Schwann cells, cardiac myocytes and peri-neuronal satellite cells, the *dm-20* isoform predominates. Selection of the distal 5′ splice site appears, therefore, to be common to all these different cell types and may well be the constitutive pathway for *plp* pre-mRNA splice site selection. This would be consistent if the appearance of PLP protein was a later evolutionary event requiring additional regulatory mechanisms.

At the present time it is very difficult to rationalise the large, and occasionally conflicting, amounts of data regarding expression of the *plp* gene. *In vitro* manipulation of *plp* genotype in several lines of mice has produced a spectrum of phenotypes, and whilst

demonstrating the ability to disrupt *plp* gene expression, it has not necessarily increased our understanding of *plp* expression. The control and effects of the *plp* gene are obviously highly complex and it is very likely that many, as yet unidentified players are involved in its co-ordinated expression. Identification and study of these factors may well provide the wider backdrop necessary to interpret the data already available. Several techniques have been reported which will allow identification of genes which are either linked with a specific target gene or protein, such as PLP, or which allow the identification of genes which are differentially expressed due to developmental or extracellular stimuli. The use of commercial *in vivo* yeast hybrid reporter systems may allow the identification of either proteins binding to *plp cis*-regulatory elements which may be involved in transcriptional regulation of the *plp* gene, or proteins interacting directly with PLP/DM-20 proteins themselves. Problems may be encountered if looking for genes encoding proteins which bind to *plp cis*-elements since these regulatory regions of the *plp* gene have yet to be fully characterised. Identification of genes encoding proteins interacting directly with PLP/DM-20 is potentially less problematic and may prove very interesting.

Identification of differentially expressed genes may be investigated by the differential display of mRNA using RT-PCR. This is a much less labour intensive approach than previously used subtractive hybridisation techniques. A combination of degenerate primers and small arbitrary primers gives a profile of RT-PCR products which will represent the numerous mRNAs present in the sample. Comparison of profiles from different samples, at different developmental stages for example, allows identification of bands which are specific or increased/decreased in intensity in one of the samples. Cloning and sequencing of these bands then gives direct access to genes which are either up or down-regulated during this developmental period. If we are interested in identifying genes which are closely linked with expression of the *plp* gene, comparison of samples taken from time points either side of the dramatic up-regulation and change in transcript ratio seen around P1 in the spinal cord would be a good starting point. There will probably be many other genes unrelated to *plp* coincidentally undergoing up/down-regulation at this time. Isolation and sequencing of numerous candidate products is potentially very time consuming, especially if many of the candidates are of such a coincidental nature. One possible way of eliminating some of these products would be to compare two sets of samples at the same time, which are at the same developmental stage with respect to the gene of interest, but at a different age chronologically. The demonstration that mid optic nerves undergo the same up-regulation and change in transcript ratio as the spinal cord, but delayed by approximately 6 days, provides such a comparison. Interest could then be concentrated on changes in differential products which are consistent across both the spinal cord and optic nerve samples.

The dramatic ratio changes seen in both spinal cord and optic nerve serve to highlight important time points in relation to myelination and expression of the *plp* gene. Study of

the wider spectrum of gene expression at these time points may well provide the additional information to allow us to understand this important, but as yet elusive gene.

# Abbreviations

| | |
|---|---|
| APES | 3-aminopropyltriethoxy-silane |
| ATP | Adenosine-triphosphate |
| BNF | Buffered neutral formaldehyde |
| bp | Base pairs |
| BSA | Bovine serum albumin |
| $^0C$ | Degrees centigrade |
| $CaCl_2$ | Calcium chloride |
| cAMP | Cyclic adenosine monophosphate |
| CCG | Cranial cervical ganglia |
| cDNA | Complementary DNA |
| CIAP | Calf intestinal alkaline phosphatase |
| CMT-1A | Charcot-Marie-Tooth disease type 1A |
| CNP | 2',3'-cyclic nucleotide 3'-phosphodiesterase |
| CNS | Central nervous system |
| cpm | Counts per minute |
| CST | Cervical sympathetic trunk |
| CTP | Cytidine-triphosphate |
| DAB | 3'-diaminobenzidine tetrachloride |
| DAPI | 4',6-diamidino-2-phenylindole |
| dCTP | 2'-Deoxy-cytidine-5'-triphosphate |
| DDSA | Dodecanyl succinic anhydride |
| DEPC | Di-ethyl pyrocarbonate |
| DIG | Digoxigenin |
| DMEM | Dulbecco's modified Eagle medium |
| DMP | 2,4,6-tri-dimethylaminomethyl-phenol |
| DNA | Deoxyribonucleic acid |
| dNTP | Deoxynucleoside-triphosphate |
| DS | Dejerine-Sottas hypertrophic neuropathy |
| DTT | Dithiothrietol |
| DW | Distilled water |
| E | Embryonic day |
| EDTA | (Ethylenedinitrilo)tetraacetic acid |
| EM | Electron microscopy |
| ER | Endoplasmic reticulum |
| FACS | Fluorescence-activated cell sorting |
| FCS | Foetal calf serum |
| FITC | Fluorescein isothiocyanate |
| g | Gram |
| GalC | Galactocerebroside |
| GFAP | Glial fibrillary acidic protein |
| GTP | Guanosine-5'-triphosphate |
| GuSCN | Guanidine thiocyanate |
| H and E | Haematoxylin and eosin |
| HBSS | Hanks' balanced salt solution |
| HCl | Hydrochloric acid |
| HEPES | (N-[2-hydroxyethyl]piperazine-N'-[2-ethane-sulphonic acid]) |
| hr | Hour |
| Ile | Isoleucine |

| | |
|---|---|
| ISH | *In situ* hybridisation |
| *jp* | Jimpy |
| $jp^{msd}$ | Jimpy myelin synthesis deficient |
| $jp^{rsh}$ | Jimpy rumpshaker |
| kb | Kilobase |
| kD | KiloDalton |
| $K_2HPO_4$ | Potassium hydrogen phosphate |
| L | Litre |
| lb | Pound |
| LB | Luria Bertani |
| LiCl | Lithium chloride |
| M | Molar |
| MAG | Myelin associated glycoprotein |
| Mb | Megabase |
| MBP | Myelin basic protein |
| *md*-rat | Myelin deficient rat |
| mg | Milligram |
| $MgCl_2$ | Magnesium chloride |
| $MgSO_4$ | Magnesium sulphate |
| min | Minute |
| ml | Millilitre |
| mM | Millimolar |
| MMLV | Moloney murine leukaemia virus |
| MOBP | Myelin-associated oligodendrocyte basic protein |
| MOG | Myelin oligodendrocyte glycoprotein |
| MOSP | Myelin oligodendrocyte-specific protein |
| mRNA | Messenger ribonucleic acid |
| NaAc | Sodium acetate |
| NaCl | Sodium chloride |
| $NaClO_4$ | Sodium chlorate |
| $NaH_2PO_4$ | Sodium hydrogen phosphate |
| NaI | Sodium iodide |
| NaOH | Sodium hydroxide |
| NBT | Nitroblue tetra-zolium chloride |
| N-CAM | Neural cell adhesion molecule |
| NF | Neurofilaments |
| ng | Nanogram |
| NGF | Nerve growth factor |
| NGS | Normal goat serum |
| $NH_4Ac$ | Ammonium acetate |
| $NH_4Cl$ | Ammonium chloride |
| O-2A | Oligodendrocyte-type2 astrocyte |
| OB | Olfactory bulb |
| OD | Optical density |
| Omgp | Oligodendrocyte-myelin glycoprotein |
| ONEC | Olfactory nerve ensheathing cell |
| ONL | Olfactory nerve layer |
| P | Post-natal day |
| $P_0$ | Protein zero |
| PAP | Peroxidase anti-peroxidase |

| | |
|---|---|
| PBS | Phosphate buffered saline |
| PCR | Polymerase chain reaction |
| PDGFα | Platelet-derived growth factor alpha |
| PDGFαR | Platelet-derived growth factor alpha receptor |
| PLP | Proteolipid protein |
| PLP-CT | Proteolipid protein-carboxy terminal |
| PMD | Pelizaeus-Merzbacher disease |
| PMP-22 | Peripheral myelin protein-22 |
| PNS | Peripheral nervous system |
| POA | Proligodendroblast antigen |
| *pt* | Paralytic tremor |
| Ran-2 | Rat neural antigen 2 |
| RER | Rough endoplasmic reticulum |
| RmAb | Ranscht monoclonal antibody |
| RNA | Ribonucleic acid |
| rpm | Revolutions per minute |
| RT-PCR | Reverse transcriptase-polymerase chain reaction |
| SDS-PAGE | Sodium dodecyl sulphate polyacrylamide gel electrophoresis |
| SDW` | Sterile distilled water |
| sec | Second |
| *sh*-pup | Shaking pup |
| SnRNA | Small nuclear RNA |
| SnRNP | Small nuclear RNA protein complex |
| SPG2 | Spastic paraplegia type 2A |
| sq. in. | Square inch |
| SSC | Standard sodium citrate |
| SUL | Sulphatide |
| TAE | Tris acetate EDTA |
| TBE | Tris borate EDTA |
| TE | Tris EDTA |
| Thr | Threonine |
| tRNA | Transfer ribonucleic acid |
| TxR | Texas red |
| U | Units |
| μCi | Microcurie |
| μg | Microgram |
| μl | Microlitre |
| μm | Micrometre |
| UTP | Uridine-5'-triphosphate |
| UV | Ultra-violet |
| vim | Vimentin |
| w/v | Weight in volume |
| X-phos | 5-bromo-4-chloro-3-indoyl-phosphate |

# References


Agrawal, H.C. and Agrawal, D. (1991) Proteolipid protein and DM-20 are synthesized by Schwann cells, present in myelin membrane, but they are not fatty acylated. *Neurochemical Research.* **16**, 855-858.

Armstrong, R.C. Kim, J.G. and Hudson L.D. (1995) Expression of myelin transcription factor I (MytI), a "zinc-finger" DNA-binding protein, in developing oligodendrocytes. *Glia.* **14**, 303-321.

Asotra, K. and Macklin, W.B. (1993) Protein kinase C activity modulates myelin gene expression in enriched oligodendrocytes. *Journal of Neuroscience Research.* **34**, 571-588.

Banik, N.L. and Smith, M.E. (1977) Protein determinants of myelination in different regions of developing rat central nervous system. *Biochemical Journal.* **162**, 247-255.

Bansal, R., Stefansson, K. and Pfeiffer, S.E. (1992) Proligodendroblast antigen (POA), a developmental antigen expressed by A007/O4-positive oligodendrocyte progenitors prior to the appearance of sulfatide and galactocerebroside. *Journal of Neurochemistry.* **58**, 2221-2229.

Barnett, S.C., Hutchins, A.M. and Noble, M. (1993) Purification of olfatory nerve ensheathing cells from the olfatory bulb. *Developmental Biology.* **155**, 337-350.

Baron, P., Kamholz, J., Scherer, S., Honda, H., Shy, M., Scarpini, E., Scarlato, G. and Pleasure, D. (1993) Appearance of PLP mRNA in specific regions of the developing rat lumbosacral spinal cord as revealed by *in situ* hybridization. *Experimental Neurology.* **121**, 139-147.

Barres, B.A. and Raff, M.C. (1993) Proliferation of oligodendrocyte precursor cells depends on electrical activity in axons. *Nature.* **361**, 258-260.

Barres, B.A. and Raff, M.C. (1994) Control of oligodendrocyte number in the developing rat optic nerve. *Neuron.* **12**, 935-942.

Bartlett, W.P. and Skoff, R.P. (1986) Expression of the jimpy gene in the spinal cords of heterozygous female mice. I. An early myelin deficit followed by compensation. *Journal of Neuroscience.* **6**, 2802-2812.

Bensted, J.P.M., Dobbing, J., Morgan, R.S., Reid, R.T.W. and Payling Wright, G. (1957) Neuroglial development and myelination in the spinal cord of the chick embryo. *Journal of Embryology and Experimental Morphology.* **5**, 428-437.

Berndt, J., Kim, J.G. and Hudson, L.D. (1992) Identification of *cis*-regulatory elements in the myelin proteolipid protein (PLP) gene. *The Journal of Biological Chemistry.* **267**, 14730-14737.

Birnboim, H.C. and Doly, J. (1979) A rapid alkaline extraction procedure for screening recombinant plasmid DNA. *Nucleic Acids Research.* **7**, 1513-1523.

Bjartmar, C., Hildebrand, C. and Loinder, K. (1994) Morphological heterogeneity of rat oligodendrocytes: Electron microscopic studies on serial sections. *Glia.* **11**, 235-244.

Black, J.A., Foster, R.E. and Waxman, S.G. (1982) Rat optic nerve: freeze-fracture studies during development of myelinated axons. *Brain Research.* **250**, 1-20.

Boison, D. and Stoffel, W. (1994) Disruption of the compacted myelin sheath of axons of the central nervous system in proteolipid protein-deficient mice. *Proceedings of the National Academy of Sciences USA.* **91**, 11709-11713.

Boison, D., Bussow, H., D'Urso, D., Muller, H. and Stoffel, W. (1995) Adhesive properties of proteolipid protein are responsible for the compaction of CNS myelin sheaths. *The Journal of Neuroscience.* **15**, 5502-5513.

Bosse, F., Zoidl, G., Wilms, S., Gillen, C.P., Kuhn, H.G. and Müller, H.W. (1994) Differential expression of two mRNA species indicates a dual function of peripheral myelin protein *PMP22* in cell growth and myelination. *Journal of Neuroscience Research.* **37**, 529-537.

Bottenstein, J.E. and Sato, G.H. (1979) Growth of a rat neuroblastoma cell line in serum-free supplemented medium. *Proceedings of the National Academy of Sciences USA.* **76**, 514-517.

Bourre, J.M., Jacque, C., Delassalle, A., Nguyen-Legros, J., Dumont, O., Lachapelle, F., Raoul, M., Alvarez, C. and Baumann, N. (1980) Density profile and basic protein measurements in the myelin range of particulate material from normal developing mouse brain and from neurological mutants (jimpy; quaking; trembler; shiverer and its mld allele) obtained by zonal centrifugation. *Journal of Neurochemistry.* **35**, 458-464.

Brown, M.C., Besio Moreno, M., Bongarzone, E.R., Cohen, P.D., Soto, E.F. and Pasquini, J.M. (1993) Vesicular transport of myelin proteolipid and cerebroside sulfates to the myelin membrane. *Journal of Neuroscience Research.* **35**, 402-408.

Bunge, M.B., Bunge, R.P. and Ris, H. (1961) Ultrastructural study of remyelination in an experimental lesion in adult cat spinal cord. *Journal of Biophysical and Biochemical Cytology.* **10**, 67.

Bunge, M.B., Bunge, R.P. and Pappas, G.D. (1962) Electron microscopic demonstrations of connections between glia and myelin sheaths in the developing mammalian central nervous system. *Journal of Cell Biology.* **12**, 448.

Bunge, R.P. (1968) Glial cells and the central myelin sheath. *Physiological Reviews.* **48**, 197.

Cambi, F. and Kamholz, J. (1994) Transcriptional regulation of the rat PLP promoter in primary cultures of oligodendrocytes. *Neurochemical Research.* **19**, 1055-1060.

Cameron-Curry, P. and Le Douarin, N.M. (1995) Oligodendrocyte precursors originate from both the dorsal and the ventral parts of the spinal cord. *Neuron.* **15**, 1299-1310.

Campagnoni, A.T., Campagnoni, C.W., Dutton, G.R. and Cohen, J. (1976) A regional study of developing rat brain: the accumulation and distribution of proteolipid proteins. *Journal of Neurobiology.* **7**, 313-324.

Campagnoni, A.T. and Hunkeler, M.J. (1980) Synthesis of the Myelin Proteolipid Protein in the Developing Mouse Brain. *Journal of Neurobiology.* **11**, 355-364.

Campagnoni, A.T. and Macklin, W.B. (1988) Cellular and molecular aspects of myelin protein gene expression. *Molecular Neurobiology.* **2**, 41-89.

Campagnoni, C.W., Garbay, B., Micevych, P., Pribyl, T., Kampf, K., Handley, V.W. and Campagnoni, A.T. (1992) DM20 mRNA splice product of the myelin proteolipid protein gene is expressed in the murine heart. *Journal of Neuroscience Research.* **33**, 148-155.

Chalfie, M., Tu, Y., Euskirchen, G., Ward, W.W. and Prasher, D.C. (1994) Green fluorescent protein as a marker for gene expression. *Science.* **263**, 802-805.

Chan, D.S. and Lees, M.B. (1974) Gel electrophoresis studies of bovine brain white matter proteolipid and myelin proteins. *Biochemistry.* **13**, 2704-2711.

Chance, P.F., Alderson, M.K., Leppig, K.A., Lensch, M.W., Matsunami, N., Smith, B., Swanson, P.D., Odelberg, S.J., Disteche, C.M. and Bird, T.D. (1993) DNA deletion associated with hereditary neuropathy with liability to pressure palsies. *Cell.* **72**, 143-151.

Choi, B.H., Kim, R.C. and Lapham, L.W. (1983) Do radial glia give rise to both astroglial and oligodendroglial cells. *Developmental Brain Research.* **8**, 119-130.

Chomczynski, P. and Sacchi, N. (1987) Single-step method of RNA isolation by acid guanidinium-thiocyanate-phenol-chloroform extraction. *Annals of Biochemistry.* **162**, 156-159.

Colello, R.J., Devey, L.R., Imperato, E. and Pott, U. (1995) The chronology of oligodendrocyte differentiation in the rat optic nerve: evidence for a signaling step initiating myelination in the CNS. *The Journal of Neuroscience.* **15**, 7665-7672.

Collarini, E.J., Kuhn, R., Marshall, C.J., Monuki, E.S., Lemke, G. and Richardson, W.D. (1992) Down-regulation of the POU transcription factor SCIP is an early event in oligodendrocyte differentiation in vitro. *Development.* **116**, 193-200.

Colman, D.R., Kreibich, G., Frey, A.B. and Sabatini, D.D. (1982) Synthesis and incorporation of myelin polypeptides into CNS myelin. *Journal of Cell Biology.* **95**, 598-608.

Cook, J.L., Irias-Donaghey, S. and Deininger, P.L. (1992) Regulation of rodent myelin proteolipid protein gene expression. *Neuroscience Letters.* **137**, 56-60.

Cox, K.H., DeLeon, D.V., Angerer, L.M. and Angerer, R.C. (1984) Detection of mRNAs in sea urchin embryos by in situ hybridization using asymmetric RNA probes. *Developmental Biology.* **101**, 485-502.

Cremers, F.P.M., Pfeiffer, R.A., van de Pol, T.J.R., Hofker, M.H., Kruse, T.A., Wieringa, B. and Ropers, H.H. (1987) An interstitial duplication of the X chromosome in a male allows physical fine mapping of probes from the Xq13-q22 region. *Human Genetics.* **77**, 23-27.

Danielson, P.E., Forss-Petter, S., Brow, M.A., Calavetta, L., Douglass, J., Milner, R.J. and Sutcliffe, J.G. (1988) p1B15: a cDNA clone of the rat mRNA encoding cyclophilin. *DNA.* **7**, 261-267.

Darnell Jr., J.E. (1982) Variety in the level of gene control in eukaryotic cells. *Nature.* **297**, 365-371.

de Ferra, F., Engh, H., Hudson, L., Kamholz, J., Puckett, C., Molineaux, S. and Lazzarini, R.A. (1985) Alternative splicing accounts for the four forms of myelin basic protein. *Cell.* **43**, 721-727.

De Leon, M., Welcher, A.A., Suter, U. and Shooter, E.M. (1991) Identification of transcriptionally regulated genes after sciatic nerve injury. *Journal of Neuroscience Research.* **29**, 437-448.

De Lorenzo, A.J. (1957) Electron microscopic observations of the olfactory mucosa and olfactory nerve. *Journal of Biophysical and Biochemical Cytology.* **3**, 839-848.

De Vitry, F., Picart, R., Jacque, C., Legault, L., Dupouey, P. and Tixier-Vidal, A. (1980) Presumptive common precursor for neuronal and glial cell lineages in mouse hypothalamus. *Proceedings of the National Academy of Sciences USA.* **77**, 4165-4169.

Devon, R. and Doucette, R. (1992) Olfactory ensheathing cells myelinate dorsal root ganglion neurites. *Brain Research.* **589**, 175-179.

Diaz, R.S., Monreal, J. and Lucas, M. (1990) Calcium movements mediated by proteolipid protein and nucleotides in liposomes prepared with the endogenous lipids from white matter. *Journal of Neurochemistry.* **55**, 1304-1309.

Diehl, H., Schaich, M., Budzinski, R. and Stoffel, W. (1986) Individual exons encode the integral membrane domains of human proteolipid protein. *Proceedings of the National Academy of Sciences USA.* **83**, 9807-9811.

Doucette, J.R. (1984) The glial cells in the nerve fiber layer of the rat olfactory bulb. *The Anatomical Record.* **210**, 385-391.

Doucette, R. (1989) Development of the nerve fiber layer in the olfactory bulb of mouse embryos. *The Journal of Comparative Neurology.* **285**, 514-527.

Doucette, R. (1990) Glial influences on axonal growth in the primary olfactory system. *Glia.* **3**, 433-449.

Doucette, R. (1991) PNS-CNS transitional zone of the first cranial nerve. *The Journal of Comparative Neurology.* **312**, 451-466.

Dubois-Dalcq, M., Behar, T., Hudson, L.D. and Lazzarini, R.A. (1986) Emergence of three myelin proteins in oligodendrocytes cultured without neurons. *Journal of Cell Biology.* **102**, 384-392.

Duncan, I.D., Hammang, J.P. and Jackson, K.F. (1986) Mosaicism in the CNS of two myelin mutants, the shaking pup and the myelin deficient (md) rat. *Journal of Neuropathology and Experimental Neurology.* **45**, 373-

Duncan, I.D., Hammang, J.P. and Trapp, B.D. (1987) Abnormal compact myelin in the myelin-deficient rat: absence of proteolipid protein correlates with a defect in the intraperiod line. *Proceedings of the National Academy of Sciences USA.* **84**, 6287-6291.

Duncan, I.D., Hammang, J.P., Goda, S. and Quarles, R.H. (1989) Myelination in the jimpy mouse in the absence of proteolipid protein. *Glia.* **2**, 148-154.

Duncan, I.D., Jackson, K.F., Hammang, J.P., Marren, D. and Hoffman, R. (1993) Development of myelin mosaicism in the optic nerve of heterozygotes of the X-linked myelin-deficient (*md*) rat mutant. *Developmental Biology.* **157**, 334-347.

Dyer, C.A., Hickey, W.F. and Geisert, E.E., Jr. (1991) Myelin/oligodendrocyte-specific protein: A novel surface membrane protein that associates with microtubules. *Journal of Neuroscience Research.* **28**, 607-613.

Einsenbarth, G.S., Walsh, F.S. and Nirenberg, M. (1979) Monoclonal antibody to a plasma membrane antigen of neurons. *Proceedings of the National Academy of Sciences USA.* **76**, 4913-4917.

Ellis, D. and Malcolm, S. (1994) Proteolipid protein gene dosage effect in Pelizaeus-Merzbacher disease. *Nature Genetics.* **6**, 333-334.

Fanaragga, M.L. Neurobiology of oligodendrocytes in the plp mutant rumpshaker: [Thesis] Faculty of Veterinary Medicine, University of Glasgow; 1993. Morphometric analysis and glial cell quantification. p.85.

Fanarraga, M., Sommer, I., Griffiths, I.R., Montague, P., Groome, N.P., Nave, K., Schneider, A., Brophy, P.J. and Kennedy, P.G.E. (1993) Oligodendrocyte development and differentiation in the rumpshaker mutation. *Glia.* **9**, 146-156.

Fanarraga M., Sommer I. and Griffiths I.R. (1995) O-2A progenitors of the mouse optic nerve exhibit a developmental pattern of antigen expression different from the rat. *Glia.* **15**, 95-104.

Flechsig, P. (1894) Gehirn und seele. *Neurol. Centralbl.*

Fok-Seang, J. and Miller, R.H. (1994) Distribution and differentiation of $A2B5^+$ glial precursors in the developing rat spinal cord. *Journal of Neuroscience Research.* **37**, 219-235.

Folch, J. and Lees, M. (1951) Proteolipids, a new type of tissue lipoproteins. *The Journal of Biological Chemistry.* **191**, 807-817.

Fox, M.W., Inman, O.R. and Himwich, W.A. (1967) The postnatal development of the spinal cord of the dog. *The Journal of Comparative Neurology.* **130**, 233-240.

Fraher, J.P. (1972) A quantitative study of anterior root fibres during early myelination. *Journal of Anatomy.* **112**, 99-124.

Fraher, J.P. (1992) The CNS-PNS transitional zone of the rat. Morphometric studies at cranial and spinal levels. *Progress in Neurobiology.* **38**, 261-316.

Franklin, R.J.M. and Blakemore, W.F. (1995) Glial-cell transplantation and plasticity in the O-2A lineage - Implications for CNS repair. *Trends in Neurosciences.* **18**, 151-156.

Gard, A.L. and Pfeiffer, S.E. (1990) Two proliferative stages of the oligodendrocyte lineage (A2B5+O4- and GalC-) under different mitogenic control. *Neuron.* **5**, 615-625.

Gardinier, M.V., Macklin, W.B., Diniak, A.J. and Deininger, P.L. (1986) Characterization of myelin proteolipid mRNAs in normal and jimpy mice. *Molecular and Cellular Biology.* **6**, 3755-3762.

Gardinier, M.V. and Macklin, W. (1988) Myelin proteolipid protein gene expression in jimpy and $jimpy^{msd}$ mice. *Journal of Neurochemistry.* **51**, 360-369.

Gardinier, V. and Macklin, W.B. (1990) Developmental expression of the myelin proteolipid protein gene. *Cellular and Molecular Biology of Myelination.* Jeserich, G. editor: Springer-Verlag , Berlin, pp. 517-532.

Gasser, H.S. (1956) Olfactory nerve fibres. *Journal of General Physiology.* **39**, 473-496.

Gencic, S. and Hudson, L.D. (1990) Conservative amino acid substitution in the myelin proteolipid protein of $jimpy^{msd}$ mice. *Journal of Neuroscience.* **10**, 117-124.

Giese, K.P., Martini, R., Lemke, G., Soriano, P. and Schachner, M. (1992) Mouse $P_0$ disruption leads to hypomyelination, abnormal expression of recognition molecules, and degeneration of myelin and axons. *Cell.* **71**, 565-576.

Gilmore, S.A. (1971) Neuroglial population in the spinal white matter of neonatal and early post-natal rats: an autoradiographic study of numbers of neuroglial and changes in their proliferative activity. *The Anatomical Record.* **171**, 283-292.

Giulian, D., Johnson, B., Krebs, J.F., Tapscott, M.J. and Honda, S. (1991) A growth factor from neuronal cell lines stimulates myelin protein synthesis in mammalian brain. *Journal of Neuroscience.* **11**, 327-336.

Gonye, G.E., Warrington, A.E., DeVito, J.A. and Pfeiffer, S.E. (1994) Oligodendrocyte precursor quantitation and localization in perinatal brain using a retrospective bioassay. *Journal of Neuroscience.* **14**, 5365-5372.

Gow, A., Friedrich, V.L., Jr. and Lazzarini, R.A. (1994a) Intracellular transport and sorting of the oligodendrocyte transmembrane proteolipid protein. *Journal of Neuroscience Research.* **37**, 563-573.

Gow, A., Friedrich, V.L., Jr. and Lazzarini, R.A. (1994b) Many naturally occurring mutations of myelin proteolipid protein impair its intracellular transport. *Journal of Neuroscience Research.* **37**, 574-583.

Graziadei, P.P.C. and Monti Graziadei, G.A. (1979) Neurogenesis and neuron regeneration in the olfactory system of mammals. I. Morphological aspects of differentiation and structural organization of the olfactory sensory neurones. *Journal of Neurocytology.* **8**, 1-18.

Greenfield, S., Brostoff, S., Eyler, E.H. and Morell, P. (1973) Protein composition of the peripheral nervous system. *Journal of Neurochemistry.* **20**, 1207-1216.

Griffiths, I.R., Duncan, I.D., McCulloch, M. and Harvey, M.J.A. (1981) Shaking pups: a disorder of central myelination in the spaniel dog. *Journal of the Neurological Sciences.* **50**, 423-433.

Griffiths, I.R., Mitchell, L.S., McPhilemy, K., Morrison, S., Kyriakides, E. and Barrie, J.A. (1989) Expression of myelin protein genes in Schwann cells. *Journal of Neurocytology.* **18**, 345-352.

Griffiths, I.R., Dickinson, P. and Montague, P. (1995a) Expression of the proteolipid protein gene in glial cells of the post natal peripheral nervous system of rodents. *Neuropathology and Applied Neurobiology.* **21**, 97-110.

Griffiths, I.R., Schneider, A., Anderson, J. and Nave, K. (1995b) Transgenic and natural mouse models of proteolipid protein (PLP) related dysmyelination and demyelination. *Brain Pathology.* **5**, 275-281.

Grinspan, J., Wrabetz, L. and Kamholz, J. (1993) Oligodendrocyte maturation and myelin gene expression in PDGF-treated cultures from rat cerebral white matter. *Journal of Neurocytology.* **22**, 322-333.

Gupta, S.K., Pringle, J., Poduslo, J.F. and Mezei, C. (1991) Levels of proteolipid protein mRNAs in peripheral nerve are not under stringent axonal control. *Journal of Neurochemistry.* **56**, 1754-1762.

Hardy, R. and Reynolds, R. (1991) Proliferation and differentiation potential of rat forebrain oligodendroglial progenitors both *in vitro* and *in vivo*. *Development.* **111**, 1061-1080.

Hayashi, S. (1978) Acetylation of chromosome squashes of Drosophilia melanogaster decreases the background in autoradiographs from hybridization with $^{125}$I-labelled RNA. *Journal of Histochemistry and Cytochemistry.* **36**, 677-679.

Helynck, G., Luu, B., Nussbaum, J.L., Picken, D., Skalidis, G., Trifilieff, E., Van Dorsselaer, A., Seta, P., Sandeaux, R., Gavach, D., *et al.* (1983) Brain proteolipids, isolation, purification and effects on ionic permeability of membranes. *European Journal of Biochemistry.* **133**, 689-695.

Hildebrand, C. and Skoglund, S. (1971) Calibre spectra of some fibre tracts in the feline central nervous system during postnatal development. *Acta Physiologica Scandinavica.* **364**, 5-41.

Hildebrand, C. and Waxman, S.G. (1984) Postnatal differentiation of rat optic nerve fibers:electron microscopic observations on the development of nodes of Ranvier and axoglial relations. *The Journal of Comparative Neurology.* **224**, 25-37.

Hirano, M. and Goldman, J.E. (1988) Gliogenesis in rat spinal cord: evidence for origin of astrocytes and oligodendrocytes from radial precursors. *Journal of Neuroscience Research.* **21**, 155-167.

Hudson, L.D., Friedrich, V.L., Jr., Behar, T., Dubois-Dalcq, M. and Lazzarini, R.A. (1989a) The initial events in myelin synthesis: orientation of proteolipid protein in the plasma membrane of cultured oligodendrocytes. *Journal of Cell Biology.* **109**, 717-727.

Hudson, L.D., Puckett, C., Berndt, J., Chan, J. and Genic, S. (1989b) Mutation of the proteolipid protein gene PLP in a human X chromosome-linked myelin disorder. *Proceedings of the National Academy of Sciences USA.* **86**, 8128-8131.

Huxley, A.F. and Staempfli, R. (1949) Evidence for saltatory conduction in peripheral myelinated nerve fibres. *Journal of Physiology.* **108**, 315-339.

Ikenaka, K., Furuichi, T., Iwasaki, Y., Moriguchi, A., Okano, H. and Mikoshiba, K. (1988) Myelin proteolipid protein gene structure and its regulation of expression in normal and *jimpy* mutant mice. *Journal of Molecular Biology.* **199**, 587-596.

Ikenaka, K., Kagawa, T. and Mikoshiba, K. (1992) Selective expression of DM-20, an alternatively spliced myelin proteolipid protein gene product, in developing nervous system and in non-glial cells. *Journal of Neurochemistry.* **58**, 2248-2253.

Jacobson, S. (1963) Sequence of myelination in the brain of the albino rat. *The Journal of Comparative Neurology.* **121**, 5-29.

Janz, R. and Stoffel, W. (1993) Characterization of a brain-specific Sp 1-like activity interacting with an unusual binding site within the myelin proteolipid protein promoter. *Biological Chemistry Hoppe-Seyler.* **374**, 507-517.

Jessen, K.R., Brennan, A., Morgan, L., Mirsky, R., Kent, A., Hashimoto, Y. and Gavrilovic, J. (1994) The Schwann cell precursor and its fate: A study of cell death and differentiation during gliogenesis in rat embryonic nerves. *Neuron.* **12**, 509-527.

Jessen, K.R. and Mirsky, R. (1991) Schwann cell precursors and their development. *Glia.* **4**, 185-194.

Johnson, R.S., Roder, J.C. and Riordan, J.R. (1995) Over-expression of the DM-20 myelin proteolipid causes central nervous system demyelination in transgenic mice. *Journal of Neurochemistry.* **64**, 967-976.

Juurlink, B.H.J. and Hertz, L. (1991) Establishment of highly enriched type-2 astrocyte cultures and quantitative determination of intense glutamine synthetase activity in these cells. *Journal of Neuroscience Research.* **30**, 531-539.

Kagawa, T., Ikenaka, K., Inoue, Y., Kuriyama, S., Tsujii, T., Nakao, J., Nakajima, K., Aruga, J., Okano, H. and Mikoshiba, K. (1994) Glial cell degeneration and hypomyelination caused by overexpression of myelin proteolipid protein gene. *Neuron.* **13**, 427-442.

Kamholz, J., Sessa, M., Scherer, S., Vogelbacker, H., Mokuno, K., Baron, P., Wrabetz, L., Shy, M. and Pleasure, D. (1992) Structure and expression of proteolipid protein in the peripheral nervous system. *Journal of Neuroscience Research.* **31**, 231-244.

Kanfer, J., Parenty, M., Goujet-Zalc, C., Monge, M., Bernier, L., Campagnoni, A.T., Dautigny, A. and Zalc, B. (1989) Developmental expression of myelin proteolipid, basic protein and 2', 3'-cyclic nucleotide 3'-phosphodiesterase transcripts in different rat brain regions. *Journal of Molecular Neuroscience.* **1**, 39-46.

Kappers, C.U.A. (1916) Further contributions on neurobiotaxis. *The Journal of Comparative Neurology.* **27**, 261.

Karthigasan, J., Bauer, T.K., Teplow, D.B., Saavedra, R.A. and Kirschner, D.A. (1991) Generation of DM-20 splice site in myelin proteolipid protein gene: A hypothesis based on analysis of the amphibian protein. *Peptide Research.* **4**, 227-229.

Kashima, T., Tiu, S.N., Merrill, J.E., Vinters, H.V., Dawson, G. and Campagnoni, A.T. (1993) Expression of oligodendrocyte-associated genes in cell lines derived from human gliomas and neuroblastomas. *Cancer Research.* **53**, 170-175.

Kidd, G.J., Hauer, P.E. and Trapp, B.D. (1990) Axons modulate myelin protein messenger RNA levels during central nervous system myelination in vivo. *Journal of Neuroscience Research.* **26**, 409-418.

Kim, J.G. and Hudson, L.D. (1992) Novel member of the zinc finger superfamily: a $C_2$-HC finger that recognises a glia-specific gene. *Molecular and Cellular Biology.* **12**, 5632-5639.

Kitagawa, K., Sinoway, M.P., Yang, C., Gould, R.M. and Colman, D.R. (1993) A proteolipid protein gene family: Expression in sharks and rays and possible evolution from an ancestral gene encoding a pore-forming polypeptide. *Neuron.* **11**, 433-448.

Knapp, P.E., Skoff, R.P. and Redstone, D.W. (1986) Oligodendroglial cell death in jimpy mice: an explanation for the myelin deficit. *Journal of Neuroscience.* **6**, 2813-2822.

Knapp, P.E. and Skoff, R.P. (1993) Jimpy mutation affects astrocytes: Lengthening of the cell cycle in vitro. *Developmental Neuroscience.* **15**, 31-36.

Kobayashi, H., Hoffman, E.P. and Marks, H.G. (1994) The *rumpshaker* mutation in spastic paraplegia. *Nature Genetics.* **7**, 351-352.

Kronquist, K.E., Crandall, B.F., Macklin, W.B. and Campagnoni, A.T. (1987) Expression of myelin proteins in the developing human spinal cord: cloning and sequencing of human proteolipid protein cDNA. *Journal of Neuroscience Research.* **18**, 395-401.

Kuhlmann-Krieg, S., Sommer, I. and Schachner, M. (1988) Ultrastructural features of cultured oligodendrocytes expressing stage-specific cell-surface antigens. *Developmental Brain Research.* **39**, 269-280.

Kumar, S., Cole, R., Chiappelli, F. and de Vellis, J. (1989) Differential regulation of oligodendrocyte markers by glucocorticoids: Post-transcriptional regulation of both proteolipid protein and myelin basic protein and transcriptional regulation of glycerol phosphate dehydrogenase. *Proceedings of the National Academy of Sciences USA.* **86**, 6807-6811.

Langworthy, O.R. (1928) The behavior of pouch young opossums correlated with the myelinization of tracts in the nervous system. *The Journal of Comparative Neurology.* **46**, 201-248.

Langworthy, O.R. (1929) A correlated study of the development of reflex activity in fetal and young kittens and the myelinization of the tracts in the nervous system. *Contributions to Embryology, Carnegie Institute of Washington* **394**, No.114 127-171.

Langworthy, O.R. (1933) Development of behavior patterns and myelinization of the nervous system in the human fetus and infant. *Contributions to Embryology, Carnegie Institute of Washington.* **443**, No139 1-57.

Laursen, R.A., Samiullah, M. and Lees, M.B. (1984) The structure of bovine brain myelin proteolipid and its organization in myelin. *Proceedings of the National Academy of Sciences USA.* **81**, 2912-2916.

LeBlanc, A.C., Poduslo, J.F. and Mezei, C. (1987) Gene expression in the presence or absence of myelin assembly. *Molecular Brain Research.* **2**, 57-67.

Lees, M.B., Brostoff, S.W. (1984) Proteins of myelin. In: *Myelin.* Morell, P. editor: Plenum Press, New York, pp. 197-224.

Lees, M.B., Sakura, J.D. (1978) Preparation of proteolipids. In: *Research methods in neurochemistry.* Marks, N. and Rodnight, R. editors: Plenum Press, New York, pp. 354-370.

Lemke, G. (1993) Transcriptional regulation of the development of neurons and glia. *Current Opinion in Neurobiology.* **3**, 703-708.

Lepage, P., Helynck, G., Chu, J., Luu, B., Sorokine, O., Trifilieff, E. and Van Dorsselaer, A. (1986) Purification and characterization of minor brain proteolipids: use of fast atom bombardment-mass spectrometry for peptide sequencing. *Biochimie.* **68**, 669-686.

Levi, G., Aloisi, F. and Wilkin, G.P. (1987) Differentiation of cerebellar bipotential glial precursors into oligodendrocytes in primary culture: developmental profile of surface antigens and mitotic activity. *Journal of Neuroscience Research.* **18**, 407-417.

LeVine, S.M., Wong, D. and Macklin, W.B. (1990) Developmental expression of proteolipid protein and DM-20 mRNAs and proteins in the rat brain. *Developmental Neuroscience.* **12**, 235-250.

LeVine, S.M. and Goldman, J.E. (1988) Spatial and temporal patterns of oligodendrocyte differentiation in rat cerebrum and cerebellum. *The Journal of Comparative Neurology.* **277**, 441-455.

Lin, L.H. and Lees, M.B. (1982) Interactions of dicyclohexylcarbodiimide with myelin proteolipid. *Proceedings of the National Academy of Sciences USA.* **79**, 941-945.

Linington, C., Webb, M. and Woodhams, P.L. (1984) A novel myelin-associated glycoprotein defined by a mouse monoclonal antibody. *Journal of Neuroimmunology.* **6**, 387-396.

López-Barahona, M., Miñano, M., Mira, E., Iglesias, T., Stunnenberg, H.G., Rodríguez-Peña, A., Bernal, J. and Muñoz, A. (1993) Retinoic acid posttranscriptionally up-regulates proteolipid protein gene expression in C6 glioma cells. *The Journal of Biological Chemistry.* **268**, 25617-25623.

Lubetzki, C., Goujet-Zalc, C., Gansmuller, A., Monge, M., Brillat, A. and Zalc, B. (1991) Morphological, biochemical, and functional characterization of bulk isolated glial progenitor cells. *Journal of Neurochemistry.* **56**, 671-680.

Lucas Keene, M.F. and Hewer, E.E. (1931) Some observations on myelination in the human central nervous system. *Journal of Anatomy.* **66**, 1-13.

Macklin, W.B., Braun, P.E. and Lees, M.B. (1982) Electroblot analysis of the myelin proteolipid protein. *Journal of Neuroscience Research.* **7**, 1-10.

Macklin, W.B., Oberfield, E. and Lees, M.B. (1983) Electroblot analysis of rat myelin proteolipid and basic protein during development. *Developmental Neuroscience.* **6**, 161-168.

Macklin, W.B., Weill, C.L. and Deininger, P.L. (1986) Expression of myelin proteolipid and basic protein mRNAs in cultured cells. *Journal of Neuroscience Research.* **16**, 203-217.

Macklin, W.B., Campagnoni, A.T., Deininger, P.L. and Gardinier, M.V. (1987) Structure and expression of the mouse proteolipid protein gene. *Journal of Neuroscience Research.* **18**, 383-394.

Macklin, W.B. (1988) The myelin proteolipid protein gene produces a non-oligodendrocyte mRNA. [Abstract] *Transactions of the American Society of Neurochemistry.* **19**, 132

Macklin, W.B., Gardinier, M.V., Obeso, Z.O., King, K.D., and Wight, P.A. (1991) Mutations in the myelin proteolipid protein gene alter oligodendrocyte gene expression in jimpy and jimpy$^{msd}$ mice. *Journal of Neurochemistry.* **56**, (1) 163-171.

Martí, E., Bumcrot, D.A., Takada, R. and McMahon, A.P. (1995) Requirement of 19K form of Sonic hedgehog for induction of distinct ventral cell types in CNS explants. *Nature.* **375**, 322-325.

Mastronardi, F.G., Ackerley, C.A., Arsenault, L., Roots, B.I. and Moscarello, M.A. (1993) Demyelination in a transgenic mouse: A model for multiple sclerosis. *Journal of Neuroscience Research.* **36**, 315-324.

Mattei, M., Alliel, P.M., Dautigny, A., Passage, E., Pham-Dinh, D., Mattei, J. and Jolles, P. (1986) The gene encoding for the major brain proteolipid (PLP) maps on the q-22 band of the human X chromosome. *Human Genetics.* **72**, 352-353.

Matthews, M.A. and Duncan, D. (1971) A quantitative study of morphological changes accompanying the initiation and progress of myelin production in the dorsal funiculus of the rat spinal cord. *The Journal of Comparative Neurology.* **142**, 1-22.

Mazia, D., Schatten, G. and Sale, W. (1975) Adhesion of cells to surfaces coated with polylysine. *Journal of Cell Biology.* **66**, 198-200.

McPhilemy, K., Mitchell, L.S., Griffiths, I.R., Morrison, S., Deary, A.W., Sommer, I. and Kennedy, P.G.E. (1990) Effect of optic nerve transection upon myelin protein gene expression by oligodendrocytes: evidence for axonal influences on gene expression. *Journal of Neurocytology.* **19**, 494-503.

Mikol, D.D., Rongnoparut, P., Allwardt, B.A., Marton, L.S. and Stefansson, K. (1993) The oligodendrocyte-myelin glycoprotein of mouse: Primary structure and gene structure. *Genomics.* **17**, 604-610.

Miller, R.H., David, S., Patel, R., Abney, E.R. and Raff, M.C. (1985) A quantitative immunohistochemical study of macroglial cell development in the rat optic nerve: *in vivo* evidence for two distinct astrocyte lineages. *Developmental Biology.* **111**, 35-41.

Milner, R.J., Lai, C., Nave, K., Lenoir, D., Ogata, J. and Sutcliffe, J.G. (1985) Nucleotide sequence of two mRNAs for rat brain myelin proteolipid protein. *Cell.* **42**, 931-939.

Mirsky, R., Dubois, C., Morgan, L. and Jessen, K.R. (1990) O4 and A007-sulphatide antibodies bind to embryonic Schwann cells prior to the appearance of galactocerebroside; regulation of the antigen by axon-Schwann cell signals and cyclic AMP. *Development.* **109**, 105-116.

Mitchell, L.S., Gillespie, C.S., McAllister, F., Fanarraga, M., Kirkham, D., Kelly, B., Brophy, P.J., Griffiths, I.R., Montague, P. and Kennedy, P.G.E. (1992) Developmental expression of the major myelin protein genes in the CNS of the X-linked hypomyelinating mutant rumpshaker. *Journal of Neuroscience Research.* **33**, 205-217.

Montague P, Barrie JA, Griffiths IR. Localization patterns of the PLP and DM-20 myelin isoproteins in a variety of transient and stable transfectants. [In Press] *Journal of Neuroscience Research.* 1995.

Nadon, N.L., Duncan, I.D. and Hudson, L.D. (1990) A point mutation in the proteolipid protein gene of the "shaking pup" interupts oligodendrocyte development. *Development.* **110**, 529-537.

Nadon, N.L., Arnheiter, H. and Hudson, L.D. (1994) A combination of PLP and DM20 transgenes promotes partial myelination in the jimpy mouse. *Journal of Neurochemistry.* **63**, 822-833.

Naismith, A.L., Hoffman-Chudzik, E., Tsui, L. and Riordan, J.R. (1985) Study of the expression of myelin proteolipid protein (lipophilin) using a cloned complementary DNA. *Nucleic Acids Research.* **13**, 7413-7425.

Nakafuku, M. and Nakamura, S. (1995) Establishment and characterisation of a multipotential neural cell line that can conditionally generate neurons, astrocytes and oligodendrocytes in vitro. *Journal of Neuroscience Research.* **41**, 153-168.

Nakajima, K., Ikenaka, K., Kagawa, T., Aruga, J., Nakao, J., Nakahira, K., Shiota, C., Kim, S.U. and Mikoshiba, K. (1993) Novel isoforms of mouse myelin basic protein predominantly expressed in embryonic stage. *Journal of Neurochemistry.* **60**, 1554-1563.

Nakao, J., Yamada, M., Kagawa, T., Kim, S.U., Miyao, Y., Shimizu, K., Mikoshiba, K. and Ikenaka, K. (1995) Expression of proteolipid protein gene is directly associated with secretion of a factor influencing oligodendrocyte development. *Journal of Neurochemistry.* **64**, 2396-2403.

Nave, K., Lai, C., Bloom, F.E. and Milner, R.J. (1986) Jimpy mutant mouse: A 74-base deletion in the mRNA for myelin proteolipid protein and evidence for a primary defect in RNA splicing. *Proceedings of the National Academy of Sciences USA.* **83**, 9264-9268.

Nave, K., Bloom, F.E. and Milner, R.J. (1987a) A single nucleotide difference in the gene for myelin proteolipid protein defines the *jimpy* mutation in mouse. *Journal of Neurochemistry.* **49**, 1873-1877.

Nave, K., Lai, C., Bloom, F.E. and Milner, R.J. (1987b) Splice site selection in the proteolipid protein (PLP) gene transcript and primary structure of the DM-20 protein of central nervous system myelin. *Proceedings of the National Academy of Sciences USA.* **84**, 5665-5669.

Nave, K., Schneider, A., Readhead, C., Griffiths, I.R., Pühlhofer, A., Bartholomä, A., Graf, S. and Kiefer, B. (1993) Molecular biology and neurogenetics of myelin proteolipid protein. In: *A Multidisciplinary Approach to Myelin Diseases.* Salvati, S. editor: Plenum Press, New York,

Nave, K.-A. and Lemke, G. (1991) Induction of the myelin proteolipid protein (PLP) gene in C6 glioblastoma cells: Functional analysis of the PLP promoter. *Journal of Neuroscience.* **11**, 3060-3069.

Noble, M., Murray, K., Stroobant, P., Waterfield, M.D. and Riddle, P. (1988) Platelet-derived growth factor promotes division and motility and inhibits premature differentiation of the oligodendrocyte/type-2 astrocyte progenitor cell. *Nature.* **333**, 560-562.

Noble, M., Wolswijk, G. and Wren, D. (1989) The complex relationship between cell division and the control of differentiation in oligodendrocyte-type-2 astrocyte progenitor cells isolated from perinatal and adult rat optic nerves. *Progress in Growth Factor Research.* **1**, 179-194.

Noll, E. and Miller, R.H. (1993) Oligodendrocyte precursors originate at the ventral ventricular zone dorsal to the ventral midline region in the embryonic rat spinal cord. *Development.* **118**, 563-573.

Noll, E. and Miller, R.H. (1994) Regulation of oligodendrocyte differentiation: A role for retinoic acid in the spinal cord. *Development.* **120**, 649-660.

Norgren, R.B., Ratner, N. and Brackenbury, R. (1992) Development of olfactory nerve glia defined by a monoclonal antibody specific for Schwann cells. *Developmental Dynamics.* **194**, 231-238.

Nornes, H.O. and Carry, M. (1978) Neurogenesis in spinal cord of mouse: an autoradiographic analysis. *Brain Research.* **159**, 1-16.

Norton, W.T. and Cammer, W. (1984) Isolation and characterization of myelin. In: *Myelin.* Morell, P. editor: Plenum Press, New York and London, pp. 147-196.

Nussbaum, J.L. and Mandel, P. (1973) Brain proteolipids in neurologically mutant mice. *Brain Research.* **61**, 295-310.

Nussbaum, J.L. and Roussel, G. (1983) Immunocytochemical demonstration of the transport of myelin proteolipids through the Golgi apparatus. *Cell and Tissue Research.* **234**, 547-559.

Ono, K., Friedrich, V.L., Jr., Hudson, L., Lazzarini, R.A. and Dubois-Dalcq, M. (1990) The unexpected expression of the major CNS myelin protein, proteolipid protein, in Schwann cells in vivo and in vitro. In: *Charcot-Marie-Tooth Disorders: Pathophysiology, Molecular Genetics and Therapy. Neurology and Neurobiology Series. Vol. 53.* Lovelace, R.E. and Shapiro, H.R. editors: Wiley Liss, New York, pp. 201-209.

Ono, K., Bansal, R., Payne, J., Rutishauser, U. and Miller, R.H. (1995) Early development and dispersal of oligodendrocyte precursors in the embryonic chick spinal cord. *Development.* **121**, 1743-1754.

Orr-Urtreger, A. and Lonai, P. (1992) Platelet-derived growth factor-A and its receptor are expressed in separate, but adjacent cell layers of the mouse embryo. *Development.* **115**, 1045-1058.

Pasquini, J.M., Guarna, M.M., Besio-Moreno, M.A., Iturregui, M.T., Oteiza, P.I. and Soto, E.F. (1989) Inhibition of the synthesis of glycosphingolipids affect the translocation of proteolipid protein to the myelin membrane. *Journal of Neuroscience Research.* **22**, 289-296.

Patel, P.I. and Lupski, J.R. (1994) Charcot-Marie-Tooth disease: A new paradigm for the mechanism of inherited disease. *Trends in Genetics.* **10**, 128-133.

Peters, A. and Muir, A.R. (1959) The relationship between axons and Schwann cells during development of peripheral nerves in the rat. *Quarterly Journal of Experimental Physiology.* **44**, 117-130.

Pfeiffer, S.E., Bansal, R., Gard, A.L. and Warrington, A.E. (1990) Regulation of oligodendrocyte progenitor development: antibody-perturbation sites. In: *Cellular and Molecular Biology of Myelination.* Jeserich, G., Althaus, H.A. and Waehneldt, T.V. editors: Springer-Verlag, Berlin, pp. 19-31.

Pham-Dinh, D., Birling, M., Dautigny, A. and Nussbaum, J.L. (1991) Proteolipid DM-20 predominates over PLP in peripheral nervous system. *Molecular Neuroscience.* **2**, 89-92.

Pinching, A.J. and Powell, T.P.S. (1971a) The neuron types of the glomerular layer of the olfactory bulb. *Journal of Cell Science.* **9**, 305-345.

Pinching, A.J. and Powell, T.P.S. (1971b) The neuropil of the glomeruli of the olfactory bulb. *Journal of Cell Science.* **9**, 347-377.

Placzek, M., Tessier-Lavigne, M., Yamada, T., Jessell, T. and Dodd, J. (1990) Mesodermal control of neuronal cell identity: floor plate induction by the notochord. *Science.* **250**, 985-988.

Popot, J.-L., Dinh, D.P. and Dautigny, A. (1991) Major myelin proteolipid: The 4-α-helix topology. *The Journal of Membrane Biology.* **120**, 233-246.

Prasher, D.C., Eckenrode, V.K., Ward, W.W., Prendergast, F.G. and Cormier, M.J. (1992) Primary structure of the *Aequorea victoria* green-fluorescent protein. *Gene.* **111**, 229-233.

Price, J. and Thurlow, L. (1988) Cell lineage in the rat cerebral cortex: a study using retroviral-mediated gene transfer. *Development.* **104**, 473-482.

Price, J.L. and Powell, T.P.S. (1970) The morphology of the granule cells of the olfactory bulb. *Journal of Cell Science.* **7**, 91-123.

Pringle, N.P., Mudhar, H.S., Collarini, E.J. and Richardson, W.D. (1992) PDGF receptors in the rat CNS: During late neurogenesis, PDGF alpha-receptor expression appears to be restricted to glial cells of the oligodendrocyte lineage. *Development.* **115**, 535-551.

Pringle, N.P. and Richardson, W.D. (1993) A singularity of PDGF alpha-receptor expression in the dorsoventral axis of the neural tube may define the origin of the oligodendrocyte lineage. *Development.* **117**, 525-533.

Privat, A., Jacque, C., Bourre, J.M., Dupouey, P. and Baumann, N. (1979) Absence of the major dense line in myelin of the mutant mouse shiverer. *Neuroscience Letters.* **12**, 107-112.

Puckett, C., Hudson, L.D., Ono, K., Benecke, J., Dubois-Dalcq, M. and Lazzarini, R.A. (1987) Myelin-specific proteolipid protein is expressed in myelinating Schwann cells but is not incorporated into myelin sheaths. *Journal of Neuroscience Research.* **18**, 511-518.

Quarles, R.H., Everly, J.L. and Brady, R.O. (1973) Evidence for the close association of a glycoprotein with myelin. *Journal of Neurochemistry.* **21**, 1177-1191.

Raff, M.C., Mirsky, R., Fields, K.L., Lisak, R.P., Dorfman, S.H., Silberberg, D.H., Gregson, N.A., Liebowitz, S. and Kennedy, M.C. (1978) Galactocerebroside is a specific marker for oligodendrocytes in culture. *Nature.* **274**, 813-816.

Raff, M.C., Miller, R.H. and Noble, M. (1983) A glial progenitor that develops *in vitro* into an astrocyte or an oligodendrocyte depending on culture medium. *Nature.* **303**, 390-396.

Raff, M.C., Abney, E.R. and Miller, R.H. (1984a) Two glial cell lineages diverge prenatally in rat optic nerve. *Developmental Biology.* **106**, 53-60.

Raff, M.C., Williams, B.P. and Miller, R.H. (1984b) The in vitro differentiation of a bipotential glial progenitor cell. *The EMBO Journal.* **3**, 1857-1864.

Raff, M.C. (1989) Glial cell diversification in the rat optic nerve. *Science.* **243**, 1450-1455.

Ranscht, B., Clapshaw, P.A., Price, J., Noble, M. and Seifert, W. (1982) Development of oligodendrocytes and Schwann cells studied with a monoclonal antibody against galactocerebroside. *Proceedings of the National Academy of Sciences USA.* **79**, 2709-2713.

Raskind, W.H., Williams, C.A., Hudson, L.D. and Bird, T.D. (1991) Complete deletion of the proteolipid protein gene (PLP) in a family with X-linked Pelizaeus-Merzbacher disease. *American Journal of Human Genetics.* **49**, 1355-1360.

Readhead, C., Schneider, A., Griffiths, I.R. and Nave, K. (1994) Premature arrest of myelin formation in transgenic mice with increased proteolipid protein gene dosage. *Neuron.* **12**, 583-595.

Remahl, S. and Hildebrand, C. (1982) Changing relation between onset of myelination and axon diameter range in developing feline white matter. *Journal of the Neurological Sciences.* **54**, 33-45.

Remahl, S. and Hildebrand, C. (1990) Relation between axons and oligodendroglial cells during initial myelination. I. The glial unit. *Journal of Neurocytology.* **19**, 313-328.

Richardson, W.D., Pringle, N., Mosley, M.J., Westermark, B. and Dubois-Dalcq, M. (1988) A role for platelet-derived growth factor in normal gliogenesis in the central nervous system. *Cell.* **53**, 309-319.

Roa, B.B., Dyck, P.J., Marks, H.G., Chance, P.F. and Lupski, J.R. (1993) Dejerine-Sottas syndrome associated with point mutation in the peripheral myelin protein 22 (*PMP22*) gene. *Nature Genetics.* **5**, 269-273.

Roach, F.C. (1945) Differentiation of the central nervous system after axial reversals of the medullary plate of Amblystoma. *The Journal of Experimental Zoology.* **99**, 53-77.

Ross, N.W. and Braun, P.E. (1988) Acylation in vitro of the myelin proteolipid protein and comparison with acylation in vivo: acylation of a cysteine occurs nonenzymatically. *Journal of Neuroscience Research.* **21**, 35-44.

Roussel, G., Neskovic, N.M., Trifilieff, E., Artault, J. and Nussbaum, J.L. (1987) Arrest of proteolipid transport through the Golgi apparatus in jimpy brain. *Journal of Neurocytology.* **16**, 195-204.

Samorajski, T. and Friede, R.L. (1968) A quantitative electron microscopic study of myelination in the pyramidal tract of rat. *The Journal of Comparative Neurology.* **134**, 323-338.

Samorajski, T., Friede, R.L. and Reimer, P.R. (1970) Hypomyelination in the quaking mouse. A model for the analysis of disturbed myelin formation. *Journal of Neuropathology and Experimental Neurology.* **29**, 507-523.

Saugier-Veber, P., Munnich, A., Bonneau, D., Rozet, J.-M., Le Merrer, M., Gil, R. and Boespflug-Tanguy, O. (1994) X-linked spastic paraplegia and Pelizaeus-Merzbacher disease are allelic disorders at the proteolipid protein locus. *Nature Genetics.* **6**, 257-262.

Scherer, S.S., Vogelbacker, H.H. and Kamholz, J. (1992) Axons modulate the expression of proteolipid protein in the CNS. *Journal of Neuroscience Research.* **32**, 138-148.

Scherer, S.S., Braun, P.E., Grinspan, J., Collarini, E., Wang, D. and Kamholz, J. (1994) Differential regulation of the 2',3'-cyclic nucleotide 3'-phosphodiesterase gene during oligodendrocyte development. *Neuron.* **12**, 1363-1375.

Schindler, P., Luu, B., Sorokine, O., Trifilieff, E. and Van Dorsselaer, A. (1990) Developmental study of proteolipids in bovine brain: a novel proteolipid and DM-20 appear before proteolipid protein (PLP) during myelination. *Journal of Neurochemistry.* **55**, 2079-2085.

Schliess, F. and Stoffel, W. (1991) Evolution of the myelin integral membrane proteins of the central nervous system. *Biological Chemistry Hoppe-Seyler.* **372**, 865-874.

Schneider, A., Montague, P., Griffiths, I.R., Fanarraga, M., Kennedy, P.G.E., Brophy, P.J. and Nave, K. (1992) Uncoupling of hypomyelination and glial cell death by a mutation in the proteolipid protein gene. *Nature.* **358**, 758-761.

Schneider, A., Griffiths, I.R., Readhead, C. and Nave, K.-A. (1995) Dominant-negative action of the *jimpy* mutation in mice complemented with an autosomal transgene for myelin proteolipid protein. *Proceedings of the National Academy of Sciences USA.* **92**, 4447-4451.

Schnitzer, J. and Schachner, M. (1982) Cell type specificity of a neural cell surface antigen recognized by the monoclonal antibody A2B5. *Cell and Tissue Research.* **224**, 625-636.

Schoenwolf, G.C. and Smith, J.L. (1990) Mechanisms of neurulation: traditional viewpoint and recent advances. *Development.* **109**, 243-270.

Schonbach, J., Hu, K.H. and Friede, R.L. (1968) Cellular and chemical changes during myelination: histologic,autoradiographic,histochemical and biochemical data on myelination in the pyramidal tract and corpus callosum of rat. *The Journal of Comparative Neurology.* **134**, 21-38.

Schwab, M.E. and Schnell, L. (1989) Region-specific appearance of myelin constituents in the developing rat spinal cord. *Journal of Neurocytology.* **18**, 161-169.

Shiota, C., Miura, M. and Mikoshiba, K. (1989) Developmental profile and differential localization of mRNAs of myelin proteins (MBP and PLP) in oligodendrocytes in the brain and in culture. *Developmental Brain Research.* **45**, 83-94.

Sidman, R.L., Dickie, M.M. and Appel, S.H. (1964) Mutant mice (quaking and jimpy) with deficient myelination in the central nervous system. *Science.* **144**, 309-311.

Sims, T.J., and Vaughn, J.E. (1979) The generation of neurones involved in an early reflex pathway of embryonic mouse spinal cord. *The Journal of Comparative Neurology.* **183**, 707-720.

Sinoway, M.P., Kitagawa, K., Timsit, S., Hashim, G.A. and Colman, D.R. (1994) Proteolipid protein interactions in transfectants: Implications for myelin assembly. *Journal of Neuroscience Research.* **37**, 551-562.

Skoff, R.P., Price, D.L. and Stocks, A. (1976a) Electron microscopic autoradiographic studies of gliogenesis in rat optic nerve. II. Time of origin. *The Journal of Comparative Neurology.* **169,** 313-334.

Skoff, R.P., Price, D.L. and Stocks, A. (1976b) Electron microscopic autoradiographic studies of gliogenesis in rat optic nerve. *The Journal of Comparative Neurology.* **169**, 291-312.

Skoff, R.P., Toland, D. and Nast, E. (1980) Pattern of myelination and distribution of neuroglial cells along the developing optic system of the rat and rabbit. *The Journal of Comparative Neurology.* **191**, 237-253.

Small, R.K., Riddle, P. and Noble, M. (1987) Evidence for migration of oligodendrocyte-type-2 astrocyte progenitor cells into the developing rat optic nerve. *Nature.* **328**, 155-157.

Smith, R., Cook, J. and Dickens, P.A. (1984) Structure of the proteolipid protein extracted from bovine central nervous system myelin with nondenaturing detergents. *Journal of Neurochemistry.* **42**, 306-313.

Snipes, G.J., Suter, U., Welcher, A.A. and Shooter, E.M. (1992) Characterization of a novel peripheral nervous system myelin protein (PMP-22/SR13). *Journal of Cell Biology.* **117**, 225-238.

Sobel, R.A., Greer, J.M., Isaac, J., Fondren, G. and Lees, M.B. (1994) Immunolocalization of proteolipid protein peptide 103-116 in myelin. *Journal of Neuroscience Research.* **37**, 36-43.

Sommer, I. and Schachner, M. (1981) Monoclonal antibodies (O1-O4) to oligodendrocyte cell surfaces: an immunocytological study in the central nervous system. *Developmental Biology.* **83**, 311-327.

Sorg, B.A., Smith, M.M. and Campagnoni, A.T. (1987) Developmental expression of the myelin proteolipid protein and basic protein mRNA in normal and dysmyelinating mutant mice. *Journal of Neurochemistry.* **49**, 1146-1154.

Sprinkle, T.J., Zarube, M.E. and McKhann, G.M. (1978) Activity of 2'3'-cyclic nucleotide 3'-phosphodiesterase in regions of rat brain during development: quantitative relationship to myelin basic protein. *Journal of Neurochemistry.* **30**, 309-314.

Stahl, N., Harry, J. and Popko, B. (1990) Quantitative analysis of myelin protein gene expression during development in the rat sciatic nerve. *Molecular Brain Research.* **8**, 209-212.

Stewart, H.J.S., Morgan, L., Jessen, K.R. and Mirsky, R. (1993) Changes in DNA synthesis rate in the Schwann cell lineage *in vivo* are correlated with the precursor-Schwann cell transition and myelination. *European Journal of Neuroscience.* **5**, 1136-1144.

Stoffel, W., Hillen, H., Schroder, W. and Deutzmann, R. (1983) The primary structure of bovine brain myelin lipophilin (proteolipid apoprotein). *Hoppe-Seyler's Zeipschrift fuer Physiologische Chemie.* **364**, 1455-1466.

Stoffel, W., Hillen, H. and Giersiefen, H. (1984) Structure and molecular arrangement of proteolipid protein of central nervous system myelin. *Proceedings of the National Academy of Sciences USA.* **81**, 5012-5016.

Sturrock, R.R. (1983) Problems of glial identification and quantification in the aging central nervous system. In: *Brain Aging: Neuropathology and Neuropharmacology.* Cervos-Navarro, J. and Sarkander, H.-I. editors: Raven Press, New York, pp. 179-209.

Suter, U., Moskow, J.J., Welcher, A.A., Snipes, G.J., Kosaras, B., Sidman, R.L., Buchberg, A.M. and Shooter, E.M. (1992a) A leucine-to-proline mutation in the putative first transmembrane domain of the 22-kDa peripheral myelin protein in the trembler-J mouse. *Proceedings of the National Academy of Sciences USA.* **89**, 4382-4386.

Suter, U., Welcher, A.A., Özcelik, T., Snipes, G.J., Kosaras, B., Francke, U., Billings-Gagliardi, S., Sidman, R.L. and Shooter, E.M. (1992b) *Trembler* mouse carries a point mutation in a myelin gene. *Nature.* **356**, 241-244.

Tennekoon, G.I., Cohen, S.R., Price, D.L. and McKhann, G.M. (1977) Myelinogenesis in optic nerve. A morphological, autoradiographic and biochemical analysis. *Journal of Cell Biology.* **72**, 604-616.

Tetzloff, S.U. and Bizzozero, O.A. (1993) Proteolipid protein from the peripheral nervous system also contains covalently bound fatty acids. *Biochemical and Biophysical Research Communications.* **193**, 1304-1310.

Tilney, F. (1933) Behaviour in its relation to development of the brain: correlation between development of brain and behaviour in the albino rat from embryonic states to maturity. *Bulletin of the Neurological Institute N.Y.* **3**, 252-358.

Tilney, F. and Casamajor, L. (1924) Myelinogeny as applied to the study of behavior. *Archives of Neurology and Psychiatry.* **12**, 1-66.

Timsit, S.G., Bally-Cuif, L., Colman, D.R. and Zalc, B. (1992a) DM-20 mRNA is expressed during the embryonic development of the nervous system of the mouse. *Journal of Neurochemistry.* **58**, 1172-1175.

Timsit, S., Sinoway, M.P., Levy, L., Allinquant, B., Stempak, J., Staugaitis, S.M. and Colman, D.R. (1992b) The DM20 protein of myelin: Intracellular and surface expression patterns in transfectants. *Journal of Neurochemistry.* **58**, 1936-1942.

Timsit, S., Martinez, S., Allinquant, B., Peyron, F., Puelles, L. and Zalc, B. (1995) Oligodendrocytes originate in a restricted zone of the embryonic ventral neural tube defined by DM-20 mRNA expression. *Journal of Neuroscience.* **15**, 1012-1024.

Tosic, M., Dolivo, M., Domanska-Janik, K. and Matthieu, J.-M. (1994) Paralytic tremor (*pt*): A new allele of the proteolipid protein gene in rabbits. *Journal of Neurochemistry.* **63**, 2210-2216.

Townsend, L.E. and Benjamins, J.A. (1983) Effects of monensin on posttranslational processing of myelin proteins. *Journal of Neurochemistry.* **40**, 1333-1339.

Trapp, B.D., Itoyama, Y., MacIntosh, T.D. and Quarles, R.H. (1983) P2 protein in oligodendrocytes and myelin of the rabbit central nervous system. *Journal of Neurochemistry.* **40,** 47-54.

Trapp, B.D., Hauer, P. and Lemke, G. (1988) Axonal regulation of myelin protein mRNA levels in actively myelinating Schwann cells. *Journal of Neuroscience.* **8,** 3515-3521.

Trapp, B.D. (1990) Distribution of myelin protein gene products in actively-myelinating oligodendrocytes. In: *Cellular and Molecular Biology of Myelination.* Jeserich, G., Althaus, H.A. and Waehneldt, T.V. editors: Springer-Verlag, Berlin, pp. 59-79.

Trapp, B.D. and Quarles, R.H. (1982) Presence of myelin-associated glycoprotein correlates with alterations in the periodicity of peripheral myelin. *Journal of Cell Biology.* **92,** 877-882.

Trapp, B.D. and Quarles, R.H. (1984) Immunocytochemical localization of the myelin-associated glycoprotein. Fact or artifact? *Journal of Neuroimmunology.* **6,** 231-249.

Trousse, F., Giess, M.C., Soula, C., Ghandour, S., Duprat, A.-M. and Cochard, P. (1995) Notochord and floor plate stimulate oligodendrocyte differentiation in cultures of the chick dorsal neural tube. *Journal of Neuroscience Research.* **41,** 552-560.

Tsuneishi, S., Takada, S., Motoike, T., Ohashi, T., Sano, K. and Nakamura, H. (1991) Effects of dexamethasone on the expression of myelin basic protein, proteolipid protein, and glial fibrillary acidic protein genes in developing rat brain. *Developmental Brain Research.* **61,** 117-123.

Uzman, L.L. and Rumley, M.K. (1958) Changes in the composition of the developing mouse brain during early myelination. *Journal of Neurochemistry.* **3,** 170-184.

Vacher-Lepretre, M., Nicot, C., Alfsen, A., Jolles, J. and Jolles, P. (1976) Study of the apoprotein of Folch-Pi bovine proteolipid. II. Characterization of the components isolated from sodium dodecyl sulfate solutions. *Biochimica et Biophysica Acta.* **420,** 323-331.

Valverde, F., Santacana, M. and Heredia, M. (1992) Formation of an olfactory glomerulus: morphological aspects of development and organization. *Neuroscience.* **49,** 255-275.

Valverde, F. and Lopez-Mascaraque, L. (1991) Neuroglial arrangements in the olfactory glomeruli of the hedgehog. *The Journal of Comparative Neurology.* **307,** 658-674.

Van Dorsselaer, A., Nebhl, R., Sorokine, O., Schindler, P. and Luu, B. (1987) The DM-20 proteolipid is a major brain protein. It is synthesised earlier in foetal life than the major myelin proteolipid (PLP). *Compte Rendu Academy Science Paris.* **305,** 555-560.

Vaughn, J. (1969) An electron microscopic analysis of gliogenesis in rat optic nerves. *Zeitschrift Zellforschung Microskopische Anatomie.* **94,** 293-324.

Verdi, J.M., Kampf, K. and Campagnoni, A.T. (1989) Translational regulation of myelin protein synthesis by steroids. *Journal of Neurochemistry.* **52,** 321-324.

Verity, A.N. and Campagnoni, A.T. (1988) Regional expression of myelin protein genes in the developing mouse brain: in situ hybridization studies. *Journal of Neuroscience Research.* **21,** 238-248.

Vermeesch, M.K., Knapp, P.E., Skoff, R.P., Studzinski, D.M. and Benjamins, J.A. (1990) Death of individual oligodendrocytes in *jimpy* precedes expression of proteolipid protein. *Developmental Neuroscience.* **12,** 303-315.

Waehneldt, T.V., Matthieu, J.-M. and Jeserich, G. (1985) Appearance of myelin proteins during vertebrate evolution. *Neuroscience Letters.* **57**, 97-102.

Waehneldt, T.V., Matthieu, J.-M. and Jeserich, G. (1986) Major central nervous system myelin glycoprotein of the African lungfish (*Protopterus dolloi*) cross reacts with myelin proteolipid protein antibodies, indicating a close phylogenetic relationship with amphibians. *Journal of Neurochemistry.* **46**, 1387-1391.

Waehneldt, T.V. (1990) Phylogeny of myelin proteins. *Annals of the New York Academy of Sciences.* **605**, 15-28.

Waehneldt, T.V. and Malotka, J. (1989) Presence of proteolipid protein in coelocanth brain myelin demonstrates tetrapod affinities and questions a chondrichthyan association. *Journal of Neurochemistry.* **52**, 1941-1943.

Warf, B.C., Fok-Seang, J. and Miller, R.H. (1991) Evidence for the ventral origin of oligodendrocyte precursors in the rat spinal cord. *Journal of Neuroscience.* **11**, 2477-2488.

Weimbs, T. and Stoffel, W. (1992) Proteolipid protein (PLP) of CNS myelin: Positions of free, disulfide-bonded, and fatty acid thioester-linked cysteine residues and implications for the membrane topology of PLP. *Biochemistry.* **31**, 12289-12296.

Weimbs, T. and Stoffel, W. (1994) Topology of CNS myelin proteolipid protein: Evidence for the nonenzymatic glycosylation of extracytoplasmic domains in normal and diabetic animals. *Biochemistry.* **33**, 10408-10415.

Wight, P.A., Duchala, C.S., Readhead, C. and Macklin, W.B. (1993) A myelin proteolipid protein-LacZ fusion protein is developmentally regulated and targeted to the myelin membrane in transgenic mice. *Journal of Cell Biology.* **123**, 443-454.

Wilkinson, H.J., Bailes, J.A. and McMahon, A.P. (1987) Expression of the proto-oncogene interleukin-1 is restricted to specific neural cells in the developing mouse embryo. *Cell.* **50**, 79-88.

Willard, H.F. and Riordan, J.R. (1985) Assignment of the gene for myelin proteolipid protein to the X chromosome: implications for X-linked myelin disorders. *Science.* **230**, 940-942.

Williams, B.P., Read, J. and Price, J. (1991) The generation of neurons and oligodendrocytes from a common precursor cell. *Neuron.* **7**, 685-693.

Windle, W.F., Fish, M.W. and O'Donnell, J.E. (1934) Myelogeny of the cat as related to development of fibre tracts and prenatal behaviour patterns. *The Journal of Comparative Neurology.* **59**, 139165-

Winter, J., Mirsky, R. and Kadlubowski, M. (1982) Immunocytochemical study of the appearance of P2 in developing rat peripheral nerve: comparison with other myelin components. *Journal of Neurocytology.* **11**, 351-362.

Wolswijk, G. (1994) $G_{D3}^{+}$ cells in the adult rat optic nerve are ramified microglia rather than O-$2A^{adult}$ progenitor cells. *Glia.* **10**, 244-249.

Yakovlev, P.I. and Lecours, A.R. (1967) The myelogenetic cycles of regional maturation of the brain. *Regional Development of the Brain in Early Life.* Minkowski, A. editor: Blackwell Scientific Publications. Oxford and Edinburgh, pp. 3-70.

Yamada, T., Placzek, M., Tanaka, H., Dodd, J. and Jessell, T.M. (1991) Control of cell pattern in the developing nervous system: polarizing activity of the floor plate and notochord. *Cell.* **64**, 635-647.

Yamamoto, Y., Mizuno, R., Nishimura, T., Ogawa, Y., Yoshikawa, H., Fujimura, H., Adachi, E., Kishimoto, T., Yanagihara, T. and Sakoda, S. (1994) Cloning and expression of myelin-associated oligodendrocytic basic protein. A novel basic protein constituting the central nervous system myelin. *The Journal of Biological Chemistry.* **269**, 31725-31730.

Yan, Y., Lagenaur, C. and Narayanan, V. (1993) Molecular cloning of M6: Identification of a PLP/DM20 gene family. *Neuron.* **11**, 423-431.

Yanagisawa, K. and Quarles, R.H. (1986) Jimpy mice: quantitation of myelin-associated glycoprotein and other proteins. *Journal of Neurochemistry.* **47**, 322-325.

Ye, P., Kanoh, M., Zhu, W., Laszkiewicz, I., Royland, J.E., Wiggins, R.C. and Konat, G. (1992) Cyclic AMP-induced upregulation of proteolipid protein and myelin associated glycoprotein gene expression in C6 cells. *Journal of Neuroscience Research.* **31**, 578-583.

Yu, W.-P., Collarini, E.J., Pringle, N.P. and Richardson, W.D. (1994) Embryonic expression of myelin genes: Evidence for a focal source of oligodendrocyte precursors in the ventricular zone of the neural tube. *Neuron.* **12**, 1353-1362.

Zahler, A.M. and Roth, M.B. (1995) Distinct functions of SR proteins in recruitment of U1 small nuclear ribonucleoprotein to alternative 5' splice sites. *Proceedings of the National Academy of Sciences USA.* **92**, 2642-2646.

Zgorzalewicz, B., Neuhoff, V. and Waehneldt, T.V. (1974) Rat myelin proteins.Compositional changes in various regions of the nervous system during ontogenetic development. *Neurobiology.* **4**, 265-276.

Zhang, S.-M., Marsh, R., Ratner, N. and Brackenbury, R. (1995) Myelin glycoprotein $P_0$ is expressed at early stages of chicken and rat embryogenesis. *Journal of Neuroscience Research.* **40**, 241-250.

Zhu, W., Kanoh, M., Ye, P., Laszkiewicz, I., Royland, J.E., Wiggins, R.C. and Konat, G. (1992) Retinoic acid-regulated expression of proteolipid protein and myelin-associated glycoprotein genes in C6 glioma cells. *Journal of Neuroscience Research.* **31**, 745-750.

Zhu, W., Wiggins, R.C. and Konat, G.W. (1994) Glucocorticoid-induced upregulation of proteolipid protein and myelin-associated glycoprotein genes in C6 cells. *Journal of Neuroscience Research.* **37**, 208-212.